

## Master Thesis

August 15, 2016

---

# Dynamic Vessel Response Modelling for Port Design and Operation

Case Study for the Port of Reykjavik

---

---

Hans Christian Bencard Nielsen (s136324)  
Supervisor: Erik Damgaard Christensen (DTU)  
Peter Sloth (DHI)  
Bjarne Jensen (DHI)  
Jens Kirkegaard (DHI)

# Table of Contents

List of Figures	iii
List of Tables	vi
<b>1 Abstract</b>	<b>1</b>
<b>2 Preface</b>	<b>2</b>
<b>3 Project Outline</b>	<b>3</b>
<b>4 Introduction</b>	<b>4</b>
<b>5 Background of the MIKE Models</b>	<b>7</b>
5.1 MIKE21 Spectral Wave Model . . . . .	7
5.2 MIKE21 Boussinesq Wave Model . . . . .	7
5.3 MIKE Dynamic Vessel Response Simulator Model . . . . .	9
5.4 Model Choice . . . . .	12
<b>6 MIKE 21 Spectral Wave Model</b>	<b>13</b>
6.1 Model Input Data . . . . .	13
6.2 Model Output . . . . .	14
<b>7 MIKE 21 Boussinesq Wave Model</b>	<b>19</b>
7.1 Bathymetrical Layout, Sponge Layer Map & Porosity Layer Map . . . . .	19
7.2 Wave Field Generation . . . . .	22
7.3 MIKE 21 BW Model Setup . . . . .	23
7.4 MIKE 21 BW Model Results . . . . .	24
<b>8 MIKE Dynamic Vessel Response Model</b>	<b>29</b>
8.1 DVRS Model Input . . . . .	29
8.2 Vessel Mooring and Fender Layout . . . . .	30
8.3 Vessel Motion Criteria . . . . .	37
8.4 Model Setup . . . . .	39
<b>9 Dynamic Vessel Response Output</b>	<b>41</b>
<b>10 DVRS Result Analysis</b>	<b>45</b>
10.1 Polypropylene Line, Polyamide Tail, no wind . . . . .	45
10.2 Ultraline Dyneema Line, Polyamide Tail, no wind . . . . .	46
10.3 Polypropylene Line, Polyamide Tail, wind $10 \frac{m}{s}$ , 0 degrees . . . . .	47
10.4 Ultraline Dyneema Line, Polyamide Tail, wind $10 \frac{m}{s}$ , 0 degrees . . . . .	48
10.5 Polypropylene Line, Polyamide Tail, wind $15 \frac{m}{s}$ , 0 degrees . . . . .	49
10.6 Ultraline Dyneema Line, Polyamide Tail, wind $15 \frac{m}{s}$ , 0 degrees . . . . .	50
10.7 Polypropylene Line, Polyamide Tail, wind $15 \frac{m}{s}$ , 250 degrees . . . . .	51
10.8 Ultraline Dyneema Line, Polyamide Tail, wind $15 \frac{m}{s}$ , 250 degrees . . . . .	52

10.9 DVRS Scenario Result Comparison . . . . .	53
10.10 Sensitivity Analysis . . . . .	56
<b>11 Discussion</b>	<b>65</b>
<b>12 Conclusion</b>	<b>69</b>
<b>13 Recommendations</b>	<b>69</b>
<b>14 References</b>	<b>71</b>
<b>A Appendix - Project Outline</b>	<b>74</b>
<b>B Appendix - Wave Plots</b>	<b>80</b>
B.1 Wave Agitation Coefficients . . . . .	80
B.2 Surface Elevation Plots . . . . .	85
B.3 $H_{m0}$ in the Total Model Area . . . . .	100
B.4 $H_{m0}$ at Hafnarbakki utan Klepps . . . . .	115
<b>C Appendix - DVRS Figures</b>	<b>130</b>
C.1 Polypropylene Line, Polyamide Tail, no wind . . . . .	130
C.2 Ultraline Dyneema Line, Polyamide Tail, no wind . . . . .	139
C.3 Polypropylene Line, Polyamide Tail, Wind $10 \frac{m}{s}$ , 0 degrees . . . . .	149
C.4 Ultraline Dyneema Line, Polyamide Tail, Wind $10 \frac{m}{s}$ , 0 degrees . . . . .	159
C.5 Polypropylene Line, Polyamide Tail, Wind $15 \frac{m}{s}$ , 0 degrees . . . . .	169
C.6 Ultraline Dyneema Line, Polyamide Tail, Wind $15 \frac{m}{s}$ , 0 degrees . . . . .	179
C.7 Polypropylene Line, Polyamide Tail, Wind $15 \frac{m}{s}$ , 250 degrees . . . . .	189
C.8 Ultraline Dyneema Line, Polyamide Tail, Wind $15 \frac{m}{s}$ , 250 degrees . . . . .	199

## List of Figures

4.1	The country of Iceland . . . . .	4
4.2	Proposed location for the port expansion at Hafnarbakki utan Klepps . . .	5
5.1	DVRS set-up showing the input data for the FVRE, DVRE models and the DVRS model's outputs . . . . .	9
5.2	A vessels six-degrees of freedom. . . . .	10
5.3	DVRS Coordinate System . . . . .	12
6.1	Initial Modelled Area in MIKE21 SW . . . . .	13
6.2	Modelled Area in MIKE21 SW . . . . .	14
6.3	Time Series for the Sig. Wave Height at B7 from 1995 to 2015 . . . . .	15
6.4	Time Series for the Peak Wave Period at B7 from 1995 to 2015 . . . . .	15
6.5	Time Series for the Mean Wave Direction at B7 from 1995 to 2015 . . . . .	16
6.6	Offshore Wave Rose for the Data from 1995 to 2015 . . . . .	16
6.7	Extreme Value Analysis from the Offshore Wave Data . . . . .	18
7.1	Hafnarbakki utan Klepps vs Kleppsbakki Grid Points . . . . .	19
7.2	MIKE21 BW Model Bathymetry . . . . .	20
7.3	Smaller MIKE21 BW Model Bathymetry . . . . .	20
7.4	3D Overview of the Bathymetry for the Modelled Area . . . . .	21
7.5	Applied Sponge Layer Map in the Model Area . . . . .	21
7.6	Applied Porosity Layer Map in the Model Area . . . . .	22
7.7	Arbitrary JONSWAP Spectrum, [14] . . . . .	23
7.8	W.A.C. for $H_{m0}$ 1m . . . . .	26
7.9	W.A.C. for $H_{m0}$ 2m . . . . .	26
7.10	W.A.C. for $H_{m0}$ 3m . . . . .	26
7.11	W.A.C. for $H_{m0}$ 4m . . . . .	27
7.12	Time Series for the Wave Height at Hafnarbakki utan Klepps from 1995-2015	27
7.13	Exceedance Plot for the Wave Height at Hafnarbakki utan Klepps . . . . .	28
8.1	Eimskips M/V Godafoss . . . . .	29
8.2	Digitalised Vessel Hull used in the DVRS Program . . . . .	30
8.3	Names and locations of mooring lines in a typical layout, [35] . . . . .	31
8.4	Fore Deck Area Mooring Line Layout provided by the Captain of Godafoss	32
8.5	Aft Deck Area Mooring Line Layout provided by the Captain of Godafoss .	32
8.6	Performance curve for the V-cap Fender . . . . .	33
8.7	Performance curve for the RTT Fender . . . . .	33
8.8	MBL % vs Elongation % curve for a typical Polypropylene Line, [3] . . . . .	36
8.9	MBL % vs Elongation % curve for a typical Ultraline Dyneema Line, [3] .	36
8.10	MBL % vs Elongation % curve for a typical Polyamide Line, [3] . . . . .	37
8.11	A vessels six degrees of freedom, [35] . . . . .	38
8.12	Suggested critical degrees of motion for various vessel types, [35] . . . . .	39
8.13	Initial setup page in the DVRS software package . . . . .	40
8.14	DVRS scenario input coordinates . . . . .	40
9.1	DVRS Surge Data for $H_{m0}$ 3m, $T_p$ 10s, MWD 315deg . . . . .	41
9.2	DVRS Sway Data for $H_{m0}$ 3m, $T_p$ 10s, MWD 315deg . . . . .	42
9.3	DVRS Heave Data for $H_{m0}$ 3m, $T_p$ 10s, MWD 315deg . . . . .	42

9.4	DVRS Roll Data for Hm0 3m, Tp 10s, MWD 315deg . . . . .	43
9.5	DVRS Pitch Data for Hm0 3m, Tp 10s, MWD 315deg . . . . .	43
9.6	DVRS Yaw Data for Hm0 3m, Tp 10s, MWD 315deg . . . . .	44
10.1	Exceedance of the Surge Motion, Polypropylene Line with no wind . . . . .	46
10.2	Time Series showing the Surge Motions from 1995-2015, Polypropylene Line with no wind . . . . .	46
10.3	Exceedance of the Mooring Line Forces, , Polypropylene Line with no wind	47
10.4	Exceedance of the Surge Motion, Ultraline Dyneema Line with no wind . .	47
10.5	Time Series showing the Surge Motions from 1995-2015, Ultraline Dyneema Line with no wind . . . . .	48
10.6	Exceedance of the Mooring Line Forces, Ultraline Dyneema Line with no wind	48
10.7	Exceedance of the Surge Motion, Polypropylene Line with wind $10 \frac{m}{s}$ from $0^\circ$	49
10.8	Time Series showing the Surge Motions from 1995-2015, Polypropylene Line with wind $10 \frac{m}{s}$ from $0^\circ$ . . . . .	49
10.9	Exceedance of the Surge Motion, Ultraline Dyneema Line with wind $10 \frac{m}{s}$ from $0^\circ$ . . . . .	50
10.10	Time Series showing the Surge Motions from 1995-2015, Ultraline Dyneema Line with wind $10 \frac{m}{s}$ from $0^\circ$ . . . . .	50
10.11	Exceedance of the Surge Motion, Polypropylene Line with wind $15 \frac{m}{s}$ from $0^\circ$	51
10.12	Time Series showing the Surge Motions from 1995-2015, Polypropylene Line with wind $15 \frac{m}{s}$ from $0^\circ$ . . . . .	51
10.13	Exceedance of the Surge Motion, Ultraline Dyneema Line with wind $15 \frac{m}{s}$ from $0^\circ$ . . . . .	52
10.14	Time Series showing the Surge Motions from 1995-2015, Ultraline Dyneema Line with wind $15 \frac{m}{s}$ from $0^\circ$ . . . . .	52
10.15	Exceedance of the Surge Motion, Polypropylene Line with wind $15 \frac{m}{s}$ from $250^\circ$ . . . . .	53
10.16	Time Series showing the Surge Motions from 1995-2015, Polypropylene Line with wind $15 \frac{m}{s}$ from $250^\circ$ . . . . .	53
10.17	Exceedance of the Surge Motion, Ultraline Dyneema Line with wind $15 \frac{m}{s}$ from $250^\circ$ . . . . .	54
10.18	Time Series showing the Surge Motions from 1995-2015, Ultraline Dyneema Line with wind $15 \frac{m}{s}$ from $250^\circ$ . . . . .	54
10.19	Sensitivity Test - Wind Directions effects of the Vessels Rotations . . . . .	57
10.20	Sensitivity Test - Wind Directions effects of the Vessels Rotations . . . . .	57
10.21	Sensitivity Test - Wind Directions effects on the Mooring Line Forces . . .	58
10.22	Sensitivity Test- Tail Lengths Effects on the Vessel Displacement . . . . .	59
10.23	Sensitivity Test - Tail Lengths Effects on the Vessel Rotation . . . . .	60
10.24	Sensitivity Test - Tail Length Effects on the Mooring Line Forces . . . . .	60
10.25	Sensitivity Test - Line Pre-Tensioning Effects on Vessel Displacement . . .	61
10.26	Sensitivity Test - Line Pre-Tensioning Effects on Vessel Rotation . . . . .	61
10.27	Sensitivity Test - Line Pre-Tension Effect on Mooring Line Forces . . . . .	62
10.28	Sensitivity Test - Seawater Density Effects on Vessel Displacement . . . . .	63
10.29	Sensitivity Test - Seawater Density Effects on Vessel Rotation . . . . .	64
10.30	Sensitivity Test - Seawater Density Mooring Line Forces . . . . .	64

11.1 The effect of long waves on larger vessels, [35] . . . . .	66
11.2 Frequency spectrum for the offshore waves . . . . .	67
11.3 Frequency spectrum for the berth waves . . . . .	67

## List of Tables

6.1	Twenty Year Wave Model Statistics for $H_{m0}$ , $T_p$ & MWD	17
7.1	Modelled Wave Scenarios	24
7.2	Mean Wave Aggitation Coefficient at Haffnarbakki utan Klepps	25
8.1	Eimskips Godafoss Vessel Dimension	29
8.2	DVRS Modelled Scenarios	30
8.3	Fender Characteristics used in the DVRS Model	32
8.4	Coordinate Location of the Bollards, Fenders, Fair Leads and Winches	34
8.5	Bollard, Fair Lead, Winch Combination used in the DVRS Model	35
8.6	Godafoss Mooring Line and Tail Length	35
8.7	Stiffness table for the Polypropylene Line and Polyamide Tail	36
8.8	Stiffness table for the Ultraline Dyneema Line and Polyamide Tail	37
8.9	Maximum amplitudes of motions for container vessels at 100% (un)loading efficiency	38
8.10	Maximum allowable significant motion amplitudes for an (un)loading efficiency of 95%	39
8.11	Initial Vessel Displacement Values after iterating the vessel	41
10.1	Result Comparison for the Surge Exceedance Plots	55
10.2	Sensitivity Test - Wind Direction Data Points	56
10.3	Sensitivity Test - Tail Length Data Points	59
10.4	Sensitivity Test - Line Pre-Tensioning Datapoints	61
10.5	Sensitivity Test - Seawater Density Data Points	63
C.1	DVRS Datapoints for $H_{m0}$ 1m	130
C.2	DVRS Datapoints for $H_{m0}$ 2m	130
C.3	DVRS Datapoints for $H_{m0}$ 3m	130
C.4	DVRS Datapoints for $H_{m0}$ 4m	130
C.5	DVRS Datapoints for Mooring Line Forces	138
C.6	DVRS Datapoints for $H_{m0}$ 1m	139
C.7	DVRS Datapoints for $H_{m0}$ 2m	139
C.8	DVRS Datapoints for $H_{m0}$ 3m	139
C.9	DVRS Datapoints for $H_{m0}$ 4m	139
C.10	DVRS Datapoints for Mooring Line Forces	148
C.11	DVRS Datapoints for $H_{m0}$ 1m	149
C.12	DVRS Datapoints for $H_{m0}$ 2m	149
C.13	DVRS Datapoints for $H_{m0}$ 3m	149
C.14	DVRS Datapoints for $H_{m0}$ 4m	149
C.15	DVRS Datapoints for Mooring Line Forces	158
C.16	DVRS Datapoints for $H_{m0}$ 1m	159
C.17	DVRS Datapoints for $H_{m0}$ 2m	159
C.18	DVRS Datapoints for $H_{m0}$ 3m	159
C.19	DVRS Datapoints for $H_{m0}$ 4m	159
C.20	DVRS Datapoints for Mooring Line Forces	168
C.21	DVRS Datapoints for $H_{m0}$ 1m	169
C.22	DVRS Datapoints for $H_{m0}$ 2m	169

---

C.23 DVRS Datapoints for $H_{m0}$ 3m . . . . .	169
C.24 DVRS Datapoints for $H_{m0}$ 4m . . . . .	169
C.25 DVRS Datapoints for Mooring Line Forces . . . . .	178
C.26 DVRS Datapoints for $H_{m0}$ 1m . . . . .	179
C.27 DVRS Datapoints for $H_{m0}$ 2m . . . . .	179
C.28 DVRS Datapoints for $H_{m0}$ 3m . . . . .	179
C.29 DVRS Datapoints for $H_{m0}$ 4m . . . . .	179
C.30 DVRS Datapoints for Mooring Line Forces . . . . .	188
C.31 DVRS Datapoints for $H_{m0}$ 1m . . . . .	189
C.32 DVRS Datapoints for $H_{m0}$ 2m . . . . .	189
C.33 DVRS Datapoints for $H_{m0}$ 3m . . . . .	189
C.34 DVRS Datapoints for $H_{m0}$ 4m . . . . .	189
C.35 DVRS Datapoints for Mooring Line Forces . . . . .	198
C.36 DVRS Datapoints for $H_{m0}$ 1m . . . . .	199
C.37 DVRS Datapoints for $H_{m0}$ 2m . . . . .	199
C.38 DVRS Datapoints for $H_{m0}$ 3m . . . . .	199
C.39 DVRS Datapoints for $H_{m0}$ 4m . . . . .	199
C.40 DVRS Datapoints for Mooring Line Forces . . . . .	208



## 1 Abstract

The Port Authorities of Reykjavik are planning to expand their berth area at Hafnarbakki utan Klepps. After the use of three MIKE software programs (MIKE21 SW, BW and DVRS) it was possible to compare the method in which harbours are currently designed regarding the wave height at the berth area with what regarding the vessel motion criteria established by PIANC 2012. The wave agitation coefficients at Hafnarbakki utan Klepps for different wave conditions was determined. By using these it was determined that the current method of looking at the wave height limitation of 0.5m has an exceedance probability of 0.154% per year (13.5 hour). The shipping company Eimskip has provided details for one of their vessels, M/V Godafoss and it has been used as the design vessel for Hafnarbakki utan Klepps. Two different vessel mooring configurations were compared, one using a Polypropylene Line and a Polyamide Tail and the other using an Ultraline Dyneema Line and Polyamide Tail. They were subject to different wind conditions of 10 & 15  $\frac{m}{s}$  coming from different angles while being under the influence of the wave climate generated by the MIKE21 BW simulations. The literature suggests that for container vessels the most critical vessel motion is the surge motion as ship-to-shore cranes can not compensate for this movement, therefore it is the only degree of motion which has been fully analysed here. The lowest exceedance time was that of an Ultraline Dyneema line with a wind speed of 15  $\frac{m}{s}$  coming at an angle of 250°, 1.516 % or 133 hours per year (surge motion of 0.2m). When comparing the expected exceedances of the berth wave height to the surge motions of a vessel it is clear to see that Godafoss will have passed the PIANC 2012 motion criteria more often than the current port design method of the wave height criteria. For this case it is worth reconsidering which of the criteria used for port designs is more critical. A series of sensitivity tests to see how the vessel will react to wind speeds of 10  $\frac{m}{s}$  coming from different directions has been undertaken. Here it was seen that when the wind is pushing the vessel off the fenders the motion increases. When the wind pushed the vessel onto the fenders the motions decreased. These sensitivity tests were also performed for the effects of changing the tail length, line pre-tensioning and seawater densities.

## 2 Preface

This thesis is the final project for my Master of Science degree in Civil Engineering at the Technical University of Denmark (DTU). It is the result of five months work, which has been done in collaboration with the Danish Hydraulic Institute (DHI), and is to be submitted on June 4<sup>th</sup>, 2016. This project represents 30 ECTS points of work and it has been conducted under the guidance of the DHI personnel of Peter Sloth, Bjarne Jensen and Jens Kirkegaard along with Professor Erik Damgaard Christensen at DTU.

It has been a long and hard process for me to write this thesis and I would not have been able to do this without the unwavering support of various people. Firstly, I would like to thank my family for supporting me and being there for me if I ever needed to speak to them. Secondly, I would like to thank the people with whom I worked at DHI as they constantly gave me useful feedback and guided me whenever I needed them. Also, the personnel in Reykjavik whom gave me the opportunity to do a case study for my thesis and always replied to any query I had about how things are done in Iceland. I would also like to thank Erik as he helped me define what was needed and to keep me on track as I would occasionally begin to veer off course and study topics which were not always relevant to my current research topic. Last but not least I can not express the gratitude I have to my girlfriend as she supported me mentally throughout this entire process. Her experience and wisdom were always guiding me and she served as my beacon of light while I navigated the rough seas of thesis writing.

### **3 Project Outline**

Before the thesis process can begin it is important to create an outline which can be used to setout a plan as to how the thesis shall proceed. After various discussions with my supervisors at both DTU and DHI a Project Outline has been created. This outline can be seen in Appendix A.

## 4 Introduction

As global trade increases the need for safe vessel berthing facilities increases as well. To safely (un)load cargo a strict set of criteria are presented. When designing a harbour the limits have been given as a maximum allowable wave height which may come into contact with the vessels. Using this limit as the only criteria may not give the harbour planner a full perspective of how the vessels will react to incoming waves or passing ships when berthed. It is therefore also necessary to know how the vessel will react to the incoming waves as this may give undesired downtime. These waves may cause the vessel to exceed its limits in either of the six degrees of freedom. They are the three displacement motions of surge, sway and heave, along with the three rotations of roll, pitch and yaw.

This thesis is a case study is done with the cooperation of DHI for the Port of Reykjavik, which plans to extend its berthing facilities at Hafnarbakki utan Klepps. Reykjavik is the capital city and it is located on the western coast of Iceland.



Figure 4.1: The country of Iceland

The expansion at Hafnarbakki utan Klepps is located in the red circle in figure 4.2.

As mentioned above, this project will look into see if the current way of designing harbours by virtue of the wave height in the berth area or if it is time to re-consider this aspect for the vessel motion criteria instead. Here this project will look at the the significant motion of amplitude for the container vessel as established in the PIANC 2012 guideline.

This will be accomplished by the use of the MIKE21 Spectral Wave, MIKE 21 Boussinesq Wave and MIKE Dynamic Vessel Response Simulator software packages.

For this report it is assumed that the reader is familiar with the basic concepts regarding waves near coastal regions & port operations/planning. Therefore not much attention has

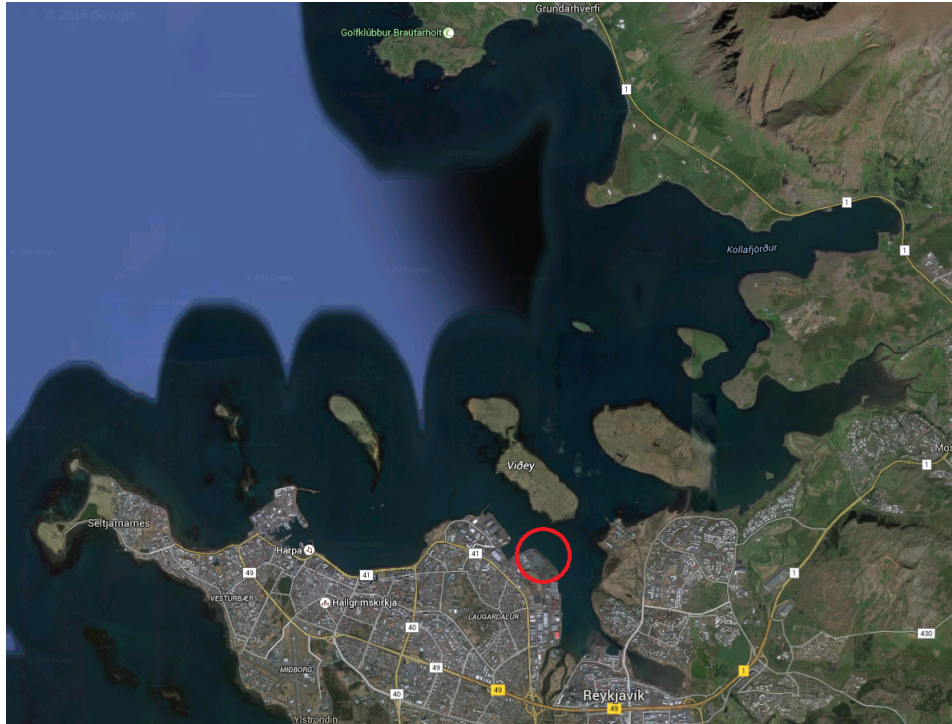


Figure 4.2: Proposed location for the port expansion at Hafnarbakki utan Klepps

been paid to the full explanation of these phenomena, yet some relevant literature for further reading is referred to in the text. This report has been divided into the following sections:

Section 5: Background information on the MIKE Models

Section 6: The MIKE 21 Spectral Wave model for the Faxaflói Bay area outside Reykjavik where a 20 year wave statistic has been used to obtain a wave data set closer to the MIKE21 BW model area

Section 7: The MIKE21 Boussinesq Wave model near Hafnarbakki utan Klepps. This is used to analyse the wave conditions at the berth along with gathering the data which is to be used in the DVRS program. The wave agitation coefficients and the exceedance of a wave height 0.5m at Hafnarbakki utan Klepps is found.

Section 8: The MIKE Dynamic Vessel Response Simulator for the vessel motion simulation at Hafnarbakki utan Klepps. This section contains the explanation of the input data and model setup.

Section 9: This section describes how the DVRS program raw output data has been analysed.

Section 10: Here the output data for each of the DVRS setup scenarios is shown independently and then compared to each other. Here the exceedance plots to see how often the vessel will surpass the motion criteria set out by PIANC 2012 is found.

Section 11: A discussion regarding this report and what other similar studies have been

undertaken.

Section 12: A conclusion with regards to the findings of this report and how they may be of use for the Port Authorities in Reykjavik.

Section 13: A short section which gives a series of recommendations for a future study or if this study was to be undertaken once more.

## 5 Background of the MIKE Models

### 5.1 MIKE21 Spectral Wave Model

The MIKE21 Spectral Wave model is a new generation spectral-wind-wave model which is based on unstructured meshes. This software package simulates the growth, decay and transformation of wind-generated waves and swell in coastal as well as offshore regions. One of the main purposes of this model is to help design offshore, port and coastal structures. MIKE21 SW includes the directional decoupled parametric formulation and the fully spectral formulation. The directional decoupled parametric formulation is based on a parameterization of the wave action conservation equation, while the parameterisation on the frequency domain is made by introducing the zeroth and first moment of the wave action spectrum as dependent variables. This has been done in Holthuijsens 1989 paper regarding the "prediction model for stationary short crested waves in shallow water with ambient currents".

The Spectral Wave program is capable of including the physical phenomena of

- Wave growth by the action of the wind
- Non-linear wave-wave interactions
- Dissipation due to white-capping/bottom friction/depth-induced wave breaking
- Refraction and shoaling due to depth variations
- Wave-current interaction

The full equations and how they are applied within the SW model can be found in [7] and they will not be discussed in length here. Some of the more important parameters which must be included in the SW model are a digitalised bathymetry which will be used to create a computerised mesh, along with the forcing parameters such as the water level data, the tidal variations, and current & wind data.

### 5.2 MIKE21 Boussinesq Wave Model

The MIKE21 BW model is based on the numerical solution of the Boussinesq equations in the time domain. This model is capable of reproducing the combined effects of the majority of the wave phenomena which are of interest in harbour & coastal engineering, such as refraction, shoaling, diffraction, wave breaking, reflection from porous structures, frequency or directional spreading, etc.

To be able to run a MIKE21 BW model the following input requirements are needed; - Digitalised bathymetry.

- Model boundary, grid spacing of the computational model grid, time step, simulation duration.
- Incident wave conditions based off a specified wave spectra.
- Porosities which describe the reflection transmission characteristics of the structures in the model.
- Sponge layers which will absorb the wave energy near the model boundaries to avoid

wave reflection off the boundary walls.

The Boussinesq equations have been enhanced to allow the waves to propagate efficiently over a varying bathymetry (from deep to shallow water), taken originally from [19] & [20]. This has increased the maximum depth to deep-water wave length ( $\frac{h}{L_o}$ ) from 0.22 to 0.5.

The model equations were extended once more to take into account the effects of wave breaking and moving shorelines, [21], [22], [33], [34].

MIKE21 BW solves the enhanced Boussinesq equations as they are expressed in the terms of the free surface elevation,  $\sigma$ , along with the depth-integrated velocity components, P & Q. The Boussinesq equation and its list of symbols are:

#### Symbol List

$P$	flux density in the x-direction, $m^3/m/s$
$Q$	flux density in the y-direction, $m^3/m/s$
$B$	Boussinesq dispersion factor
$F_x$	Horizontal stress term in x-direction
$F_y$	Horizontal stress term in y-direction
$x, y$	Cartesian co-ordinates, m
$t$	time, s
$h$	total water depth (=d+ $\xi$ ), m
$d$	still water depth, m
$g$	gravitational acceleration (= 9.81 $m/s^2$ )
$n$	porosity
$C$	Chezy resistance number, $m^{0.5}/s$
$\alpha$	resistance coefficient for laminar flow in porous media
$\beta$	resistance coefficient for turbulent flow in porous media
$\xi$	water surface level above datum, m

The Continuity Equation:

$$n \frac{\delta \xi}{\delta t} + \frac{\delta P}{\delta x} + \frac{\delta Q}{\delta y} = 0 \quad (5.1)$$

X-momentum:

$$n \frac{\delta P}{\delta t} + \frac{\delta}{\delta x} \left( \frac{P^2}{h} \right) + \frac{\delta}{\delta y} \left( \frac{PQ}{h} \right) + \frac{\delta R_{xx}}{\delta x} + \frac{\delta R_{xy}}{\delta y} + F_x n^2 g h \frac{\delta \xi}{\delta x} + n^2 P \left( \sigma + \beta \frac{\sqrt{P^2 + Q^2}}{h} \right) + \frac{gP \sqrt{P^2 + Q^2}}{h^2 C^2} + n \Psi_1 = 0 \quad (5.2)$$

Y-momentum:

$$n \frac{\delta Q}{\delta t} + \frac{\delta}{\delta y} \left( \frac{Q^2}{h} \right) + \frac{\delta}{\delta x} \left( \frac{PQ}{h} \right) + \frac{\delta R_{yy}}{\delta y} + \frac{\delta R_{xy}}{\delta x} + F_y n^2 g h \frac{\delta \xi}{\delta y} + n^2 Q \left( \sigma + \beta \frac{\sqrt{P^2 + Q^2}}{h} \right) + \frac{gQ \sqrt{P^2 + Q^2}}{h^2 C^2} + n \Psi_2 = 0 \quad (5.3)$$

For the X-momentum and the Y-momentum equations the Boussinesq dispersion terms,  $\Psi_1$  and the  $\Psi_2$  are defined in [8]. The horizontal stress terms are described using a gradient-



stress relation which is defined in [8] as, where  $v_t$  is the horizontal eddy viscosity.

$$F_x = -\left(\frac{\delta}{\delta x}(v_t \frac{\delta P}{\delta x}) + \frac{\delta}{\delta y}(v_t(\frac{\delta P}{\delta y} + \frac{\delta Q}{\delta x}))\right) \quad (5.4)$$

$$F_y = -\left(\frac{\delta}{\delta y}(v_t \frac{\delta Q}{\delta y}) + \frac{\delta}{\delta x}(v_t(\frac{\delta Q}{\delta x} + \frac{\delta P}{\delta y}))\right) \quad (5.5)$$

For a further explanation on the derivation of the Boussinesq equations, their components, the numerical implementation, and the verification of the MIKE21 BW model please refer to [8].

### 5.3 MIKE Dynamic Vessel Response Simulator Model

For a full description of the derivation of the formulae used in the DVRS program and its capabilities please refer to [9]. This section will give a brief overview of how the software package works and it will mention some of the main formulae behind the calculation of the vessel motion.

Dynamic Vessel Response Simulator (DVRS) is a software program which has been developed by DHI by combining Frequency Vessel Response Engine (FVRE) and the Dynamic Vessel Response Engine (DVRE). FVRE is a “diffraction/radiation panel program used for calculating the frequency response functions of the floating structures”, [9]. DVRE is a “time-domain floating body engine, which computes the temporal body dynamics on the basis of the obtained frequency response functions (from FVRE), moorings and environmental forcings (wave, current and wind data)” [9]. How these components interact with each other can be seen in the figure 5.1.

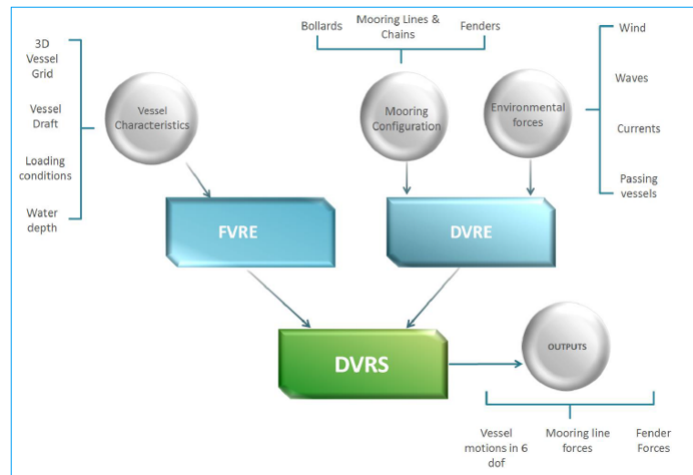


Figure 5.1: DVRS set-up showing the input data for the FVRE, DVRE models and the DVRS model’s outputs

The purpose behind the DVRS program is to solve the six degrees of motion for a berthed vessel, as shown in figure 5.2.

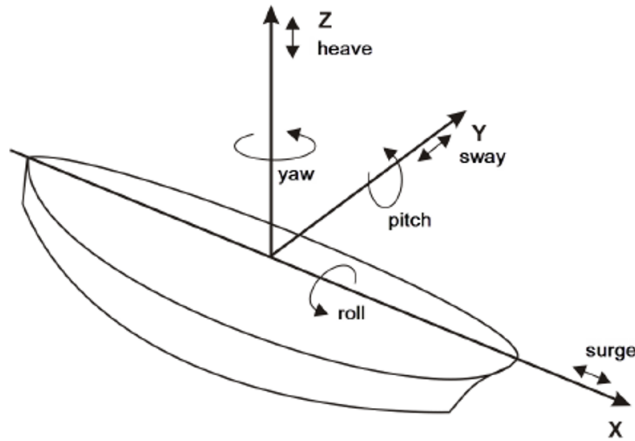


Figure 5.2: A vessels six-degrees of freedom.

### Frequency Vessel Response Engine

The FVRE engine is run first to create the geometry and hydrostatics of the floating body (vessel) which is to be modelled. This floating body surface is obtained by integrating the grid file in each of the three directions independently,  $n_1$ ,  $n_2$ ,  $n_3$  are the x,y,z unit vectors normal to the body boundary and the median of these three volumes ( $\nabla$ ) is used.

$$\nabla = - \int \int_{S_b} n_1 x dS = - \int \int_{S_b} n_2 y dS = - \int \int_{S_b} n_3 z dS \quad (5.6)$$

The location of the centre of bouyancy is used for some of the components of the hydrostatic restoring matrix. The surfaces which have been obtained from the mesh are integrated.

$$x_b = \frac{-1}{2\nabla} \int \int_{S_b} n_1 x^2 dS y_b = \frac{-1}{2\nabla} \int \int_{S_b} n_2 y^2 dS z_b = \frac{-1}{2\nabla} \int \int_{S_b} n_3 z^2 dS \quad (5.7)$$

The potential for radiated waves needs to be found, even though part of the surface elevation and flow field are solved with the Boussinesq waves in the DVRE. The total wave potential can be decomposed into the scattered, incident and radiated waves. Here  $\xi_j$  refers to the six degrees of freedom shown in figure 5.2.

$$\phi = \phi_0 + \phi_7 + i\omega \sum_{j=1}^6 \xi_j \phi_j \quad (5.8)$$

The explanation regarding the derivation for each of the degrees of motion for the radiation potential can be found on pages 41-42 in [9] and by using the boundary conditions the Laplacian of the wave potential is to be solved for 8 modes ( $j=0,\dots,7$ ). This is one for each of the six degrees of motion along with one for the incident and scattered radiated wave.

$$\nabla^2 \phi_j = 0 \quad (5.9)$$

The description of how the frequency boundary problems which are governed by 5.9 are solved in FVRE to obtain the radiation potential  $\phi_j$  on a floating bodies surface. This is accomplished by applying the free-surface Green's function,  $G(x_i; x_k)$  in which  $x_i$  is the field point while  $x_k$  is the source point. This is done in order to derive the boundary integral equations that are to be solved using the Boundary Element Method (BEM). A full description of how this is done can be found on pages 42-44 in [9], along with the smoothing of irregular frequencies, adding mass and damping coefficients & second order drift forces.

### Dynamic Vessel Response Engine

One of the first things which is done in the DVRE engine is to set up an inertia matrix,  $M$ . This is done using the mass and the horizontal centre of gravity which has been found when determining the coordinate center of buoyancy.

$$m = \rho \forall \quad (5.10)$$

The moment of inertia is obtained from the radii of gyration of the vessel.

$$I_{ij} = \rho \forall r_{ij} |r_{ij}| \quad (5.11)$$

How the added mass and damping coefficients are obtained from  $\phi_j$  is explained on page 45-47 in [9]. These pages also describe how  $F_{jD}(\omega)$  consists of the two terms  $p_I(\vec{x}, \omega)$  and  $\phi_{In}(\vec{x}, \omega)$  are derived from the Boussinesq wave calculations, based on the Haskind relation.

$$F_{jD}(\omega) = \int_0^\infty dt F_{jD}(t) e^{-i\omega t} F_{jD}(\omega) = \int \int_{S_b} d\vec{x} p_1(\vec{x}, \omega) n_j(\vec{x}) + i\omega \rho \int \int_{S_b} d\vec{x} \phi_j(\vec{x}, \omega) \phi_{1n}(\vec{x}, \omega) \quad (5.12)$$

As the vessel is at berth it is subject to a series of external forces. The sum of the total external forces,  $F_{jnl}$ , is the sum of the mooring, viscous damping, wind, current, slow wave drift and frictional damping forces in the mooring system for each of the six degrees of freedom  $j$ .

$$F_{jnl}(t) = F_{jmoor}(t) + F_{jvisc}(t) + F_{jwind}(t) + F_{jcur}(t) + F_{jdrift}(t) + F_{jfric}(t) \quad (5.13)$$

The floating bodies movement is governed by its equations of motion. In the DVRE package the equation of motion is transformed from the time domain to the frequency domain. This has been done as it may be difficult to solve certain factors in the time domain. How this has been accomplished can be seen in pages 48-49 in [9].

When the DVRS program is to be run the coordinate system is with regards to the vessel. This would require the user to translate the coordinates from a global perspective to those which are presented in figure 5.3.

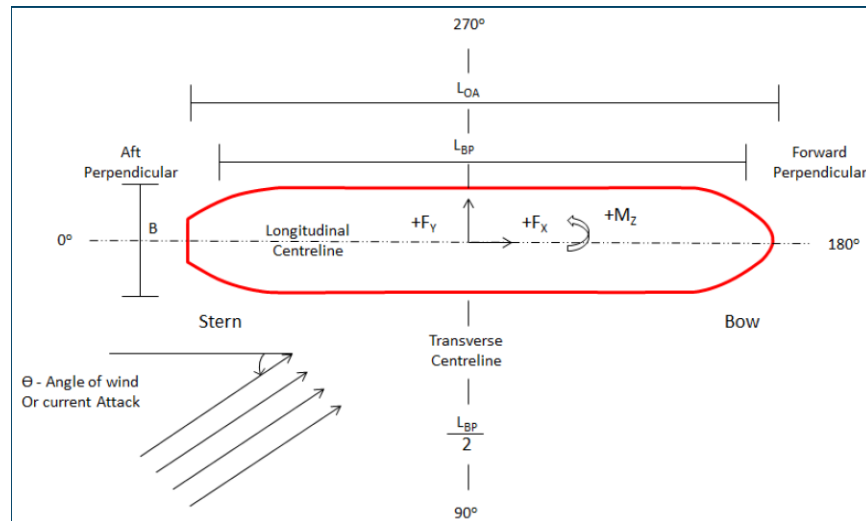


Figure 5.3: DVRS Coordinate System

#### 5.4 Model Choice

The MIKE software package is chosen as it is considered to be the most sophisticated software to model non-linear wave interactions in the time domain. In the MIKE 2016 update release the Dynamic Vessel Response Simulator has been incorporated. This allowed the author to test how the files which have been extracted from MIKE21 BW can be used in the DVRS program. As the author did this project in cooperation with DHI these were the software packages which were presented.

There are other software tools which can be used such as the SWAN model, Delf3d or Moortex/Moormaster. A feasibility study for creating open container ports has been undertaken in a Master Thesis, [2], in which these software packages were used.

The difference between the used and other software packages will not be discussed as they are out of the scope of this project.

## 6 MIKE 21 Spectral Wave Model

### 6.1 Model Input Data

The input data used in this MIKE21SW model was provided by the Port Authorities of Reykjavik as they had run a similar model, [15]. This hindcast data is for a period from 1995-2015 and it consists of a wind profile, the tidal variations, a bathymetric layout, wave data from the North Atlantic which was run in the model along a series of generation lines. Each wave data point consists of the significant wave height ( $H_{m0}$ ), the peak wave period ( $T_p$ ) and the mean wave direction (MWD) and it is given every six hours, giving 29219 number of time steps.

The layout for the SW model used in [15] is shown in figure 6.1 and the layout used in this report is shown in figure 6.2. The bathymetric layout has been slightly altered here to reduce the run time. This removed the possibility to compare the results between the MIKE21 SW & BW models, but it was decided to prioritise PC run time.

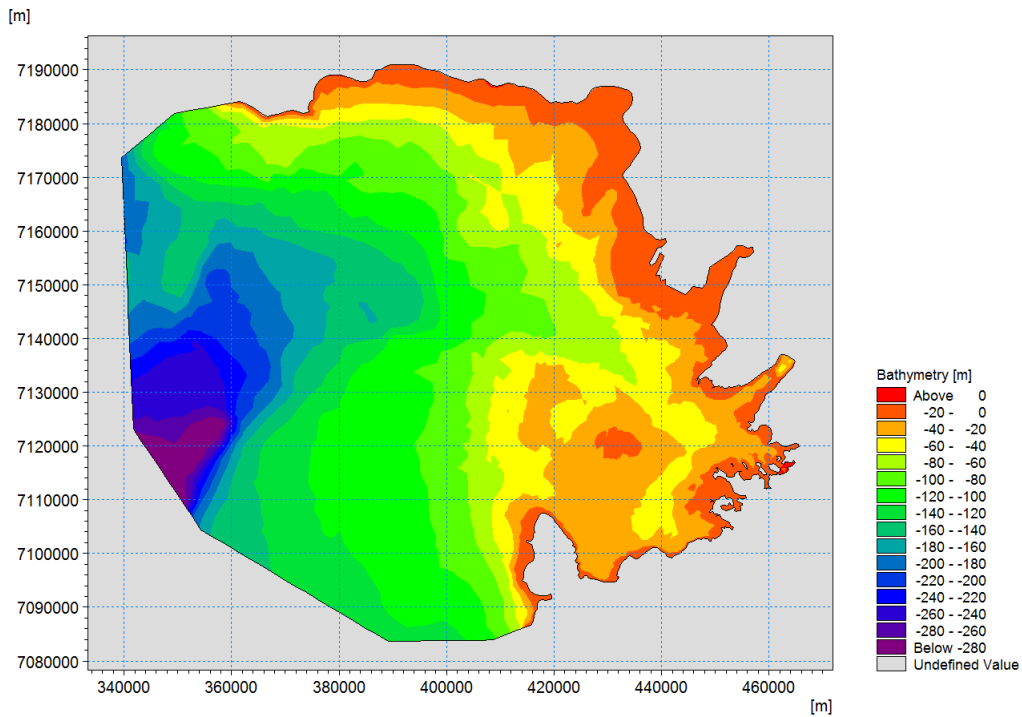


Figure 6.1: Initial Modelled Area in MIKE21 SW

In figure 6.2 the red dot which is located in the black square is used as the basis for the 20 year (1995-2015) wave statistics which have been extracted and used for the rest of this project, referred hereafter as B7. The location within the blue box is the region around the modelled MIKE21 BW area.

When running the model wave breaking and a current variation were not included, the effects of the wind were included. A fully spectral formulation was applied with a JONSWAP fetch growth expression. The maximum fetch was 100km and the shape parameters and peakness parameter were set at the standard values of 0.07, 0.09 and 3.3. A more detailed

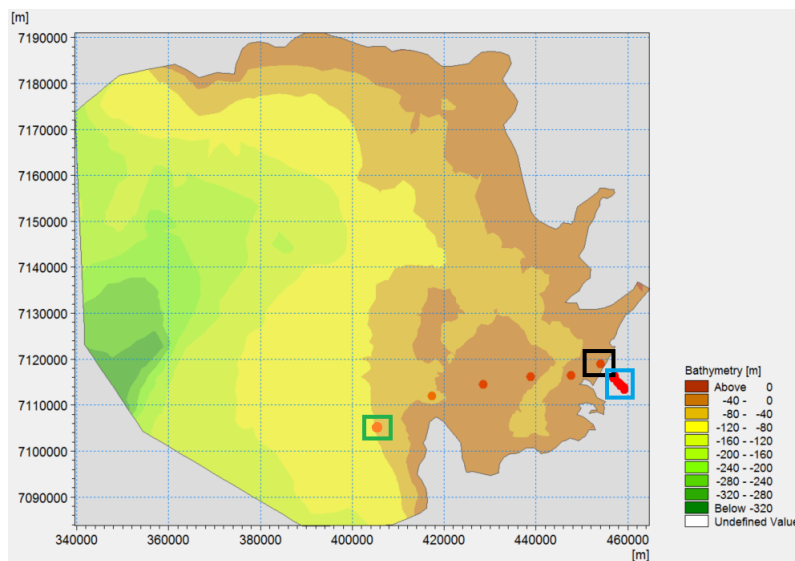


Figure 6.2: Modelled Area in MIKE21 SW

explanation of the JONSWAP spectrum and its components will be discussed later on.

## 6.2 Model Output

By creating a set of time series it is possible to see when the Port of Reykjavik has experienced any storm conditions and when one would expect unfavourable wave scenarios to occur. This has given the author an impression of when one would expect the wave height at Hafnarbakki utan Klepps to be above 0.5m, [35], and the vessel to have exceeded its motion criteria which is set out in [28]. The x-axis for the three time series presented below is the time period of 1995-2015 while the y-axis represents the value being viewed. For the sig. wave height it is in metres, for the peak wave period it is in seconds, and for the mean wave direction it is in degrees.

A similar time series has been created for the expected wave height at Hafnarbakki utan Klepps and the resultant vessel motion. This can be useful to compare the offshore data with that which is obtained after running the MIKE21 BW and MIKE DVRS models.

Also, from this output data a wave rose (figure 6.6) has been made to visualise from which direction is most frequent and which may be most critical with regards to the proposed layout. In this wave rose it has been decided that any incoming wave heights below 0.5m will be considered to be a "calm" situation as they are not expected to have a great influence on neither the wave height at the berth nor the vessel motions.

From the wave rose it is clear to see that the majority of the incoming waves are from around  $260^\circ$  to  $290^\circ$ .

A series of pivot tables have been created to show the wave statistics and by seeing how the wave field is statistically distributed a series of modelled scenarios have been decided to be run in the MIKE21 BW simulation.

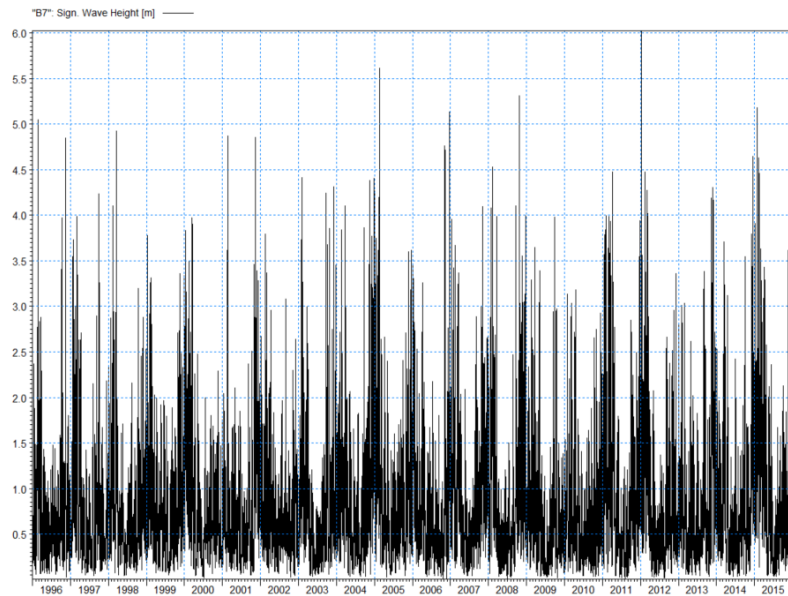


Figure 6.3: Time Series for the Sig. Wave Height at B7 from 1995 to 2015

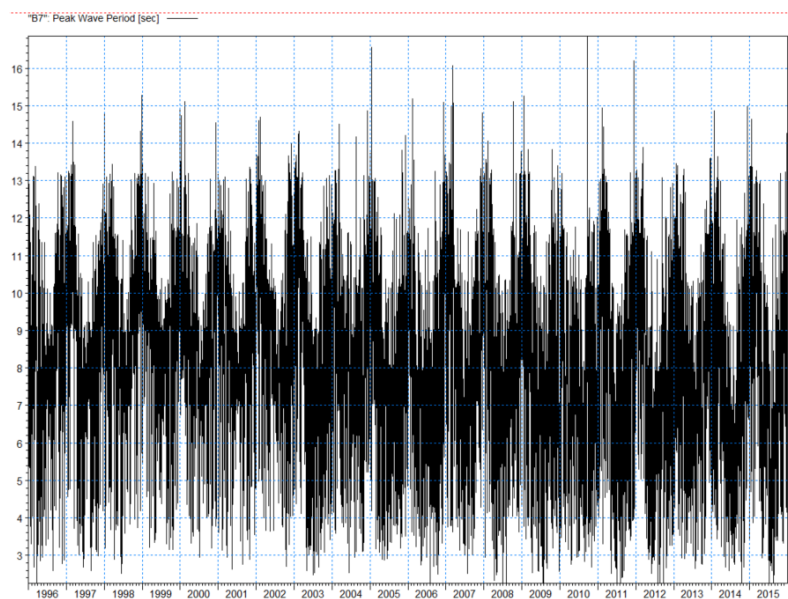


Figure 6.4: Time Series for the Peak Wave Period at B7 from 1995 to 2015

When the proposed port expansion is to be underway it may be worth considering what the return periods for the different waves may be. For the superstructure the designer would like to know what wave can be expected for a series of different return periods, such as 50 year or 100 year events. However, with regards to the motions of a berthed vessel it may be more prudent to consider an event which may occur once a year. Thus an Extreme Value Analysis has been performed by using the offshore statistics provided at location B7 from the MIKE21 SW model.

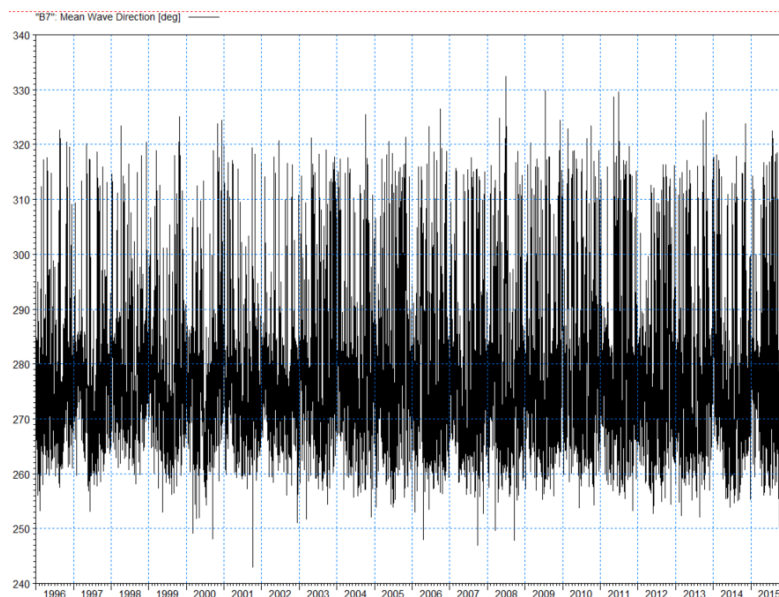


Figure 6.5: Time Series for the Mean Wave Direction at B7 from 1995 to 2015

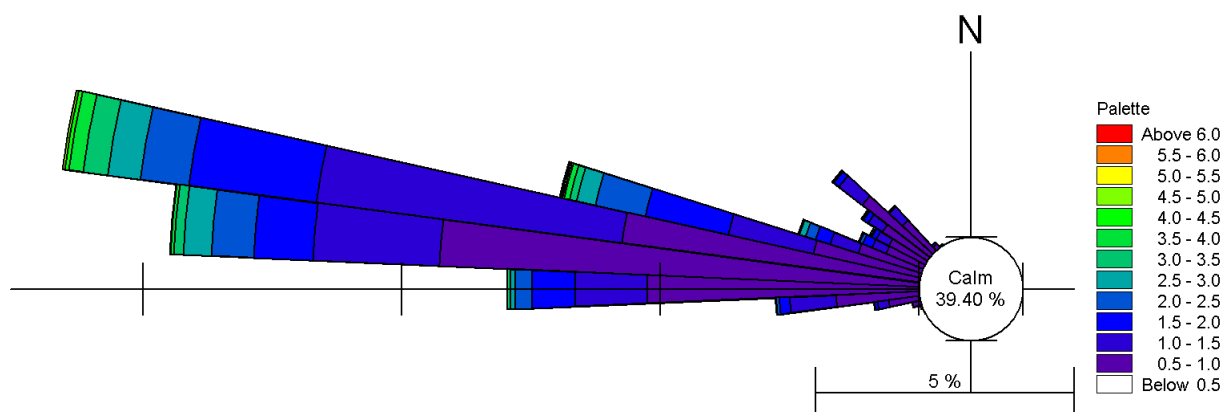


Figure 6.6: Offshore Wave Rose for the Data from 1995 to 2015

The Extreme Value Analysis has been done using the MIKE Zero tool EVA Editor. The chosen method was using a Gumbel Distribution. The estimation method for each Gumbel Distribution was the Method of Moments, Maximum Likelihood and Method of L-Moments.

From figure 6.7 it was deduced that the Port of Reykjavik can expect to encounter a 4m wave once a year. By combining this with the results shown in table 6.1 it was deduced that a 4m will be modelled for  $280^\circ$ ,  $290^\circ$  and  $300^\circ$ . It is worth noting that an Extreme Value Analysis for the peak wave period has not been undertaken. It was not deemed to be necessary after the wave height for a one year return period was found and by viewing table 6.1 the corresponding wave periods were chosen along with the mean wave direction.



Table 6.1: Twenty Year Wave Model Statistics for  $H_{m0}$ ,  $T_p$  & MWD

Hm0 (m)	Tp (s)															Total
	2.0- 3.0	3.0- 4.0	4.0- 5.0	5.0- 6.0	6.0- 7.0	7.0- 8.0	8.0- 9.0	9.0- 10.0	10.0- 11.0	11.0- 12.0	12.0- 13.0	13.0- 14.0	14.0- 15.0	15.0- 16.0	16.0- 17.0	
0.00 - 0.50	0.650	2.012	3.748	2.115	4.603	7.673	6.390	5.948	4.477	1.632	0.116	0.027	0.003	-	-	39.396
0.50 - 1.00	0.007	0.623	1.513	3.292	5.017	5.695	4.446	3.857	3.946	2.218	0.513	0.253	0.031	-	-	31.411
1.00 - 1.50	-	-	0.404	0.760	1.239	2.594	2.379	2.334	2.776	1.793	0.424	0.305	0.027	0.003	0.007	15.045
1.50 - 2.00	-	-	0.010	0.236	0.349	0.661	0.989	1.266	1.728	1.324	0.318	0.308	0.058	0.007	-	7.256
2.00 - 2.50	-	-	-	0.034	0.082	0.226	0.315	0.582	0.886	0.801	0.195	0.250	0.048	0.024	0.007	3.450
2.50 - 3.00	-	-	-	-	0.017	0.075	0.157	0.257	0.476	0.483	0.178	0.161	0.031	0.010	-	1.845
3.00 - 3.50	-	-	-	-	0.003	0.021	0.055	0.103	0.253	0.277	0.086	0.086	0.021	0.007	0.003	0.914
3.50 - 4.00	-	-	-	-	-	0.007	0.003	0.021	0.099	0.151	0.072	0.068	0.014	0.007	-	0.441
4.00 - 4.50	-	-	-	-	-	-	-	0.007	0.027	0.051	0.027	0.034	-	-	-	0.147
4.50 - 5.00	-	-	-	-	-	-	-	-	0.007	0.014	0.027	0.014	-	-	-	0.062
5.00 - 5.50	-	-	-	-	-	-	-	-	0.003	-	0.007	0.003	0.014	-	-	0.027
5.50 - 6.00	-	-	-	-	-	-	-	-	-	-	-	0.003	-	-	-	0.003
6.00 - 6.50	-	-	-	-	-	-	-	-	-	-	-	0.003	-	-	-	0.003
Total	0.657	2.635	5.674	6.438	11.311	16.951	14.734	14.378	14.675	8.751	1.961	1.526	0.233	0.058	0.017	100

Hm0 (m)	Direction (degrees)											Total
	240 - 250	250 - 260	260 - 270	270 - 280	280 - 290	290 - 300	300 - 310	310 - 320	320 - 330	330 - 340		
0.00 - 0.50	0.003	1.513	15.925	12.978	3.214	3.361	1.684	0.637	0.075	0.003	-	39.394
0.50 - 1.00	0.021	0.400	3.967	16.213	5.041	1.732	2.279	1.704	0.055	-	-	31.412
1.00 - 1.50	-	0.116	1.643	6.068	5.120	0.678	0.702	0.715	0.003	-	-	15.046
1.50 - 2.00	-	0.027	0.592	2.303	3.631	0.400	0.212	0.089	-	-	-	7.256
2.00 - 2.50	-	-	0.161	1.437	1.657	0.127	0.051	0.017	-	-	-	3.450
2.50 - 3.00	-	-	0.041	0.989	0.722	0.062	0.027	0.003	-	-	-	1.845
3.00 - 3.50	-	-	0.010	0.551	0.335	0.017	-	-	-	-	-	0.914
3.50 - 4.00	-	-	-	0.175	0.253	0.014	-	-	-	-	-	0.442
4.00 - 4.50	-	-	0.003	0.034	0.110	-	-	-	-	-	-	0.147
4.50 - 5.00	-	-	-	0.017	0.044	-	-	-	-	-	-	0.062
5.00 - 5.50	-	-	-	0.003	0.021	0.003	-	-	-	-	-	0.027
5.50 - 6.00	-	-	-	-	0.003	-	-	-	-	-	-	0.003
6.00 - 6.50	-	-	-	-	0.003	-	-	-	-	-	-	0.003
Total	0.024	2.057	22.342	40.769	20.155	6.393	4.956	3.166	0.133	0.003	-	100

Tp (s)	Direction (degrees)										Total	
	240 - 250	250 - 260	260 - 270	270 - 280	280 - 290	290 - 300	300 - 310	310 - 320	320 - 330	330 - 340		
2.0- 3.0	-	0.038	0.113	0.055	0.055	0.147	0.072	0.116	0.055	0.003	-	0.654
3.0- 4.0	0.014	0.120	0.602	0.226	0.205	0.572	0.356	0.472	0.068	-	-	2.635
4.0- 5.0	0.007	0.147	1.294	0.311	0.435	1.126	1.253	1.095	0.007	-	-	5.675
5.0- 6.0	-	0.284	1.318	0.626	0.746	0.979	1.311	1.171	0.003	-	-	6.438
6.0- 7.0	0.003	1.051	3.669	2.639	1.366	1.160	1.164	0.260	-	-	-	11.312
7.0- 8.0	-	0.308	7.133	5.863	1.978	1.116	0.534	0.021	-	-	-	16.952
8.0- 9.0	-	0.082	4.395	7.598	1.831	0.671	0.151	0.007	-	-	-	14.734
9.0- 10.0	-	0.027	2.598	9.525	1.872	0.311	0.034	0.010	-	-	-	14.378
10.0- 11.0	-	-	1.027	9.939	3.470	0.171	0.055	0.014	-	-	-	14.676
11.0- 12.0	-	-	0.185	3.214	5.216	0.116	0.021	-	-	-	-	8.751
12.0- 13.0	-	-	0.010	0.572	1.359	0.017	0.003	-	-	-	-	1.961
13.0- 14.0	-	-	-	0.181	1.335	0.007	0.003	-	-	-	-	1.526
14.0- 15.0	-	-	-	0.021	0.212	-	-	-	-	-	-	0.233
15.0- 16.0	-	-	-	-	0.058	-	-	-	-	-	-	0.058
16.0- 17.0	-	-	-	-	0.017	-	-	-	-	-	-	0.017
Total	0.024	2.057	22.342	40.769	20.155	6.393	4.956	3.166	0.133	0.003	-	100

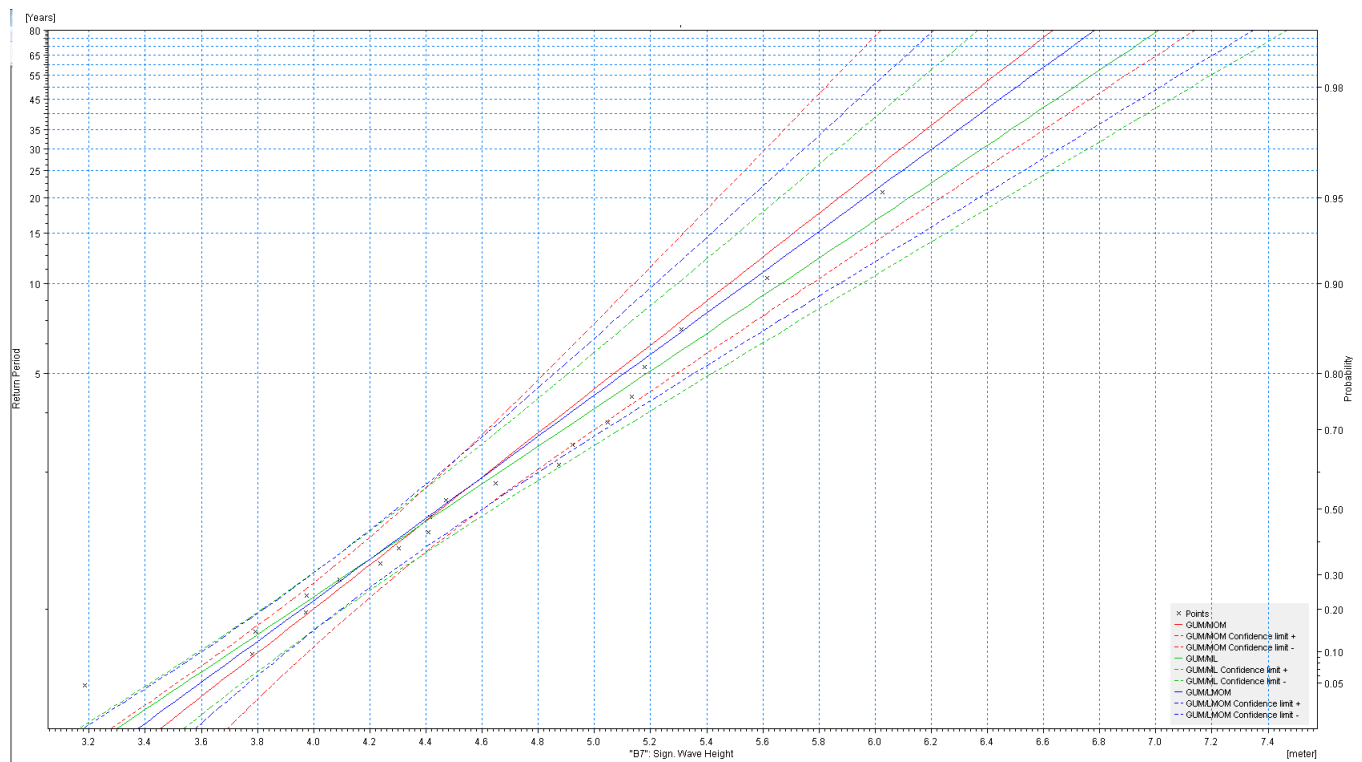


Figure 6.7: Extreme Value Analysis from the Offshore Wave Data

## 7 MIKE 21 Boussinesq Wave Model

Before creating the input files for the MIKE21 BW model, the MIKE 21 BW Setup Planner was used to determine what the maximum spatial resolution ( $dx$ ), the minimum wave period ( $T_{min}$ ) and maximum time step ( $dt$ ) should be. By stating that the maximum water depth and minimum water depth will be 35 metres and 5 metres the setup planner suggested the values were  $dx=6.20$ ,  $T_{min}= 6.7s$  and  $dt=0.191s$ . These were determined using the enhanced boussinesq equations which were described in the Model Background Section. Knowing these values the spacial resolution used for this model was 5m, the author was also advised to make sure the spacial resolution would be less than the expected wave length. This is to guarantee that a wave is not "lost" in the spacial resolution. The author was advised that 5m would be a sufficiently small spacial resolution for the waves which will be generated in this study. In total the modelled area is 2440 points wide and 1645 long, which is 12.2 x 8.225 km.

The grid has been rotated 47 degrees. This is to make sure the berth at Hafnarbakki utan Klepps is horizontal, with regards to the model layout (figure 7.1). It was suggested to do so as the horizontal surface would reduce the possibility of numerical instabilities due to the step like shape of the grid points. A comparison between the proposed Hafnarbakki utan Klepps and the current Kleppsbakki shows how the grid points do not make a smooth surface.

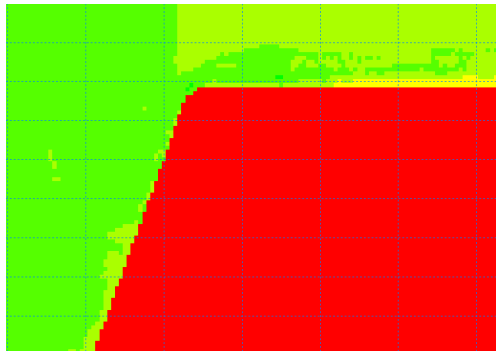


Figure 7.1: Hafnarbakki utan Klepps vs Kleppsbakki Grid Points

### 7.1 Bathymetrical Layout, Sponge Layer Map & Porosity Layer Map

The Port Authorities of Reykjavik have provided a digitalised copy of the bathymetry for the area which will be used for the MIKE21 BW models. This bathymetry is in correspondence to the Chart Datum of 2.2 metres. The data was in relation to UTM-27 and the grid point 0,0 corresponds to 448824 East, 7117184 North or the geographical coordinates 22° 3' 11" W & 64° 10' 38" N.

As one can see from figure 7.2 the total model area is substantially large. To model the waves over a long enough period which would satisfy the requirements for the DVRS programs would take too much time. Therefore after having run a couple of simulations with the larger modelled area it was decided to reduce the model area to save time, as can

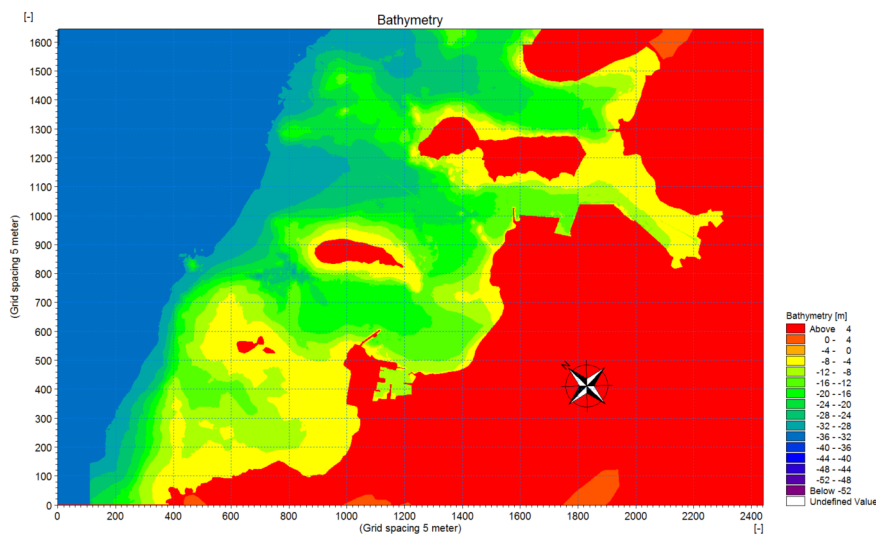


Figure 7.2: MIKE21 BW Model Bathymetry

be seen in figure 7.3.

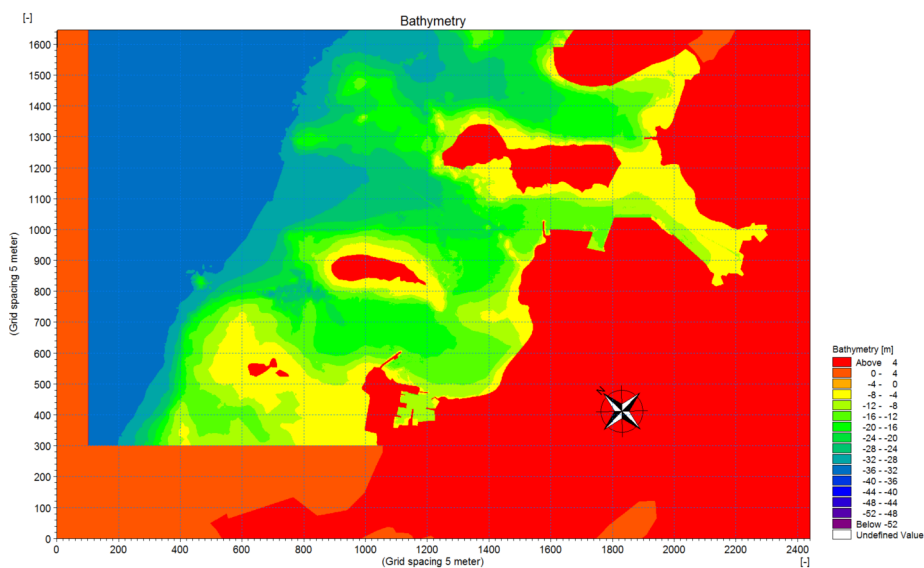


Figure 7.3: Smaller MIKE21 BW Model Bathymetry

The main difference one can see is the exclusion of a rather substantial area in the southern region. This was removed as the initial wave runs showed that the waves which entered the southern area had no effect on the waves in the vicinity of Hafnarbakki utan Klepps. A 3D bathymetry has been created by using the program MIKE Animator.

From the bathymetrical figures it is possible to estimate how shoaling, refraction and diffraction will affect the waves when moving deeper to shallower water. These effects will not be discussed in further detail but they can be seen when observing the figures in Appendix B2 and B3.

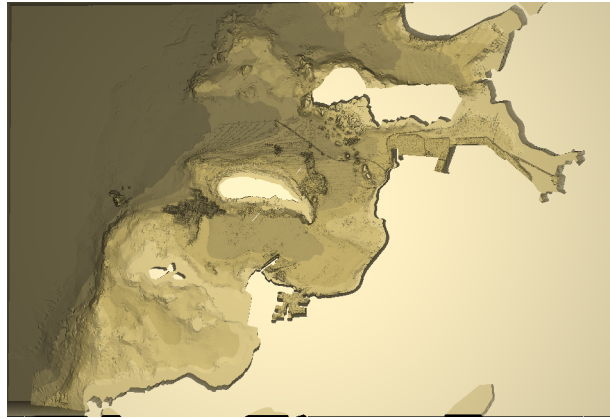


Figure 7.4: 3D Overview of the Bathymetry for the Modelled Area

When the waves are generated they propagate in both directions from their respective generation line. To avoid model blow-up a sponge layer is created along the model boundaries which are not land values. It is important that this sponge layer is wide enough to absorb all the wave energy so none is reflected back into the model. The sponge layer map has been created using the MIKE Zero Toolbox function. For this set-up a sponge layer map of 100 layers was created with the base value 10 and power value 0.92. These values were presented as recommended sponge layer values in the MIKE Zero Toolbox Guide. As mentioned the sponge layer was generated along the non-land values in the model edges. Here is a screen shot of the sponge layer, note that it is corresponding to the bathymetry from figure 7.3.

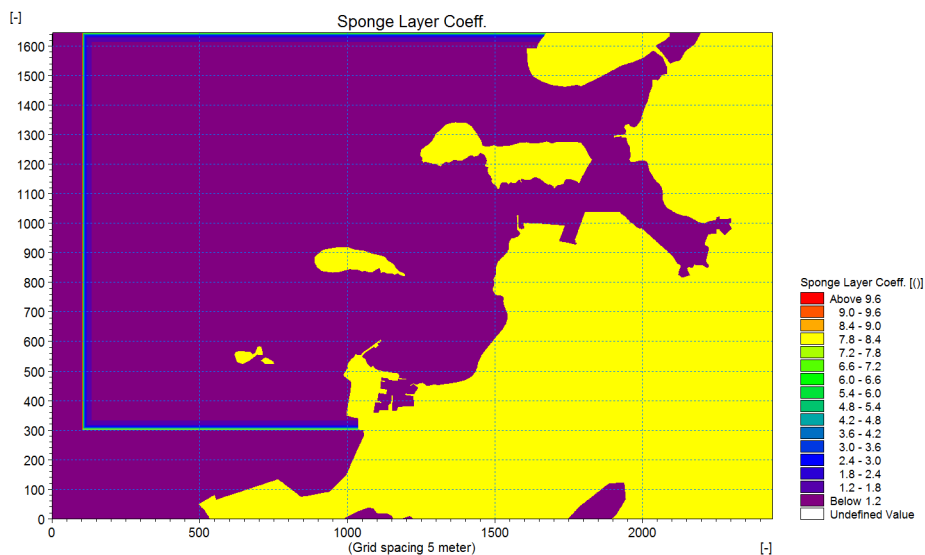


Figure 7.5: Applied Sponge Layer Map in the Model Area

After the sponge layer map has been created a porosity layer map has been created to demonstrate the reflectiveness of the various physical structures (natural or man made)

which are present. As for the sponge layer map, the porosity layer map was created using the MIKE Zero Toolbox.

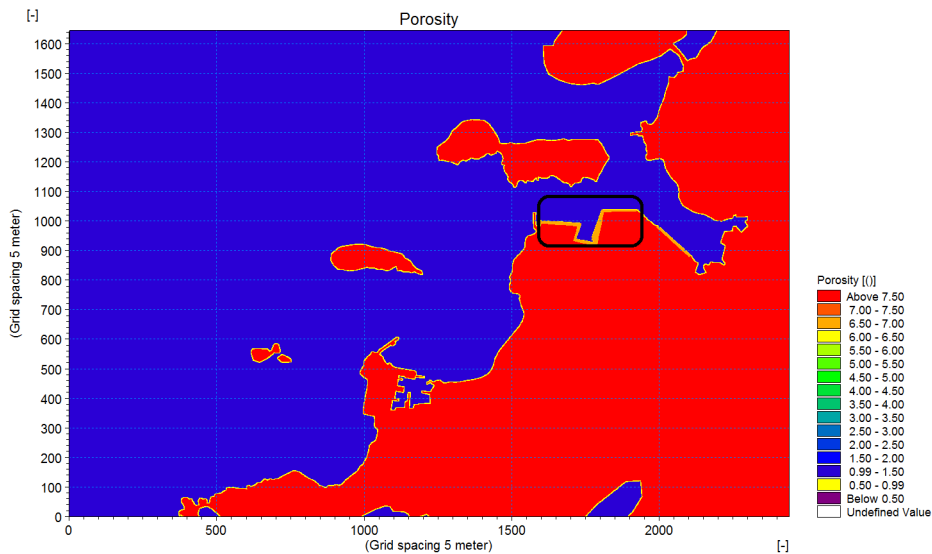


Figure 7.6: Applied Porosity Layer Map in the Model Area

The region in figure 7.6 which is encircled in the black box is the berth area of Hafnarbakki utan Klepps. Because it is a vertical berth which consists of interlocking sheet piles the porosity value has been set to a single layer with a value of 0.99. This represents almost perfect reflective properties which will influence the waves in the area. For the other areas a porosity which was three layers thick with a value of 0.85 was used. This may not be ideal as it does not fully represent the true reflective nature of the surrounding environment. But this was done as the majority of the land area in the model will not have any significant influence on the waves in the desired berth location.

## 7.2 Wave Field Generation

After the sponge and porosity maps have been created the wave generation line was made. This generation line is the location in which the waves that will propagate towards Hafnarbakki utan Klepps will be created. Once again, this was created using the MIKE Zero Toolbox Random Wave Generation. The wave generation line is located just in front of the sponge layer and the edges of it are located just inside. The start and end point were located inside the sponge layer because there were instances of model blow-ups due to numerical instabilities. By doing so this removed the problem. In the model the generation lines start and end grid points are 203,1574 & 203, 371.

In this project the Joint North Sea Wave Project (JONSWAP) frequency spectrum which was used to create the wave climate. It was also possible to select the Pierson-Moskowitz spectrum or various other spectrum types. Although fetch during the JONSWAP is somewhat limited there is no development towards a fully developed sea state. Various studies have shown that JONSWAP is ideal for the fetches related to engineering design purposes,

and that "the JONSWAP spectrum has been shown to be rather universal, not only for idealised fetch-limited conditions, but also for arbitrary wind conditions in deep water." [14].

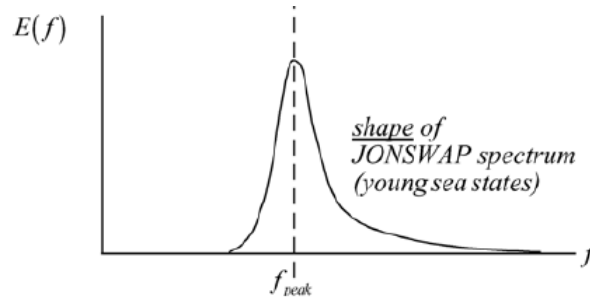


Figure 7.7: Arbitrary JONSWAP Spectrum, [14]

In this report the wave spectrum will be defined by the significant wave height, peak period and the shape parameters. The shape parameters used for the JONSWAP spectrum are taken to be  $\gamma = 3.3$ ,  $\sigma_a = 0.07$  and  $\sigma_b = 0.09$ . These values are taken to be the averages of the scatter from different shape parameters, [14]. The directional distribution was  $\cos^8$ .

The time step interval which used for this project was 0.04s with 135001 steps. This will create a wave field which lasts 90 minutes, and the number of time steps was chosen as it would satisfy the minimum requirements for the DVRS model after the wave field has reach Hafnarbakki utan Klepps.

The significant wave height ( $H_{m0}$ ), peak wave period ( $T_p$ ) and main wave direction are changed for each generated wave field. The wave scenarios which have been modelled are shown in table 7.1.

### 7.3 MIKE 21 BW Model Setup

In the MIKE 21 BW model a 2D Boussinesq Wave Module is selected with a Time Step Interval of 0.04s and 135001 time steps (corresponding to the generated wave field). Bottom friction, Eddy Viscosity, Filtering, Wave Breaking and a Moving Shoreline have all been excluded. The Surface Elevation is a constant value and there is no Boundary Data.

The output file which is required to run the DVRS model is the location of Hafnarbakki utan Klepps. This is taken to be gridpoints 1809,1038 to 1925,1054, with the output files to be measured from time step 0 to 135000 every 13 time step intervals. For the DVRS model to run the output file must be atleast 4096 seconds after warm-up, a time step of 0.5 seconds and the Water Level, P-flux & Q-flux across the modelled berth area.

Along with this, the surface elevation has been extracted over the entire model area every 200 time step intervals. The same has been done for the significant wave height. In Appendix B the surface elevation and significant wave height varies from from each simulation can be found.

## 7.4 MIKE 21 BW Model Results

The scenarios which have been run are shown in table 7.1. These wave scenarios have been chosen by a combination of looking at the results given by MIKE21 SW, and [16] states that the important wave directions along with their sig. wave height and wave periods are to be considered.

For each of these wave simulations the wave agitation coefficient (W.A.C.) has been found and data has been extracted which will be used for the DVRS model (this will be described in detail further on in the report). The W.A.C. is the ratio between the mean wave height at the modelled berth area (grid points 1809,1039 to 1848,1044) and the mean wave height offshore near the generation line.

Table 7.1: Modelled Wave Scenarios

Mean Wave Direction (degrees)	Sig. Wave Height (m)	Peak Wave Period (s)
270	1, 2, 3	10, 12, 15
280	1, 2, 3, 4	10, 12, 15
280	3	13
285	1	17
290	1, 2, 3, 4	8, 10, 12, 15
292.5	1, 2, 3	10, 15
300	1, 2, 3, 4	8, 10 12
305	1, 2 ,3	8, 10
315	1, 2, 3	8, 10

The W.A.C. for the simulations presented in table 7.1 are presented in table 7.2.

The wave agitation coefficients can be plotted to see the general tendency for the coefficients. Below the figures show how the W.A.C. changes for each significant wave height and their respective periods. The W.A.C. for each MWD can be found in Appendix B.

By analysing the W.A.C. figures it can be seen that the W.A.C. increases with the MWD. This is to be expected as waves with a MWD of approximately 315 degrees can travel unimpeded into Hafnarbakki utan Klepps.

With the W.A.C. tendency a MATLAB code for linear interpolation was done to obtain the wave statistics at the berth throughout the 20 year time period of available data, see Appendix ?? for the code. A time series and exceedance plot has been created to highlight when the wave height is expected to be above 0.5m and for how long.

From the time series plot it can be seen that it is primarily during the winter period in when the wave height at the modelled berth exceeds the criteria of 0.5m. The criteria which dictates that the wave height at a berth for a container vessel must not exceed 0.5m during the (un)loading operation is presented in [35] & [18].



Table 7.2: Mean Wave Aggitation Coefficient at Haffnarbakki utan Klepps

Hs	Tp	Deg	WAC
1	10	270	0.091
2	10	270	0.079
3	10	270	0.075
1	12	270	0.096
2	12	270	0.080
3	12	270	0.077
1	15	270	0.098
2	15	270	0.079
3	15	270	0.097

Hs	Tp	Deg	WAC
1	10	280	0.110
2	10	280	0.096
3	10	280	0.092
4	10	280	0.094
1	12	280	0.113
2	12	280	0.094
3	12	280	0.089
4	12	280	0.094
3	13	280	0.097
1	15	280	0.109
2	15	280	0.095
3	15	280	0.117
4	15	280	0.121

Hs	Tp	Deg	WAC
1	8	290	0.139
2	8	290	0.126
3	8	290	0.125
4	8	290	0.122
1	10	290	0.154
2	10	290	0.144
3	10	290	0.137
4	10	290	0.138
1	12	290	0.139
2	12	290	0.125
3	12	290	0.123
4	12	290	0.130
1	15	290	0.129
2	15	290	0.124
3	15	290	0.146
4	15	290	0.150

Hs	Tp	Deg	WAC
1	8	300	0.198
2	8	300	0.187
3	8	300	0.181
4	8	300	0.182
1	10	300	0.204
2	10	300	0.190
3	10	300	0.184
4	10	300	0.184
1	12	300	0.180
2	12	300	0.166
3	12	300	0.168
4	12	300	0.174

Hs	Tp	Deg	WAC
1	10	292.5	0.167
2	10	292.5	0.153
3	10	292.5	0.144
1	15	292.5	0.138
2	15	292.5	0.130
3	15	292.5	0.153

Hs	Tp	Deg	WAC
1	8	305	0.215
2	8	305	0.203
3	8	305	0.196
1	10	305	0.221
2	10	305	0.207
3	10	305	0.200

Hs	Tp	Deg	WAC
1	8	315	0.258
2	8	315	0.241
3	8	315	0.235
1	10	315	0.278
2	10	315	0.237
3	10	315	0.232

The exceedance plot for the data points show that the wave height is above the proposed criteria 0.154% of the time, which is roughly 13.5 hours per year. This exceedance will be used as a basis of comparison for the vessel motion. Having the various exceedance plots and time series will allow the author to conclude which of the criteria, the wave height at the berth or the vessel motion, are more significant for this study, see figures 7.12 and 7.13.

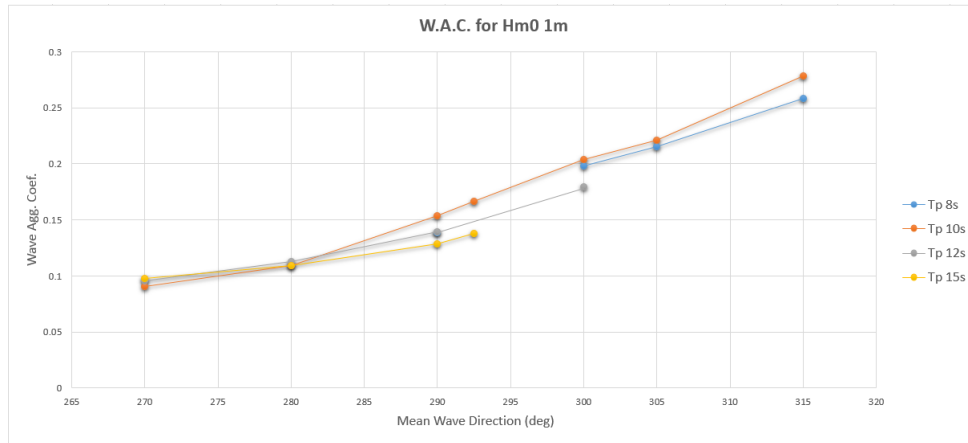


Figure 7.8: W.A.C. for  $H_{m0}$  1m

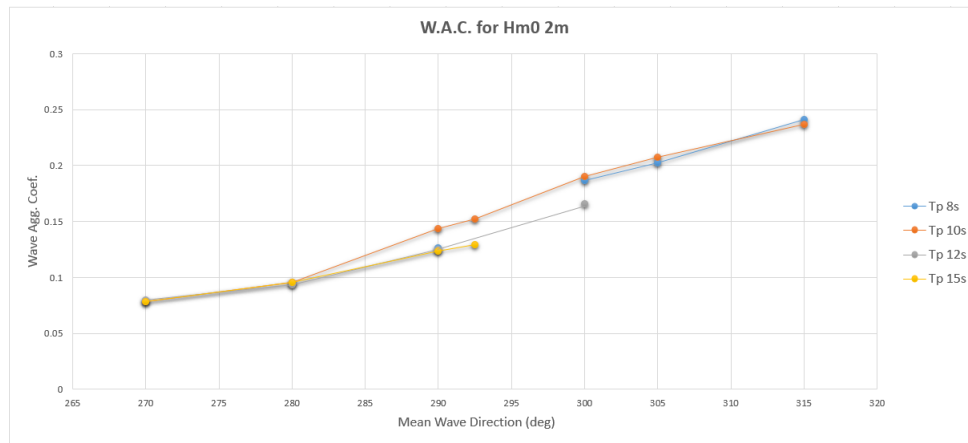


Figure 7.9: W.A.C. for  $H_{m0}$  2m

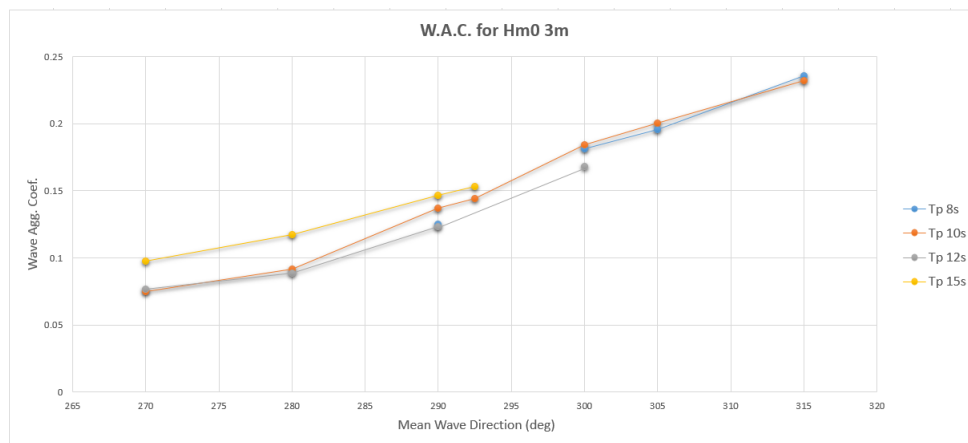


Figure 7.10: W.A.C. for  $H_{m0}$  3m

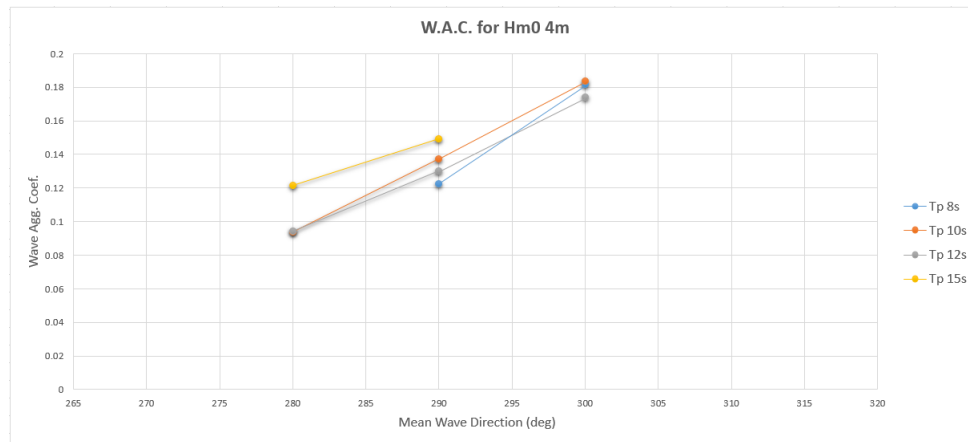
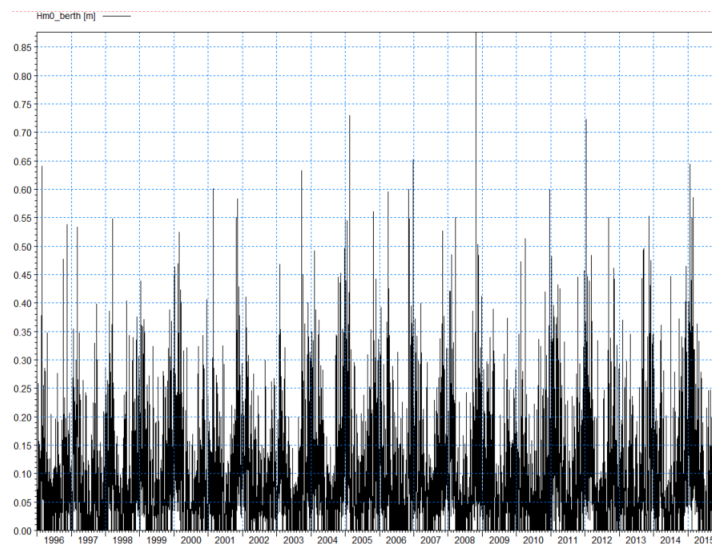
Figure 7.11: W.A.C. for  $H_{m0}$  4m

Figure 7.12: Time Series for the Wave Height at Hafnarbakki utan Klepps from 1995-2015

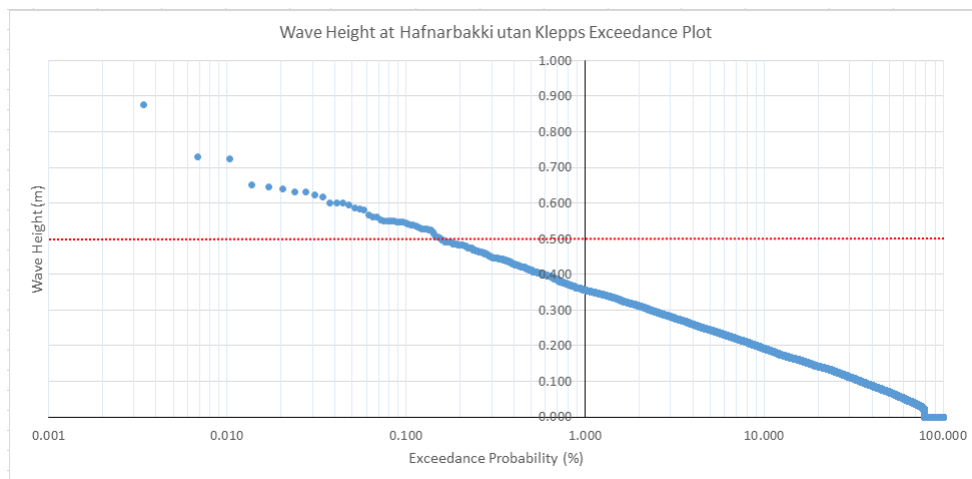


Figure 7.13: Exceedance Plot for the Wave Height at Hafnarbakki utan Klepps

## 8 MIKE Dynamic Vessel Response Model

### 8.1 DVRS Model Input

The vessel which will be used for this project is Eimskips M/V Godafoss. It's dimensions can be found in table 8.1.

Table 8.1: Eimskips Godafoss Vessel Dimension

DWT (tonnes)	GT (tonnes)	TEU	Loa (m)	Lpp (m)	B (m)	D (m)
17034	14664	1457	165.6	153	28.6	8.95
Rxx (m)	Ryy (m)	Rzz (m)	C.O.G. (m)	Deck Plane Height (m)	$\delta$ (m <sup>3</sup> )	
8.25	41.4	41.4	3.15	6	26909	

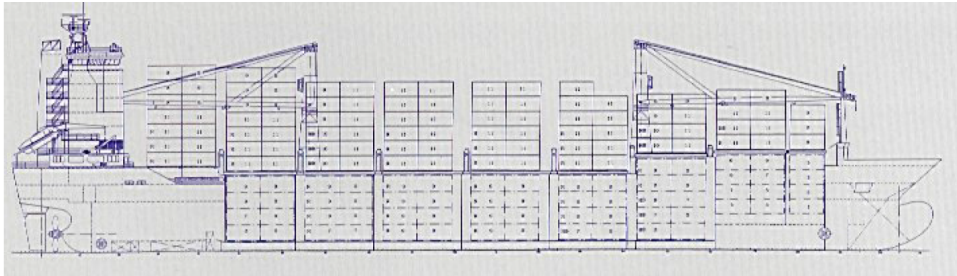


Figure 8.1: Eimskips M/V Godafoss

Unfortunately the author was not able to obtain a digitalised copy of the hull as this is sensitive material. Instead, DHI provided a digitalised hull for a container vessel and it was scaled to match that of Godafoss, see figure 8.2 for the digitalised ship hull symmetrical along the y-axis. The vessel scaling was 0.85 (x-direction), 1.003 (y-direction) and 0.88 (z-direction) and is made of 1201 panels.

After having run the MIKE21 BW model the output file which has been selected to be the berth location of Hafnarbakki utan Klepps will be used to model the vessel motions during the different wave conditions. The output MIKE21 BW files to be used in the DVRS model have been previously described.

When running these simulations the wave files which have been extracted from MIKE21 BW are used, however the addition of wind is possible, as this effect is not reflected in the wave files. After speaking to the Port Authorities in Reykjavik it was advised that they stop the (un)loading operations when the wind speed is around 15-17  $\frac{m}{s}$  and the most critical wind direction was at 250° (with respect to figure 5.3). With this in mind a series of simulations have been run to determine the vessel motion with different wind speeds and directions, as shown below.

It is worth noting that each of these simulations has been run for both the mooring line combinations of Polypropylene with Polyamide and Ultraline Dyneema with Polyamide.

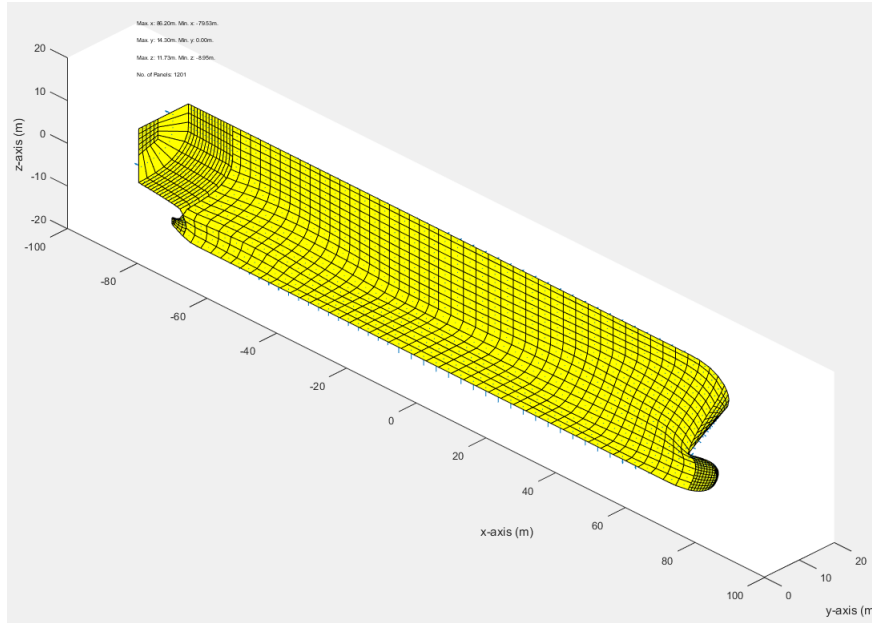


Figure 8.2: Digitalised Vessel Hull used in the DVRS Program

Table 8.2: DVRS Modelled Scenarios

Wind Speed $\frac{m}{s}$	Wind Direction (degrees)
0	-
10	0
15	0
15	250

A study has been done by [36] to suggest that it may not always be advisable to assume the wind velocity to be constant. The effects of gusts in the wind patterns and how they affect the container handling equipment are discussed in [36]. Here a gust is defined as the wind speed over a period of three seconds and a gust factor is determined by the "relation between the maximum wind speed and the measure time interval." An example is given where they discuss how the maximum gust wind for a Beaufort Scale 6 wind of  $13.8 \frac{m}{s}$  is actually  $13.8 \frac{m}{s} * 1.5$ ,  $20.7 \frac{m}{s}$ . Furthermore, another example explains how the Port of Rotterdam suspends operations when the gusts reach  $25 \frac{m}{s}$ , which is a mean wind speed of  $25 \frac{m}{s} / 1.5$ ,  $17 \frac{m}{s}$ . This coincides with the data provided by Reykjavik and the gust factor is not taken into consideration in this report.

## 8.2 Vessel Mooring and Fender Layout

Mooring systems are used to "tie" the vessel to the berth. This is done to assure that the vessel will not move while the (un)loading process is underway to reduce the downtime

and for safety measures. Thorensen (2010) states that the traditional the mooring system consists of:

- Breast mooring lines which are used to reduce the sway and yaw motions.
- Spring mooring lines that aim to reduce the surge motion, thus they shall be placed as parallel to the berth as possible with an angle equal to or less than  $10^\circ$ .
- Head and stern mooring lines may be used along with the breast and spring lines as an additional method to reduce the ship motions.

A layout of how these mooring lines are applied to an arbitrary vessel are shown in the figure 8.3, note the difference between bow (head) and stern (rear). This does not have an effect on the mooring line capabilities but rather to distinguish their location. The mooring lines are usually symmetrical to the centreline of a vessel to acquire an even load distribution. To minimize the motion of the vessel the mooring lines are to be kept taut and only slackened when (un)berthing.

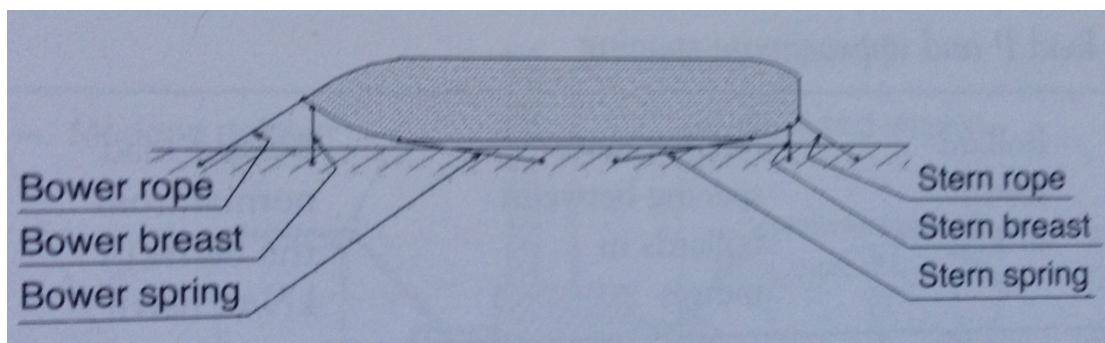


Figure 8.3: Names and locations of mooring lines in a typical layout, [35]

The captain of Godafoss has provided a sample of the mooring layout which is commonly used when they berth at Reykjavik, figures 8.4 and 8.5. This layout has been used as the basis for the DVRS mooring simulations. This sketch shows the location of the Fair Leads, and Winches on the vessel along with the Mooring Line length, and this sketch has been used as the basis for determining the locations of the aforementioned structures.

Along with the vessel mooring lines, the quay wall has a series of fenders which will absorb the vessel impact during berthing. Fenders are used to protect the ship's hull and the berthing structure from the created loads when a vessel is berthing. A quay wall without fenders would be inoperable as the vessels and structure would be too damaged and unsafe to use. At Hafnarbakki utan Klepps the Reykjavik Truck Tire (RTT) system in which 9 truck tires are stacked upon each other. They are then placed within the shutes of the sheet pile quay wall. Together with the RTT a V-cap fender TLT-BA600x2500 Type Rubber Fender is used.

The performance curve for the V-cap fender was provided by Iceland and the RTT fender performance curve is taken from the Fentek catalogue, [10].

The RTT-fenders are 1.1m wide however, since they are located 0.2m into the sheet pile shutes the maximum deflection is taken to be 0.9m. The V-cap fender is 0.6m wide and

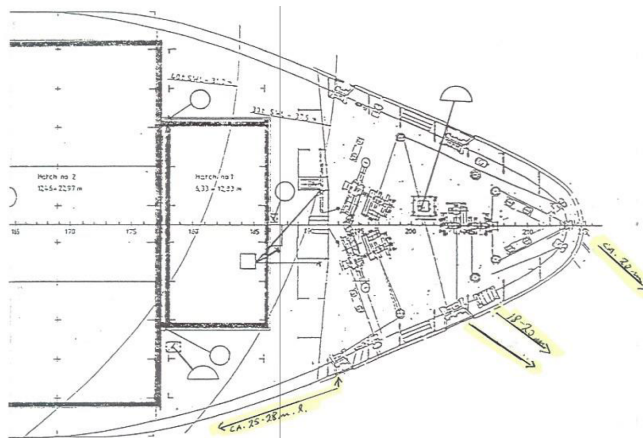


Figure 8.4: Fore Deck Area Mooring Line Layout provided by the Captain of Godafoss

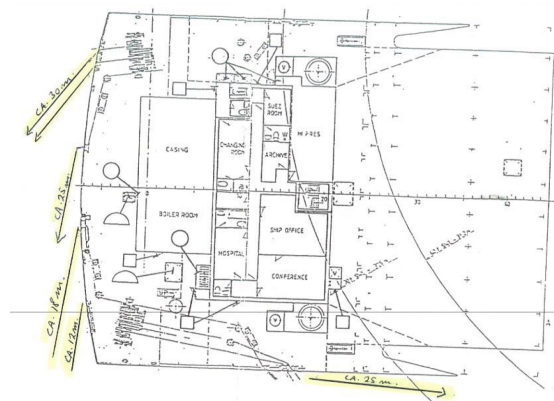


Figure 8.5: Aft Deck Area Mooring Line Layout provided by the Captain of Godafoss

Table 8.3: Fender Characteristics used in the DVRS Model

	Reaction force (kN)	Energy Absorption (kJ/m)	Max. Deflection (%)
RTT	286	70	100
V-cap fender	1500	325	52.5

has a maximum deflection of 0.315m.

Bollards are used to secure the mooring lines to the berth structure. They are located along the seaward edge of the berth and are typically spaced 5-30 metres apart so as to accommodate a variety of ship sizes, [35]. These bollards are also meant to withstand a certain load placed upon them by the mooring lines from the vessel. As storms are an occurrence which cannot be factored out then special storm bollards are to be installed which will be able to support twice the load of a regular bollard. It is also advisable to not have two vessels use the same bollard simultaneously. This is because one ship may be



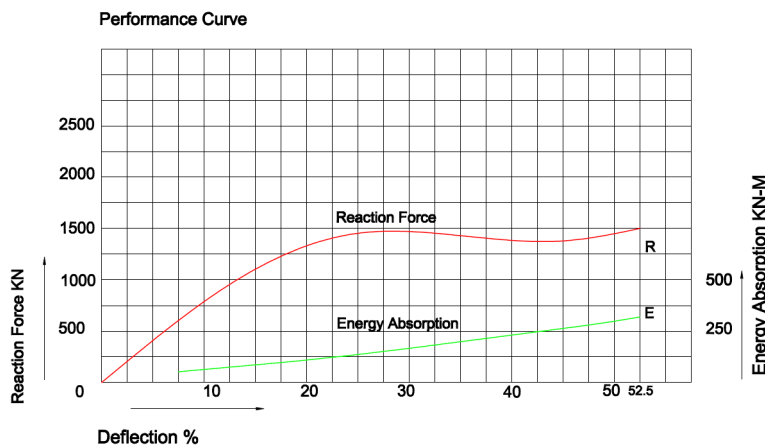


Figure 8.6: Performance curve for the V-cap Fender

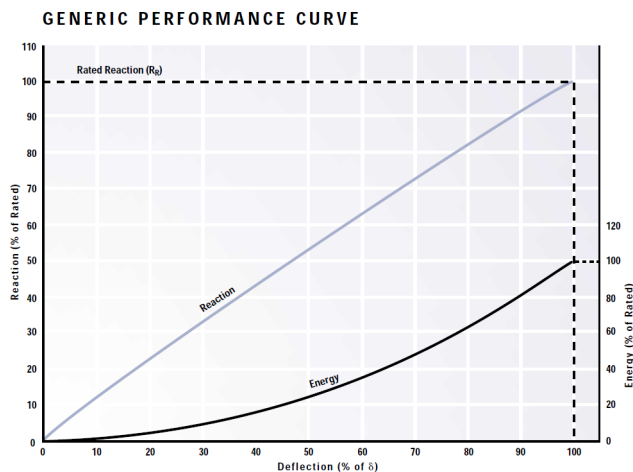


Figure 8.7: Performance curve for the RTT Fender

unwilling to slacken its mooring line, in unfavourable conditions, to allow the first vessel to unberth.

The location of the bollards, fenders, mooring lines, winches and fair leads have been placed in the DVRS program. It is worth noting that in the DVRS program the location of these objects are in relation to the centre point Godafoss. This (0,0) point is located at UTM-27 East 458867, North 7114049, and the Z-coordinates are with respect to the water surface. From this point forward any locations in the DVRS program will be with regards to this point.

The RTT-fenders continue along the quay wall at 2.2m intervals until X-coordinate 77.8 as they are located within the shutes of the sheet pile quay wall. The V-cap fenders continue along the quay wall at 4.3m intervals until X-coordinate 78.8. The combination of the bollard, fair lead, winch dictates how long the mooring line is. This combination can be see in table 8.5.

Table 8.4: Coordinate Location of the Bollards, Fenders, Fair Leads and Winches

	X (m)	Y (m)	Z (m)
Bollard 1	-101.3	-15.7	4.5
Bollard 3	-85.88	-15.7	4.5
Bollard 8	-38.35	-15.7	4.5
Bollard 14	34.44	-15.7	4.5
Bollard 19	84.95	-15.7	4.5
Bollard 20	96.98	-15.7	4.5
Fair Lead 1	82.8	0	6.5
Fair Lead 2	81.48	-1.76	6.5
Fair Lead 3	76.42	-5.94	6.5
Fair Lead 4	66.52	-10.12	6.5
Fair Lead 5	-65.42	-14.3	6.5
Fair Lead 6	-82.8	-8.8	6.5
Fair Lead 7	-82.8	-3.52	6.5
Fair Lead 8	-82.8	3.08	6.5
Fair Lead 9	-82.8	9.46	6.5
Fair Lead 10	-82.8	10.78	6.5
Winch 1	74	0	6.5
Winch 2	68.72	-1.32	6.5
Winch 3	68.72	1.32	6.5
Winch 4	-78.4	-10.34	6.5
Winch 5	-78.4	10.34	6.5
RTT-Fender	-80.6	-14.3	2
V-cap Fender	-78.5	-14.6	4

The mooring line and tail lengths are found via this combination and they can be seen in table 8.6.

For this study it was assumed that the mooring lines would either be a Polypropylene ISO 1346 8 strand with a diameter of 96 mm and a MBL of 1050 kN or Ultraline Dyneema 8 strand core with a diameter of 80 mm and an MBL of 4272 kN. The tail is Polyamide ISO 1140 8 strand with a diameter of mm and an MBL of 1078 kN. The line specifications are all provided by BEXCO. The MBL% vs Elongation % curve for each of the line types can be provided by [3], see figures 8.8, 8.9 and 8.10. From these figures the curve which indicates the line is 'used' has been applied. This was chosen as Godafoss will most likely

Table 8.5: Bollard, Fair Lead, Winch Combination used in the DVRS Model

Mooring Line No.	Bollard No.	Fair Lead No.	Winch No.
1	20	1	1
2	19	3	1
3	19	3	3
4	14	4	2
5	8	5	4
6	3	6	4
7	3	7	4
8	3	8	5
9	1	9	5
10	1	10	5

Table 8.6: Godafoss Mooring Line and Tail Length

Line Number	Mooring Line Length (m)	Tail Length (m)
1	16	5
2	8	5
3	8	5
4	27	5
5	22	5
6	2.5	5
7	7.5	5
8	14	5
9	26	5
10	27	5

have used mooring lines.

For the two different line type scenarios which have been run the Polyamide tail remains constant while the mooring line is changed between a Polypropylene & Ultraline Dyneema Line. As one of the tests will run with a synthetic line while the other uses a steel wire it may be worth noting the stiffness of the line system. This can give an indication as to how the lines will react to the external forces, by the maximum allowable motion of the vessel and the mooring line forces.

From tables 8.7 and 8.8 it is clear to see that the Ultraline Dyneema line is much more rigid

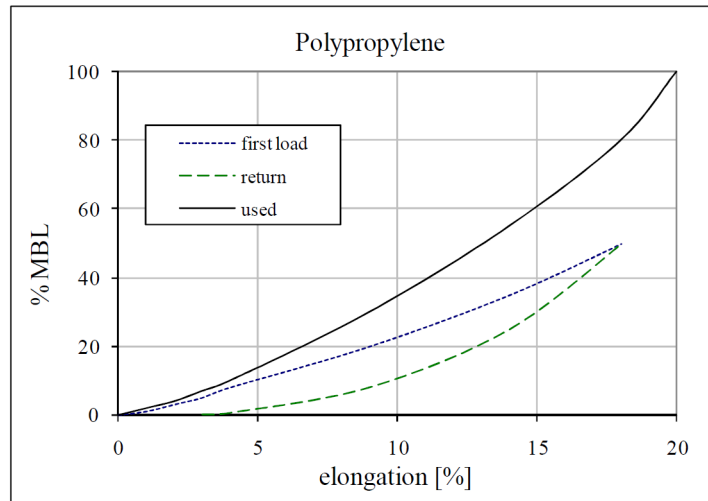


Figure 8.8: MBL % vs Elongation % curve for a typical Polypropylene Line, [3]

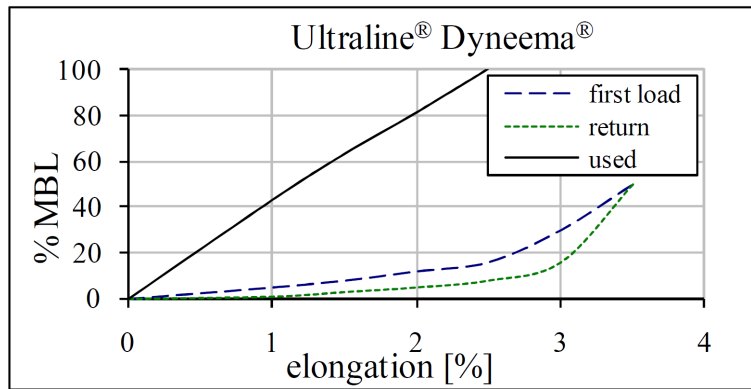


Figure 8.9: MBL % vs Elongation % curve for a typical Ultraline Dyneema Line, [3]

Table 8.7: Stiffness table for the Polypropylene Line and Polyamide Tail ( $\frac{kN}{m}$ )

Line	0% MBL	10% MBL	20% MBL	30% MBL	40% MBL	50% MBL	60% MBL	70% MBL	80% MBL	90% MBL	100% MBL
1	0	105.57	125.75	151.73	170.73	183.82	193.85	212.45	220.91	236.57	250.00
2	0	152.22	189.19	231.62	265.82	287.20	307.32	338.69	355.56	381.39	403.85
3	0	152.22	189.19	231.62	265.82	287.20	307.32	338.69	355.56	381.39	403.85
4	0	74.27	86.07	102.92	114.44	122.97	128.57	140.46	145.27	155.42	164.06
5	0	85.84	100.48	120.55	134.62	144.75	151.81	166.03	172.04	184.13	194.44
6	0	218.64	289.66	363.01	430.77	468.23	514.29	572.65	612.02	658.54	700.00
7	0	156.54	195.35	239.50	275.41	297.66	318.99	351.76	369.64	396.56	420.00
8	0	114.33	137.25	166.05	187.50	202.00	213.56	234.28	244.01	261.38	276.32
9	0	76.33	88.61	106.02	117.98	126.78	132.63	144.92	149.93	160.43	169.35
10	0	74.27	86.07	102.92	114.44	122.97	128.57	140.46	145.27	155.42	164.06

than the Polypropylene line as once the stiffness is in the region of 20-25% the Polyamide tail will have ruptured. For this reason the table was not continued past this point as the

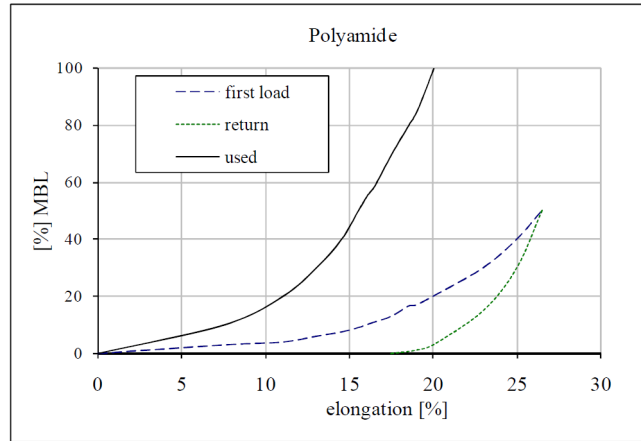


Figure 8.10: MBL % vs Elongation % curve for a typical Polyamide Line, [3]

Table 8.8: Stiffness table for the Ultraline Dyneema Line and Polyamide Tail ( $\frac{kN}{m}$ )

Line	0% MBL	5% MBL	10% MBL	15% MBL	20% MBL	25% MBL	30% MBL
1	0	380.91	563.75	719.77	854.83	1531.60	-
2	0	387.39	578.56	744.34	890.46	1648.39	-
3	0	387.39	578.56	744.34	890.46	1648.39	-
4	0	372.34	544.59	688.51	810.24	1395.64	-
5	0	376.18	553.14	702.37	829.92	1454.32	-
6	0	391.98	589.19	762.23	916.74	1739.59	-
7	0	387.80	579.51	745.93	892.79	1656.28	-
8	0	382.51	567.38	725.76	863.47	1559.22	-
9	0	373.10	546.28	691.24	814.10	1406.99	-
10	0	372.34	544.59	688.51	810.24	1395.64	-

author deemed it unnecessary to continue past this point.

The stiffness value was determined by taking the ratio of the MBL and the corresponding elongation of the line and tail at the MBL for the weaker part of the system. Since the Polypropylene and Polyamide are very similar it was decided that they act as one system with regards to the elongation % at the corresponding MBL.

### 8.3 Vessel Motion Criteria

As previously mentioned, a vessel has six degrees of freedom in which it can move due to the interaction of the waves, wind, and other forces, they are illustrated once more in figure 8.11.

When a vessel is at berth there are certain safety requirements which must be met in order to maintain a safe (un)loading operation. When a vessels motion is too large it is no longer safe to continue. Therefore a set of criteria have been established and if they are surpassed operations cease until the motion decreased to an acceptable level. The Permanent International Association of Navigation Congresses (PIANC) has set a series of guidelines as to how much these movements can be, as provided by [28]. There are different

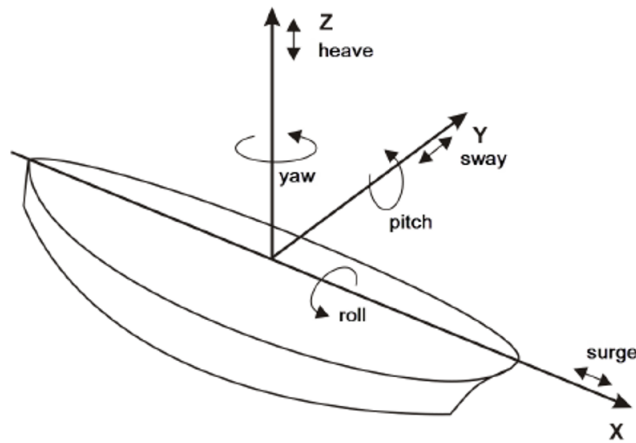


Figure 8.11: A vessels six degrees of freedom, [35]

motion criteria depending on which approach is used and they are presented in table 8.9.

Table 8.9: Maximum amplitudes of motions for container vessels at 100% (un)loading efficiency

Principal Motion	Jensen et al., 1990	Smitz, 1992	PIANC, 1995	D'Hondt, 1999	Moes, 2000
Surge (m)	0.50	0.50	0.50	0.24	0.30
Sway (m)	0.40	0.30	0.60	0.22	0.30
Heave (m)	0.45	0.30	0.40	0.20	0.30
Roll (deg)	1.50	1.00	1.50	0.24	0.50
Pitch (deg)	0.75	-	0.50	0.40	0.50
Yaw (deg)	0.25	-	0.50	0.10	0.50

It is worth noting that to maintain a 100% (un)loading efficiency there are a series of different criteria. This discrepancy is discussed in [23]. PIANC has further developed their vessel motion criteria. This was due to some misunderstandings on how to accurately measure the vessel motions, [16]. The new PIANC 2012 report was created to state the vessel motions are to be defined as a significant amplitude of motion. Here a set of maximum allowable significant motion of amplitudes criteria were set for an (un)loading efficiency of 95%. They can be seen in table 8.10 and will be used as the criteria for this report, please note that these values are those for container vessels.

Thorensen has created a figure which shows what vessel motions are more critical for different vessel types. In figure 8.12 container vessels are labelled as Lo/Lo (Load on/Load off) and show that the more critical motions are surge, sway, yaw and roll.

Along with the vessel motion criteria which have been set out by PIANC the OCIMF also has a set of guidelines as to how much force a mooring line can be subjected. The

Table 8.10: Maximum allowable significant motion amplitudes for an (un)loading efficiency of 95%

Principal Motion	Max. allowable significant motion amplitude
Surge (m)	0.20 to 0.40
Sway (m)	0.40
Heave (m)	0.30
Roll (deg)	1.00
Pitch (deg)	0.30
Yaw (deg)	0.30

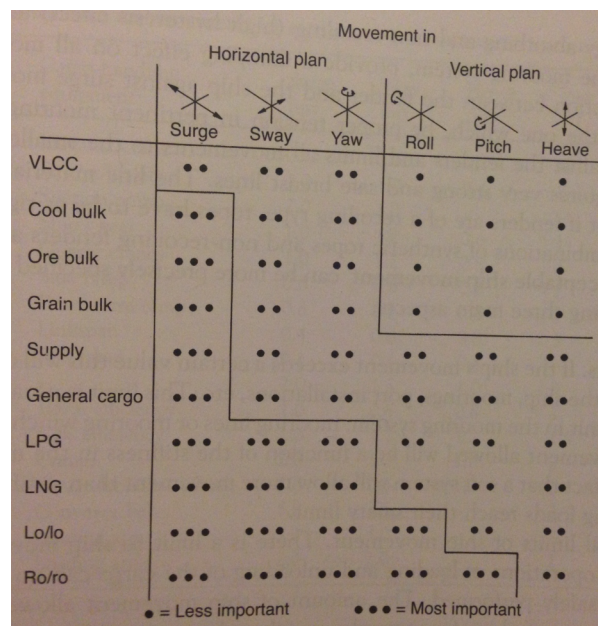


Figure 8.12: Suggested critical degrees of motion for various vessel types, [35]

Minimum Breaking Load (MBL) is that which is defined to be the smallest amount of loading a line can take before breaking. When a vessel is at berth the lines any (un)loading operations should stop if the mooring line force exceeds what is known as the Safe Working Limit (SWL). For steel wires this is 55% of the MBL, other synthetic materials (such as polypropylene) it is 50% of the MBL. For Polyamide tails a safety factor (SF) of 2.5 is applied, where the SF is  $\frac{MBL}{SWL}$ , [27].

## 8.4 Model Setup

After the input data has been acquired the DVRS model setup can begin. The grid file provided by DHI has been uploaded and scaled to match Godafoss, as seen in figure 8.2. Before proceeding the Frequency Vessel Response Engine (FVRE) was executed to rescale

the vessel.

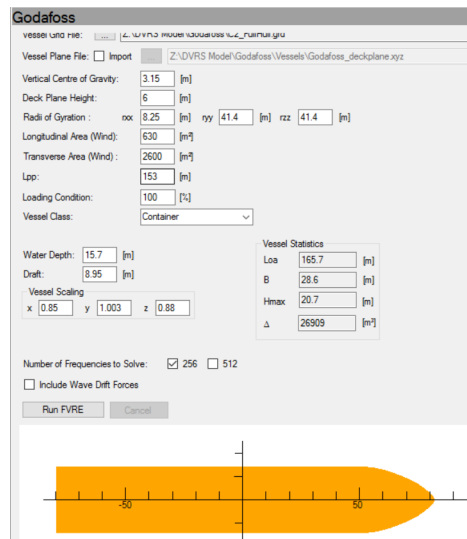


Figure 8.13: Initial setup page in the DVRS software package

The fender and mooring line characteristics are uploaded and the various scenarios are created. For this report the input coordinates for each scenario is shown in figure 8.13. Before running the DVRE engine the vessel is iterated, this is to "relocate" Godafoss along the berth as the mooring lines are set to be within 2.5% of the pretension values. If this is not achieved the vessel is "not iterated". The forces on the mooring lines and the vessel motion can be checked and if there is not significant change between the iteration steps then it simply means the mooring lines were not able to be within the 2.5% limit of the defined pretension.

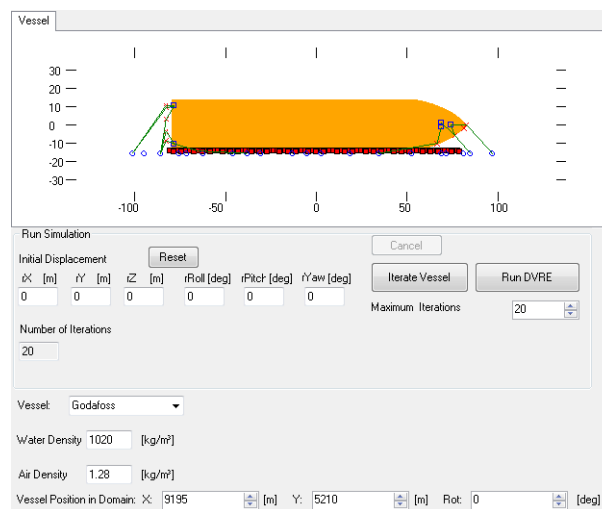


Figure 8.14: DVRS scenario input coordinates

As the mooring lines have different characteristics the initial displacement values are dif-



ferent for each case. When iterating the vessel for the scenarios with a wind speed of  $15 \frac{m}{s}$  the wind data was not included in the iteration process as it displaced the vessel too greatly, this was not the case for the wind speed  $10 \frac{m}{s}$ . The initial displacement values are shown in table 8.11.

Table 8.11: Initial Vessel Displacement Values after iterating the vessel

	rX (m)	rY (m)	rZ (m)	rRoll (deg)	rPitch (deg)	rYaw (deg)
Polypropylene, no wind	0.004	-0.0467	-0.001	0.290	-0.001	0.025
Ultralyne Dyneema, no wind	0.009	-0.025	-0.001	0.12	-0.000	0.011
Polypropylene, wind $10 \frac{m}{s}$ , $0^\circ$	0.226	-0.047	-0.001	0.281	-0.001	0.022
UltralyneDyneema, wind $10 \frac{m}{s}$ , $0^\circ$	0.881	-0.023	-0.001	0.121	-0.000	0.016

## 9 Dynamic Vessel Response Output

Once the input data has been placed into the DVRS program and the simulations have been run successfully a time series for the vessel motion is produced. An example of the output files are shown below, these results are taken from the scenario for wind speed  $10 \frac{m}{s}$ , wind direction 0 degrees, Polypropylene Line and Polyamide tail, wave file  $H_{m0}$  3m,  $T_p$  10s, MWD 315deg (here the MWD is according to true north).

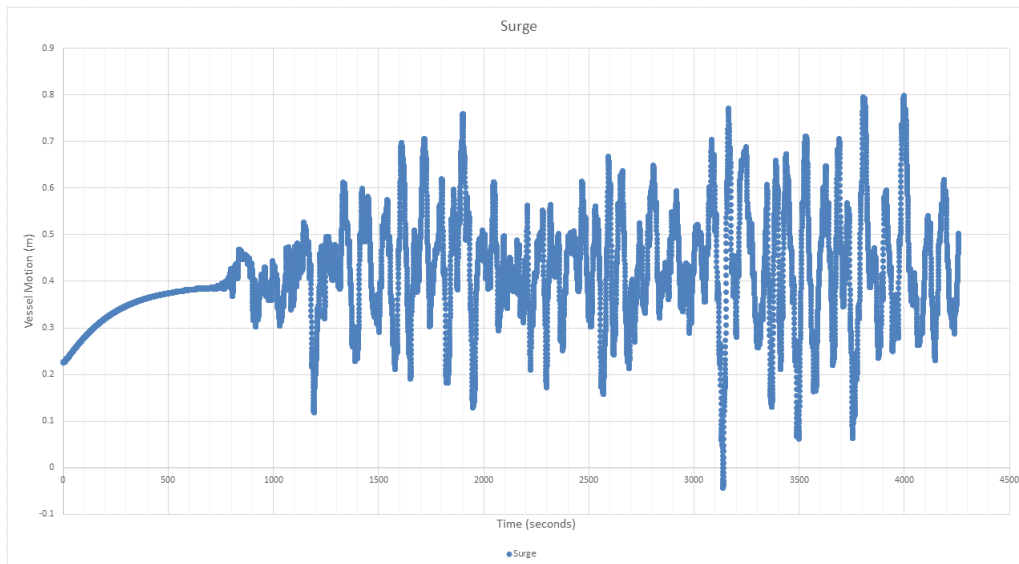


Figure 9.1: DVRS Surge Data for  $H_{m0}$  3m,  $T_p$  10s, MWD 315deg

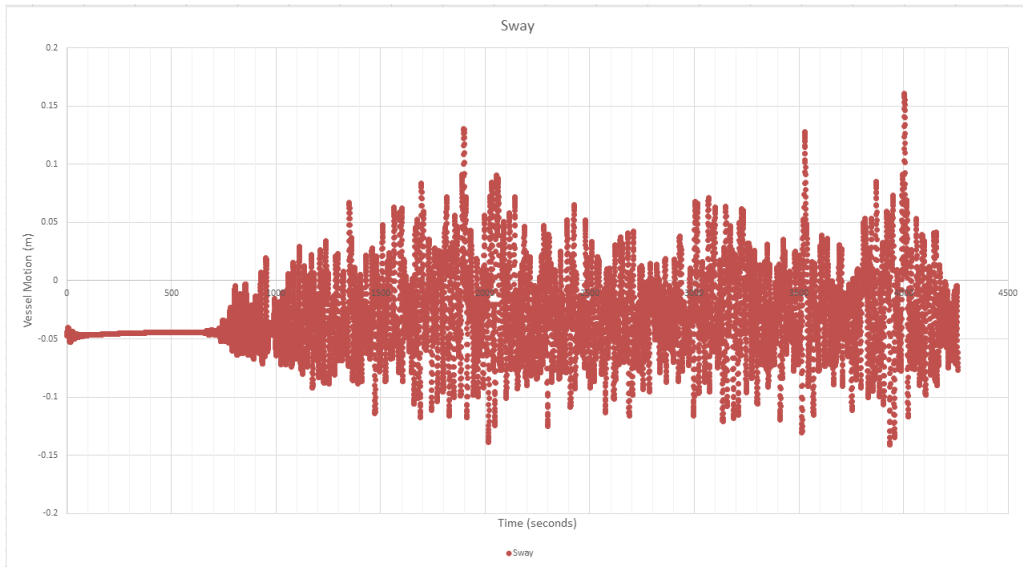


Figure 9.2: DVRS Sway Data for Hm0 3m, Tp 10s, MWD 315deg

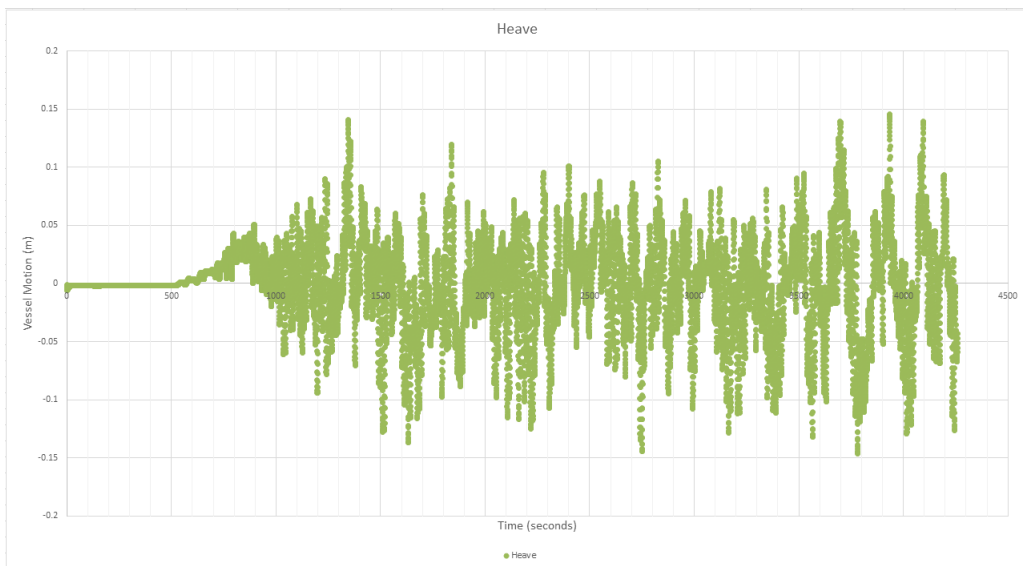


Figure 9.3: DVRS Heave Data for Hm0 3m, Tp 10s, MWD 315deg

Each time a single DVRS run is made these files are created. However it is necessary to process this data in order to get the significant amplitude of motion to verify whether or not the motion criteria has exceeded according to table 8.10 from [28]. This is done by using the method of upward zero crossings and it is described as:

- Cut the data points from before 1200 seconds (for surge) or 1000 seconds (sway, heave, roll, pitch, yaw).
- This is done as the data is not necessary since this is before the generated wave field comes into contact with the vessel and it may distort the results.

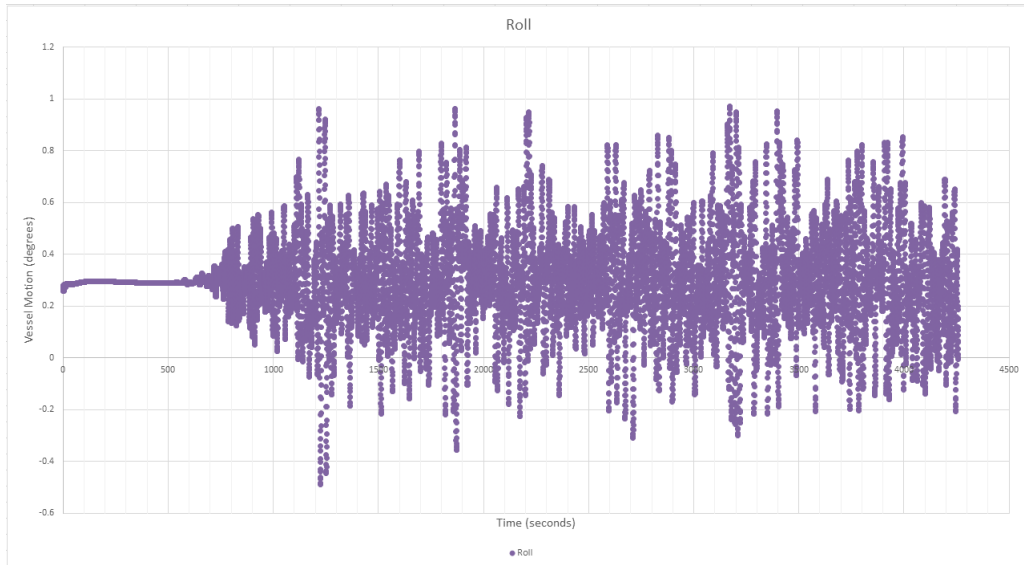


Figure 9.4: DVRS Roll Data for Hm0 3m, Tp 10s, MWD 315deg

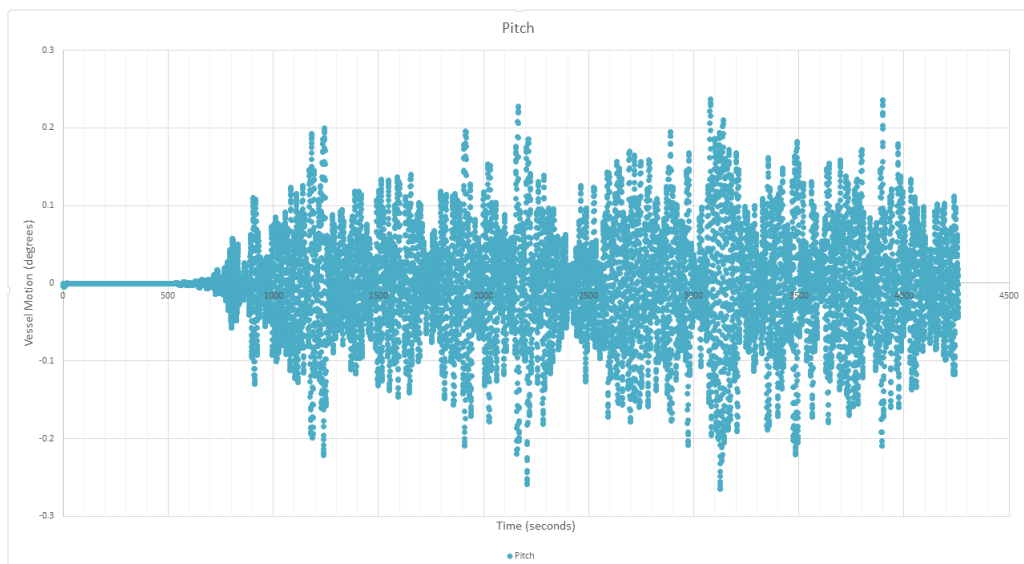


Figure 9.5: DVRS Pitch Data for Hm0 3m, Tp 10s, MWD 315deg

- Find the mean value of the remaining data points to make this the new "zero line" as the vessel may have moved from the original "zero line".
- Determine the number of times the data does an upward crossing of the new "zero line".
- The distance between the maximum and minimum value for each upward zero crossing determines the individual amplitude.
- Determine the number of amplitudes, order them numerically and find the average of the top one third of the results.
- This gives the result for the significant amplitude of motion for that degree of motion.

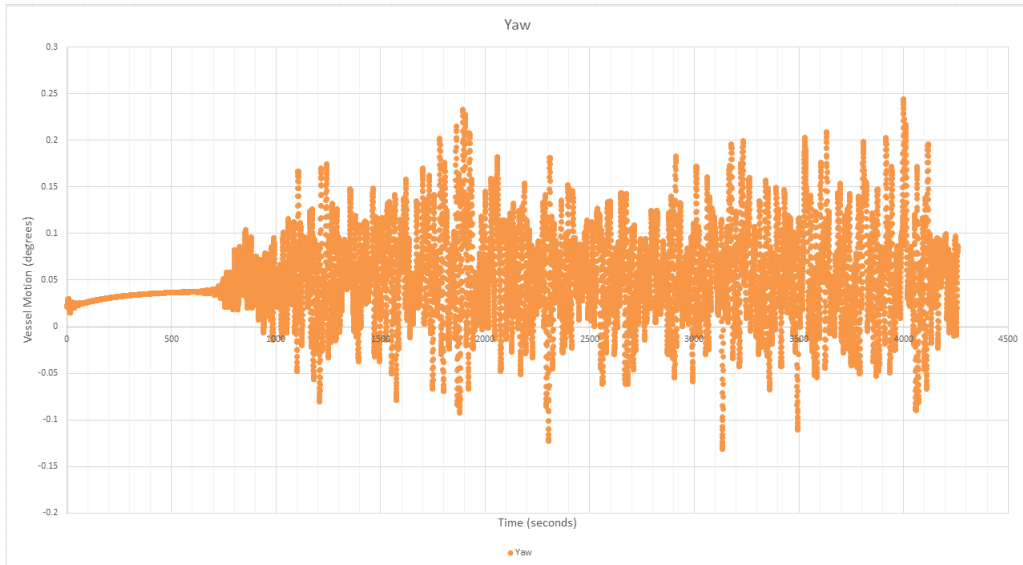


Figure 9.6: DVRS Yaw Data for Hm0 3m, Tp 10s, MWD 315deg

- Repeat this process for all the degrees of motion and for all the run scenarios.

It is worth noting that by using this method one does not obtain the maximum motion which the vessel is subjected to. This being said, the author understood the task was to be solved using this method.

The results which have been taken from the DVRS program have been analysed using the upward zero crossing method and the results are discussed in the following section.

## 10 DVRS Result Analysis

After the DVRS model has been run and the results have been extracted to show the significant amplitude of motion for the six degrees of motion. As mentioned earlier a series of scenarios have been run to simulate different conditions with regards to the wind speed and wind direction, see table 8.2 The analysis of their results will be discussed in this section.

After the analysing the raw data using the upward zero crossing method a value has been extracted for the six degrees of freedom. Using this data it is possible to find a trend for the results and by using this trend an exceedance plot has been created. This is done in order to evaluate the predicted amount of downtime the vessel will have during the (un)loading procedures. It is worth noting that for this project only the surge motion has been considered. Although it is important that the vessel does not exceed the limitations presented by table 8.10 in many cases the surge motion is considered to be the most important motion for the operational safety. Thorensen goes on to say that from a safety perspective the movements in the horizontal plane (surge, sway, yaw) must be minimised as these can break the mooring lines and cause the vessel to break loose from the berth. This notion is explained further in [23], where the authors go on to discuss how surge is "the principal motion of interest for (un)loading efficiency, due to the slow motion of the ship-to-shore crane in the direction along the quay."

Each DVRS scenario is run and the results are described in their respective subsections. To see the data points which have been extracted from the DVRS program please see Appendix C. Here the data points and their corresponding figures are shown. In the subsections below an exceedance curve which is used to determine how often the vessels surge motion will be above the limitations is presented along with a time series to see when the vessel motion can be expected to be exceeded. The results from the scenarios will be discussed and compared in further detail after they have been presented here.

### 10.1 Polypropylene Line, Polyamide Tail, no wind

The scenario which is described here is when there is no wind present while a Polypropylene Line and Polyamide Tail are being used. This can be seen as one of the two "control" situations.

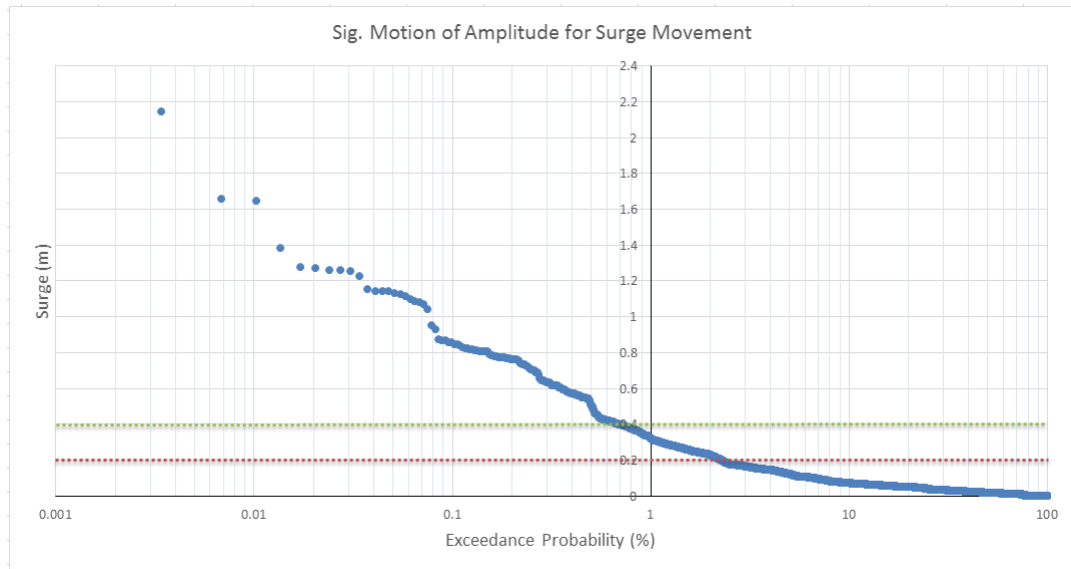


Figure 10.1: Exceedance of the Surge Motion, Polypropylene Line with no wind

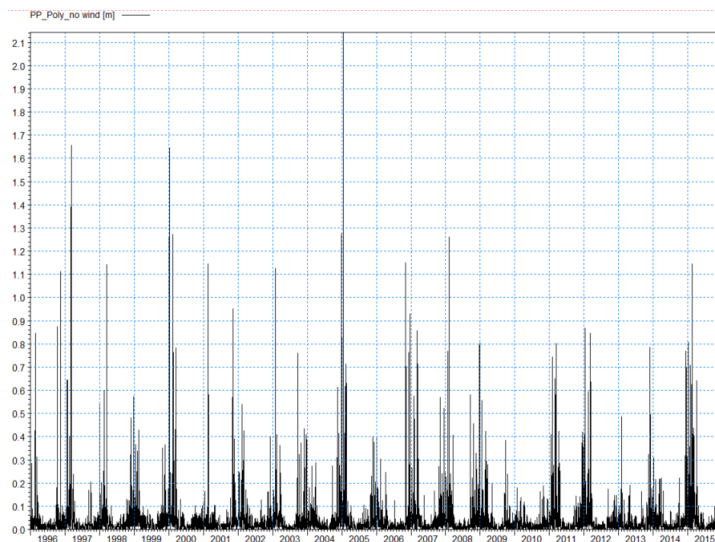


Figure 10.2: Time Series showing the Surge Motions from 1995-2015, Polypropylene Line with no wind

### 10.2 Ultraline Dyneema Line, Polyamide Tail, no wind

The scenario which is described here is when there is no wind present while a Ultraline Dyneema Line and Polyamide Tail are being used. This can be seen as the second "control" situation.

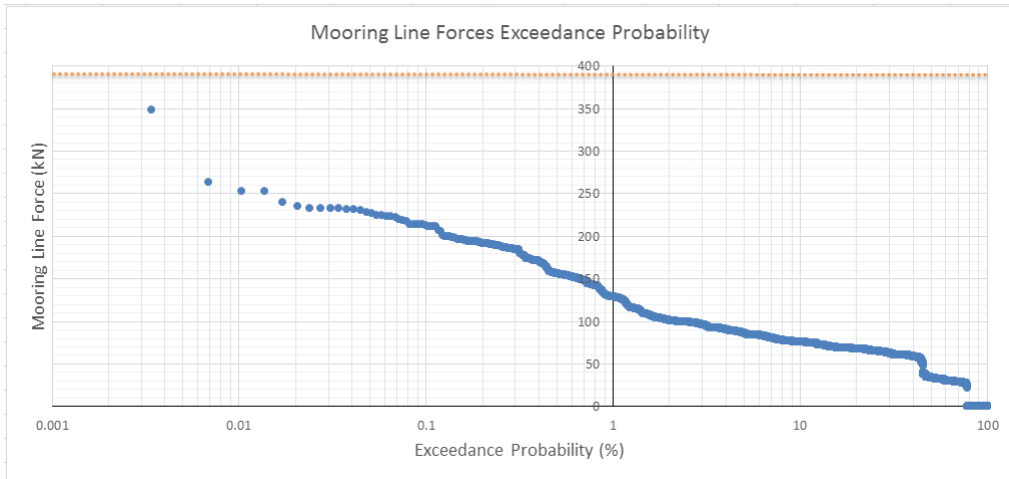


Figure 10.3: Exceedance of the Mooring Line Forces, Polypropylene Line with no wind

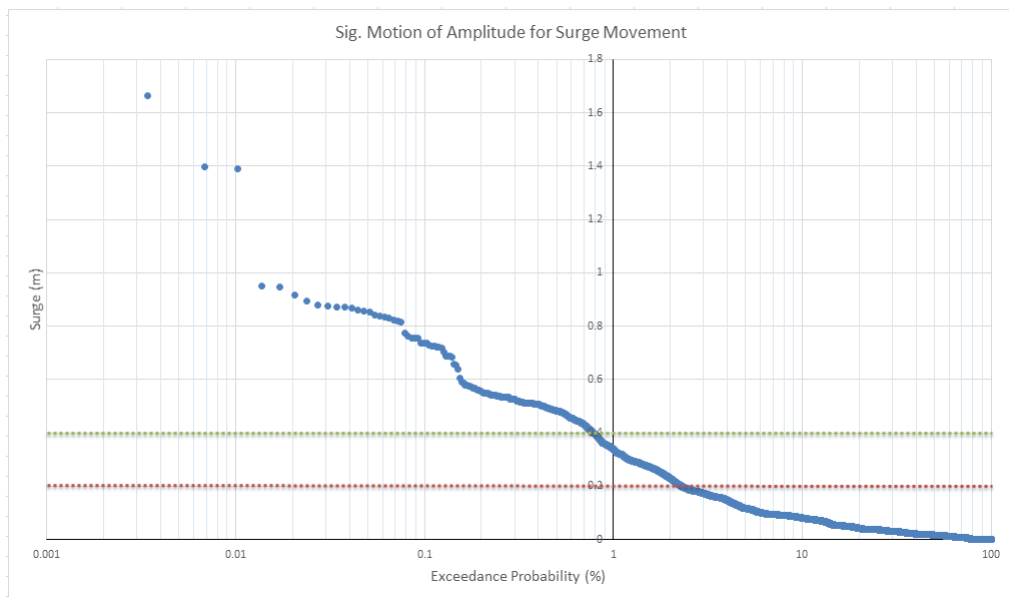


Figure 10.4: Exceedance of the Surge Motion, Ultraline Dyneema Line with no wind

### 10.3 Polypropylene Line, Polyamide Tail, wind $10 \frac{m}{s}$ , 0 degrees

These are the results from running the DVRs Scenarios with wind and a mooring line combination of Polypropylene and Polyamide. The wind speed of  $10 \frac{m}{s}$  is a fresh breeze or Beaufort level 5 in which one can expect 2-3m waves.

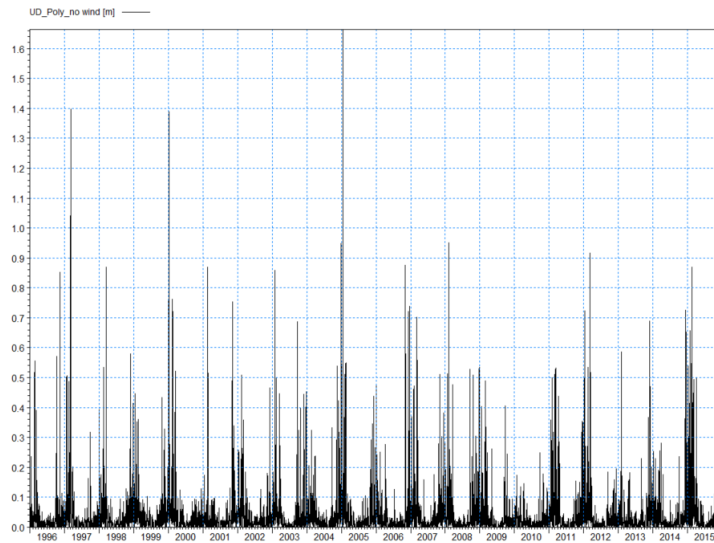


Figure 10.5: Time Series showing the Surge Motions from 1995-2015, Ultraline Dyneema Line with no wind

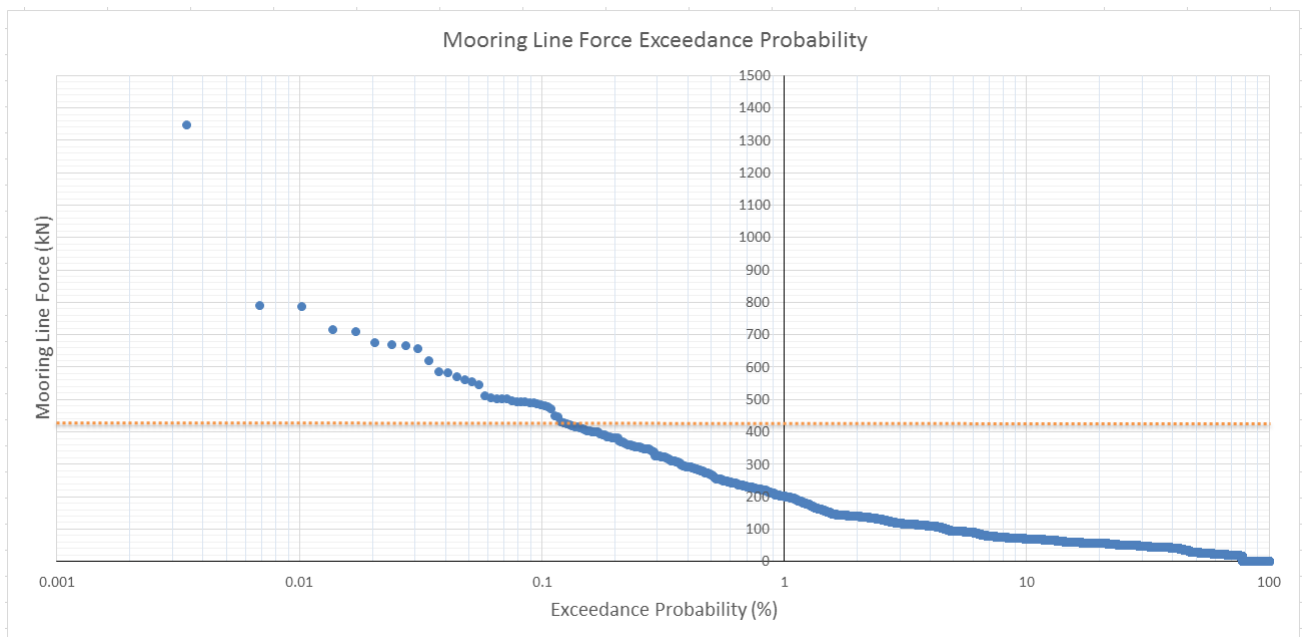


Figure 10.6: Exceedance of the Mooring Line Forces, Ultraline Dyneema Line with no wind

#### 10.4 Ultraline Dyneema Line, Polyamide Tail, wind $10 \frac{m}{s}$ , 0 degrees

These are the results from running the DVRS Scenarios with wind and a mooring line combination of Ultraline Dyneema and Polyamide. The wind speed of  $10 \frac{m}{s}$  is a fresh breeze or Beaufort level 5 in which one can expect 2-3m waves.



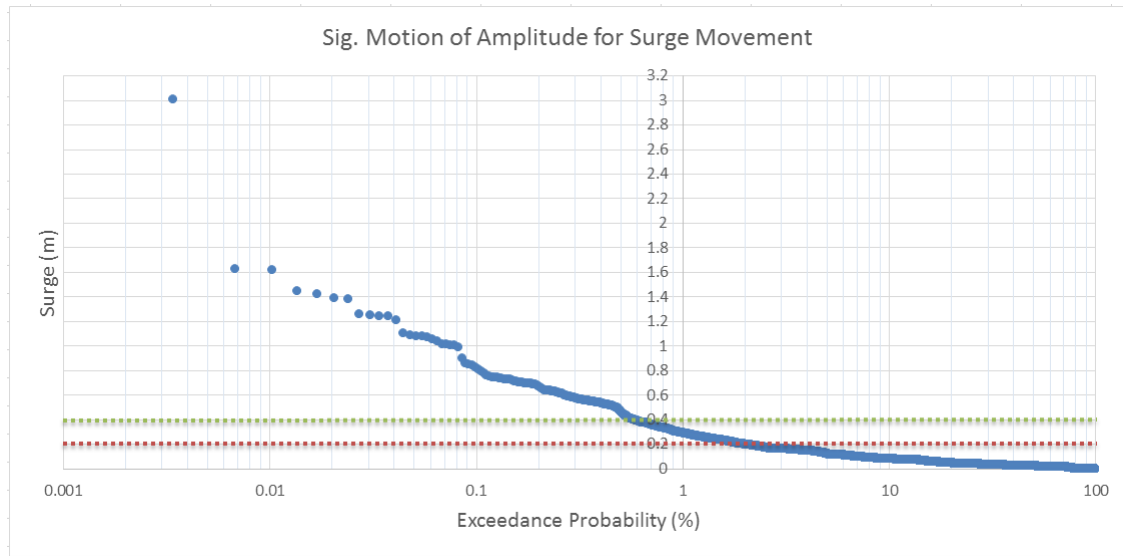


Figure 10.7: Exceedance of the Surge Motion, Polypropylene Line with wind 10  $\frac{m}{s}$  from 0°

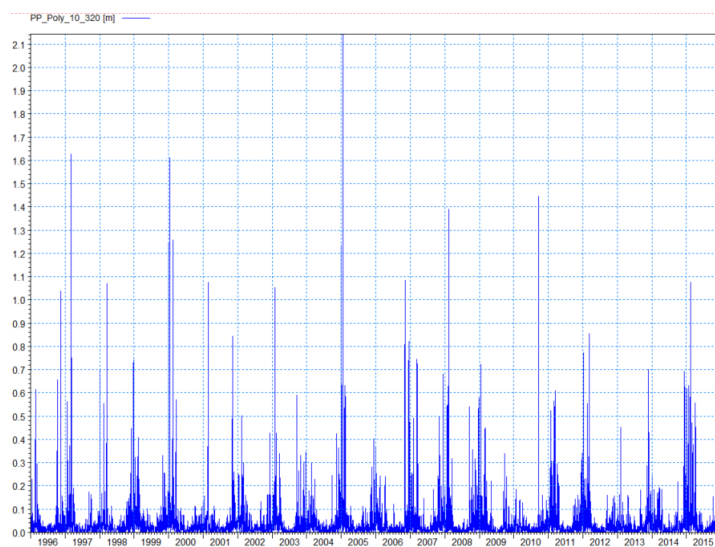


Figure 10.8: Time Series showing the Surge Motions from 1995-2015, Polypropylene Line with wind 10  $\frac{m}{s}$  from 0°

### 10.5 Polypropylene Line, Polyamide Tail, wind 15 $\frac{m}{s}$ , 0 degrees

These are the results from running the DVRS Scenarios with wind and a mooring line combination of Polypropylene and Polyamide. The wind speed of 15  $\frac{m}{s}$  is a fresh breeze or Beaufort level 7 in which one can expect 4-5.5m waves.

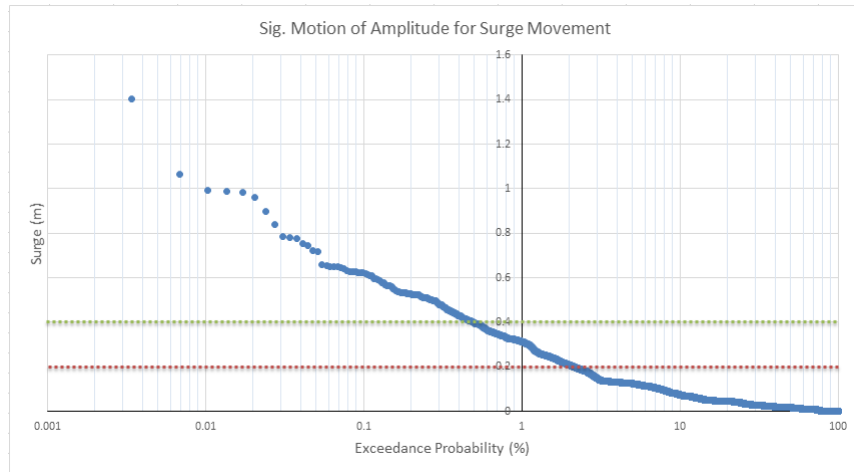


Figure 10.9: Exceedance of the Surge Motion, Ultraline Dyneema Line with wind 10  $\frac{m}{s}$  from 0°

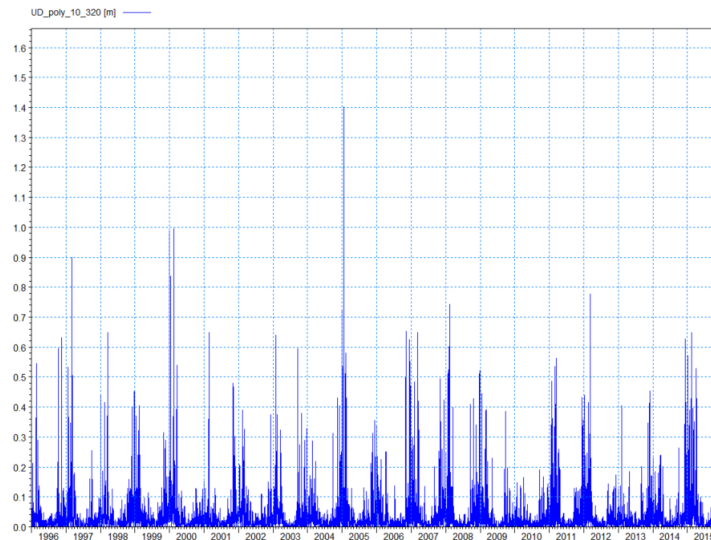


Figure 10.10: Time Series showing the Surge Motions from 1995-2015, Ultraline Dyneema Line with wind 10  $\frac{m}{s}$  from 0°

### 10.6 Ultraline Dyneema Line, Polyamide Tail, wind 15 $\frac{m}{s}$ , 0 degrees

These are the results from running the DVRS Scenarios with wind and a mooring line combination of Ultraliny Dyneema and Polyamide. The wind speed of 15  $\frac{m}{s}$  is a fresh breeze or Beaufort level 7 in which one can expect 4-5.5m waves.

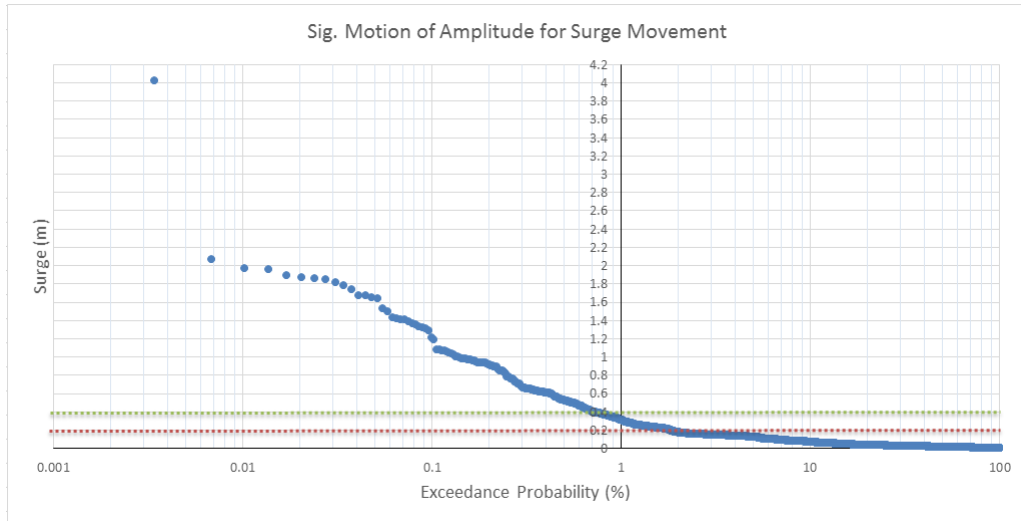


Figure 10.11: Exceedance of the Surge Motion, Polypropylene Line with wind 15  $\frac{m}{s}$  from  $0^\circ$

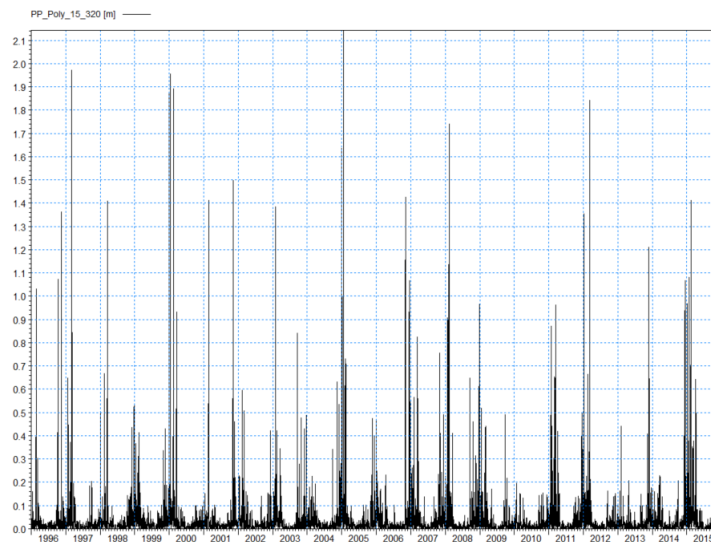


Figure 10.12: Time Series showing the Surge Motions from 1995-2015, Polypropylene Line with wind 15  $\frac{m}{s}$  from  $0^\circ$

### 10.7 Polypropylene Line, Polyamide Tail, wind 15 $\frac{m}{s}$ , 250 degrees

These are the results from running the DVRS Scenarios with wind and a mooring line combination of Polypropylene and Polyamide. The wind speed of 15  $\frac{m}{s}$  is a fresh breeze or Beaufort level 7 in which one can expect 4-5.5m waves. The wind direction here was that which was determined to be the most critical direction with regards to the (un)loading operations.

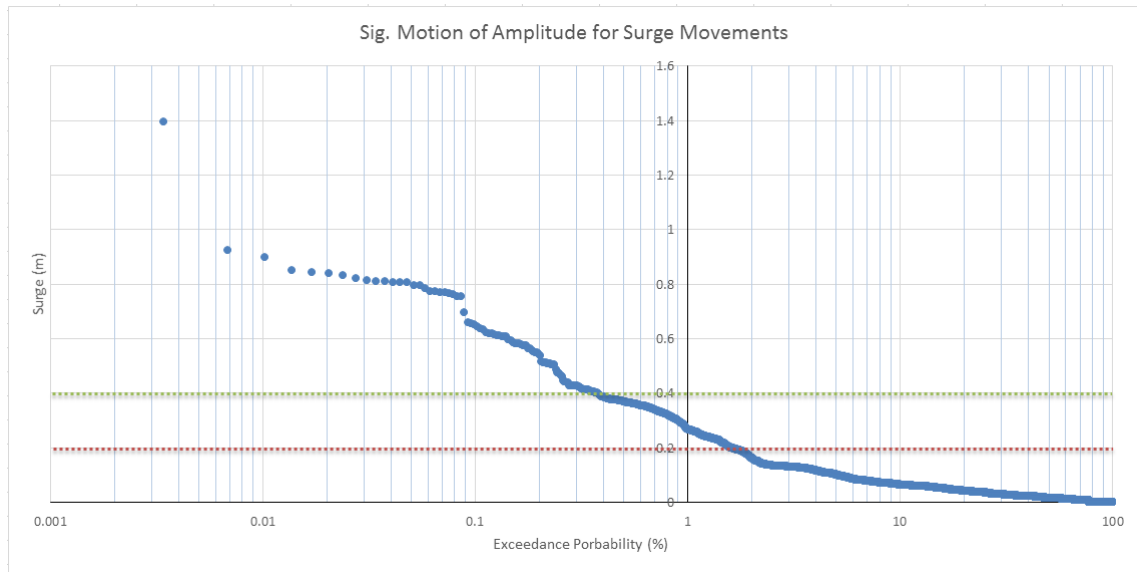


Figure 10.13: Exceedance of the Surge Motion, Ultraline Dyneema Line with wind 15  $\frac{m}{s}$  from 0°

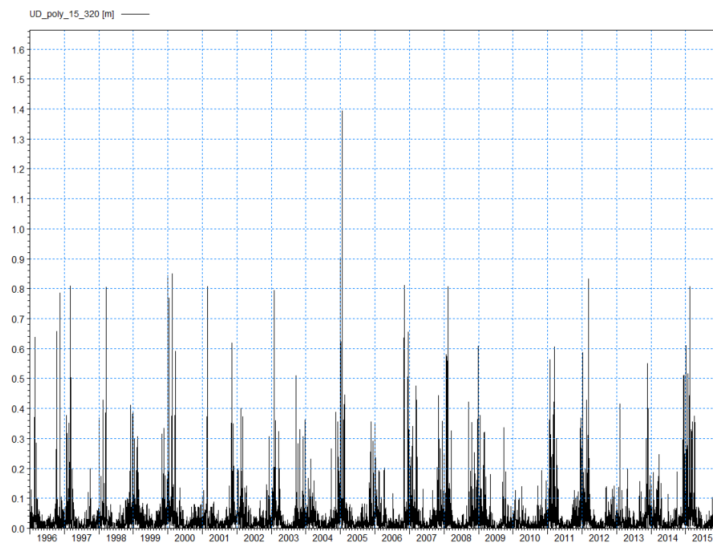


Figure 10.14: Time Series showing the Surge Motions from 1995-2015, Ultraline Dyneema Line with wind 15  $\frac{m}{s}$  from 0°

### 10.8 Ultraline Dyneema Line, Polyamide Tail, wind 15 $\frac{m}{s}$ , 250 degrees

These are the results from running the DIVERS Scenarios with wind and a mooring line combination of Ultraline Dyneema and Polyamide. The wind speed of 15  $\frac{m}{s}$  is a fresh breeze or Beaufort level 7 in which one can expect 4-5.5m waves. The wind direction here was that which was determined to be the most critical direction with regards to the (un)loading operations.

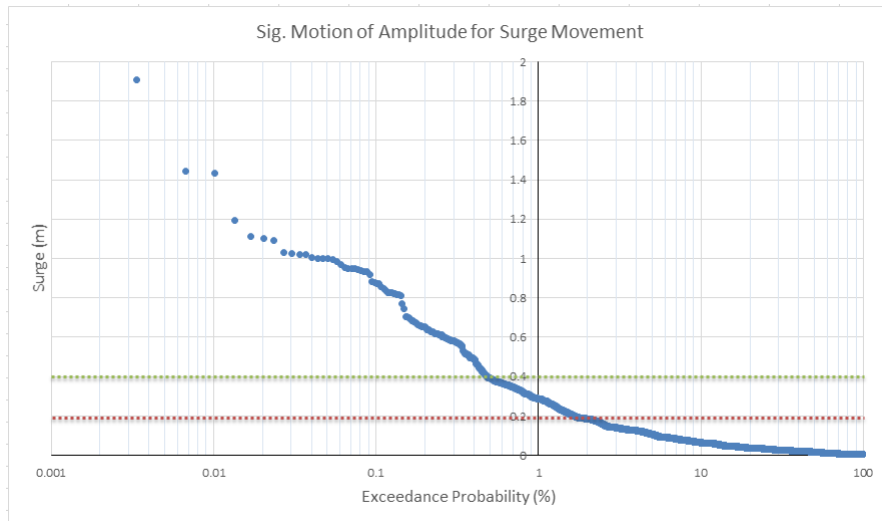


Figure 10.15: Exceedance of the Surge Motion, Polypropylene Line with wind  $15 \frac{m}{s}$  from  $250^\circ$

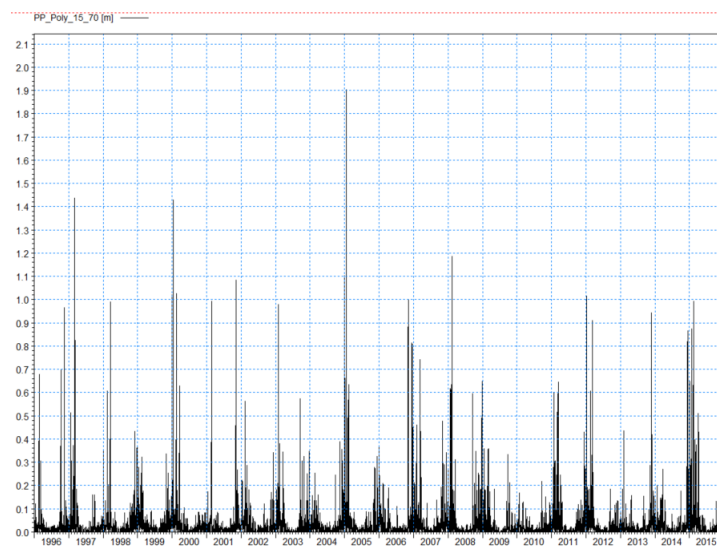


Figure 10.16: Time Series showing the Surge Motions from 1995-2015, Polypropylene Line with wind  $15 \frac{m}{s}$  from  $250^\circ$

## 10.9 DVRS Scenario Result Comparison

After the DVRS scenarios have been run their corresponding exceedance figures have been created. They were shown for each corresponding scenario in their respective subsections above. However, to better understand how these results compare to one another it is best to compare them side by side. Therefore the table below has been created to show the amount of time Godafoss have exceeded the surge motion criteria set out by [28]. Note that as all the scenarios have a Polyamide Tail this will not be written specifically in the table.

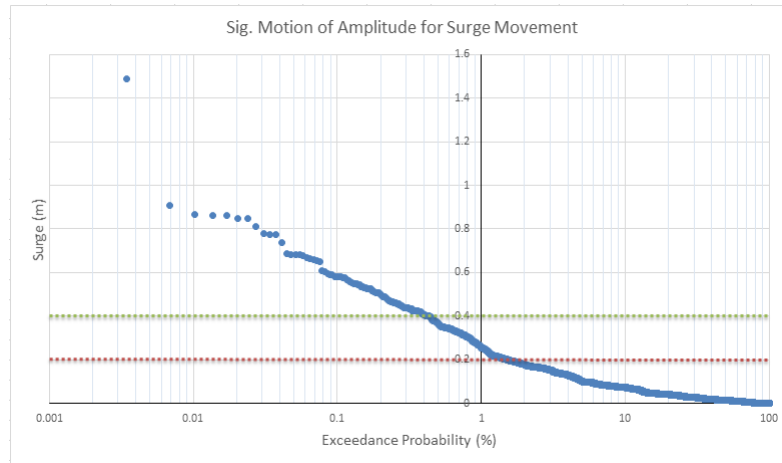


Figure 10.17: Exceedance of the Surge Motion, Ultraline Dyneema Line with wind  $15 \frac{m}{s}$  from  $250^\circ$

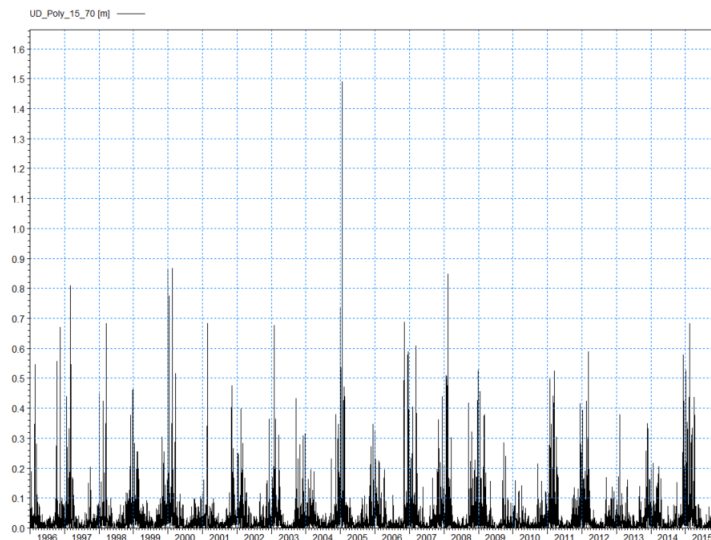


Figure 10.18: Time Series showing the Surge Motions from 1995-2015, Ultraline Dyneema Line with wind  $15 \frac{m}{s}$  from  $250^\circ$

In table 10.1 the amount of hours in which the surge motion is above the motion criteria is the total amount of hours per year. So, for a Polypropylene Line and Polyamide Tail when there is no wind one can expect the surge motion to be above 0.2m for 199 hours out of 8760 hours. The data points which were provided by the Port Authorities in Reykjavik was given as for every six hours over a 20 years. With this data set the author has assumed that it is possible to do such an iteration where the exceedance plots can be taken to represent the total amount of hours per year.

When viewing the Time Series plots it can be seen that the surge motion appears to exceed the criteria of motion during the winter time. This coincides with figures 6.7 and 7.12 as

Table 10.1: Result Comparison for the Surge Exceedance Plots

Line Type & Wind Combination	0.2m		0.4m	
	%	(hrs)	%	(hrs)
Polypropylene, no wind	2.276	199	0.688	60
Ultraline Dyneema, no wind	2.307	202	0.780	68
Polypropylene, wind $10 \frac{m}{s}$ , $0^\circ$	1.937	169	0.575	50
Ultraline Dyneema, wind $10 \frac{m}{s}$ , $0^\circ$	2.146	188	0.493	43
Polypropylene, wind $15 \frac{m}{s}$ , $0^\circ$	1.814	159	0.705	62
Ultraline Dyneema, wind $15 \frac{m}{s}$ , $0^\circ$	1.591	139	0.376	33
Polypropylene, wind $15 \frac{m}{s}$ , $250^\circ$	1.632	143	0.479	42
Ultraline Dyneema, wind $15 \frac{m}{s}$ , $250^\circ$	1.516	133	0.431	38

it would appear the winter storms are not to be underestimated. The report presented by [15] focuses on a series of winter storms and how they have affected the region around Kleppsbakki. After having created the time series plots for the surge motion it can be seen that during the winter storms the port authorities can expect increased surge motions at Hafnarbakki utan Klepps.

With these results it does however seem somewhat counter-intuitive that when there is no wind applied the stiffer Ultraline Dyneema line is subject to a larger amount of surge downtime. One may argue that for the motion criteria of 0.2m a 3 hour difference over the course of a year may be insignificant. What is particularly strange is that the introduction of wind into the model decreases the surge exceedance. One would expect as the wind arrives at the aft of the vessel the surge motion will increase as it "pushes" the vessel. It can be seen that the wind direction does influence the surge motion exceedance when comparing the wind speed  $15 \frac{m}{s}$   $0^\circ$  vs  $250^\circ$ . From this a series of sensitivity analysis have been undertaken to see how different individual factors influence the six degrees of motion.

The mooring line forces have been determined to see if they will be exceeded more often than the surge motion. This way it is possible to see which of the two is more critical. It is worth noting that the mooring line force exceedance plots have only been created for the scenarios where there is no wind present. In figure 10.3 and figure 10.6 it is clear to see that the mooring line forces will only be exceeded in the situation for an Ultraline Dyneema Line and Polyamide Tail mooring line system. The safe working load, as defined by [27], of 431.2 kN has been exceeded 0.120% per year which is equivalent to 10.5 hours per year. By comparing this to table 10.1 Godafoss will exceed the surge motion before the mooring line forces have passed the Safe Working Load.

### 10.10 Sensitivity Analysis

The scenarios which have been run above can be used to determine how the vessel will react to a very specific set of circumstances. It may be worth analysing how Godafoss will react under various different conditions. In this section the MIKE21 BW file for the condition  $H_{m0}$  1m, Tp 10s, MWD 292.5 degrees, Polypropylene Line and Polyamide Tail has been used in all circumstances. The tail length is 5m and the pre-tension is 5 tonnes. In the control scenario for a Polypropylene Line and Polyamide Tail, Godafoss' movement for surge, sway, heave, roll, pitch and yaw were 0.060 m, 0.082m, 0.053m,  $0.293^\circ$ ,  $0.070^\circ$ , and  $0.079^\circ$  respectively. The forces acting upon the mooring lines is 79.79 kN.

#### Wind Direction

The influence of the wind can sometimes be underestimated when it comes to how it affects the movement of berthed vessels. In this situation the affect of the incoming wind from different directions has been analysed. For this situation a wind speed of  $10 \frac{m}{s}$  has been applied for all the possible wind directions. In this section the wind direction is determined by the coordinate system which is shown in figure 5.3.

Table 10.2: Sensitivity Test - Wind Direction Data Points

	Wind Direction (degrees)																		
	0	10	20	30	40	50	60	70	80	90	100	110	120	130	140	150	160	170	180
Surge (m)	0.056	0.059	0.061	0.059	0.061	0.063	0.061	0.057	0.059	0.057	0.055	0.053	0.052	0.052	0.052	0.051	0.049	0.048	0.047
Sway (m)	0.084	0.087	0.084	0.082	0.081	0.082	0.085	0.084	0.084	0.085	0.084	0.085	0.086	0.086	0.087	0.087	0.087	0.088	0.088
Heave (m)	0.052	0.052	0.052	0.052	0.051	0.051	0.051	0.052	0.052	0.052	0.052	0.052	0.052	0.052	0.052	0.052	0.052	0.052	0.053
Roll (deg)	0.303	0.313	0.315	0.314	0.314	0.313	0.308	0.295	0.284	0.278	0.274	0.265	0.261	0.256	0.252	0.251	0.253	0.254	0.253
Pitch (deg)	0.078	0.078	0.079	0.079	0.079	0.079	0.079	0.078	0.078	0.077	0.077	0.077	0.077	0.076	0.076	0.076	0.076	0.075	0.075
Yaw (deg)	0.069	0.075	0.074	0.071	0.070	0.070	0.076	0.069	0.069	0.069	0.068	0.065	0.065	0.065	0.064	0.064	0.064	0.064	0.064

	Wind Direction (degrees)																			
	190	200	210	220	230	240	250	260	270	280	290	292.5	300	305	310	320	330	340	350	360
Surge (m)	0.045	0.043	0.041	0.045	0.045	0.046	0.048	0.051	0.054	0.054	0.052	0.051	0.056	0.056	0.056	0.056	0.055	0.055	0.059	0.056
Sway (m)	0.088	0.088	0.088	0.088	0.088	0.088	0.088	0.088	0.087	0.086	0.085	0.085	0.084	0.083	0.083	0.084	0.084	0.085	0.086	0.084
Heave (m)	0.053	0.053	0.053	0.053	0.053	0.053	0.053	0.053	0.053	0.053	0.052	0.052	0.052	0.052	0.052	0.052	0.052	0.052	0.052	0.052
Roll (deg)	0.253	0.251	0.248	0.251	0.251	0.256	0.260	0.266	0.270	0.277	0.287	0.291	0.304	0.309	0.311	0.317	0.318	0.317	0.314	0.303
Pitch (deg)	0.075	0.075	0.074	0.074	0.074	0.074	0.074	0.075	0.075	0.075	0.076	0.076	0.077	0.078	0.078	0.078	0.078	0.078	0.078	0.078
Yaw (deg)	0.064	0.063	0.062	0.063	0.063	0.064	0.066	0.066	0.066	0.067	0.068	0.069	0.069	0.069	0.070	0.071	0.073	0.074	0.074	0.069

Using the data points which have been extracted and presented above it is possible to see a trend of how the different wind directions affect the movements of Godafoss.

From figures 10.19 and 10.20 it is possible to determine which of the six degrees of motion are more sensitive to the incoming wind and which are possibly the more critical directions.

Initially it can be seen that Godafoss' pitch, yaw and heave seem to be unaffected by the wind direction, thus one can say that they are not greatly affected by the incoming wind. The sway motion seems to be somewhat affected by the wind. There is an 8% difference between the maximum and minimum sway motion, with a wind direction of 180 & 40 degrees respectively. What is of interest is to see what the difference between the maximum and minimum value were with respect to the control scenarios where no wind was applied. When the wind is in the least favourable direction there is a 7% increase. While the wind is in a more favourable direction there is a 1% decrease in the sway motion.

From the two figures presented above it can be seen that the surge and roll motions are those which are mostly affected by the incoming wind direction. The difference between



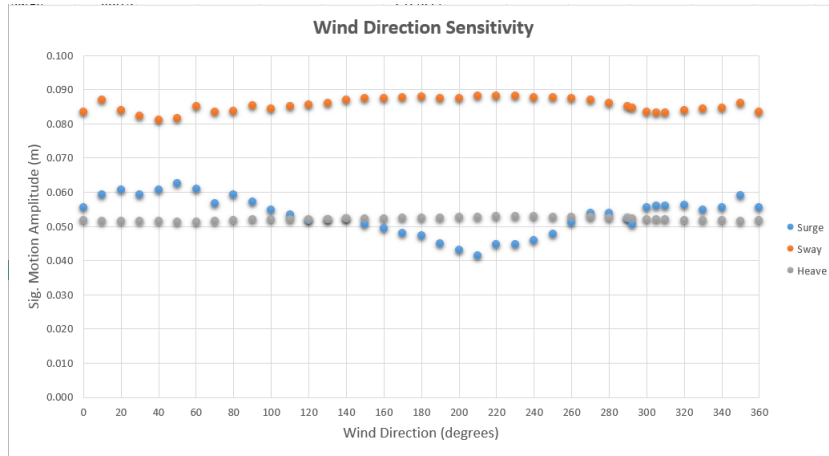


Figure 10.19: Sensitivity Test - Wind Directions effects of the Vessels Rotations

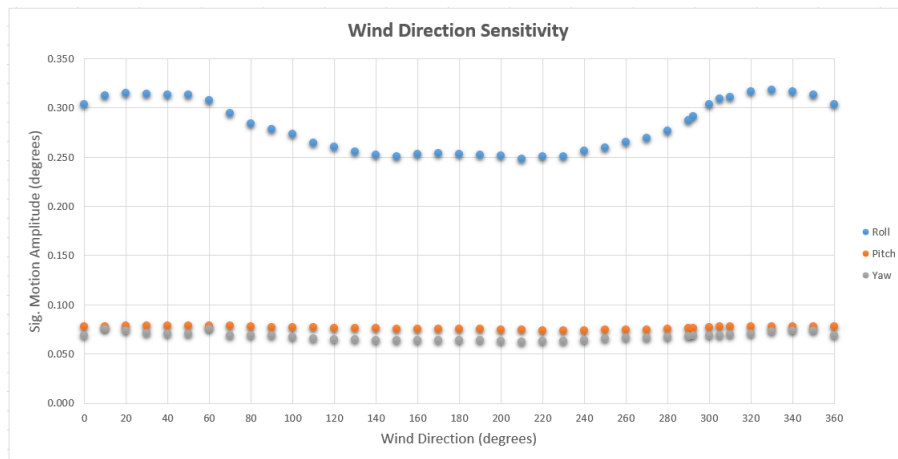


Figure 10.20: Sensitivity Test - Wind Directions effects of the Vessels Rotations

the maximum and minimum surge values is 34%, at wind directions 50 & 210 degrees respectively. This is a significant difference which can not be ignored. Once again, if it is assumed that this difference is constant for all the modelled wave scenarios then the difference can be found between the most critical and favourable wind direction when compared to the control situation. The most unfavourable wind direction increases the surge motion by 4% while the more favourable wind direction decreases the surge motion by 45%. This is a significant change and one can not argue against the influence of the wind when it comes to modelling the surge motion.

One can also see how the roll motion greatly varies as the wind direction changes. The difference between the maximum and minimum roll values is 22% at wind directions 330 & 210 degrees. Again, if this is a constant change for all situations then one can see how this would affect the control scenario. When the wind is in the least favourable direction the roll motion is increased by 8%. For a more favourable wind direction the roll rotation is decreased by 18%. Once again it can be seen that the incoming wind direction has an

important influence on how the roll motion will be affected.

When one looks at figures 10.19 and 10.20 it is clear to see which wind directions are the least favourable. As one would expect, when the wind is in the same general direction as the incoming waves then the motions have been amplified. This is compared to when the wind is opposing the incoming waves. For this sensitivity test it is worth noting that they have been performed for a wind speed of  $10 \frac{m}{s}$ .

The forces which act upon the mooring lines will also be affected by the wind direction since the vessel motions are not constant. How the forces vary with regards to the wind direction can be seen in the figure below.

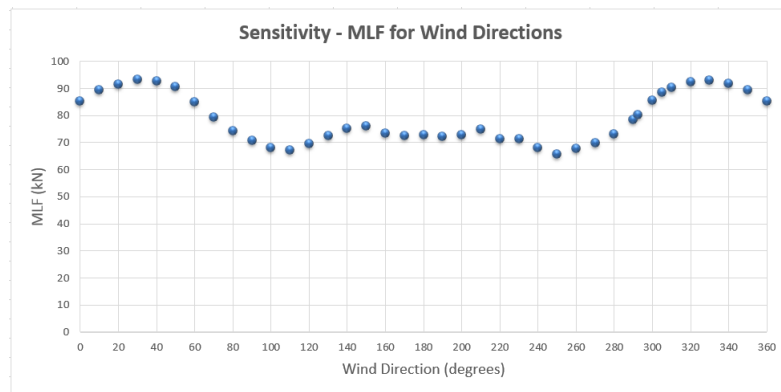


Figure 10.21: Sensitivity Test - Wind Directions effects on the Mooring Line Forces

As with the vessel motions the mooring line forces can be seen to be affected by the incoming wind direction. Here there is a 30 % difference between the maximum and minimum force, at the respective wind directions of 30 & 250 degrees. Once again it is assumed that the change in the forces will be constant so this can be compared to the control scenario. The wind direction of  $30^\circ$  increases the mooring line force by 14.5%. Compared to the wind direction  $250^\circ$  which decreased the mooring line force by 21.5%. When comparing figures 10.20 and 10.21 it can be seen that the mooring line force curve has a very similar pattern to that of Godafoss' roll motion. This may suggest that the roll motion has the greatest influence on the mooring line forces experienced by the set-up used on Godafoss.

After these tests were performed the author was made aware that the maximum allowable wind speed before the (un)loading process is stopped is  $15 \frac{m}{s}$ . It may be worth doing these simulations once more with the higher wind speed to determine what the difference would be with the control scenario.

When speaking to the port authorities they were not aware if there was a critical wind speed or direction which made it too dangerous for Godafoss proceed with its berthing operation. After having spoken to [25] it was made clear to the author that when the ferry is to call at Hirthals harbour in Northern Jutland there are certain wind conditions which do not allow the ferry to call at the port. The increased wind speed does not allow the ferry sufficient time to reduce its incoming velocity to a level which would give too high a risk for the ferry to collide with the superstructure is too great. Due to the sensitive

nature of the material the author was asked not to mention any specific wind conditions in this report. However, the port does not say there are any limitations and the vessels captain along with the shipping company is to decide whether or not it is safe to berth. After having spoken to the Port Authorities in Reykjavik it was made clear they set no limitations as to when it is safe for the vessel to call at the port. Unfortunately the author was not able to speak to Eimskip to determine if they had any requirements.

### Tail Length

Another sensitivity test which has been carried out is to determine what effect the tail length has on the six degrees of motion along with the forces felt by the mooring lines. It is worth noting that there is no wind applied to this sensitivity tests.

The data points which have been extracted from the DVRS simulations and the figures used to show the development of the vessel motion are shown here.

Table 10.3: Sensitivity Test - Tail Length Data Points

	Tail Length (m)						
	0	1	3	5	7	9	10
Surge (m)	0.053	0.054	0.055	0.060	0.065	0.071	0.067
Sway (m)	0.081	0.081	0.082	0.082	0.082	0.082	0.083
Heave (m)	0.053	0.053	0.053	0.053	0.052	0.052	0.052
Roll (deg)	0.294	0.293	0.294	0.293	0.293	0.296	0.294
Pitch (deg)	0.069	0.069	0.070	0.070	0.071	0.071	0.072
Yaw (deg)	0.083	0.082	0.080	0.079	0.077	0.075	0.076

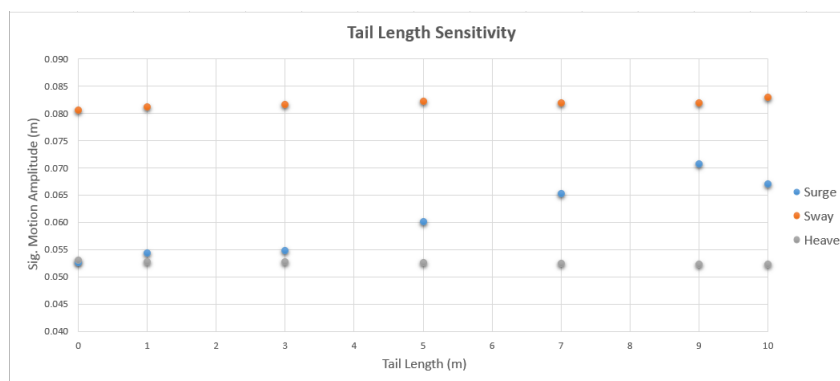


Figure 10.22: Sensitivity Test- Tail Lengths Effects on the Vessel Displacement

Here the control situation is equivalent to the results given with the tail length of 5m. When looking at figures 10.22 and 10.23 it can be seen that the effects of changing the tail length is not necessarily so significant, apart from the surge motion. As the tail length increases so does the surge motion. It would appear that the surge motion would begin to decrease once the tail length is greater than 9m. When comparing to the control situation the surge motion increases by 15%. The surge motion is the lowest when there is no tail present and this has decreased the surge motion by 14%. This would suggest that it may

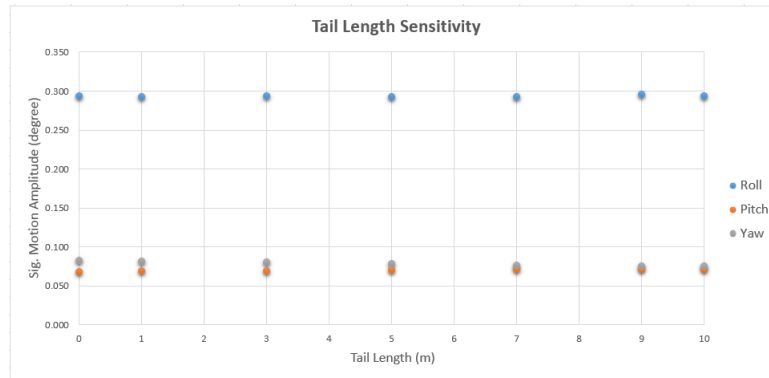


Figure 10.23: Sensitivity Test - Tail Lengths Effects on the Vessel Rotation

be beneficial to either reduce or remove the tail when using a Polypropylene Line and Polyamide Tail.

The effect on the mooring line forces by changing the tail length are illustrated here.

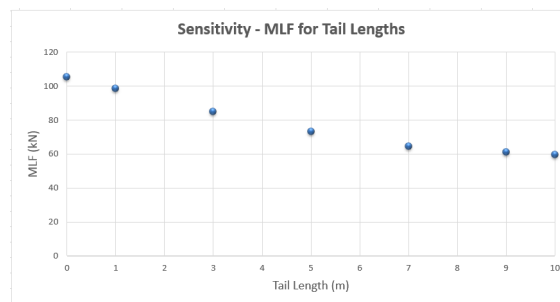


Figure 10.24: Sensitivity Test - Tail Length Effects on the Mooring Line Forces

As one would expect the forces which act upon the mooring line decrease as the tail length increases. This would seem appropriate as the forces become more distributed amongst the mooring line and the tail. It is worth noting that there is a 43% decrease in the forces when the tail length is 0m compared to when it is 10m. This is rather substantial and may influence how one would want to configure their mooring line set-up.

The effect may have been more pronounced if one were to have done this study with a mooring line and tail which had greater differences in their material properties. Such as using the Ultraline Dyneema Line rather than a Polypropylene Line.

### Line Pre-Tension

Here the influence of pre-tensioning the lines will affect the six-degrees of motion along with the mooring line forces. Here the data points and the figures showing the development of the data can be seen. It is also worth noting that there is no wind applied to these tests.

From figures 10.25 and 10.26 it can be seen that only the heave motion seem to be the least affected by the increase in the line pre-tension. By increasing the pre-tension from

Table 10.4: Sensitivity Test - Line Pre-Tensioning Datapoints

	Line Tension (t)						
	0	1	3	5	7	9	10
Surge (m)	0.126	0.075	0.062	0.060	0.048	0.034	0.032
Sway (m)	0.132	0.131	0.082	0.082	0.083	0.084	0.084
Heave (m)	0.051	0.051	0.051	0.053	0.053	0.054	0.054
Roll (deg)	0.187	0.236	0.277	0.293	0.296	0.291	0.287
Pitch (deg)	0.077	0.076	0.073	0.070	0.067	0.063	0.060
Yaw (deg)	0.100	0.106	0.076	0.079	0.080	0.080	0.081

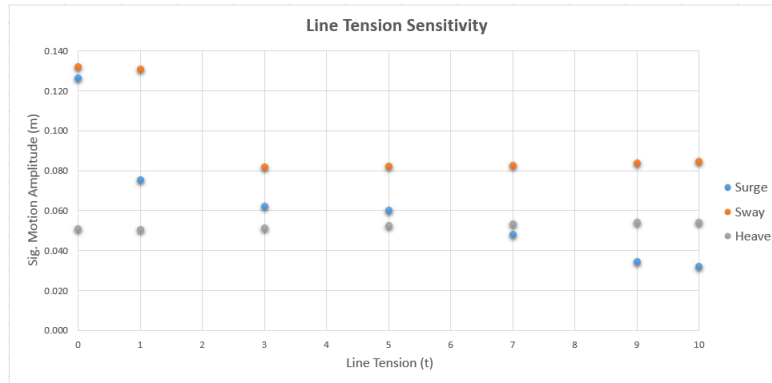


Figure 10.25: Sensitivity Test - Line Pre-Tensioning Effects on Vessel Displacement

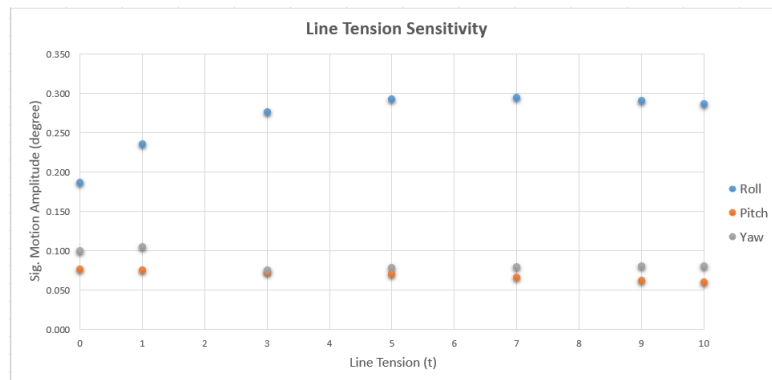


Figure 10.26: Sensitivity Test - Line Pre-Tensioning Effects on Vessel Rotation

0 to 10 tonnes the pitch is decreased by 21% while the yaw is decreased by 18%. These changes are significant if this change is also applicable for other wave conditions.

Once again the surge and roll motions greatly vary while the sway motion appears to settle after the pre-tensioning is increased to 3 tonnes, thus it will not be analysed further as it would be highly unlikely that a vessel will not have any pre-tension when berthed.

When comparing the surge motion at pre-tension 0 tonnes to 10 tonnes there is a 75% decrease. When comparing the pre-tension of 0 tonnes and 10 tonnes to the control situation

there is a surge motion decrease of 52% from 0 to 5 tonnes, and 47% when doing from 5 to 10 tonnes. Such drastic changes may suggest that the surge motion will continue to decrease as the line pre-tension is increased.

When comparing the roll motion at pre-tension 0 tonnes to 10 tonnes there is a 54% increase. When comparing the pre-tension of 0 tonnes and 10 tonnes to the control situation there is a roll motion increase of 56% from 0 to 5 tonnes, and a 2% decrease when doing from 5 to 10 tonnes. This would suggest that the roll motion may reach an equilibrium value as the pre-tension is increased.

Comparing the effect pre-tensioning has on the surge and roll motion it is clear to see that they work in opposite directions. Here one must decide whether it is more important to decrease the surge while increasing the roll motion. However, if the roll motion will appear to have reached an equilibrium at approximately 5-7 tonnes then one may suggest the vessels captain to increase the mooring line pre-tension to decrease the overall surge motion.

A study has been conducted by [1] in which they look at how different pre-tensions affect a floating platform. They go on to discuss that mooring lines are pre-tensioned so their energy absorption can be used to reduce the motion of the platform. It is worth noting that this study is done for a floating platform but the concept is similar to that used for berthed vessels. A similar study was done by [30]. This study showed how by increasing the pre-tension it is possible to reduce the RAO of a moored ship. It is worth noting that, once again, this study was done for a floating body and not a berthed vessel in a port.

This being said, it is also important to see the effect of changing the pre-tension with regards to how the mooring line forces will react. The forces are shown in the figure below.

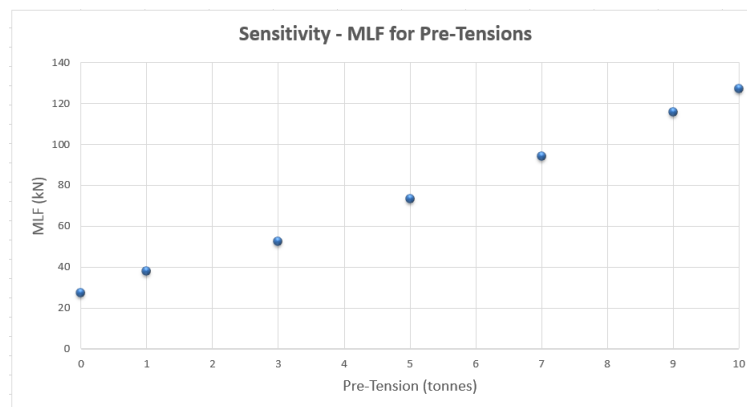


Figure 10.27: Sensitivity Test - Line Pre-Tension Effect on Mooring Line Forces

Here it is worth noting that as the line pre-tension increases then forces on the mooring lines increase. By increasing the pre-tension from 0 to 10 tonnes the forces on the mooring lines have also been increased by 366%. This can very quickly lead to unsafe working conditions when the wave climate increases, assuming that this increase will be the same for all wave conditions. Therefore a compromise must be made between decreasing the vessels surge motion to an extent in which the forces on the mooring lines must be kept

sufficiently low to ensure safe working conditions.

### Seawater Density

The final sensitivity analysis which has been performed is that which discusses effects of various seawater densities. For this study the density is increased from that of fresh water ( $1000 \frac{kg}{m^3}$ ) to that of a highly dense condition ( $1050 \frac{kg}{m^3}$ ). This does not have any major effects for the expansion of the Port of Reykjavik as the density of the surface seawater does not vary greatly throughout the course of the year.

Table 10.5: Sensitivity Test - Seawater Density Data Points

	Seawater Density (kg/m3)										
	1000	1005	1010	1015	1020	1025	1030	1035	1040	1045	1050
Surge (m)	0.061	0.060	0.062	0.061	0.060	0.063	0.063	0.063	0.061	0.059	0.059
Sway (m)	0.082	0.082	0.082	0.082	0.082	0.082	0.082	0.082	0.082	0.082	0.082
Heave (m)	0.053	0.053	0.053	0.053	0.053	0.053	0.053	0.053	0.053	0.053	0.053
Roll (deg)	0.294	0.294	0.293	0.293	0.293	0.293	0.292	0.292	0.292	0.291	0.291
Pitch (deg)	0.070	0.070	0.070	0.070	0.070	0.070	0.070	0.070	0.070	0.070	0.070
Yaw (deg)	0.080	0.079	0.079	0.079	0.079	0.078	0.078	0.078	0.078	0.077	0.077

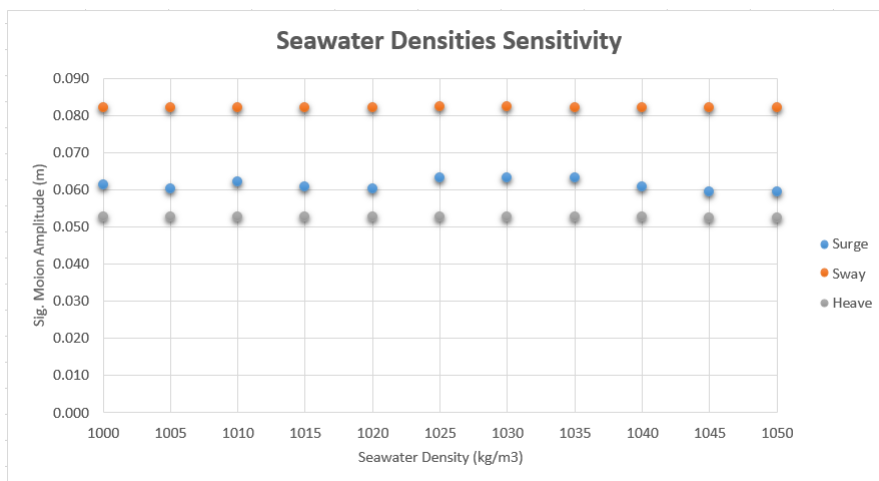


Figure 10.28: Sensitivity Test - Seawater Density Effects on Vessel Displacement

As seen in figures 10.28 and 10.29 a change in the seawater density does not have any major impact on any of the six degrees of motion.

Seeing as there is no large variation in the six degrees of motion one would expect a similar result when looking at the mooring line forces.

As expected there is no major difference between the mooring forces. There is a 0.4kN difference between the maximum and minimum value and this may be ignored as it accounts to a 0.5% difference.

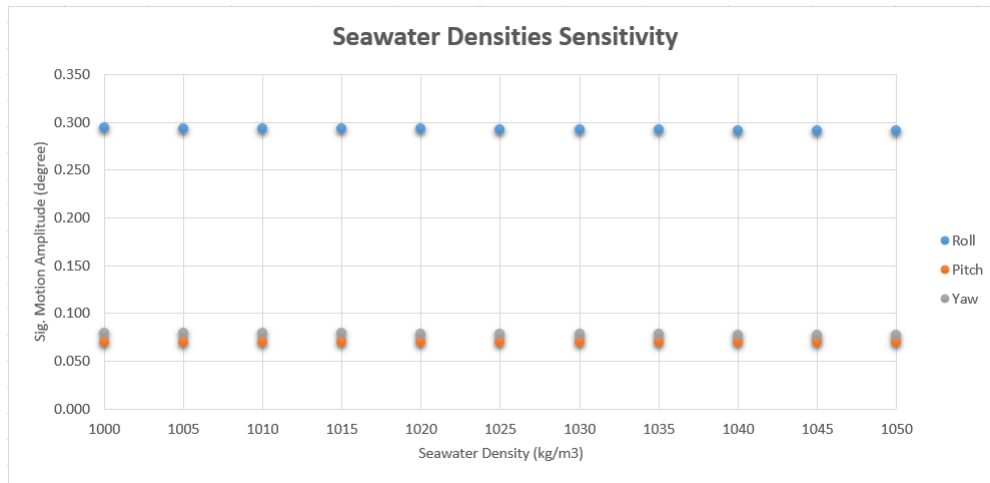


Figure 10.29: Sensitivity Test - Seawater Density Effects on Vessel Rotation

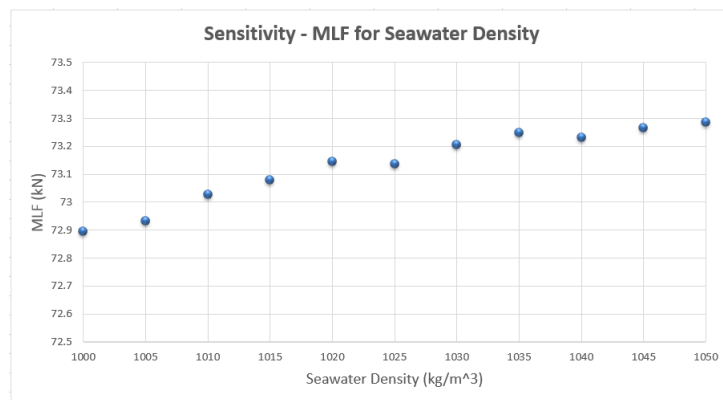


Figure 10.30: Sensitivity Test - Seawater Density Mooring Line Forces



## 11 Discussion

When the MIKE21 BW model was run the depth at Hafnarbakki utan Klepps was 15.7m, as per the recommendations from Reykjavik. They were however not able to state whether or not a new navigation channel would be dredged and if so where it would be located. A study done by [12] compares the effect of including a detailed bathymetry for the Port of Zeebrugge by using two different software packages, MILDwave and MIKE21 BW, and comparing the long and short crested waves.

Here they compared the effects of including a navigation channel or not on the wave agitation coefficients at different location. They concluded that by adding the navigation channel into the bathymetry the MIKE21 BW model gave a higher W.A.C. as this was most likely due to non-linear wave effects caused by the varying bathymetry around the navigation channel. It would therefore be advised to run the MIKE21 BW simulations for the Port of Reykjavik once again if there is to be a new navigation channel as it may alter the W.A.C. and in turn alter the vessel motion.

By comparing the exceedance results from the surge motions and the wave height at Hafnarbakki utan Klepps it is clear to see that Godafoss will have surpassed the surge motion criteria set out by [28] more often than Hafnarbakki utan Klepps will have a wave height above 0.5m as suggested by [35] & [18]. For this specific case it may be worth reconsidering the way in which the proposed expansion should take place. A suggestion may be to extend the breakwater or possibly making a minor structural extension in front of the area in which the vessel is currently berthed to protect the vessel from incoming waves.

It is worth noting that for this report and for other studies the focus is to look at each motion individually. It may not be realistic to do this as it is highly unlikely that a vessel only moves in one direction at a time, but rather a combination of movements. The work done by [11] describes how port operators and Ship-to-Shore crane drivers deal with the movements of berthed container vessels when (un)loading containers. Twenty-nine questionnaires were sent to different harbours to ask them if they felt the guidelines from PIANC were in relation to field observations, here the aforementioned guideline is PIANC 1995. Unfortunately only two questionnaires were returned successfully. Although this is a poor return and no definitive conclusion was drawn, [11] noticed that there were some similarities to the answers. These conclusions were that there was a difference in the handling reduction with respect to the vessel size.

With regards to the PIANC guidelines, both harbour masters agreed that the criteria for surge, sway and heave should be stricter than those presented in the PIANC guidelines. However, (un)loading operations were usually stopped due to heavy winds making it unsafe to continue. This study also included a view as how the six degrees of freedom effect the (un)loading capabilities of STS crane operators. An interesting conclusion from the study was that there is no current guideline of how to design for a combination of motions. The quickest decrease in handling rate was the combination of surge and sway than for surge or sway individually. This may lead to the question of how to find an adequate standard for the combination of motions.

The peak wave period which was present from the MIKE21 SW modelling may not necessarily be considered to be seiching (wave with a period of 0.5-30 minutes) it is still

important to understand the effects of long waves on berthed vessels. A paper by [17] discusses these effects in two different harbours, Torsminde (Denmark) and Long Beach (USA). In both instances a MIKE21 BW model has been used. In this paper the harbour entrance to Torsminde was changed and this reduced the effects of the long wave inside the harbour basin. Such a similar approach may be applicable to the expansion of the Port of Reykjavik, if this is deemed necessary.

Although seiching is not necessarily present it is clear to see that the long waves had a greater effect on the vessel motion than the shorter waves. When analysing the graphical results presented in Appendix C a clear assessment can be made. Waves with a larger peak period produced larger vessel motions. This was clear for each case and it is due to the fact that longer wave allow greater vessel movement. This concept is explained in figure 11.1. From this it may be advisable for the Port Authorities in Reykjavik to see if it is possible to reduce the effects of long waves by possibly extending the current breakwater or extending the berth at Kleppsbakki so it may provide some additional protection.

A study regarding the effects of long waves on a harbour in Japan has been conducted by [31]. They discovered that low-frequency motion of ships is induced by a resonance effect between the surge motions & long-period waves or harbour oscillations. This gave an increased vessel motion which compromised the safety of the mooring lines and the cargo handling efficiency. Although no structural changes to the harbour were made [31] determined that an efficient counter measure to the increased vessel motion was to change the mooring configuration/system.

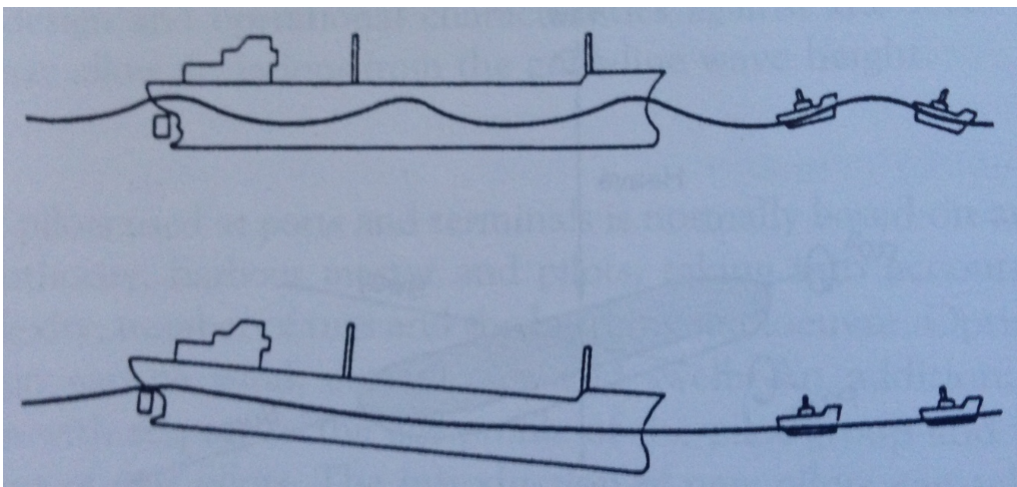


Figure 11.1: The effect of long waves on larger vessels, [35]

When running the MIKE21 BW simulations a time series for the surface elevations at grind points 1900,1050 (berth) and 460,1050 (offshore) has been extracted for the simulation of  $H_{m0}$  1m,  $T_p$  /10/12/15s, MWD 290 degrees. Using the program WS Linear Spectral Analysis, from the MIKE Zero toolbox, a frequency spectra has been created to compare the waves offshore to those at the berth area, see figures 11.2 & 11.3 where the X-axis is the frequency (Hz) and the Y-axis is the spectral density ( $\frac{m^2}{Hz}$ ).

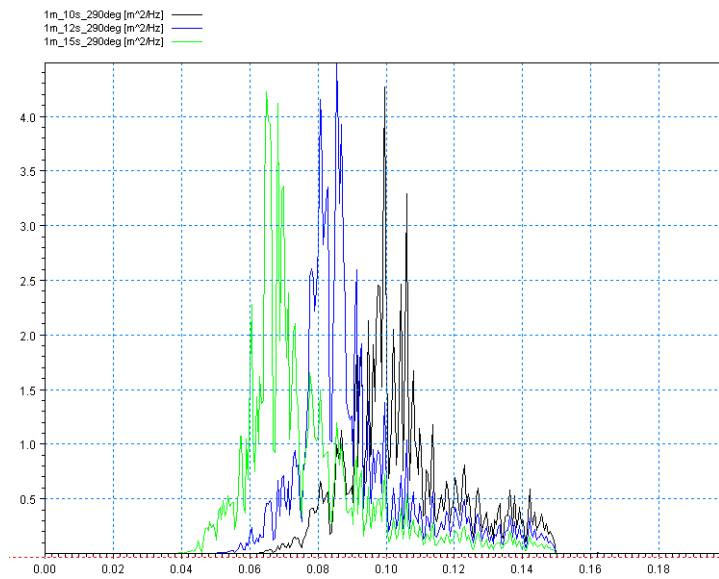


Figure 11.2: Frequency spectrum for the offshore waves

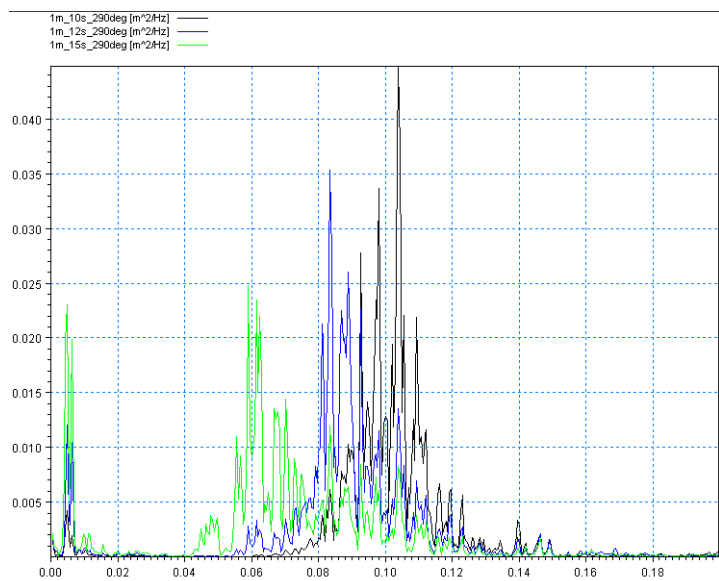


Figure 11.3: Frequency spectrum for the berth waves

It is clear to see in figure 11.3 that there is a small concentration of long waves at the berth. This appears to be very prominent when the wave fields peak wave period is 15s, with a frequency range between 0.004 and 0.008. Thus one can expect a small amount of waves at the berth to be between 125 to 250 seconds (2-4 minutes). It is out of the scope of this thesis to analyse the potential effects they may have but the author felt it was worth mentioning this phenomena.

Climate change is a serious issue which shall not be taken lightly. Unfortunately these

effects where not included in this project. A study on how harbour agitation may change in Catalan ports due to climate change has been undertaken in [32]. They go on to see how a change in the offshore wave height due to climate change would influence the waves within the port area of the 13 chosen ports. Although there was not a significant change during the winter months the wave agitation did increase during the summer months in some of the chosen ports. In some instances they mention there was up to a 20% increase in the wave height within the port area. This can not be underestimated, however there were some uncertainties regarding their models and input data. Yet, as large winter storms are becoming more frequent it may be advisable to forecast the wave climate near Reykjavik. Since the surge motion was mostly exceeded during the winter months this may increase the motion which in turn may lead to failures in the mooring lines.

## 12 Conclusion

After having run the three MIKE programs and determined the exceedance plots it is clear to see that using the current design method of a maximum wave at the berth of 0.5m is not applicable. This is only exceeded 13.5 hours a year while the nearest surge motion was 133 hours, for the Ultraline Dyneema Line & Polyamide tail with a wind speed of  $15 \frac{m}{s}$  coming at  $250^\circ$ . This may lead to a new thinking of how ports are to be designed. It is clear to see that when the vessel has exceeded the surge criteria of motion it is no longer to proceed with the (un)loading operation and this results in unwanted downtime. When comparing the highest and lowest surge exceedance times, both for the Ultraline Dyneema Line and Polyamide tail, there is a large difference between the two. Comparing 133 hours (roughly 5.5 days) while 202 hours (approximately 8.4 days) there is almost an additional 3 days of downtime. This is assuming the wind conditions will remain constant throughout the entire year. Since this is not feasible it is better to see the surge time series for the 20 year time period. Here it can be seen that the surge motion will exceed the criteria set out by PIANC 2012 primarily during the winter period. Therefore the Port Authorities in Reykjavik can expect Godafoss to exceed the surge motion criteria during this time. If possible it may be advisable to not have any vessels at berth during the larger winter storms as this may cause excessive vessel motions which in turn may break the mooring lines. This may cause the vessel to drift and damage the superstructure and itself.

## 13 Recommendations

In this section a few recommendations have been created if this project were to be undertaken once more, along with some future recommendations for similar studies.

The main recommendation the author would have for this study is to change the approach to how the DVRS scenarios were modelled. It may be advisable not to model each all the wave scenarios for one wind direction as it may vary during time. Therefore the author would suggest to expand the wind sensitivity study. It may be advised to use different wind speeds such as 5, 10, &  $15 \frac{m}{s}$  along with different wave input data. From this it may be possible to see how the vessel motion scale with regards to the wind speed and if the motion changes proportionally or not to the wave input data. Initially the test can be done using the same significant wave height and mean wave direction but altering the wave peak period. A second series of tests can be done where only the significant wave height is changed. Although this would be a rather extensive study it can give an indication as to which wind directions are the most critical with regards to the different wave input data.

When using the DVRS program it was assumed that the winches onboard the vessels are brake winches. This may not be the case for all vessels as some have self tensioning winches. A downside to using these self tensioning winches is that they can cause the vessel to "walk" along the berth. How the effects of self tensioning winches would be applied to the DVRS model is uncertain yet it may be worth considering if the shipping company does not specify if they are used or not.

In this project only one location at Hafnarbakki utan Klepps was considered and it was the most exposed location. If the Port Authorities in Reykjavik consider the surge motion

exceedance to be too great then the project can be redone by moving Godafoss further down the berth. This may help to minimize the surge motions and reducing the surge motions to an acceptable level. If possible it would be interesting to compare any measurements which can be taken at Hafnarbakki utan Klepps with those presented in this report, if no other structural changes are done in the vicinity.

## 14 References

- [1] Ahmed, M.O, et al. (2014). *Behaviour of Mooring Systems for Different Line Pretensions*. Applied Mechanics and Materials. Vol 567. PP 205-209. trans Tech Publications. Switzerland.
- [2] Bakermans, B.A. (2014). *Open Ports for Container Vessel. An exploratory study into the possibilities for offshore and exposed container ports*. Master Thesis. Delft University of Technology. Delft, the Netherlands.
- [3] BEXCO. (2007). *Product Catalogue*. BEXCO NV. Hamme, Belgium.
- [4] Christensen, E.D. et al. (2008). *Numerical Simulation of Ship Motion in Offshore and Harbour Areas*. Proceedings of the ASME 27th International Conference on Offshore Mechanics and Arctic Engineering. Estoril, Portugal.
- [5] Clarke, Ian. *Mooring - getting it right. Protecting people and ports from damaging and fatal accidents*. Port Technology International. The Nautical Institute. London, The United Kingdom.
- [6] Cunff, C.L. et al. (2008). *Frequency-Domain Calculations of Moored Vessel Motion Including Low Frequency Effect*. roceedings of the ASME 27th International Conference on Offshore Mechanics and Arctic Engineering. Estoril, Portugal.
- [7] DHI. (2016). *MIKE21 Spectral Wave Module, Scientific Documentation*. MIKE 2016. Hørsholm, Denmark.
- [8] DHI. (2016). *MIKE21 Boussinesq Wave Module, Scientific Dcoumentation*. MIKE 2016. Hørsholm, Denmark.
- [9] DHI. (2016). *Dynamic Vessel Response Simulator, User Guide Incl. Step-by-step guide and Scientific Documentation*. MIKE 2016. Hørsholm, Denmark.
- [10] Fentek. (2000). *Marine Fendering Systems*. Product Catalogue. Fentek Marine Systems GmbH. Hamburg, Germany.
- [11] Goedhart, G.J. (2002). *Criteria for (un)loading Container ships*. Master Thesis. Delft University of Technology. Delft, The Netherlands.
- [12] Gruwez, Vincent et al. (2012). *Numerical wave penetration modelling and comparison with physical model and field measurements for the harbour of Zeebrugge*. Flanders Marine Institute. Oostende, Belgium.
- [13] Hansen, H.F. et al. (2009). *Multi Vessel Interaction in Shallow Water*. Proceedings of the ASME 2009 28th International Conference on Offshore Mechanics and Arctic Engineering. Honolulu, USA.
- [14] Holthuijsen, Leo O. (2007). *Waves in Oceanic and Coastal Waters*. First edition. Cambridge University Press. New York, USA.

- 
- [15] Jónsdóttir, I.E & S. Sigudarson. (2014). *Öldufar á Sundunum. Öldufarsrannsóknir og mat á vidleguskilyrdum í Sundahöfn*. Faxaflóahafnir sf, Associated Icelandic Ports. Reykjavik, Iceland.
- [16] Kirkegaard, Jens. *Wave Agitation Modelling for Ports and Terminals*. DHI. Hørsholm, Denmark.
- [17] Kofoed-Hansen, H., et al. (2005). *Simulation of Long Wave Agitation in Ports and Harbours using a Time-Domain Boussinesq Model*. Fifth International Symposium on Ocean Wave Measurement and Analysis. 3-7 July, 2005. Madrid, Spain.
- [18] Ligteringen, H. & H. Velsink.(2012). *Ports and Terminals*. First edition. VSSD. Delft, the Netherlands.
- [19] Madsen, P.A., et al. (1991). *A new form of the Boussinesq equations with improved linear dispersion characteristics*. (Part 1). Coastal Engineering, 15. PP 371-388. Elsevier Science Publishers B.V. Amsterdam, the Netherlands.
- [20] Madsen, P.A. O.R. Sørensen. (1992). *A new form of the Boussinesq equations with improved linear dispersion characteristics. Part 2. A slowly-varying bathymetry*. (Part 2). Coastal Engineering, 18. PP 183-204. Elsevier Science Publishers B.V. Amsterdam, the Netherlands.
- [21] Madsen, P.A., et al. (1997). *Surf zone dynamics simulated by a Boussinesq type model. Part I. Model description and cross-shore motion of regular waves*. Coastal Engineering, 32. PP 255-287. Elsevier Science Publishers B.V. Amsterdam, the Netherlands.
- [22] Madsen, P.A. et al. (1997). *Surf zone dynamics simulated by a Boussinesq type model. Part II: surf beat and swash oscillations for wave groups and irregular waves*. Coastal Engineering, 32. PP 289-319. Elsevier Science Publishers B.V. Amsterdam, the Netherlands.
- [23] Moes, H. & Luther Terblanche. (2010). *Motion criteria for the efficient (un)loading of container vessels*. Stellenbosch, South Africa. Web link: [http://repository.tudelft.nl/assets/uuid:4b2de4a2-9200-4d74-b825-6085618916ee/Motion\\_criteria\\_for\\_the\\_efficient\\_unloading\\_of\\_container\\_vessels\\_Hans\\_Moes.pdf](http://repository.tudelft.nl/assets/uuid:4b2de4a2-9200-4d74-b825-6085618916ee/Motion_criteria_for_the_efficient_unloading_of_container_vessels_Hans_Moes.pdf)
- [24] Murdoch, E. et al. (2012). *A Mesters Guide to: Berthing*. Second Edition. The Standard P& I Club. Standard House. London, England.
- [25] Nielsen, B.M. (2016). *Hirsthals Harbour Vessel Entrance Criteria*. Personal communication via telephone.
- [26] OCIMF. (1989). *Effective Mooring*. Publisher: Witherby & Co. LTD. London, England.
- [27] OCIMF. (2009). *Mooring Equipment Guidelines*. Third Edition. Oil Companies International Marine Forum. Withersby Seamanship International. Livingston, the United Kingdom.



- 
- [28] PIANC. (2012). *Criteria for the (un)loading of container vessels*. Report n° 115-2012. The World Association for Waterborne Transport Infrastructure. Bruxelles, Belgium.
- [29] Rosa-Santos, P.J. & F. Taveira-Pinto. (2013). *Experimental study of solutions to reduce downtime problems in ocean facing ports: the Port of Leixões, Portugal, case study*. Journal of Applied Water Engineering and Research.
- [30] Sajjan, S.C. & S. Surendran. (2013). *Effect of Pretension on Moored Ship Response*. International Journal of Ocean System Engineering. PP. 175-187.
- [31] Sakakibara, S. & M. Kubo. (2008). *Characteristics of low-frequency motions of ships moored inside ports and harbors on the basis of field observations*. Marine Structures, 21. PP 196-223. Elsevier Science Publishers B.V. Amsterdam, the Netherlands.
- [32] Sierra, J.P., et al. (2015). *Impacts on wave-driven harbour agitation due to climate change in Catalan ports*. Natural Hazards and Earth System Sciences. PP 1695-1709. Copernicus Publications.
- [33] Sørensen, O.R. et al. (1998). *Surf zone dynamics simulated by a Boussinesq type model. Part III. Wave-induced horizontal nearshore circulations*. Coastal Engineering, 33. PP 155-176. Elsevier Science Publishers B.V. Amsterdam, the Netherlands.
- [34] Sørensen, O.R. et al. (2004). *Boussinesq-type modelling using an unstructured finited element technique*. Coastal Engineering, 50. PP 181-198. Elsevier Science Publishers B.V. Amsterdam, the Netherlands.
- [35] Thorensen, C.A. (2010). *Port Designer's Handbook*. Second Edition. Thomas Telford Limited. London, The United Kingdom.
- [36] van den Bos, W. *Wind influence on container handling, equipment and stacking*. Port Technology International. [https://www.porttechnology.org/images/uploads/technical\\_papers/PT29-19.pdf](https://www.porttechnology.org/images/uploads/technical_papers/PT29-19.pdf)

## A Appendix - Project Outline

# Master Thesis Project Outline/Plan - Dynamic Vessel Response Modelling for Port Design and Operation

Hans Christian Bencard Nielsen (s136324)

The Technical University of Denmark (DTU)

Supervisor: Erik Damgaard Christensen (DTU)

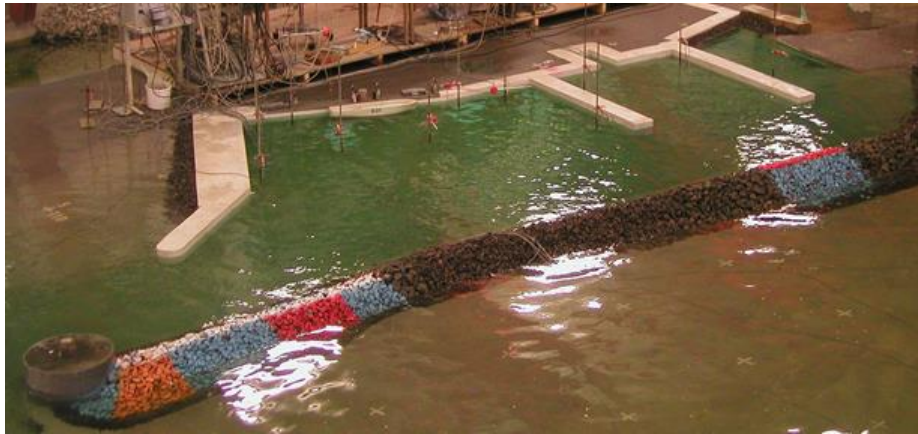
Co-Supervisor: Peter Sloth, Senior Project Manager and Specialist Consultant, DHI DK-POT  
Bjarne Jensen, Research Engineer, DK-POT (support on DVRS)  
Jens Kirkegaard, Port specialist Consultant (40+ years' experience on ports)

Company: DHI, Agern Alle 5, 2970 Hørsholm, Denmark

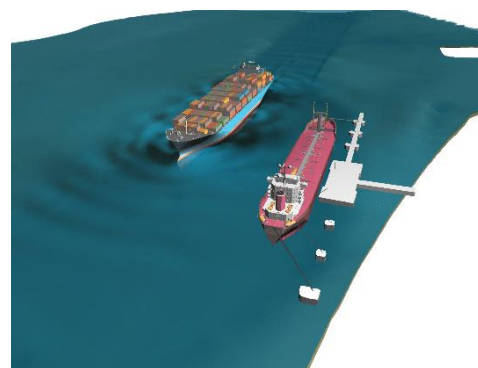
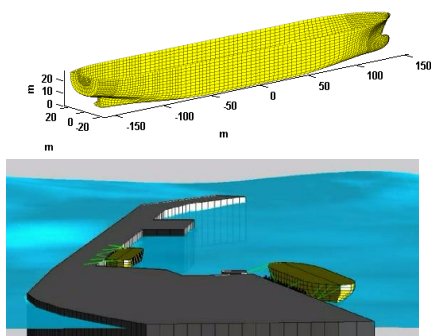
Timeline: January 4<sup>th</sup> to June 4<sup>th</sup>, 2016

## Abstract:

Downtime in ports and terminals is often related to excessive vessel motions caused by wind and waves and particularly long period waves. Accurate estimation of downtime is an important task for planning and designing new harbours as well as for increasing the operation efficiency of existing facilities. Often downtime (caused by waves) is estimated based on numerical results from wave agitation models only and experienced/empirical based criteria such as PIANC (1995)<sup>1</sup> or similar guidelines. Physical modelling of waves, vessel motions and mooring/fender forces has been best practice for decades, but nowadays often replaced by usage of numerical wave and vessel response modelling tools.



*Physical modelling of wave agitation and vessel response.*



*Numerical modelling of wave agitation and vessel response.*

---

<sup>1</sup> PIANC (1995). *Criteria for movements of moored ships in harbours: a practical guide (Supplement to bulletin No 88). Report of working group PTC II-24.*

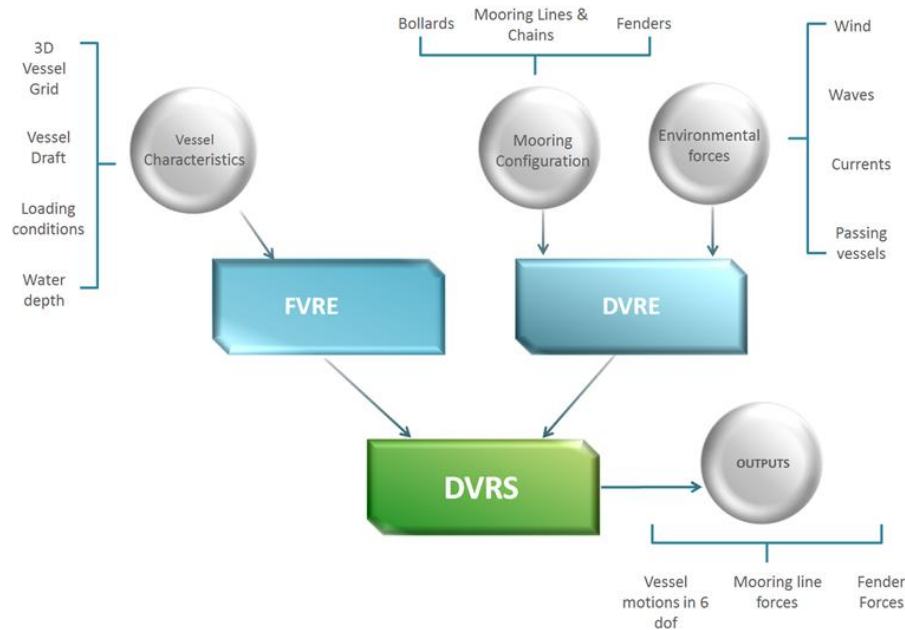
## Objective:

The objective of the project is to assess the value of using state-of-the-art numerical models to estimate the downtime of a port compared to more traditional and often applied methods - such as the PIANC & OCIMF guidelines and wave height related criteria. It is proposed to illustrate this value by considering a case study – in this project the Port of Reykjavik.

The project will cover following aspects:

- Wind and wave statistics at the port
- Calculation of wave agitation using MIKE 21 BW
- Calculation of vessels response for one or more vessel types using DHI's new model DVRS included in MIKE Powered by DHI Release 2016<sup>2</sup>
- Assessment of port/vessel downtime using various methods
  - New DVRS Model created by DHI
  - PIANC and OCIMF guidelines
  - Comparison of the results
- Use different mooring configurations to evaluate possible downtime reduction

## Overview of the DVRS Model



## Project Background:

Port downtime is often estimated using simple empirical methods where only the wave conditions are considered. This may lead to inaccurate estimates resulting in ineffective port facilities or in designs being unnecessary expensive. Ultimately, the downtime should be based on expected ship movements, as in most cases this defines the downtime.

---

<sup>2</sup> Released December 2015. The model is similar to the WAMSIM model DHI invented 10-15 years ago and used in various R&D and commercial projects worldwide.

# Master Thesis Project Outline/Plan - Dynamic Vessel Response Modelling for Port Design and Operation

Hans Christian Bencard Nielsen (s136324)

The Technical University of Denmark (DTU)

To compare the different methods and to document the value of conducting ship movement modelling a case study has been selected.

The port authorities in Reykjavik have done a preliminary study for the Port of Reykjavik in which they discuss the potential for an expansion including new berth facilities. The study included modelling of wave conditions but not any ship movement modelling. Therefore, the conclusions were solely based on empirical wave height criteria.

In the present project, the Reykjavik port expansion case will be investigated including advanced wave agitation and ship movement models to obtain accurate estimates of the vessel downtime at the new berths and to be able to optimise the port layout as well as the mooring arrangements.

## Schedule:

The proposed project will be subdivided into the following sections and a work schedule has been proposed to allow for a full completion of the project itself. It is worth noting that the timeframe may alter as the work progresses. The project end date is June 4<sup>th</sup>, 2016.

Task	Timeframe
Thesis Writing	Continuous
Input Data <ul style="list-style-type: none"><li>• Wind and wave data</li><li>• Bathymetry, port layout</li><li>• Vessel data</li></ul>	January - February
MIKE 21 BW Modelling <ul style="list-style-type: none"><li>• Model Set-up</li><li>• Input data</li><li>• Bathymetry, sponge layer, wave characteristics, current, port layout, porosity map, etc</li><li>• Simulations</li></ul>	January - February
DVRS Modelling <ul style="list-style-type: none"><li>• Set-up</li><li>• Simulation</li></ul>	February - April
Vessel Downtime <ul style="list-style-type: none"><li>• Compare DVRS with PIANC/OCIMF</li></ul>	March - April
Mooring Configuration <ul style="list-style-type: none"><li>• What mooring system is being used</li><li>• What mooring system should be used</li></ul>	April
Port Optimization <ul style="list-style-type: none"><li>• Longer breakwater</li><li>• Maybe over efficient</li><li>• Acceptable downtime</li></ul>	May
Generic Simulations	May

<ul style="list-style-type: none"><li>• Container Vessels</li><li>• Dry Bulk Carriers</li><li>• Liquid Bulk Carriers</li><li>• Ro-Ro Vessels</li><li>• Cruise Vessels</li></ul>	
Literature Study	Continuous

### Thesis Outline

Combining the abovementioned task subdivision it is possible to make a preliminary Table of Contents for the project. This will give an insight into how the thesis will be subdivided into various sections, giving the reader an idea of the final layout.

1. Preface
  - a. Acknowledgements
  - b. Abstract
2. Table of Contents
3. List of Symbols
4. List of Figures
5. List of Tables
6. Introduction
7. Case Study Background Information
  - a. Current layout and issues
8. Literature Review
9. MIKE 21 BW Modelling
  - a. Wind & Wave & Bathymetry Data
  - b. Model for current layout
10. DVRS Modelling
  - a. Vessel motion with current layout
11. Downtime and Mooring Systems
  - a. Waves heights which affect downtime
  - b. Forces on mooring system
  - c. Downtime using DVRS method
  - d. Downtime using PIANC/OCIMF guidelines
  - e. Applicability of new mooring systems
12. Layout Improvements
  - a. Ways to reduce downtime
13. Applicability to other locations
14. Recommendations & Conclusions
15. References
16. Appendices

## General Learning Objectives for the Student:

While writing the master thesis project it is important for the student to set themselves a series of learning objectives. Listed below are the objectives which are expected for the student to achieve.

- can identify and reflect on technical scientific issues and understand the interaction between the various components that make up an issue
- can, on the basis of a clear academic profile, apply elements of current research at international level to develop ideas and solve problems
- masters technical scientific methodologies, theories and tools, and has the capacity take a holistic view of and delimit a complex, open issue, see it in a broader academic and societal perspective and, on this basis, propose a variety of possible actions
- can, via analysis and modelling, develop relevant models, systems and processes for solving technological problems
- can communicate and mediate research-based knowledge both orally and in writing
- is familiar with and can seek out leading international research within his/her specialist area.
- can work independently and reflect on own learning, academic development and specialisation
- masters technical problem-solving at a high level through project work, and has the capacity to work with and manage all phases of a project – including preparation of timetables, design, solution and documentation

## NOTE:

After completion of this thesis project it was, unfortunately, not possible to complete all the tasks which were set out in the time line above. No Generic Simulations or Port Optimization studies were undertaken. This may be due to an over ambitious work load in the presented time schedule and that it was not feasible to continuously do the thesis writing while modelling and analyzing the results.

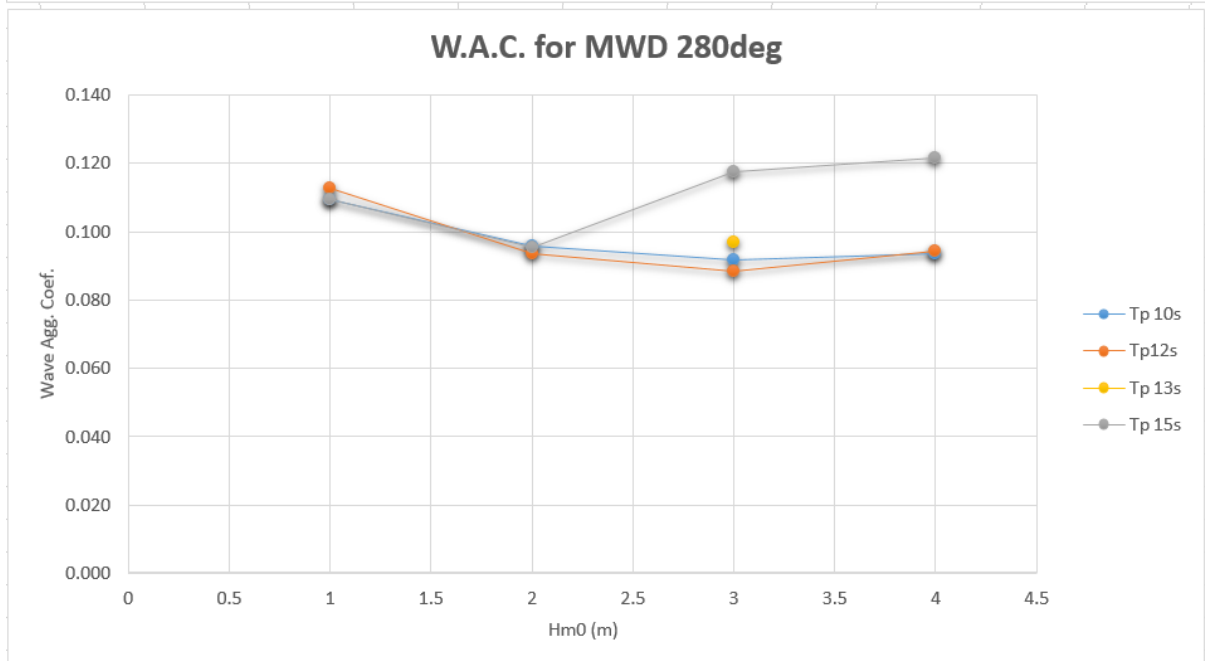
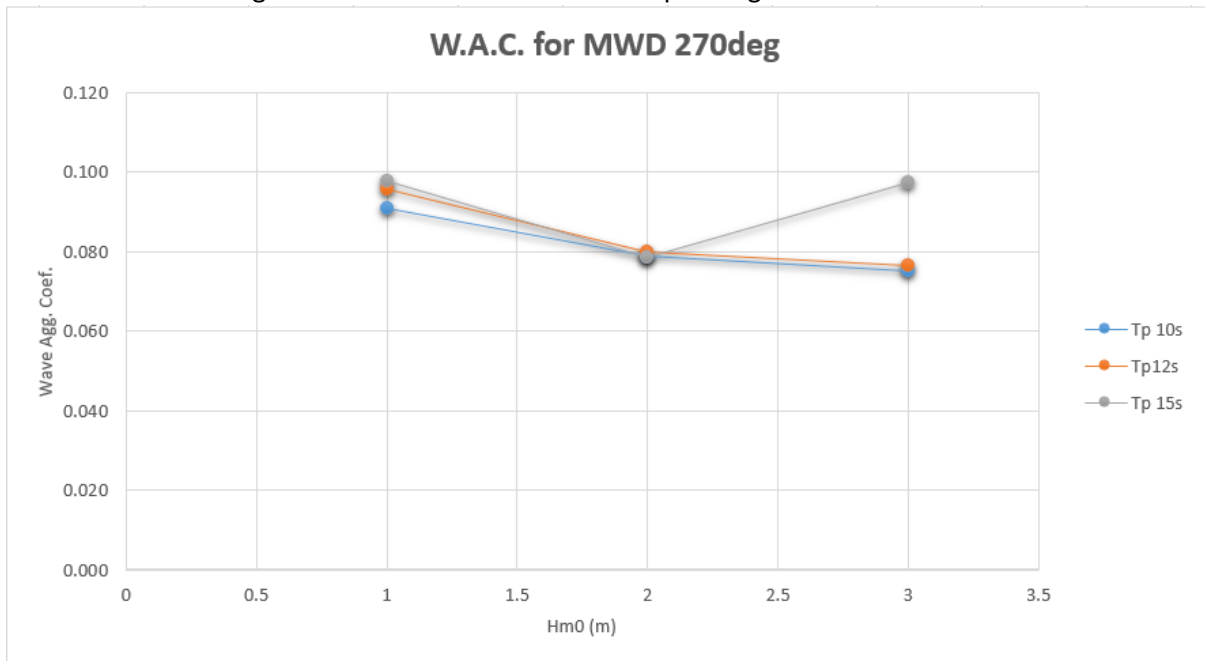
## **B Appendix - Wave Plots**

This appendix shows the plots from all the MIKE21 BW simulations. The first plots are the W.A.C. for all the simulations to demonstrate how they develop, the second series of plots are the surface elevations, followed by  $H_{m0}$  plots of the modelled area finally the  $H_{m0}$  at Hafnarbakki utan Klepps.

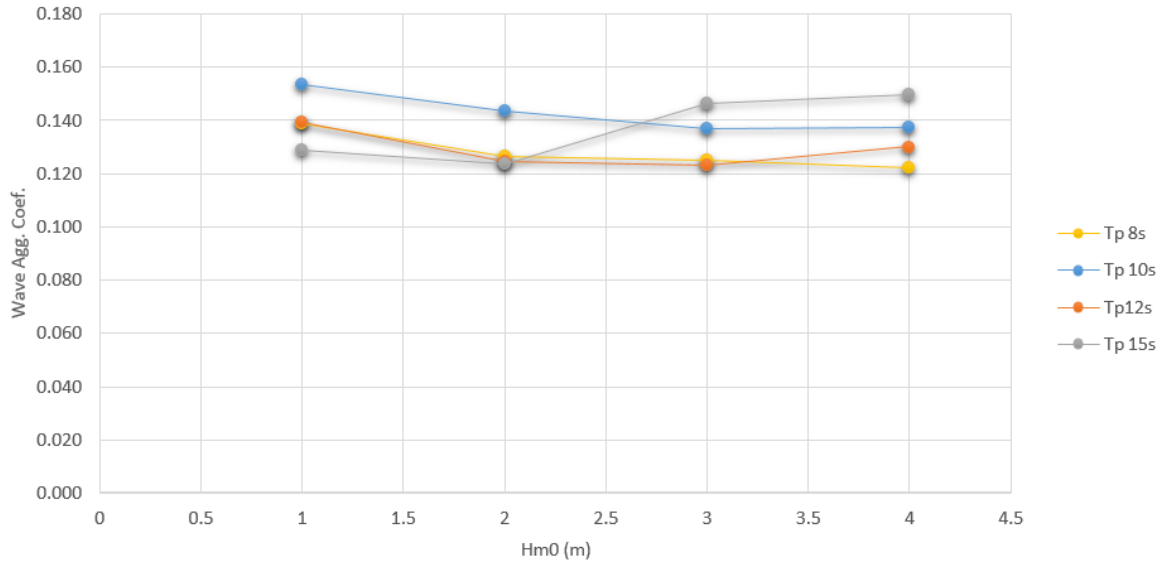
### **B.1 Wave Agitation Coefficients**



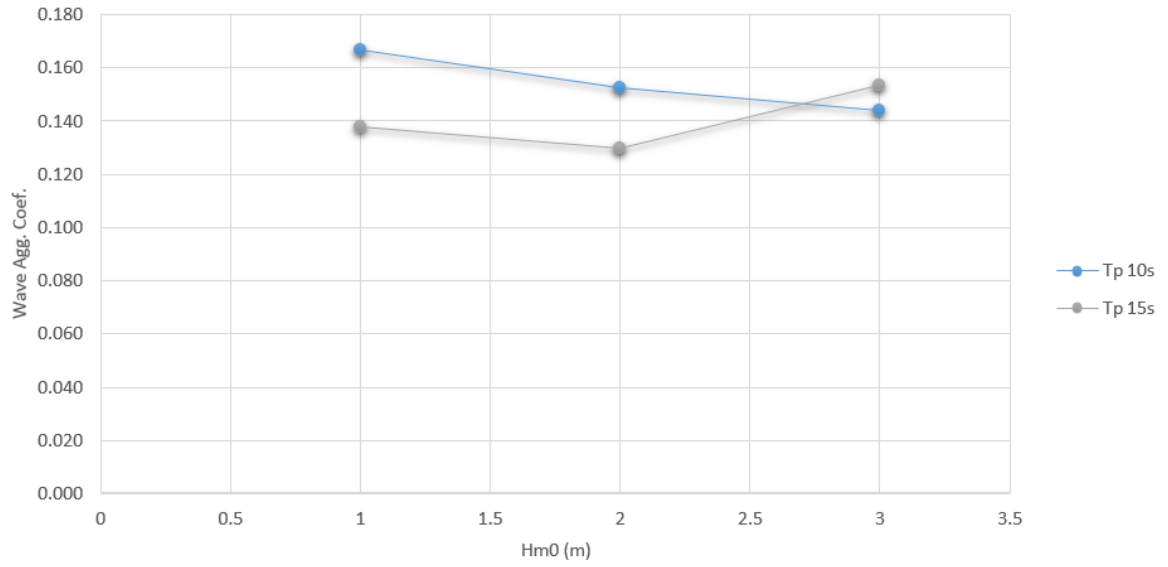
### Wave Agitation Coefficients for the Corresponding Mean Wave Direction



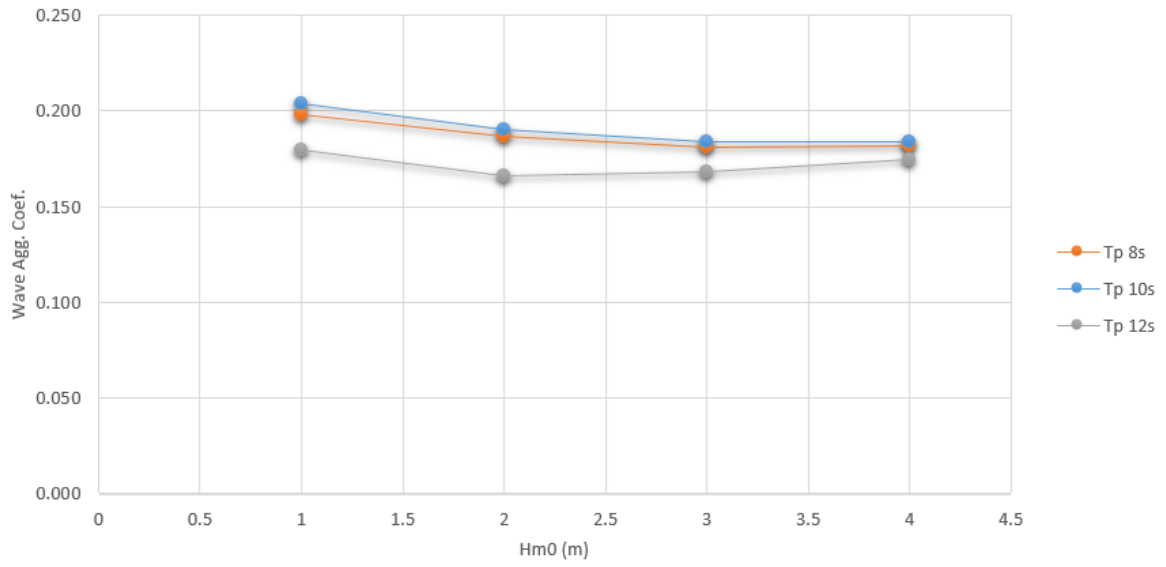
W.A.C. for MWD 290deg



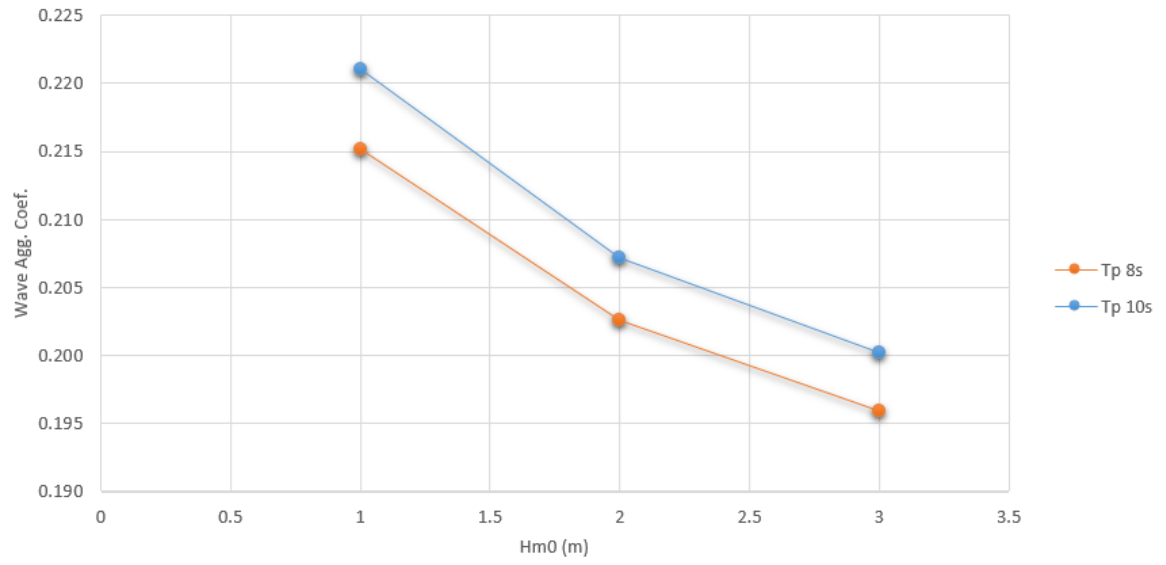
W.A.C. for MWD 292.5deg



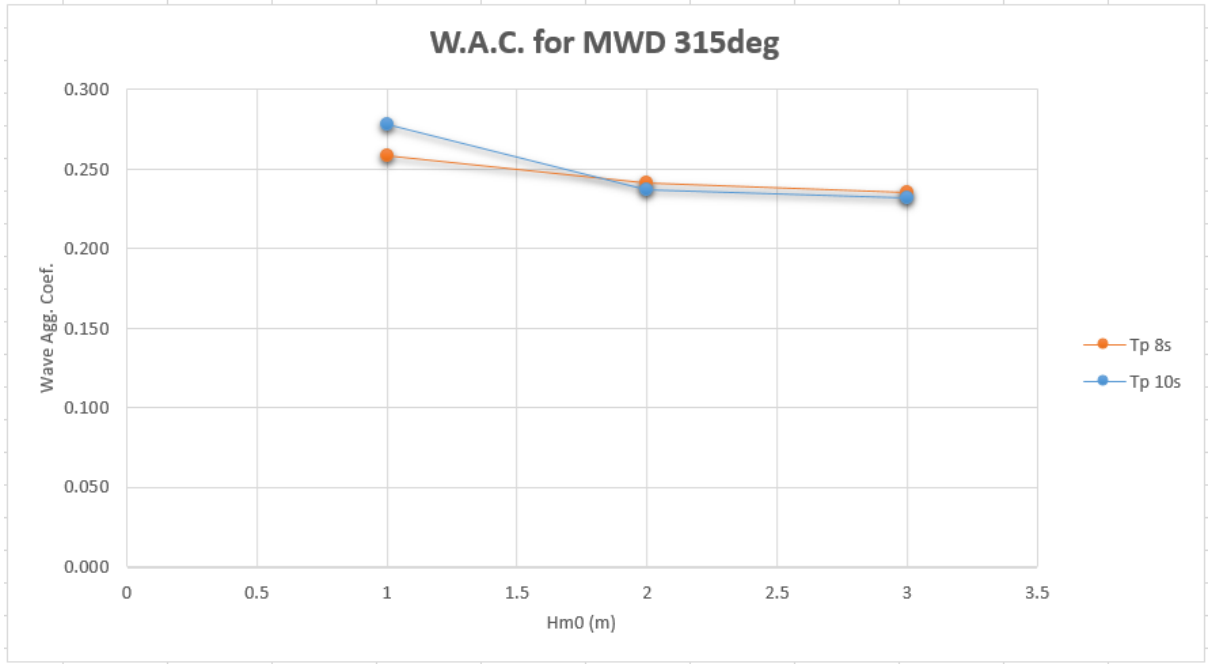
### W.A.C. for MWD 300deg



### W.A.C. for MWD 305deg



### W.A.C. for MWD 315deg

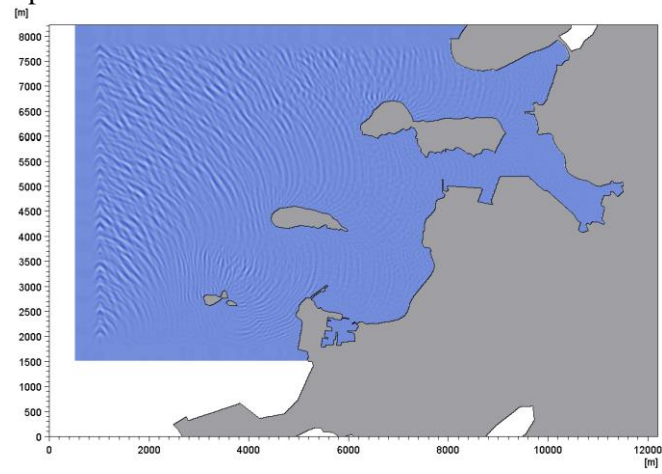


**B.2 Surface Elevation Plots**

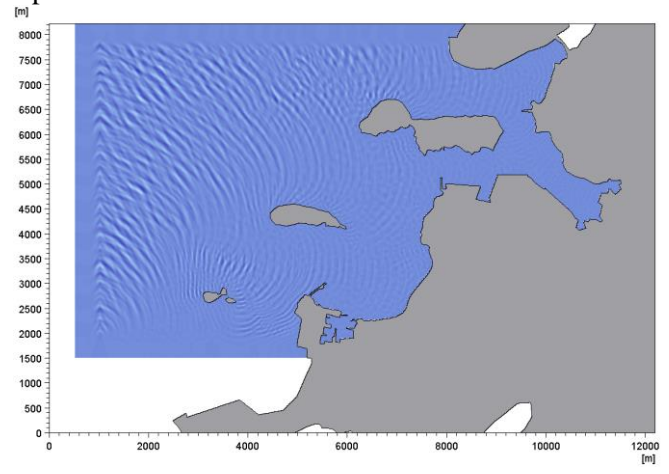
**MWD: 270 degrees**

$H_{m0}$  1m

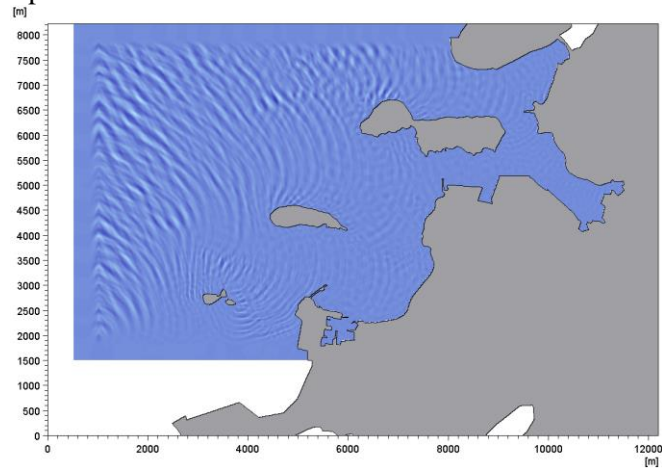
$T_p$  10s



$T_p$  12s

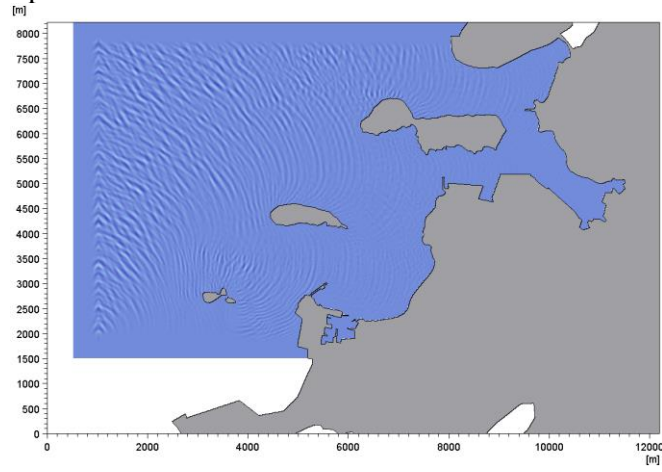


$T_p$  15s

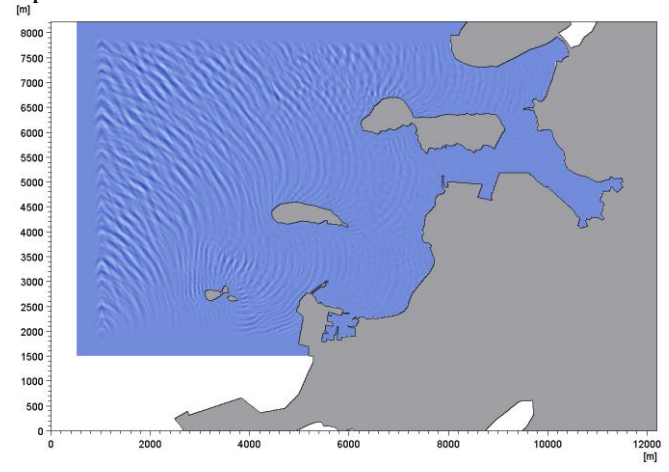


$H_{m0}$  2m

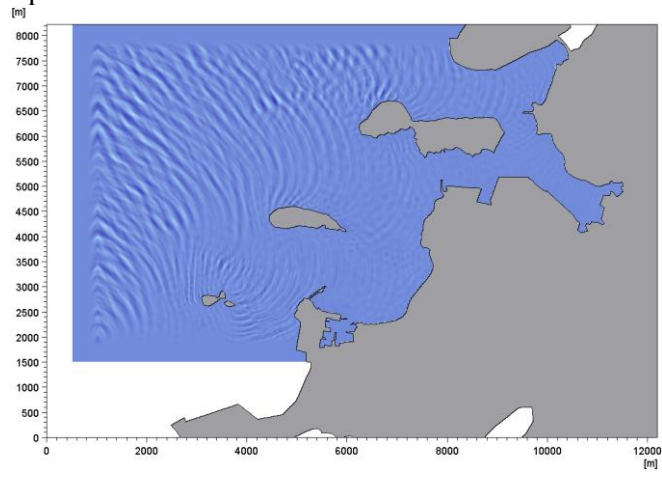
$T_p$  10s



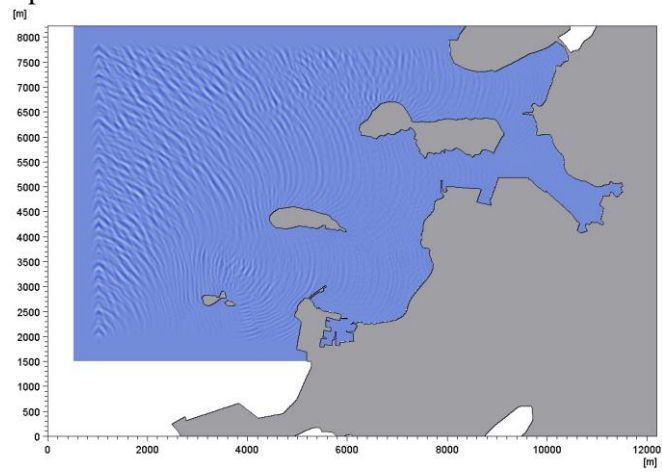
$T_p$  12s



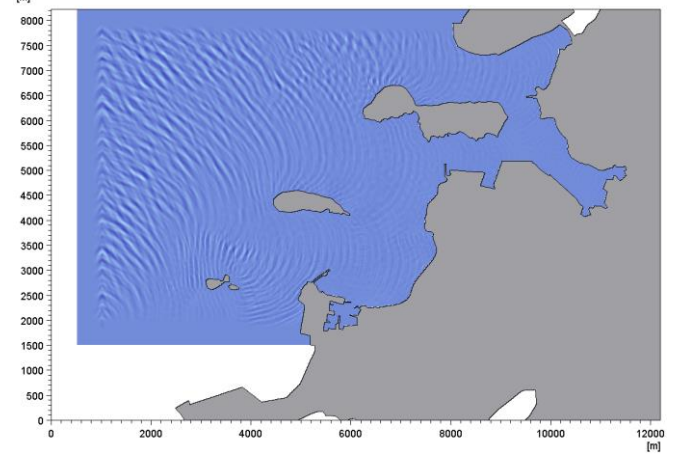
Tp 15s



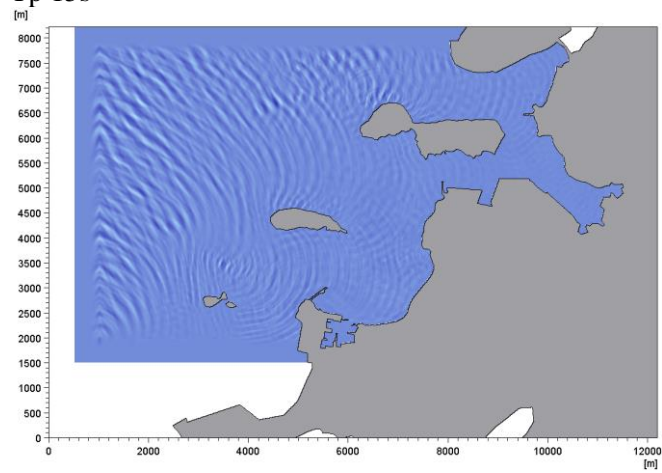
$H_{m0}$  3m  
Tp 10s



Tp 12s



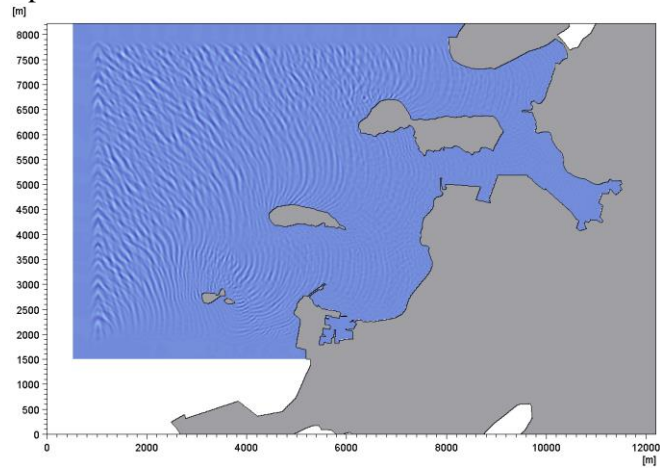
Tp 15s



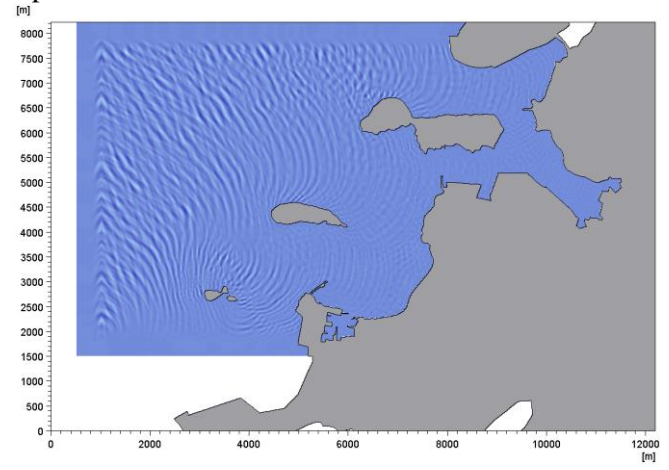
**MWD: 280 degrees**

$H_{m0}$  1m

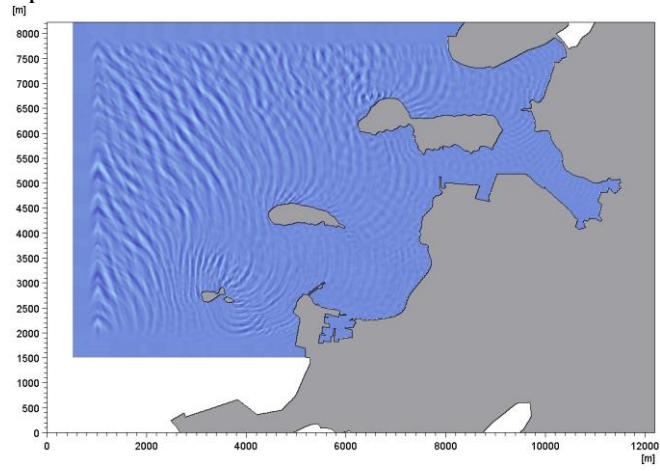
$T_p$  10s



$T_p$  12s

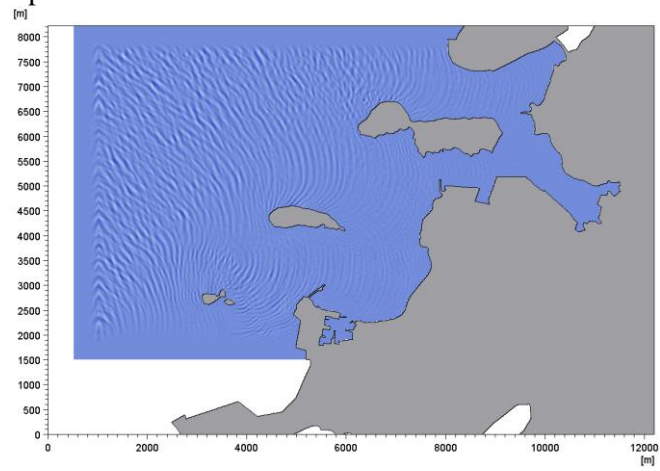


$T_p$  15s

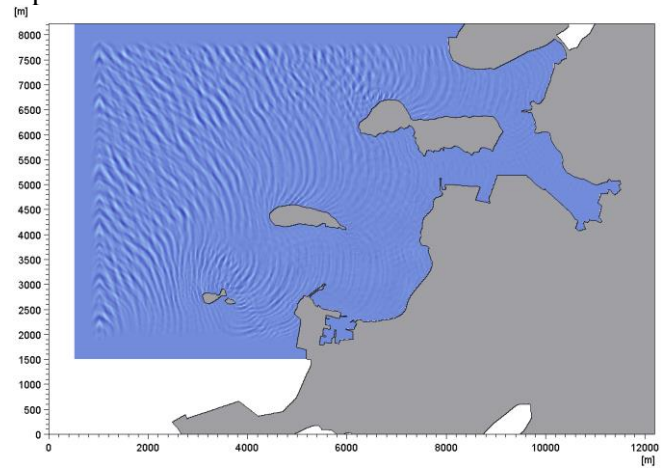


$H_{m0}$  2m

$T_p$  10s

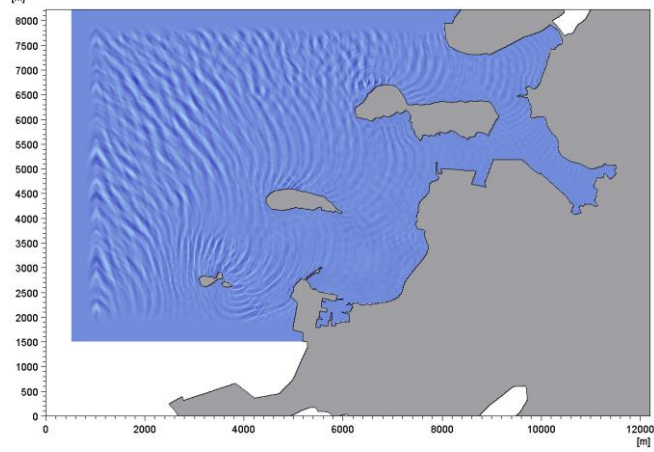


$T_p$  12s



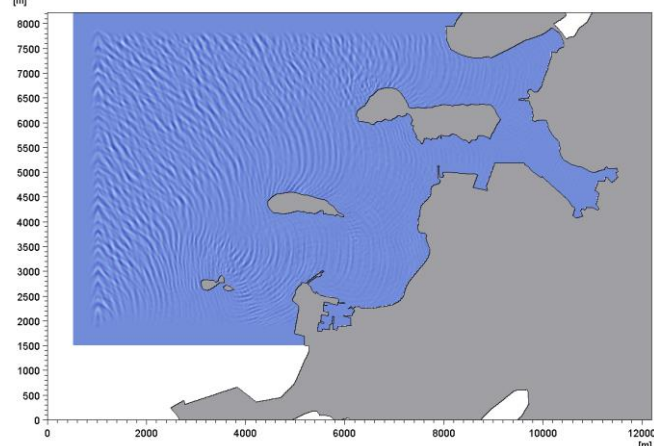


Tp 15s

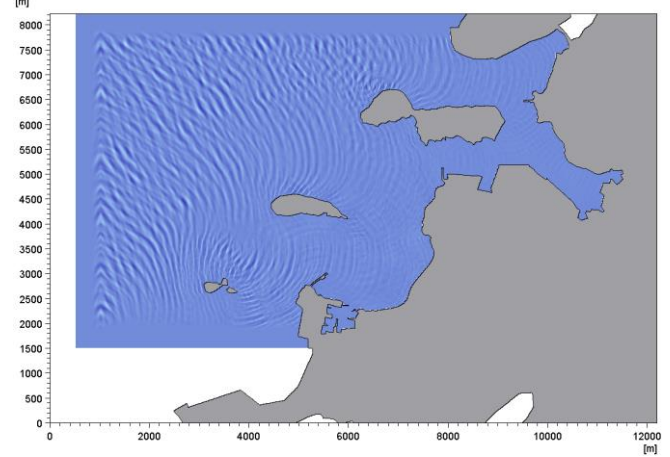


$H_{m0}$  3m

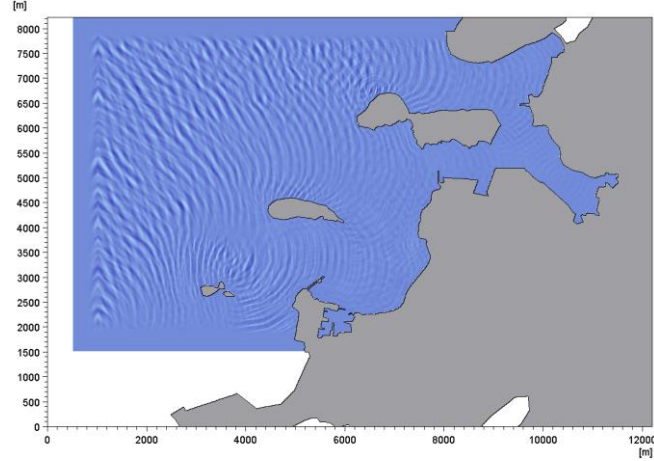
Tp 10s



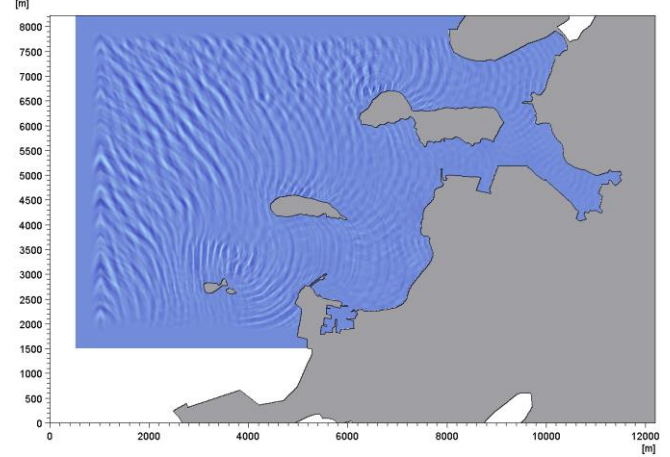
Tp 12s



Tp 13s

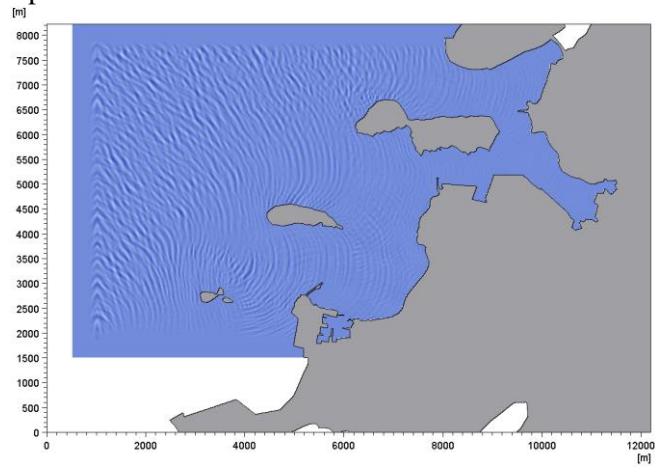


Tp 15s

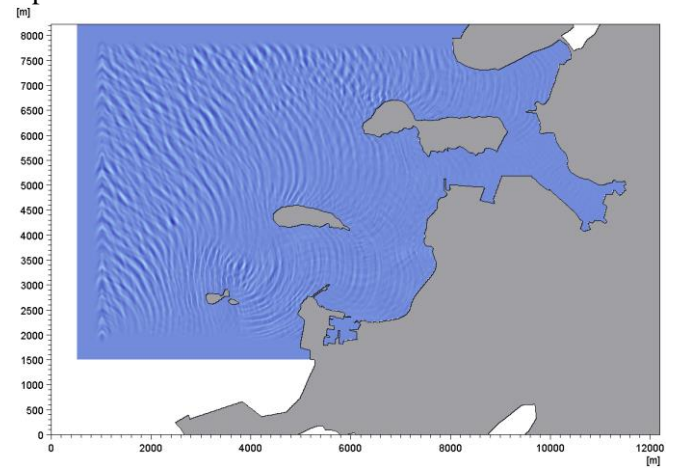


$H_{m0}$  4m

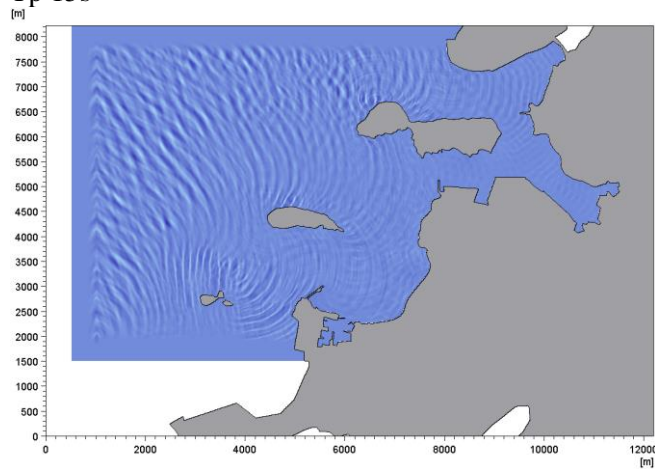
$T_p$  10s



$T_p$  12s



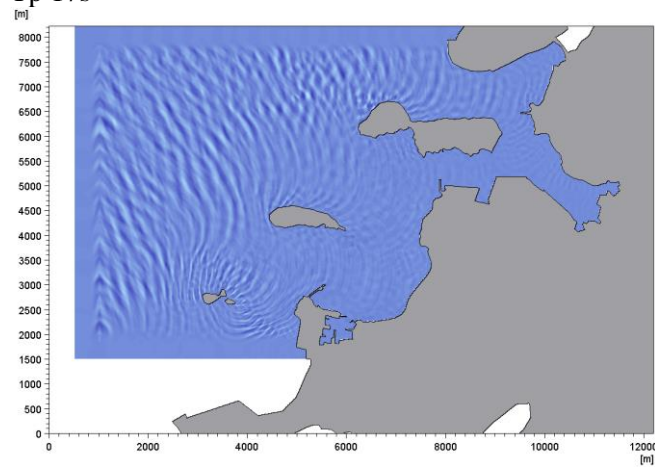
$T_p$  15s



MWD: 285 degrees

$H_{m0}$  1m

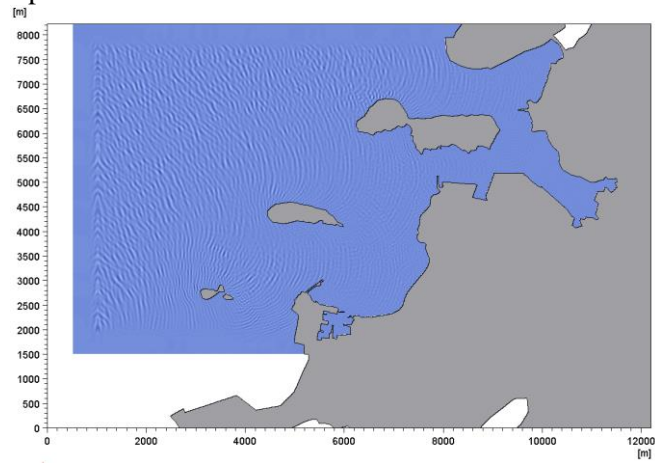
$T_p$  17s



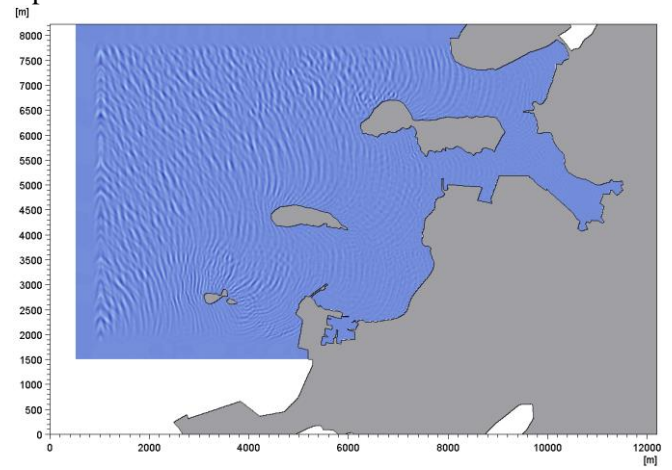
**MWD: 290 degrees**

$H_{m0}$  1m

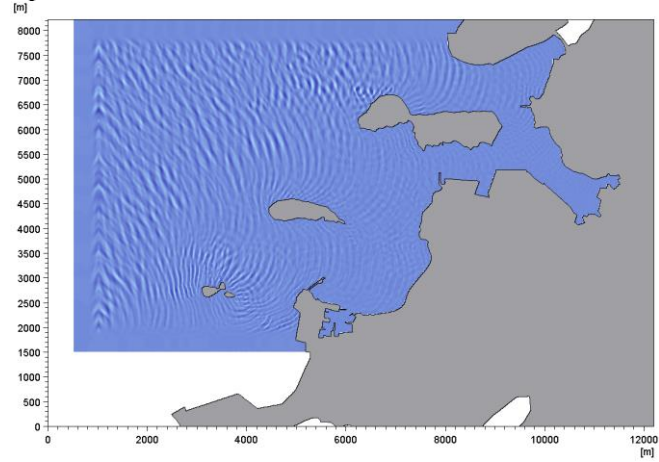
$T_p$  8s



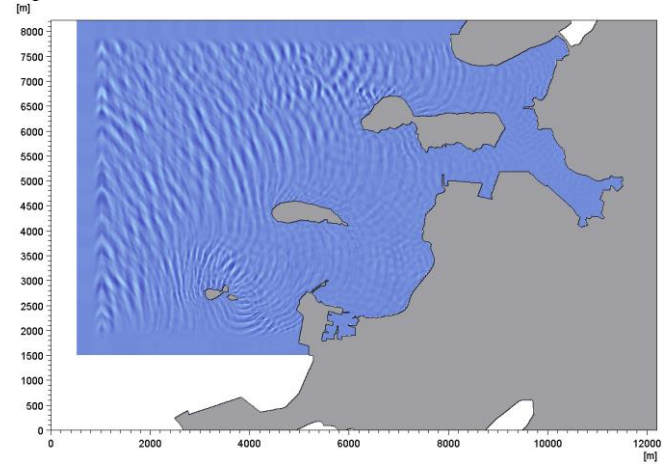
$T_p$  10s



$T_p$  12s

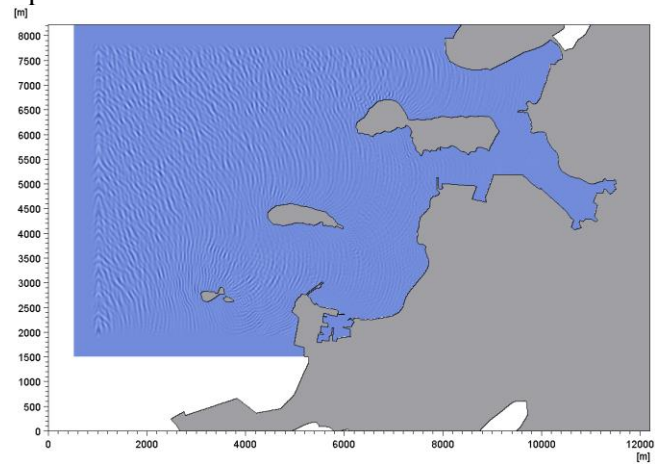


$T_p$  15s

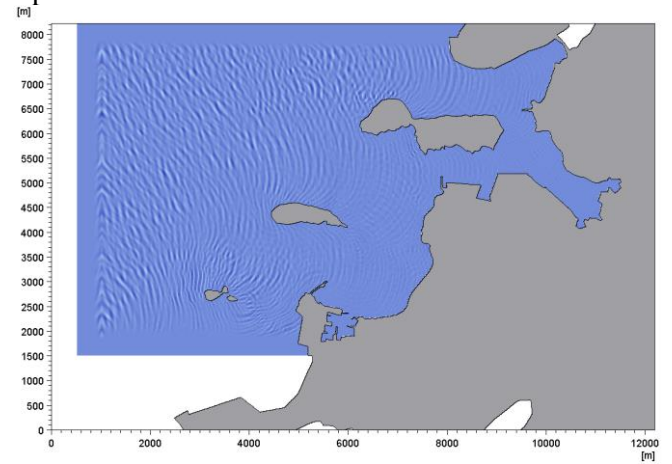


$H_{m0}$  2m

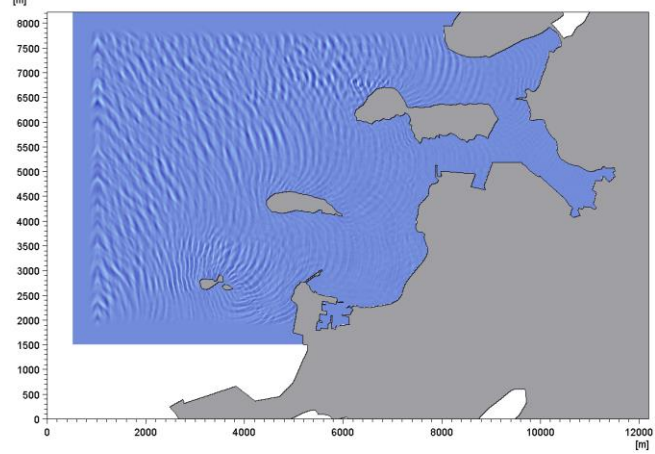
$T_p$  8s



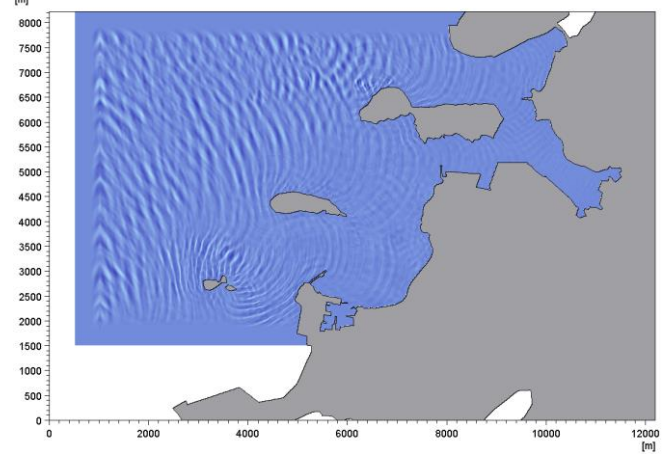
$T_p$  10s



Tp 12s

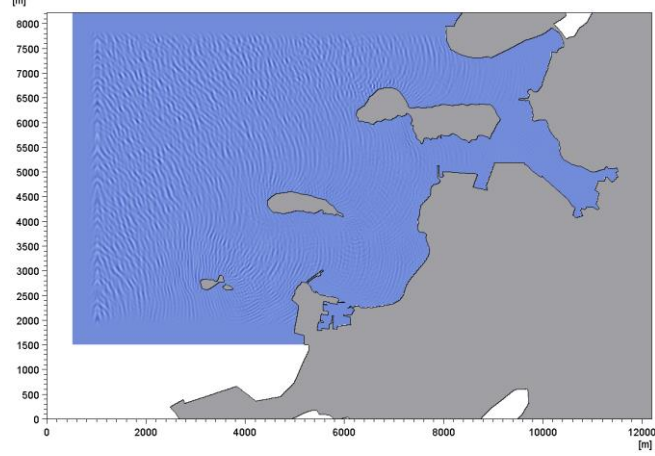


Tp 15s

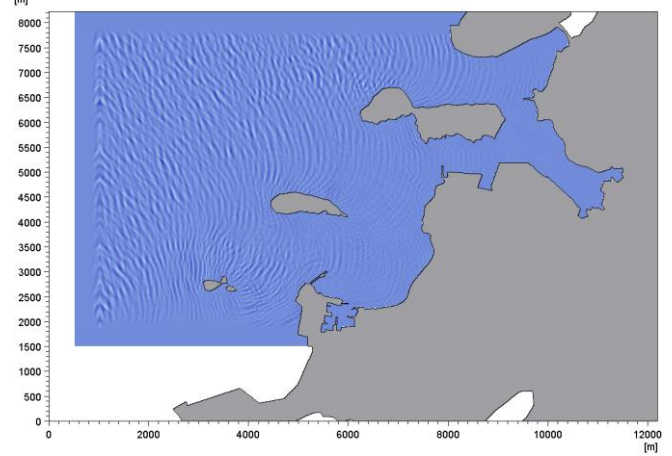


$H_{m0}$  3m

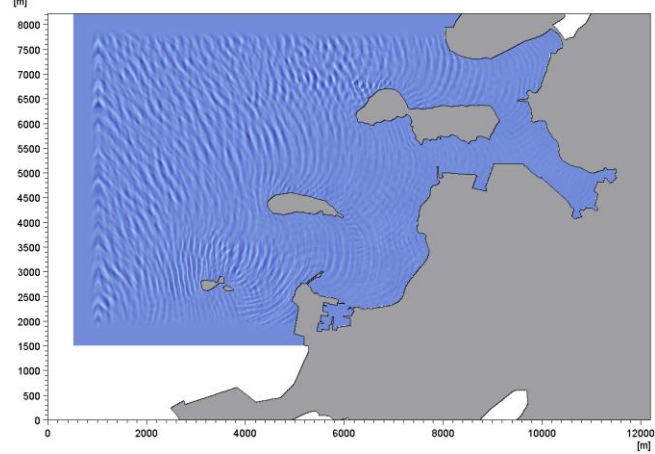
Tp 8s



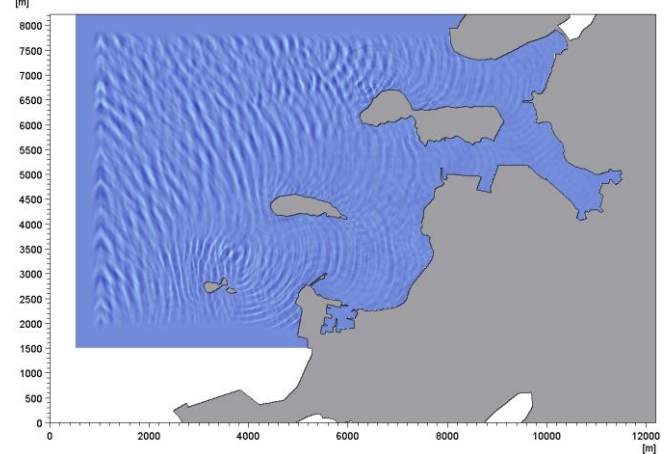
Tp 10s



Tp 12s

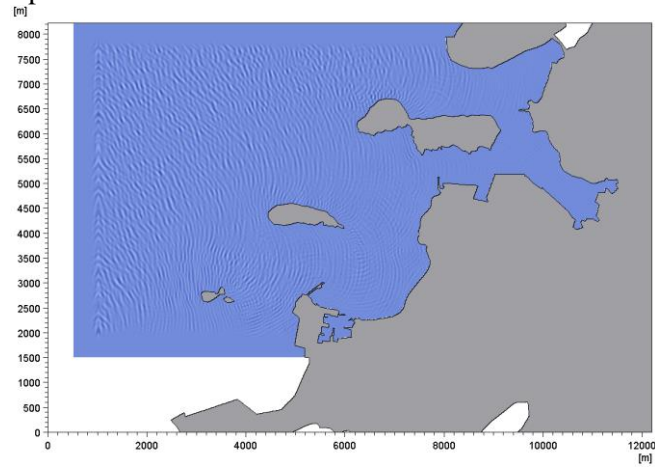


Tp 15s

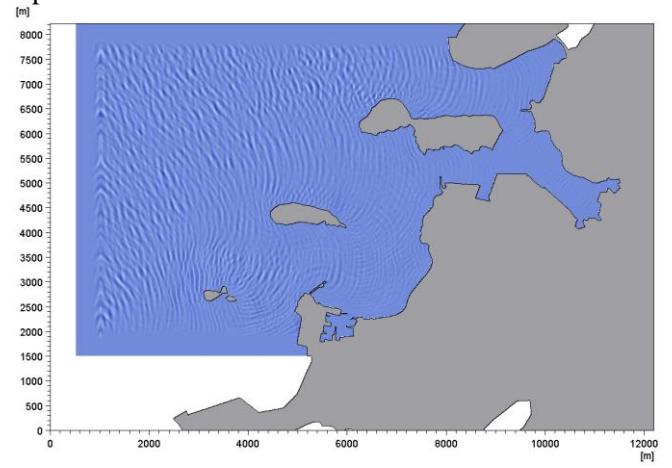


$H_{m0}$  4m

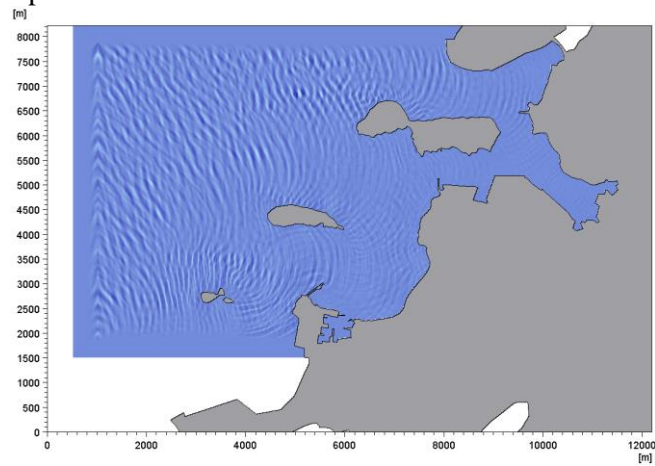
$T_p$  8s



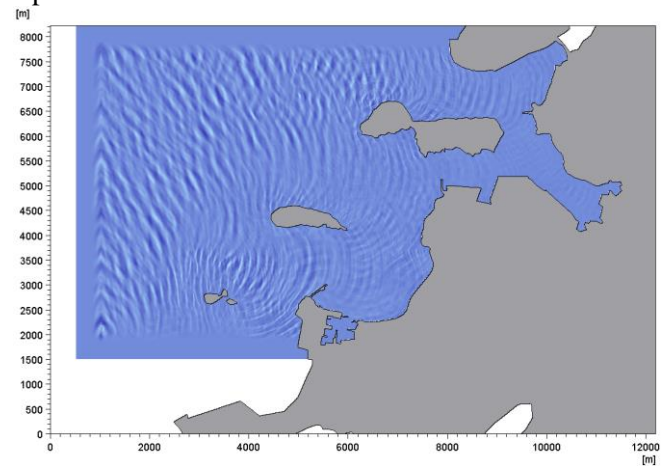
$T_p$  10s



$T_p$  12s



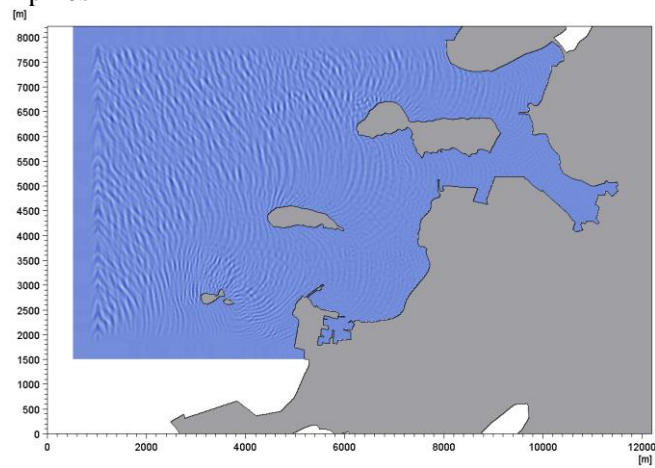
$T_p$  15s



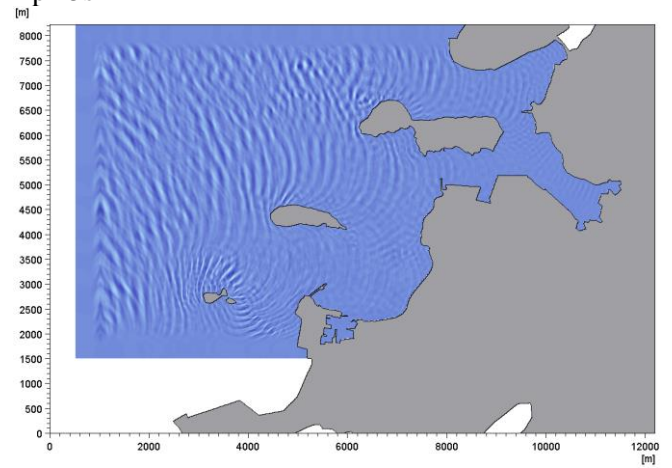
**MWD: 292.5 degrees**

$H_{m0}$  1m

$T_p$  10s

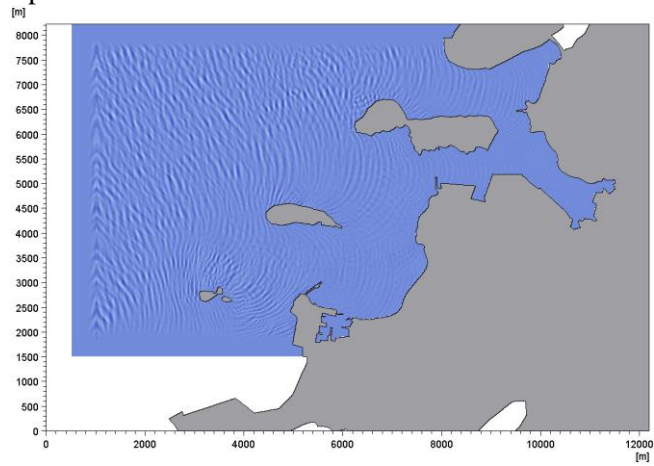


$T_p$  15s

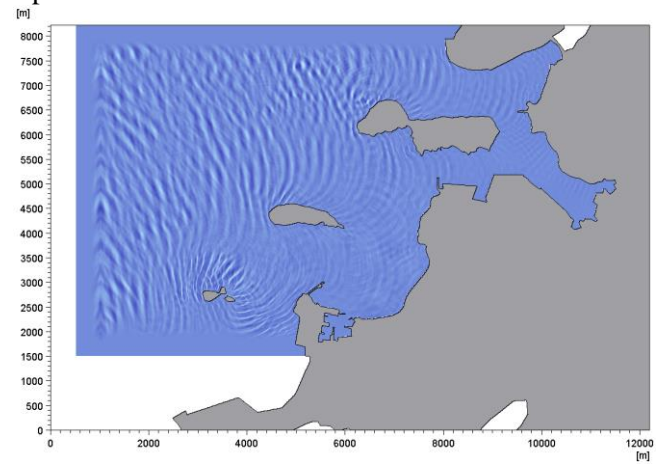


$H_{m0}$  2m

$T_p$  10s

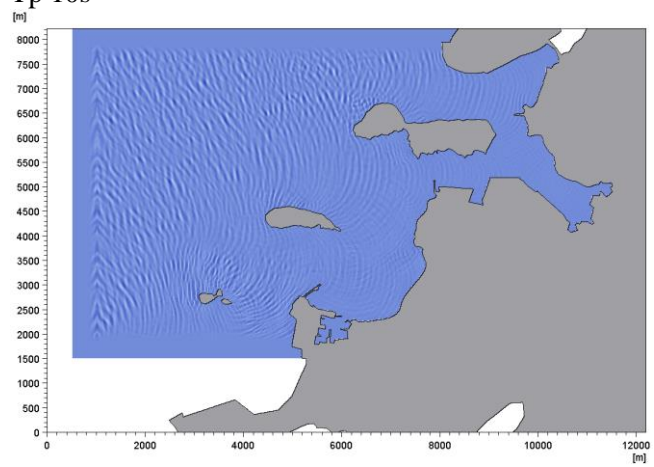


$T_p$  15s

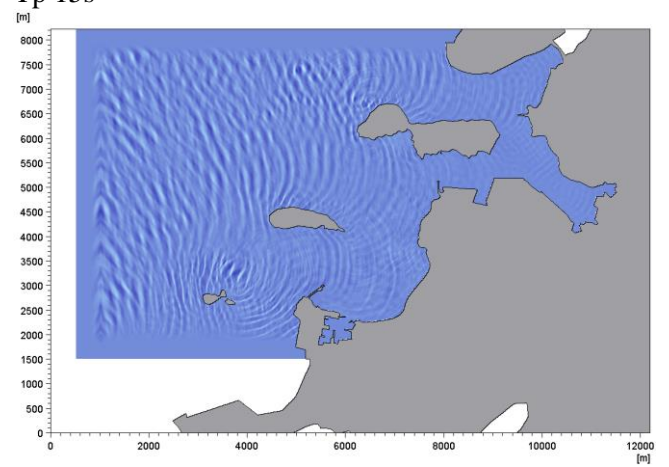


$H_{m0}$  3m

$T_p$  10s



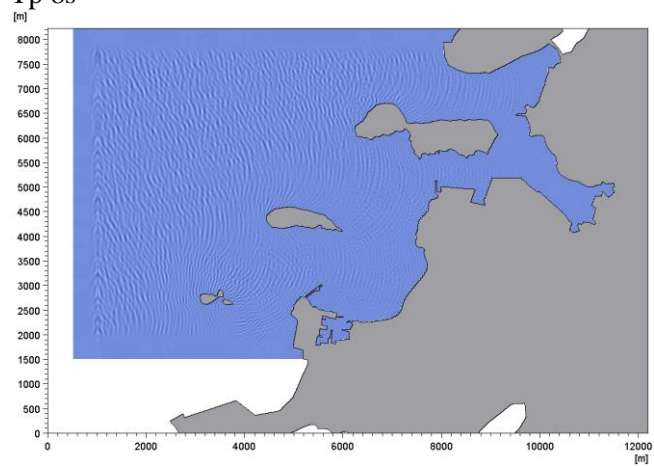
$T_p$  15s



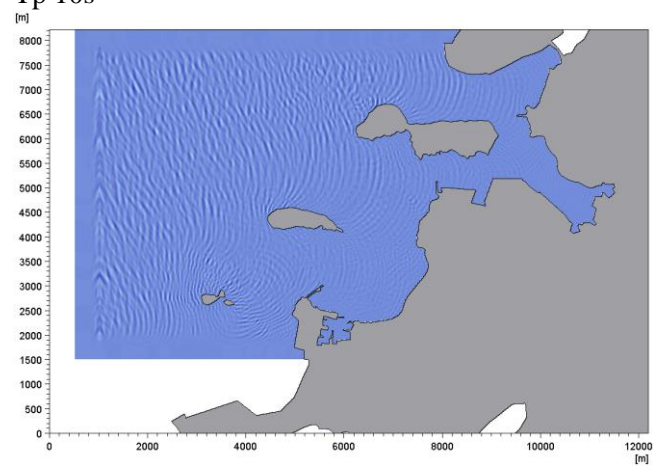
**MWD: 300 degrees**

$H_{m0}$  1m

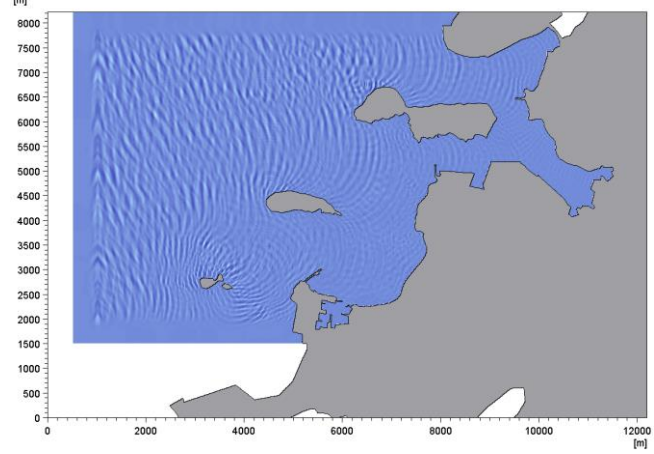
$T_p$  8s



$T_p$  10s

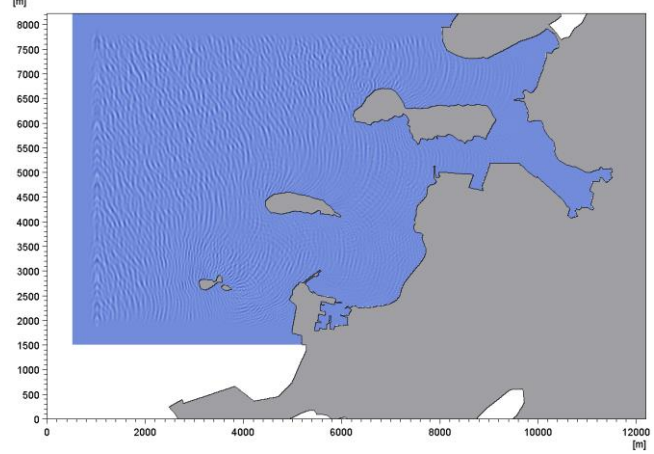


Tp 12s

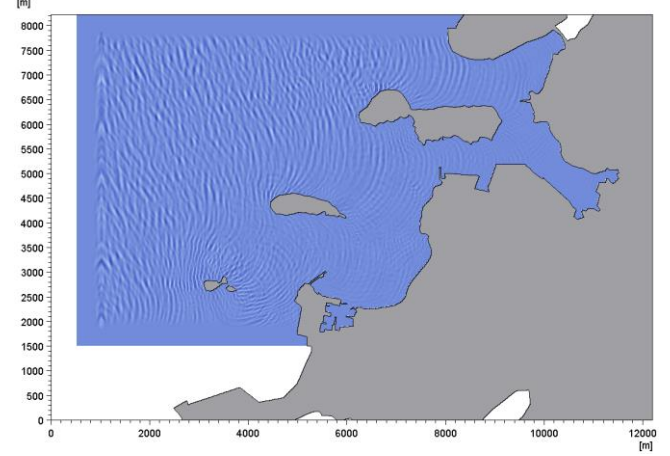


$H_{m0}$  2m

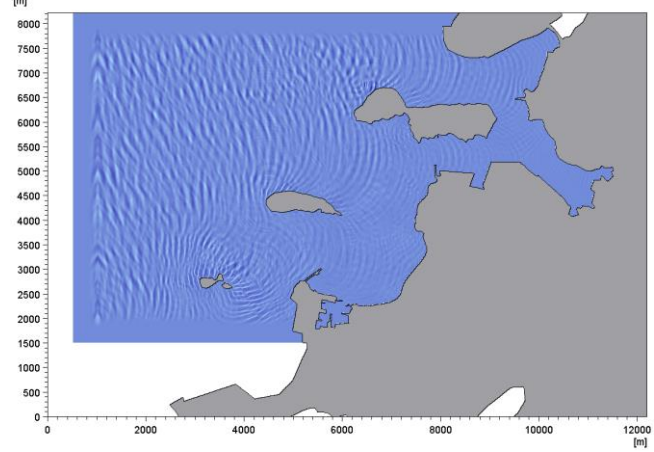
Tp 8s



Tp 10s

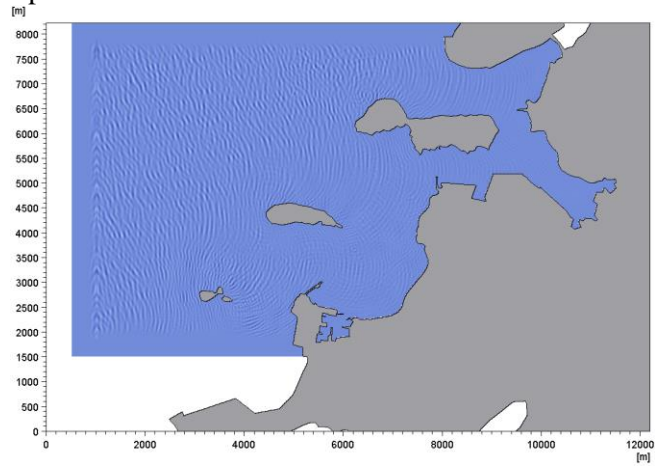


Tp 12s

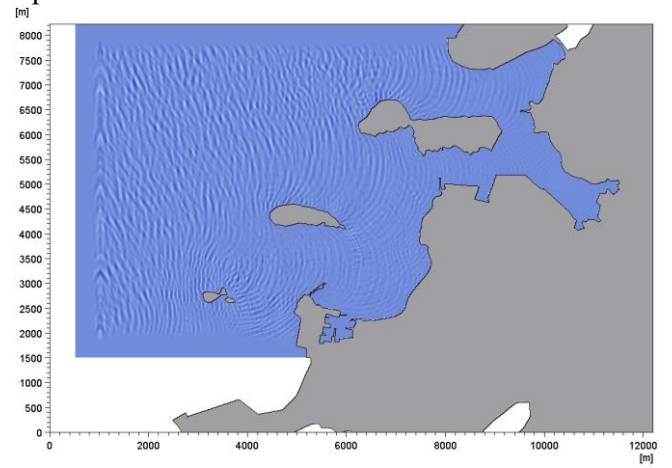


$H_{m0}$  3m

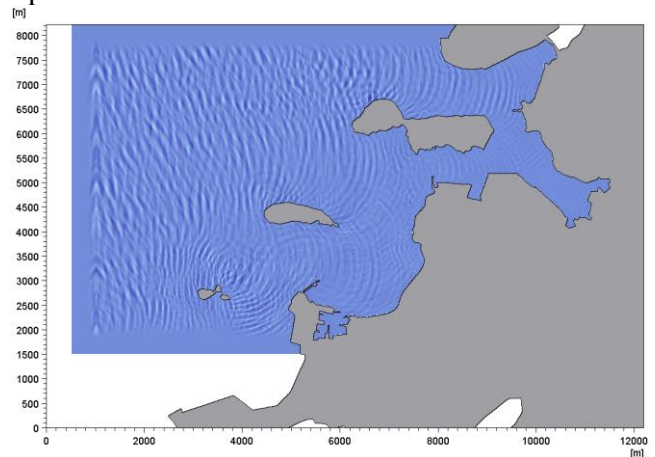
$T_p$  8s



$T_p$  10s

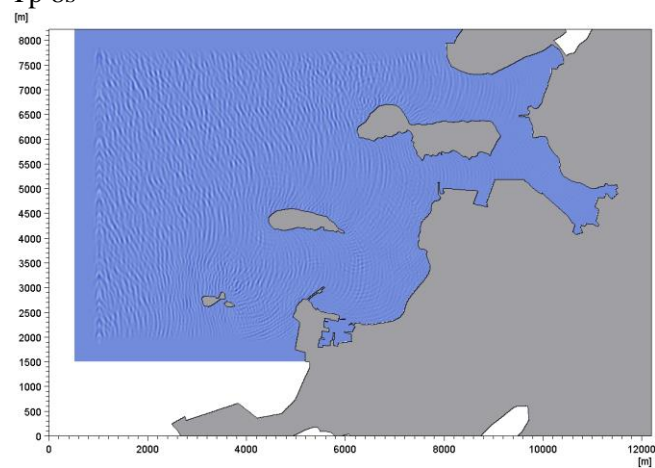


$T_p$  12s

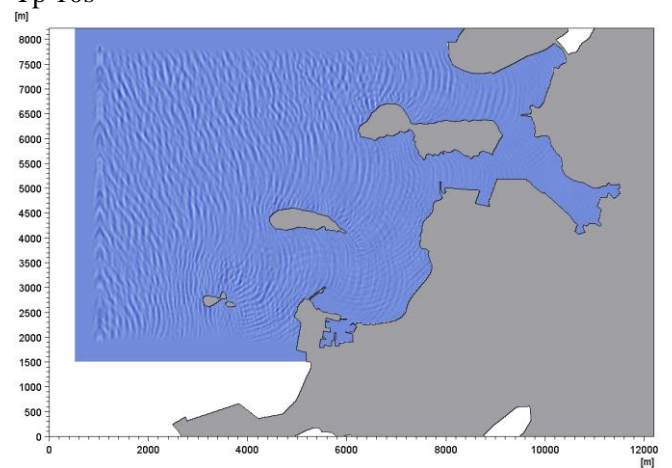


$H_{m0}$  4m

$T_p$  8s

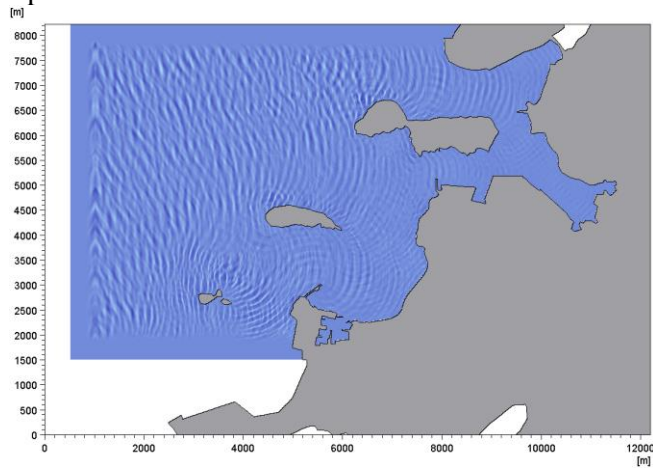


$T_p$  10s





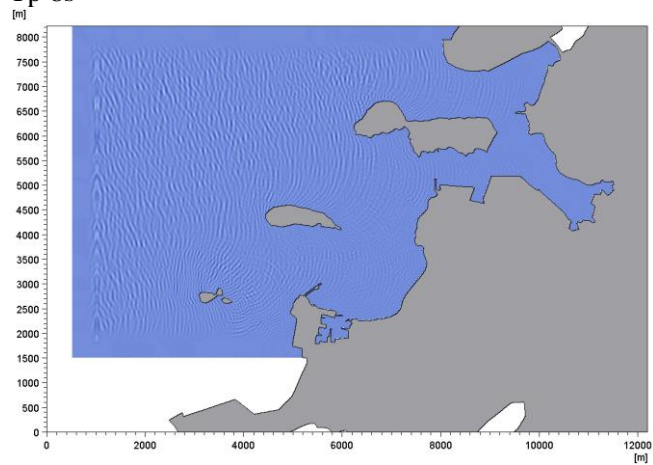
**Tp 12s**



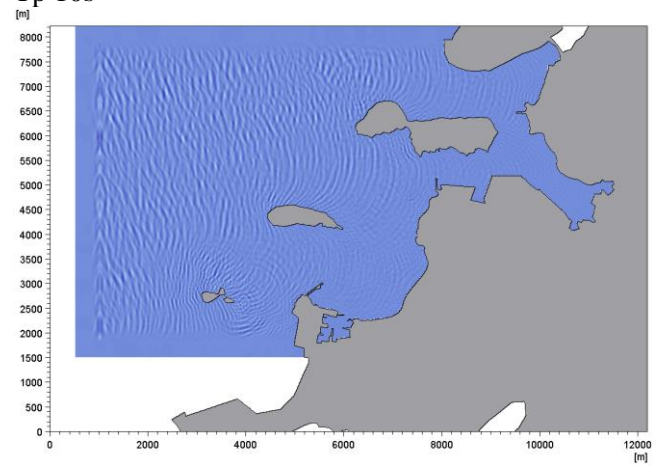
**MWD: 305 degrees**

**$H_{m0}$  1m**

**Tp 8s**

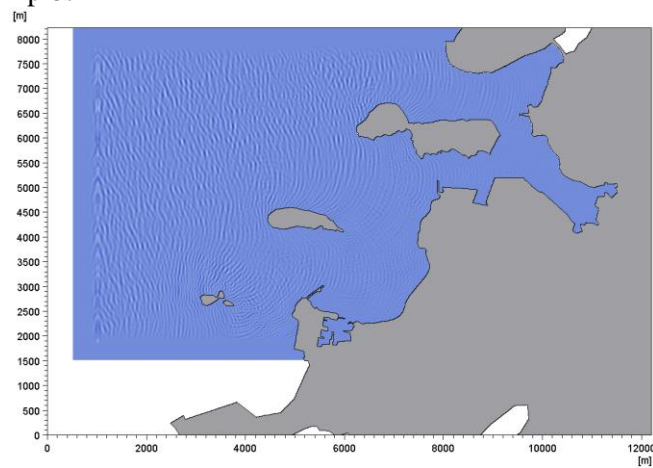


**Tp 10s**

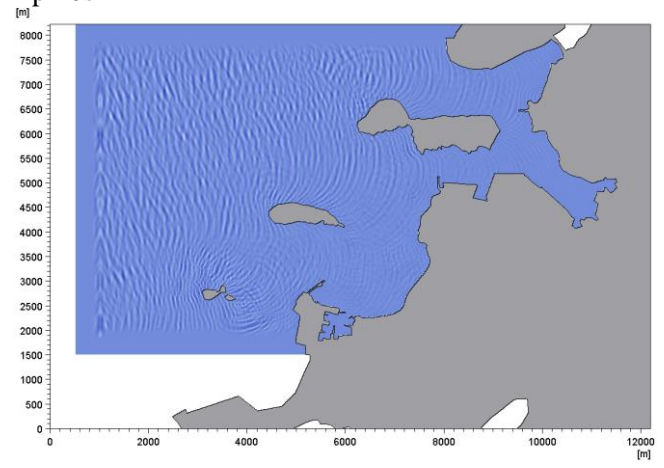


**$H_{m0}$  2m**

**Tp 8s**

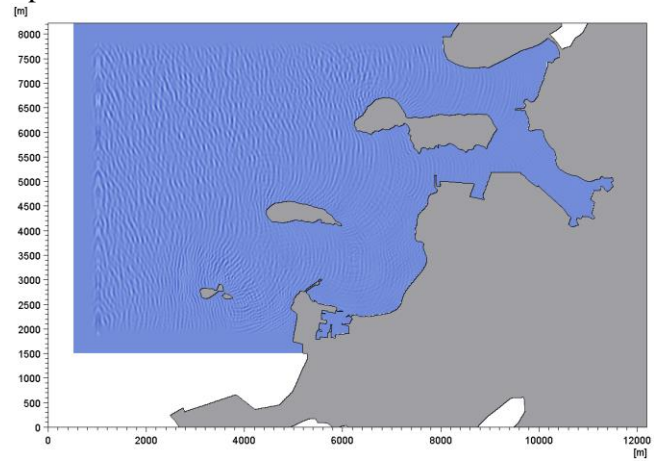


**Tp 10s**

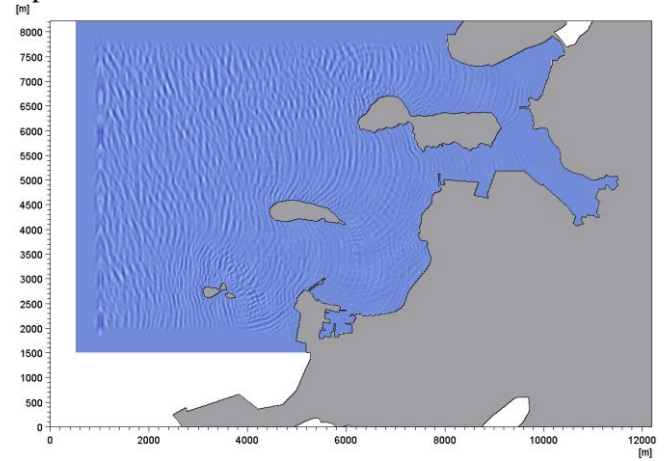


$H_{m0}$  3m

$T_p$  8s



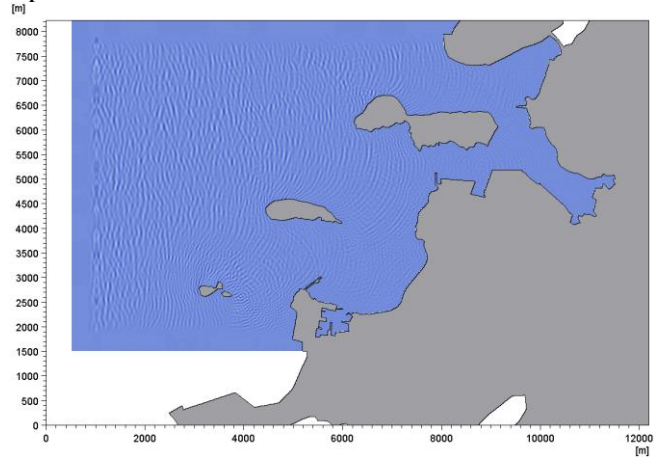
$T_p$  10s



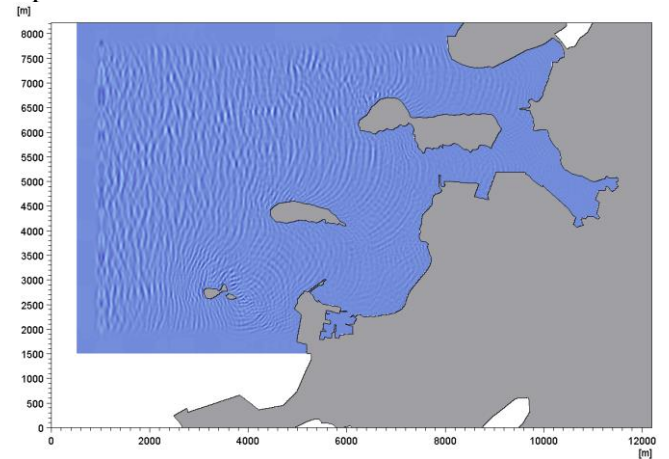
MWD: 315 degrees

$H_{m0}$  1m

$T_p$  8s

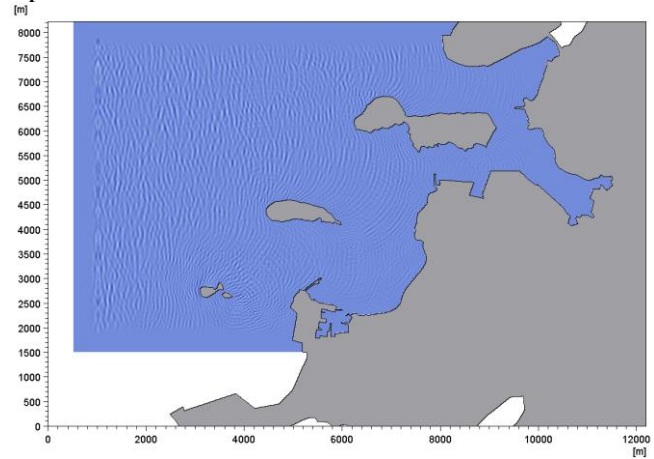


$T_p$  10s

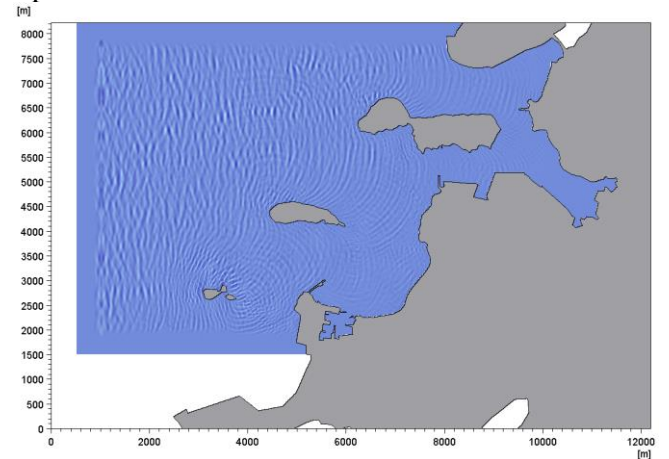


$H_{m0}$  2m

$T_p$  8s

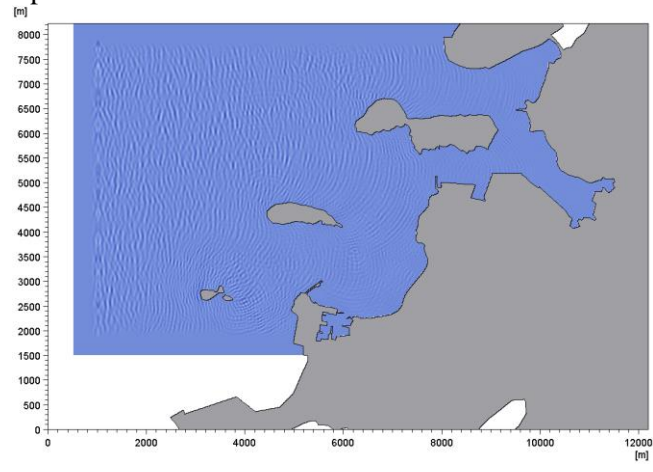


$T_p$  10s

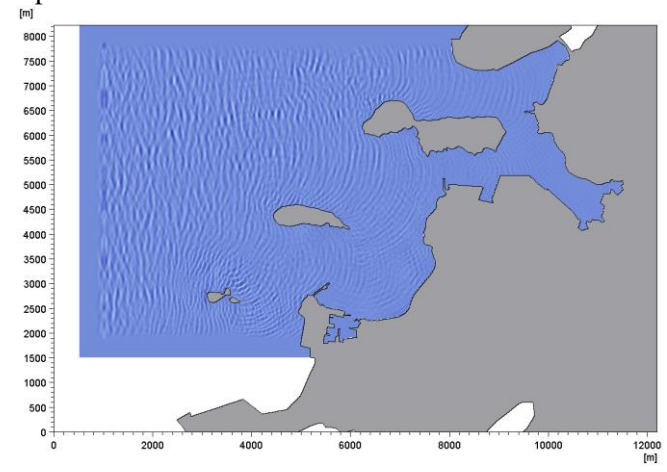


$H_{m0}$  3m

$T_p$  8s



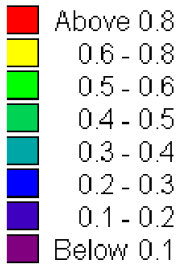
$T_p$  10s



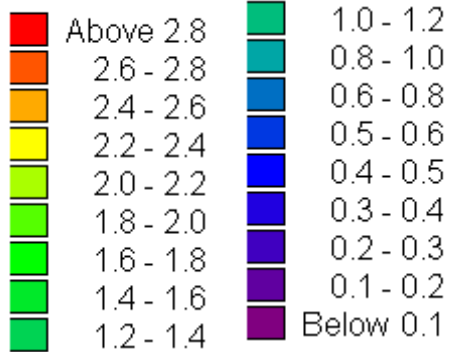
**B.3  $H_{m0}$  in the Total Model Area**

**Legend**

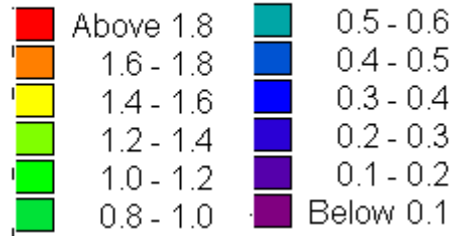
$H_{m0}$  1m  
Hm0 (meter)



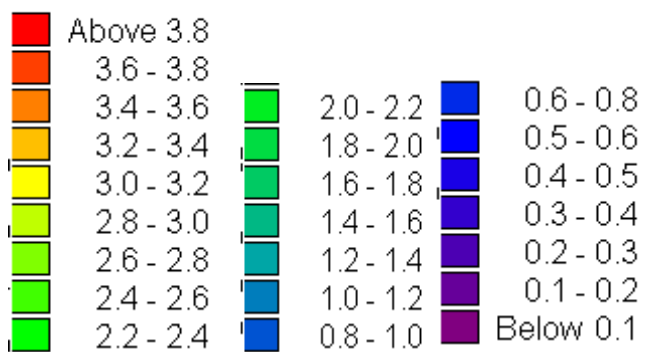
$H_{m0}$  3m  
Hm0 (meter)



$H_{m0}$  2m  
Hm0 (meter)



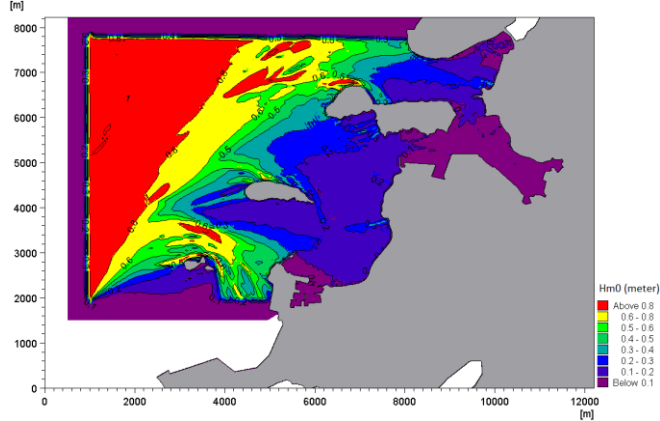
$H_{m0}$  4m  
Hm0 (meter)



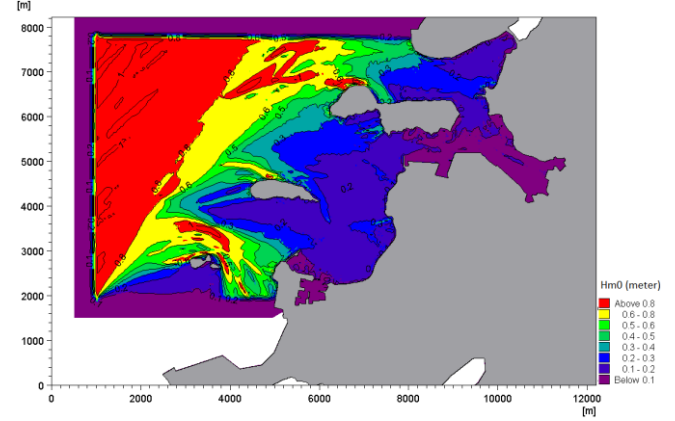
**MWD: 270 degrees**

$H_{m0}$  1m

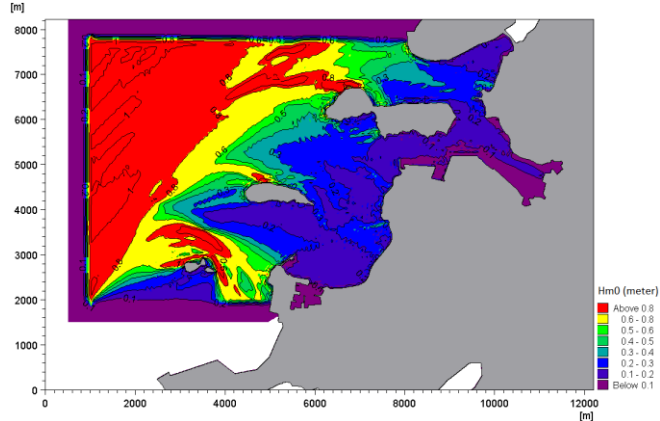
Tp 10s



Tp 12s

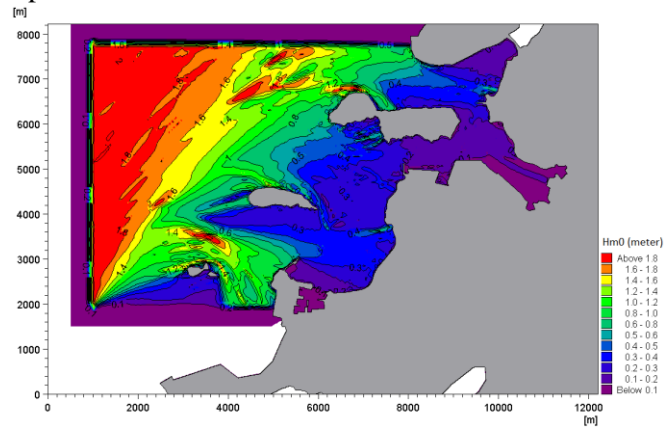


Tp 15s

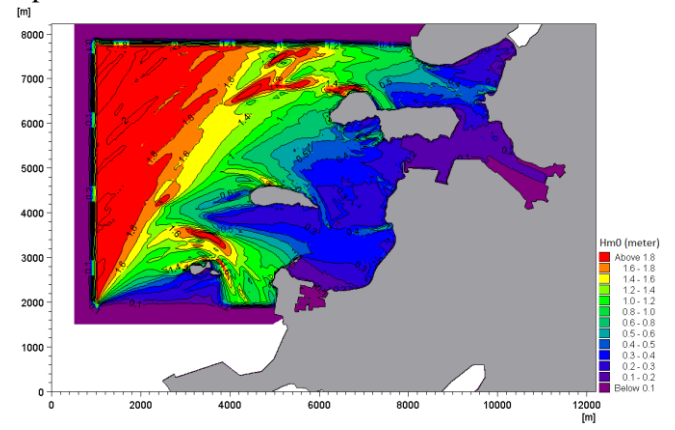


$H_{m0}$  2m

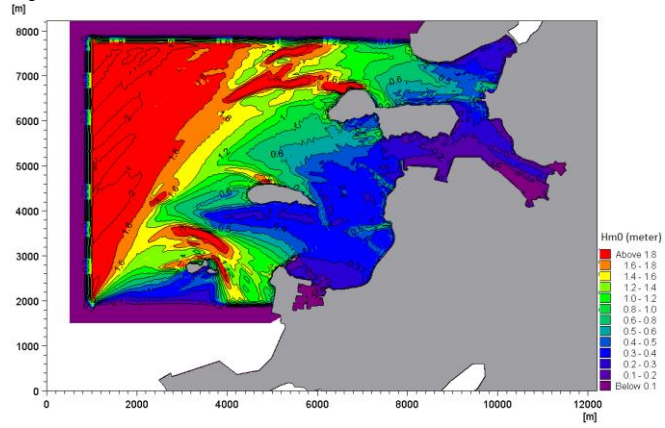
$T_p$  10s



$T_p$  12s

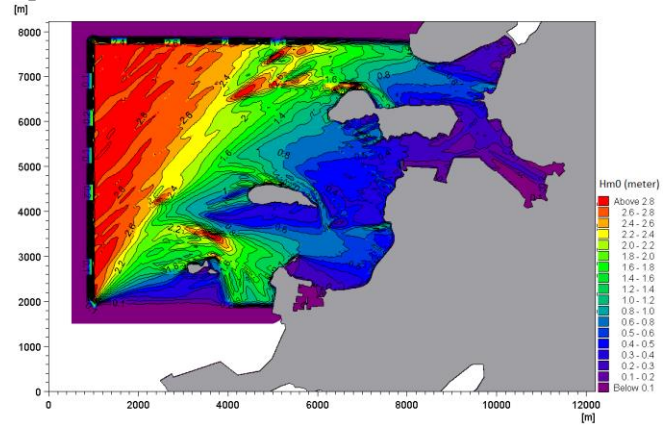


$T_p$  15s

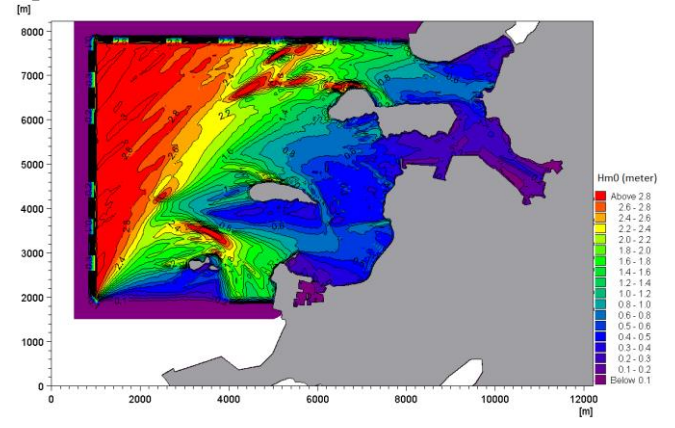


$H_{m0}$  3m

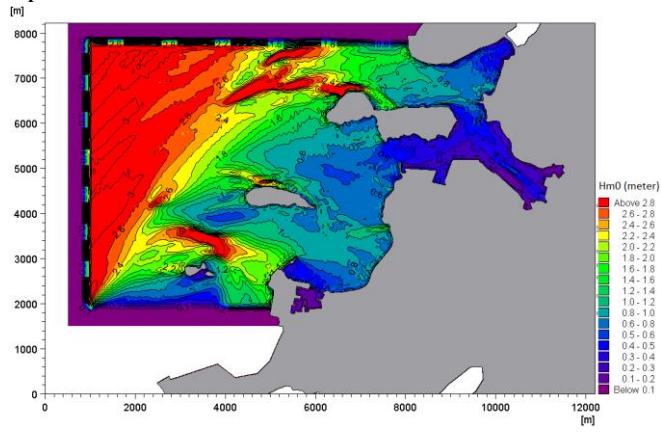
$T_p$  10s



$T_p$  12s



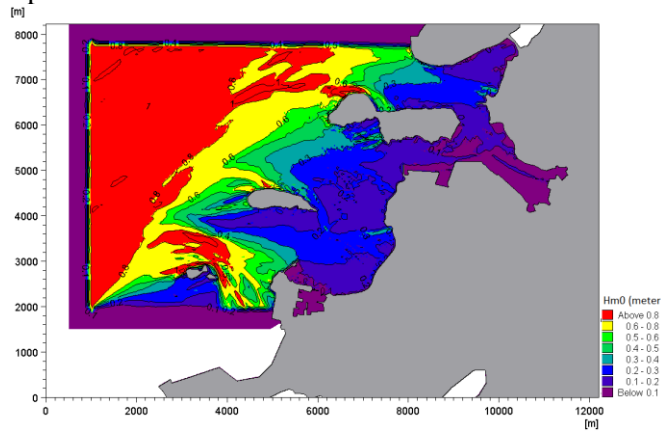
Tp 15s



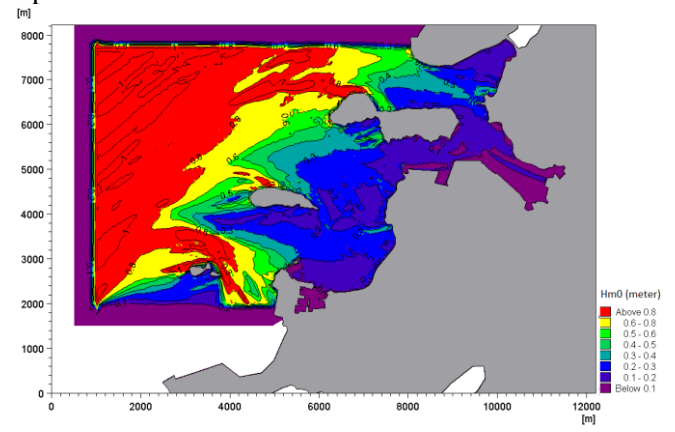
MWD: 280 degrees

$H_{m0}$  1m

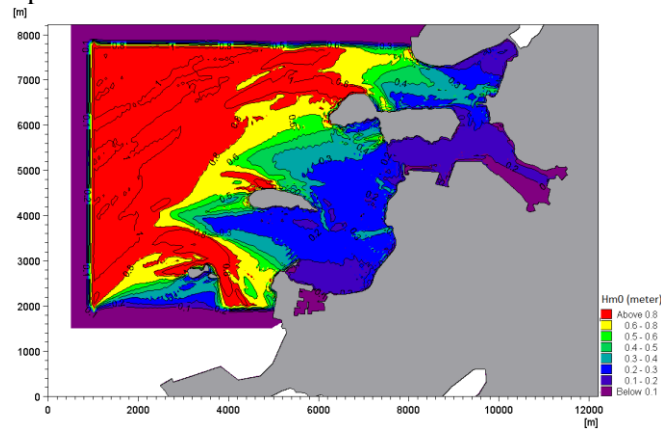
Tp 10s



Tp 12s

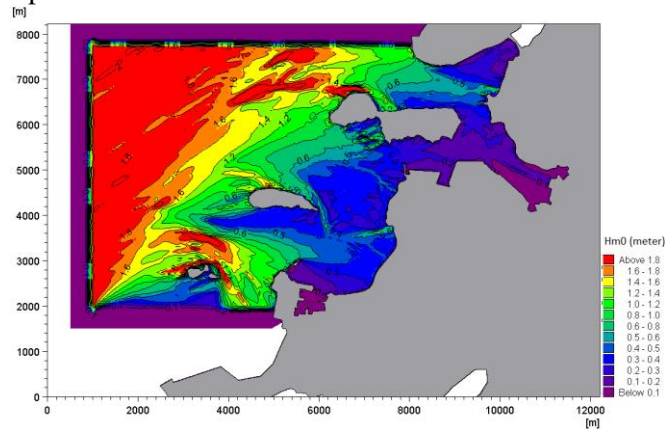


Tp 15s

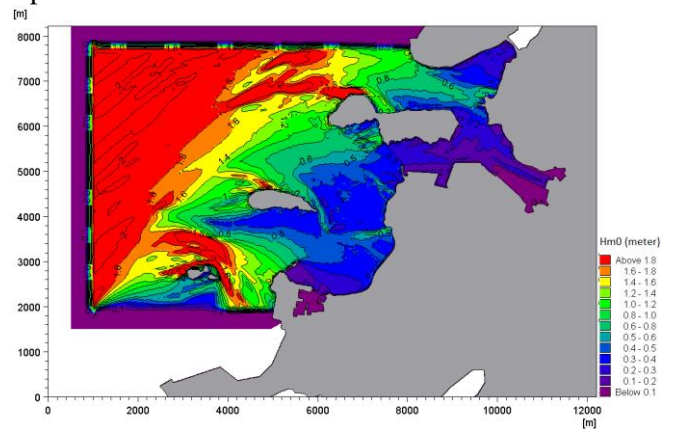


$H_{m0}$  2m

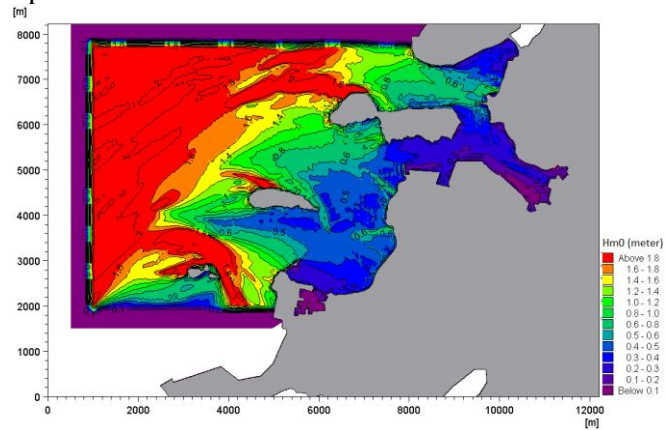
$T_p$  10s



$T_p$  12s

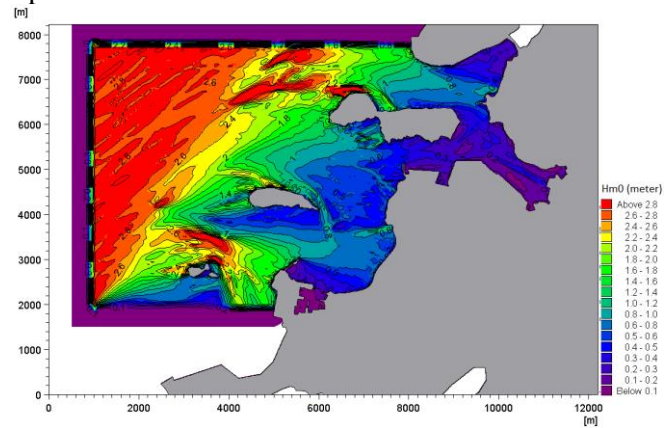


$T_p$  15s

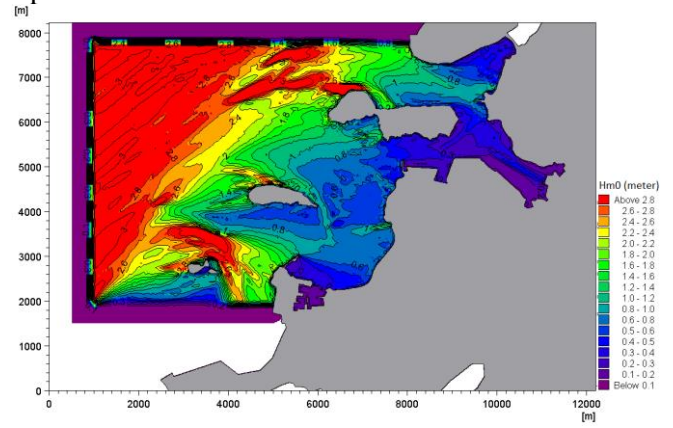


$H_{m0}$  3m

$T_p$  10s

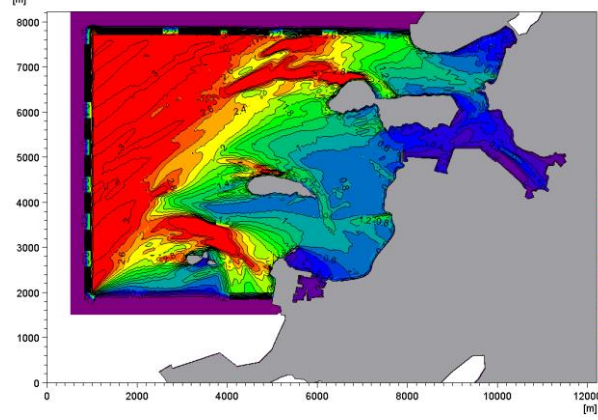


$T_p$  12s

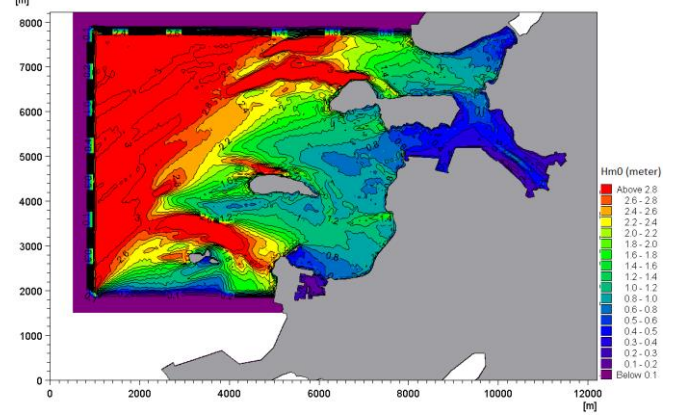




Tp 13s

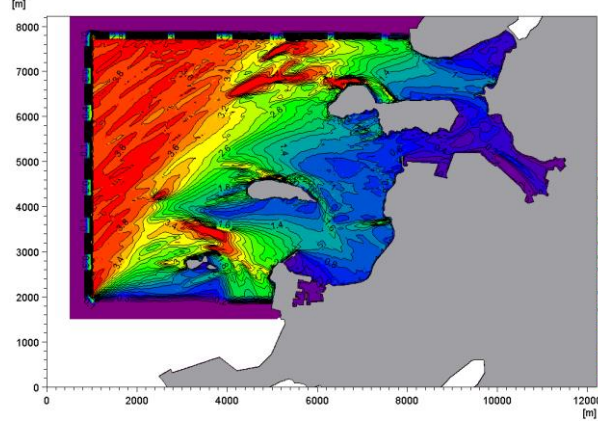


Tp 15s

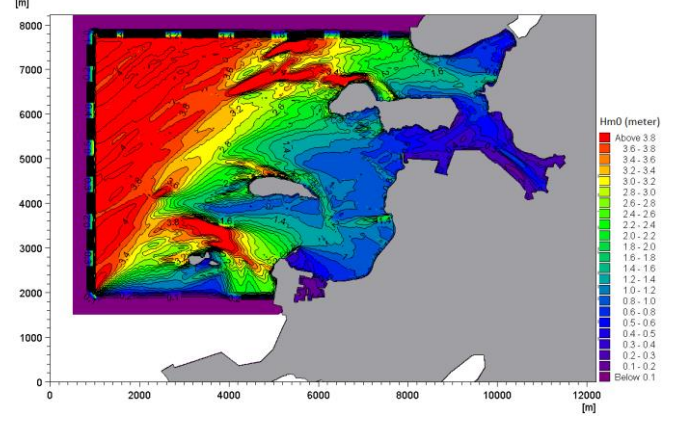


H<sub>m0</sub> 4m

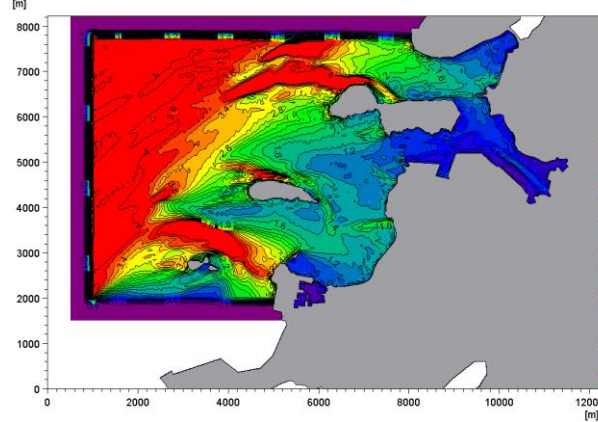
Tp 10s



Tp 12s



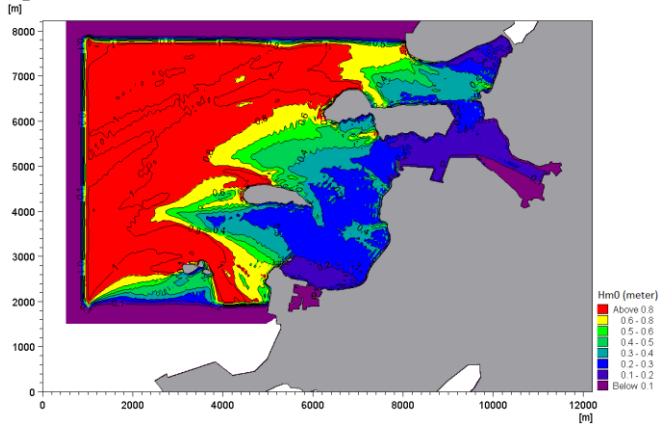
Tp 15s



MWD: 285 degrees

$H_{m0}$  1m

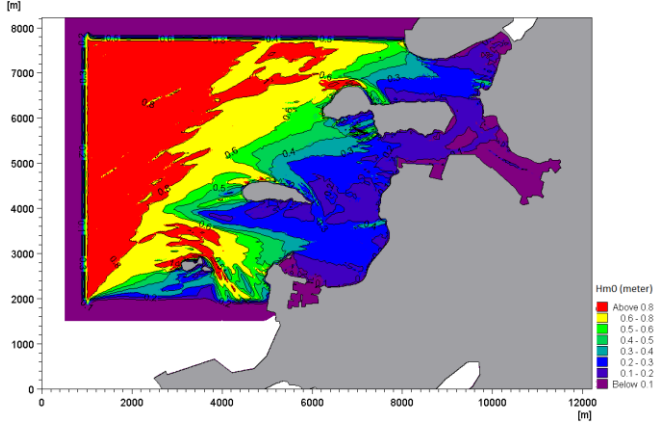
Tp 17s



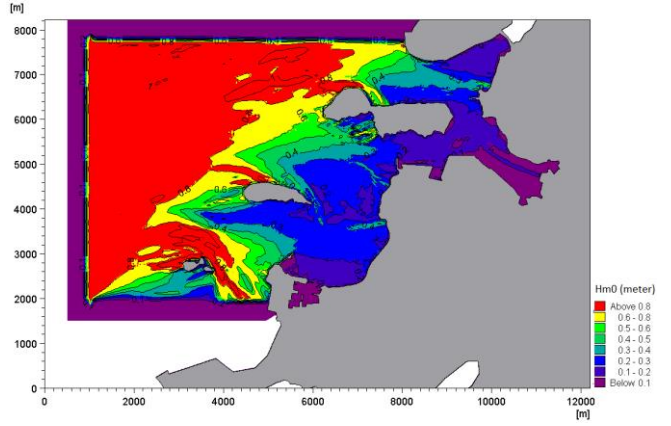
MWD: 290 degrees

$H_{m0}$  1m

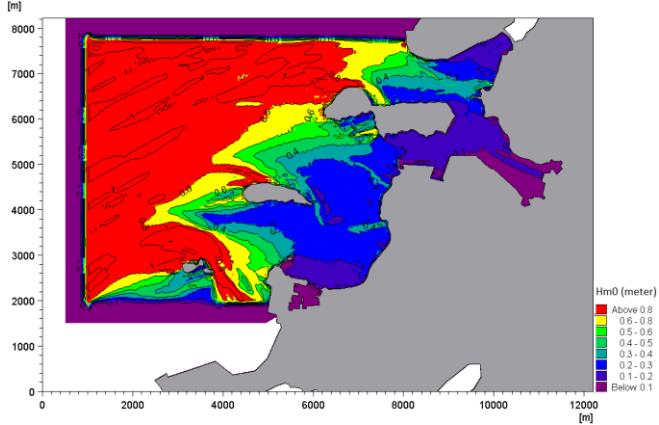
Tp 8s



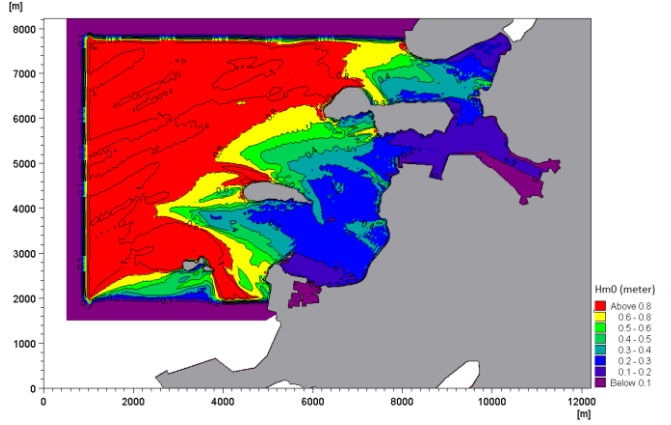
Tp 10s



Tp 12s

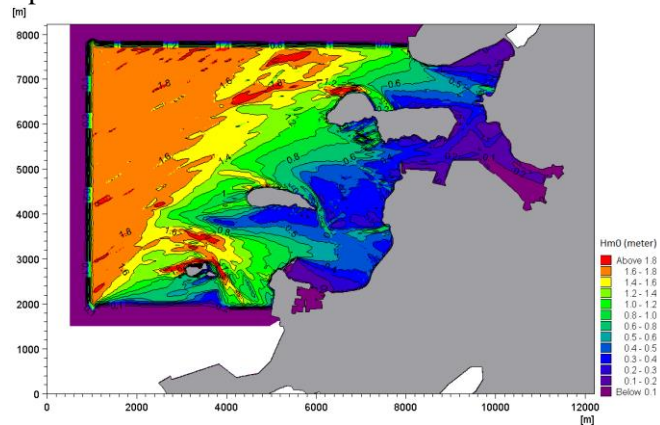


Tp 15s

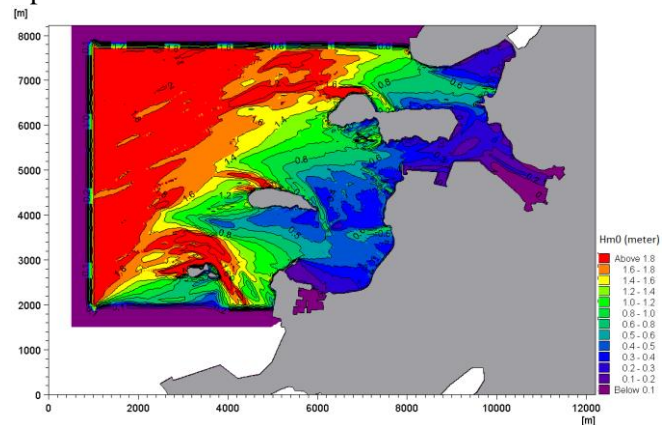


$H_{m0}$  2m

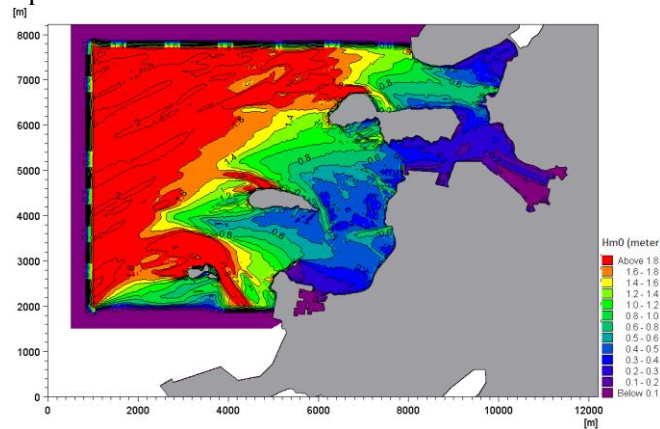
Tp 8s



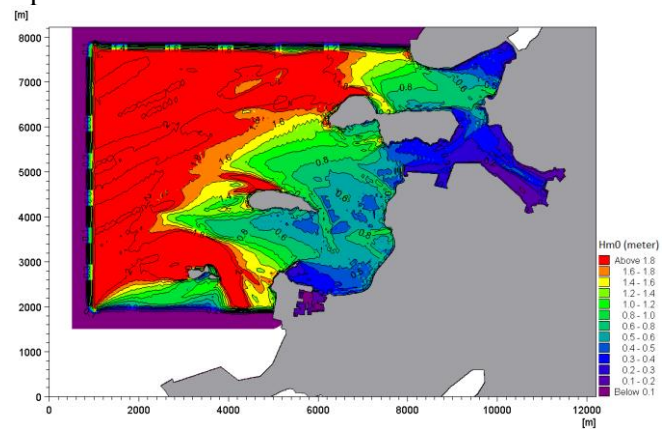
Tp 10s



Tp 12s

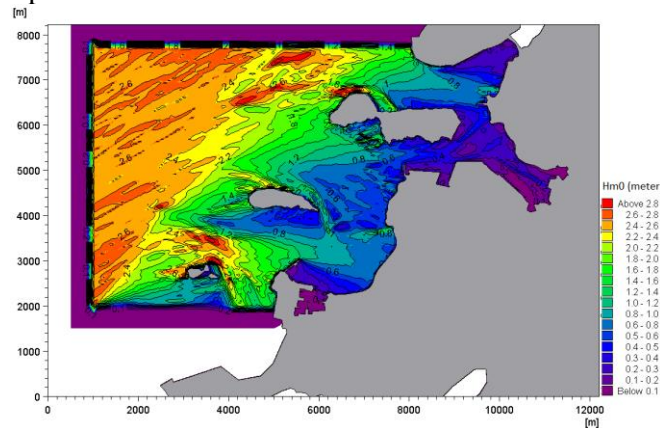


Tp 15s

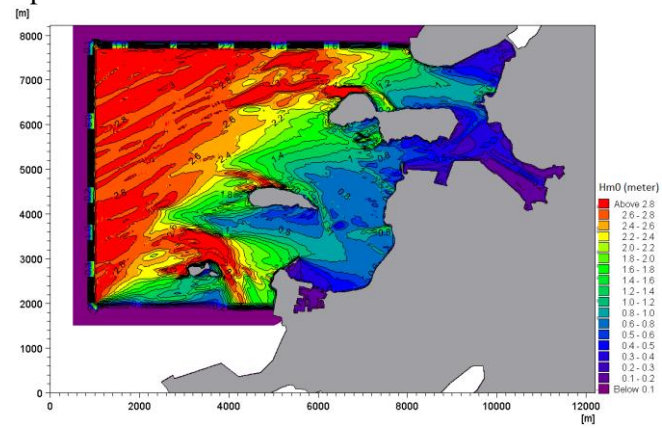


$H_{m0}$  3m

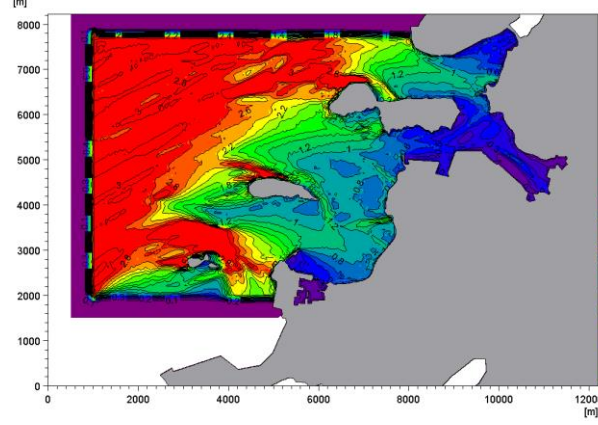
Tp 8s



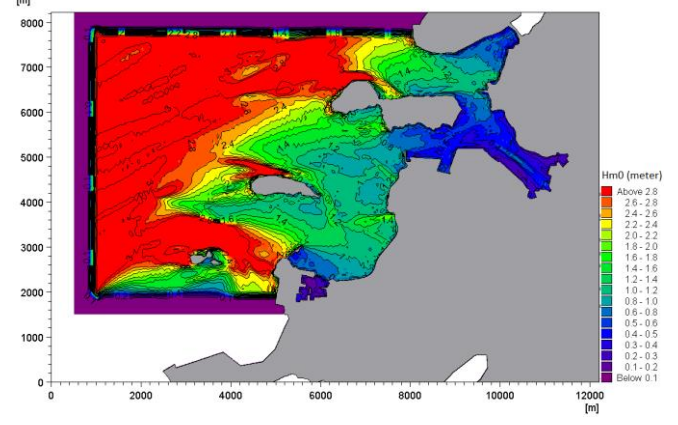
Tp 10s



Tp 12s

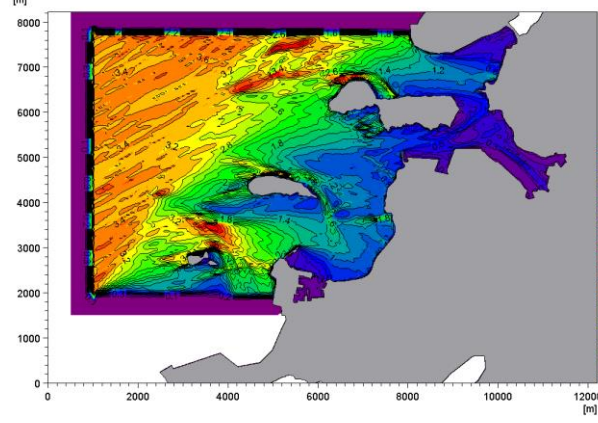


Tp 15s

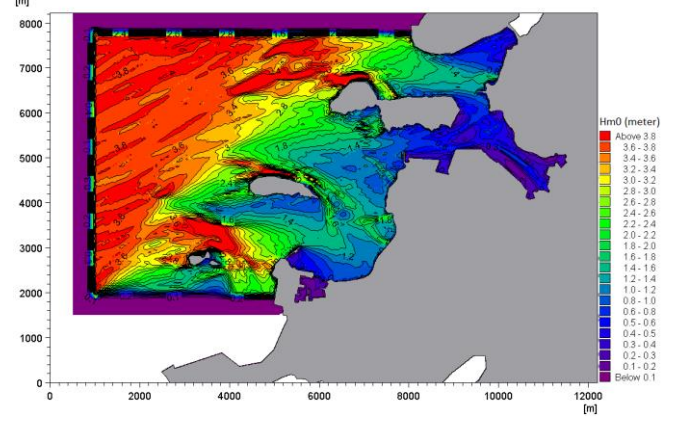


H<sub>m0</sub> 4m

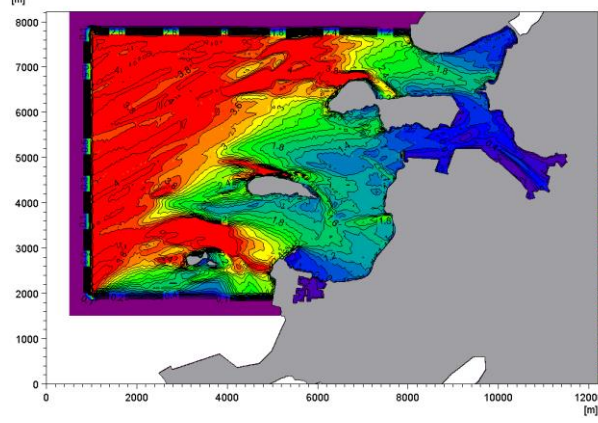
Tp 8s



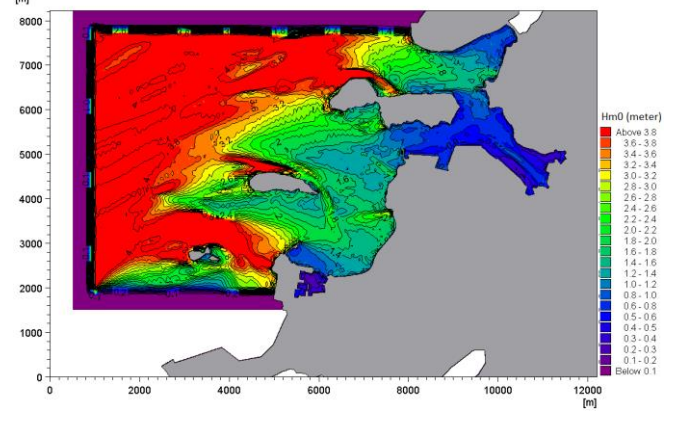
Tp 10s



Tp 12s



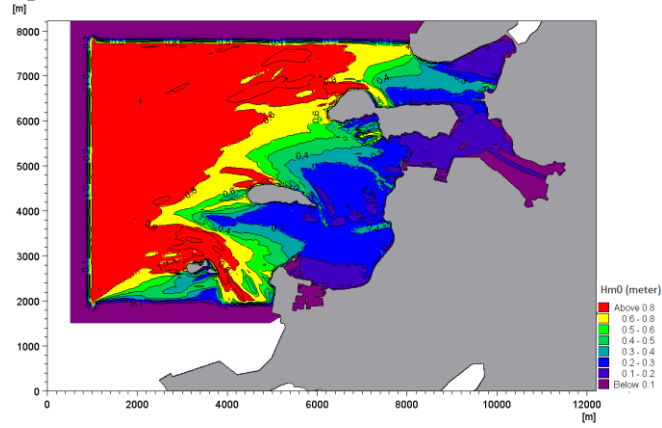
Tp 15s



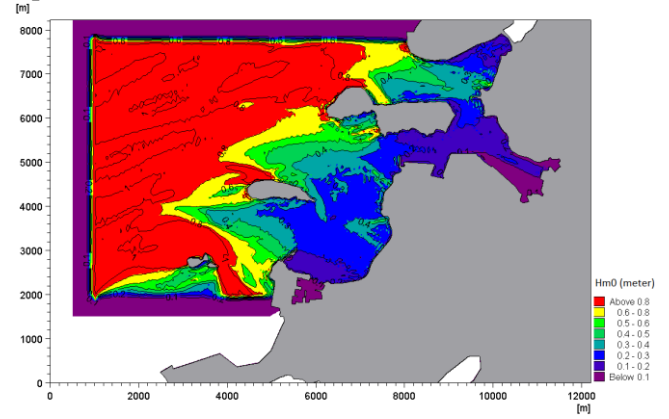
MWD: 292.5 degrees

$H_{m0}$  1m

$T_p$  10s

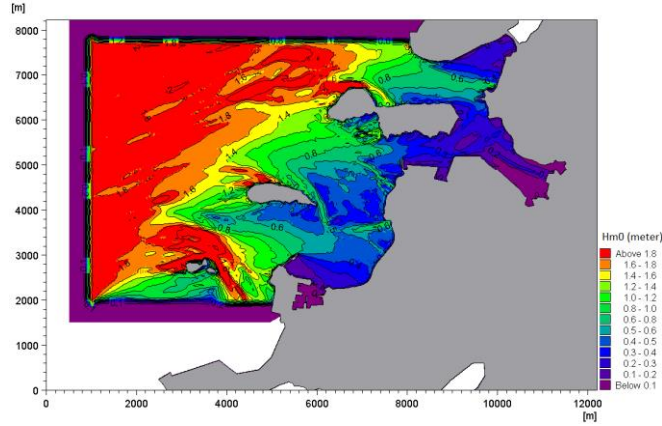


$T_p$  15s

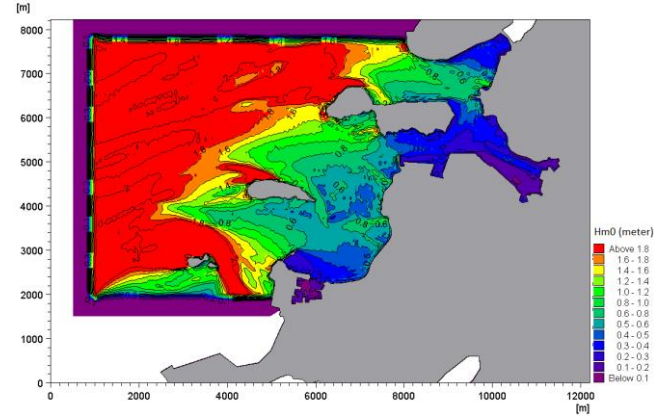


$H_{m0}$  2m

$T_p$  10s

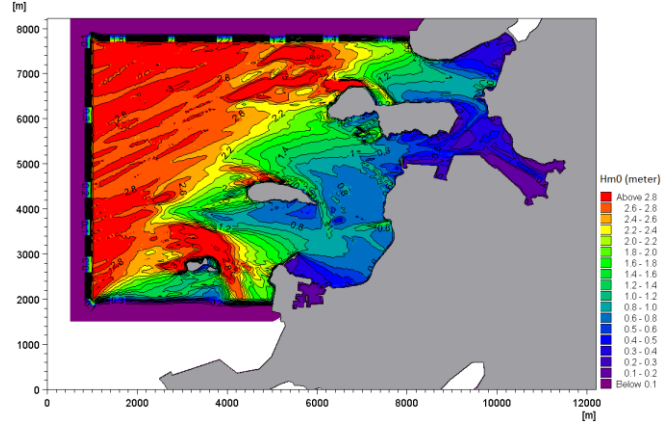


$T_p$  15s

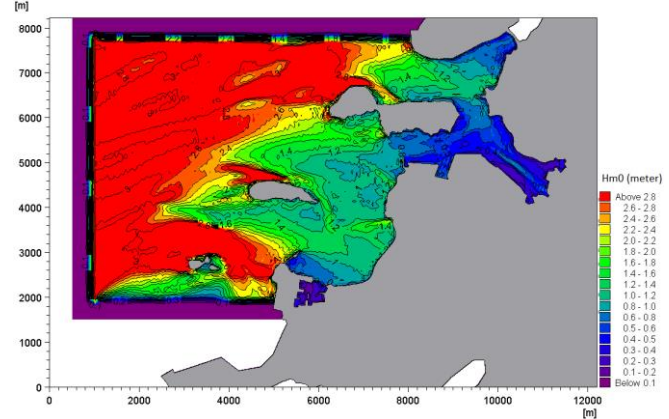


$H_{m0}$  3m

$T_p$  10s



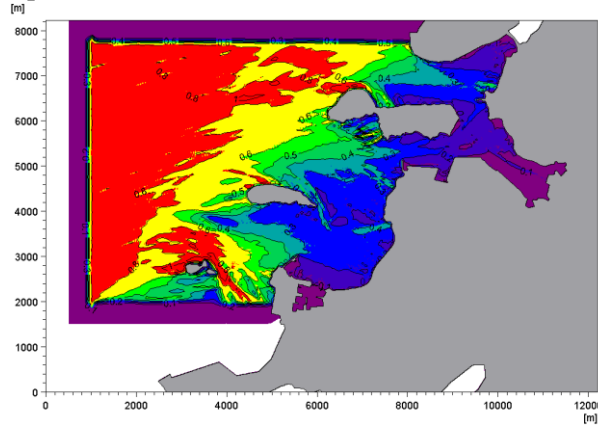
$T_p$  15s



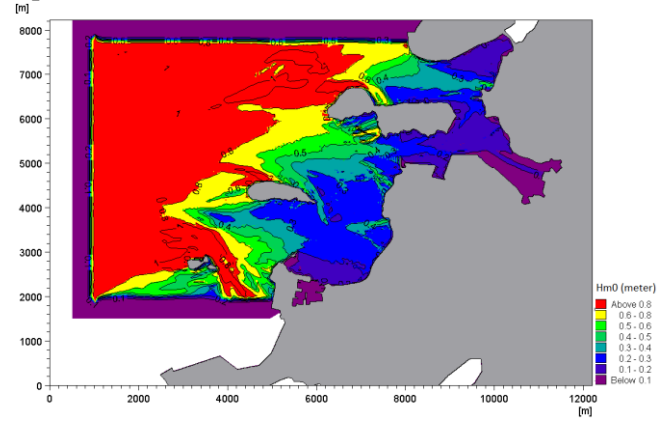
MWD: 300 degrees

$H_{m0}$  1m

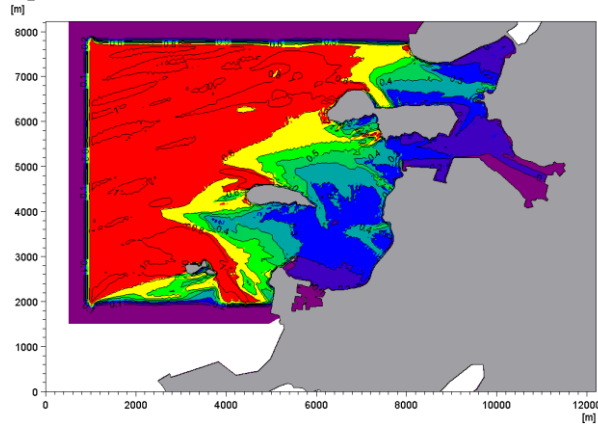
$T_p$  8s



$T_p$  10s

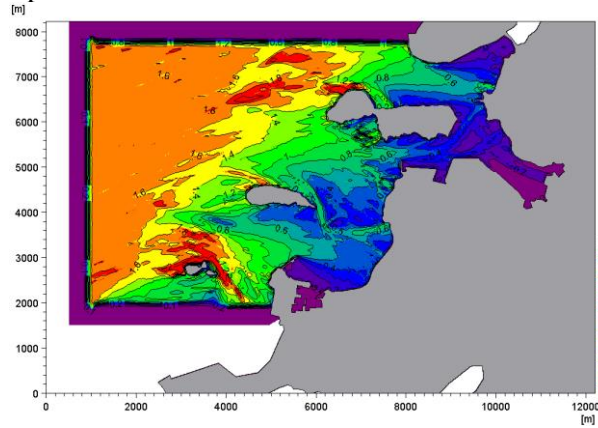


$T_p$  12s

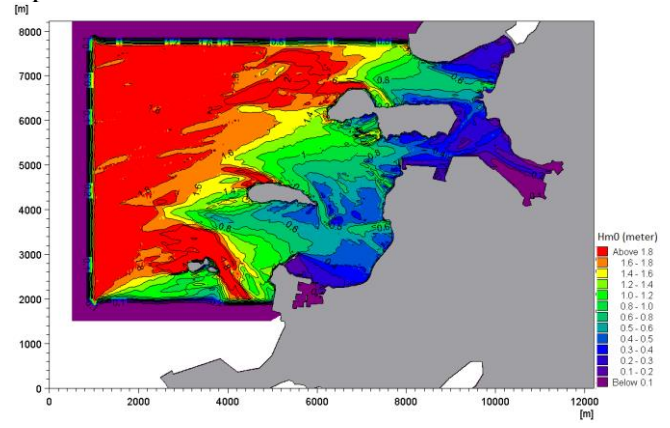


$H_{m0}$  2m

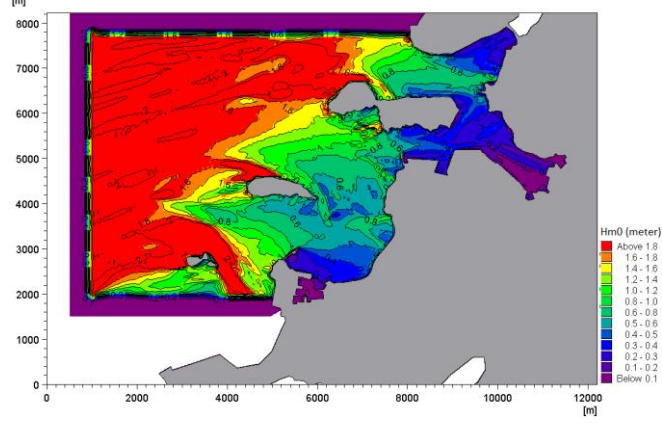
$T_p$  8s



$T_p$  10s

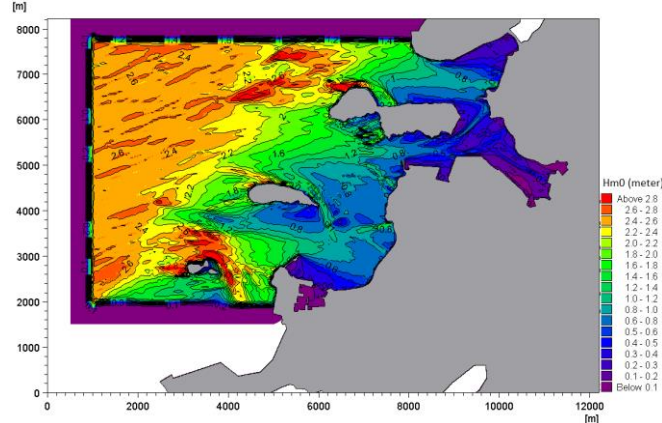


Tp 12s

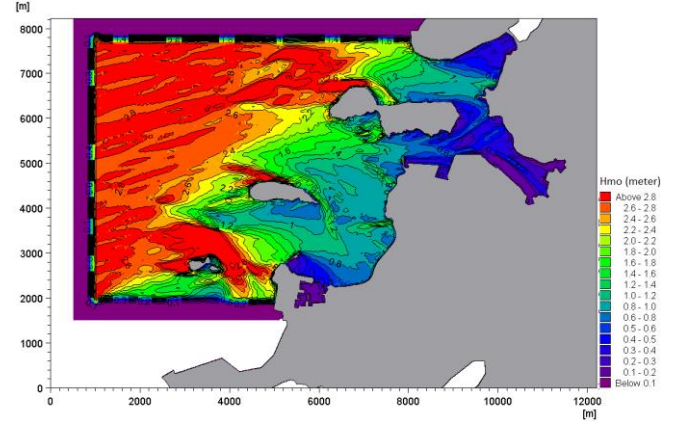


H<sub>m0</sub> 3m

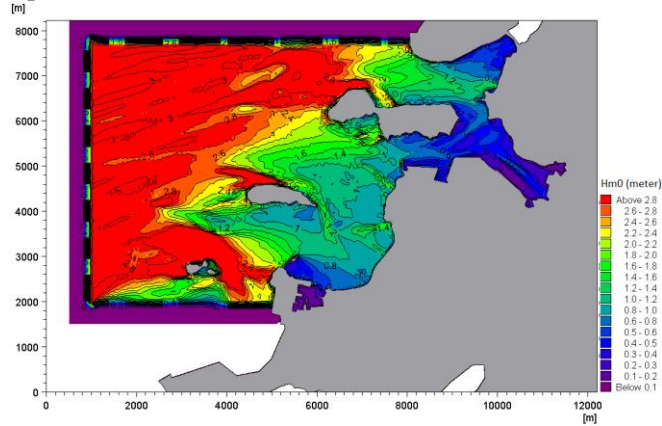
Tp 8s



Tp 10s

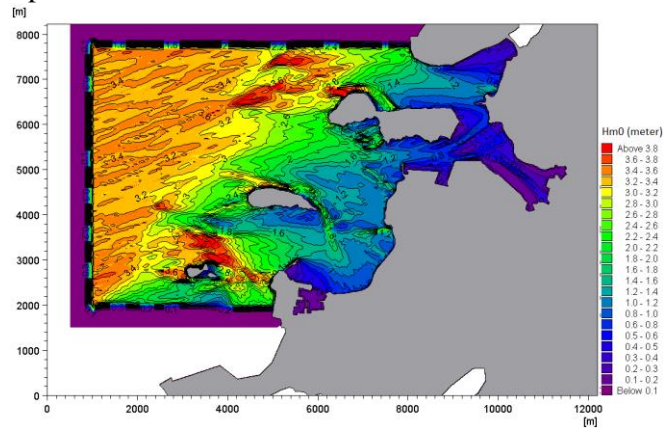


Tp 12s

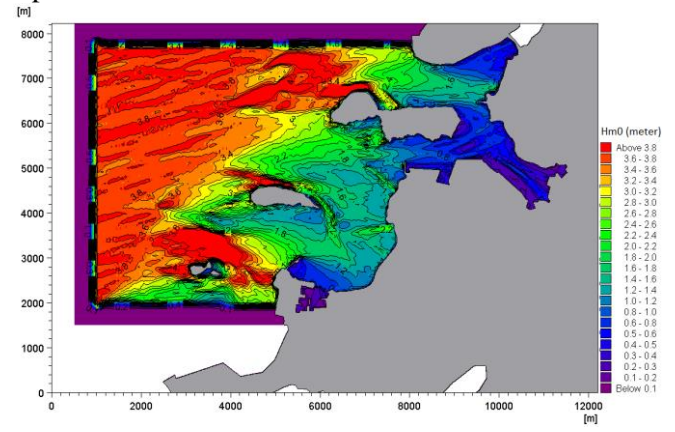


$H_{m0}$  4m

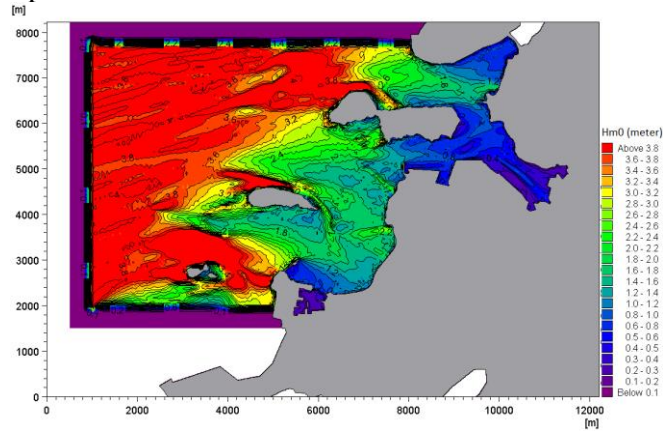
$T_p$  8s



$T_p$  10s



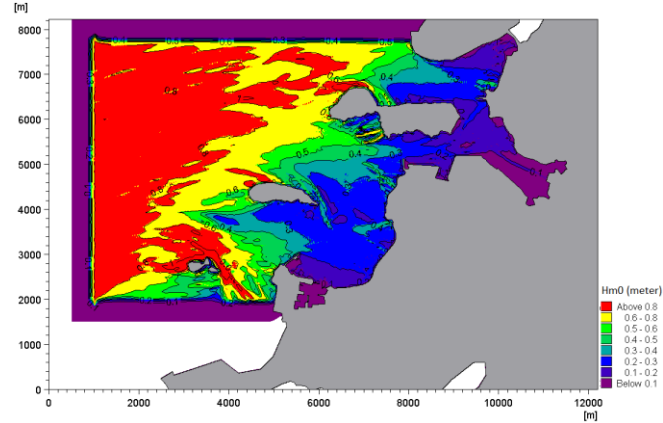
$T_p$  12s



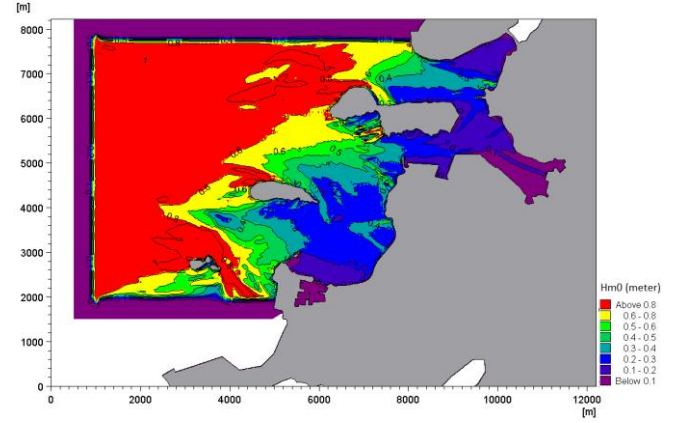
MWD: 305 degrees

$H_{m0}$  1m

$T_p$  8s



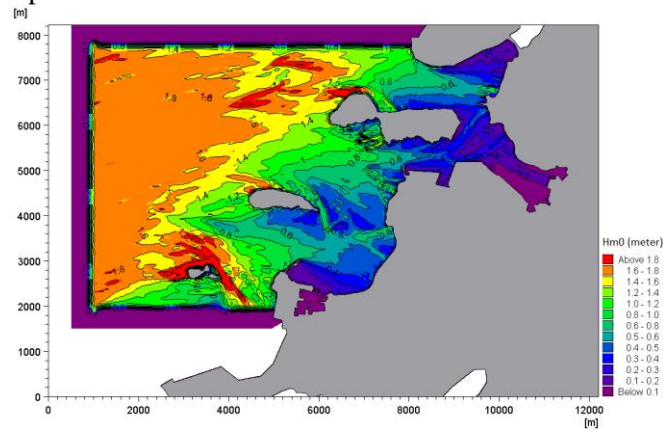
$T_p$  10s



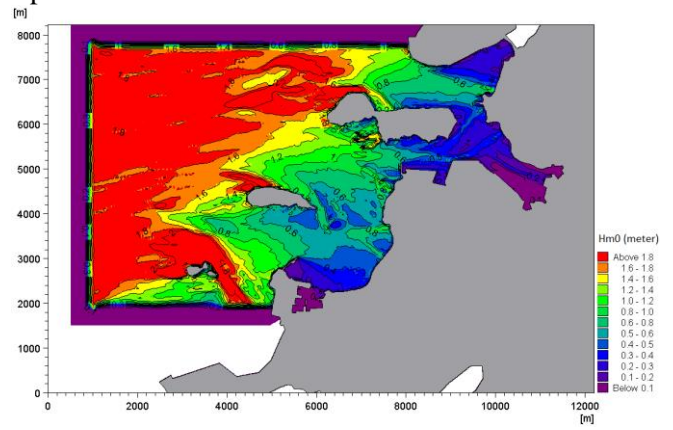


$H_{m0}$  2m

$T_p$  8s

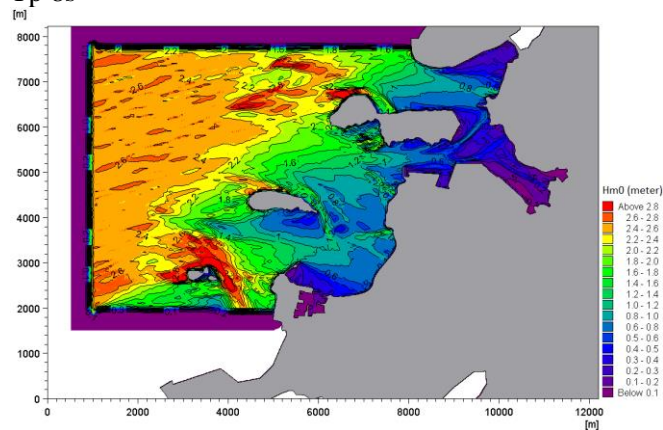


$T_p$  10s

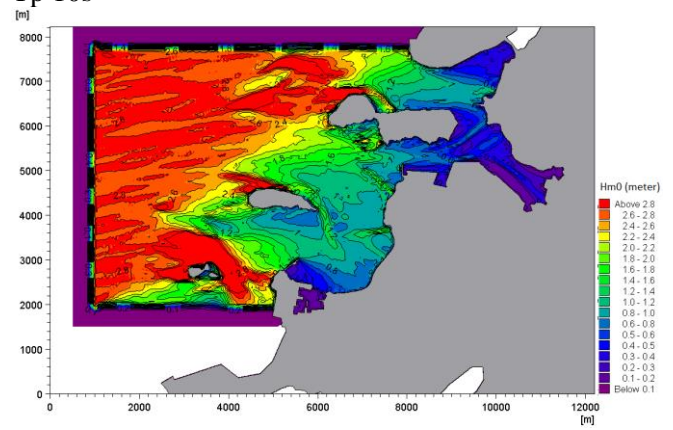


$H_{m0}$  3m

$T_p$  8s



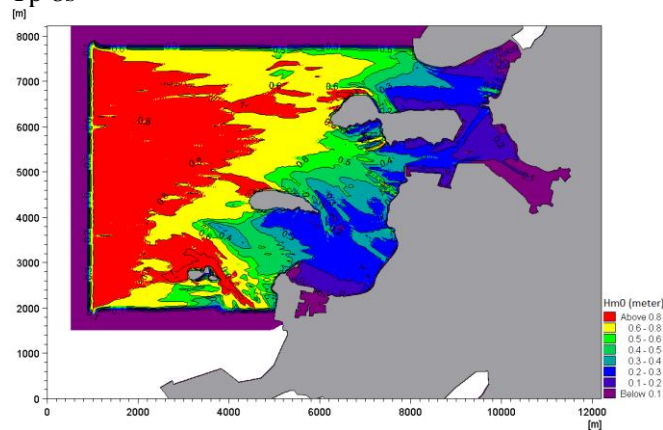
$T_p$  10s



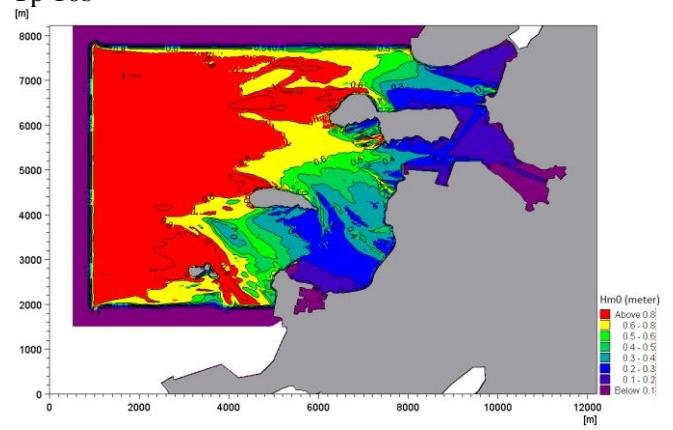
MWD: 315 degrees

$H_{m0}$  1m

$T_p$  8s

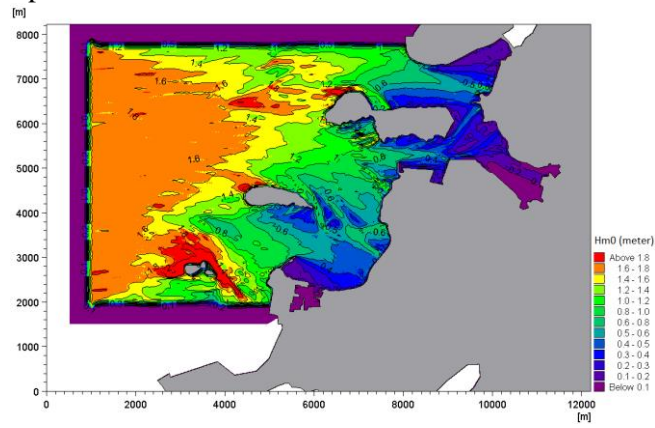


$T_p$  10s

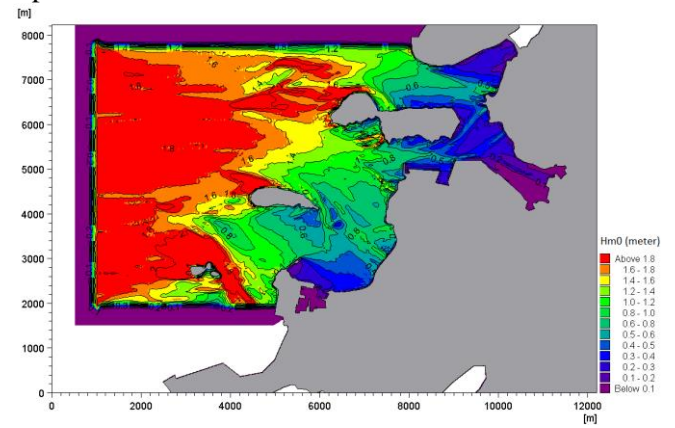


$H_{m0}$  2m

$T_p$  8s

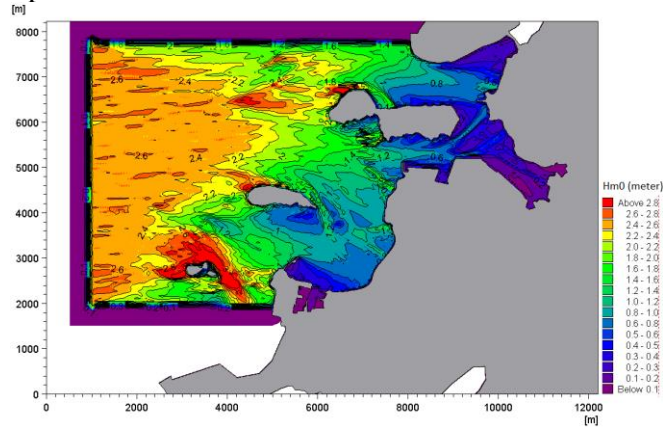


$T_p$  10s

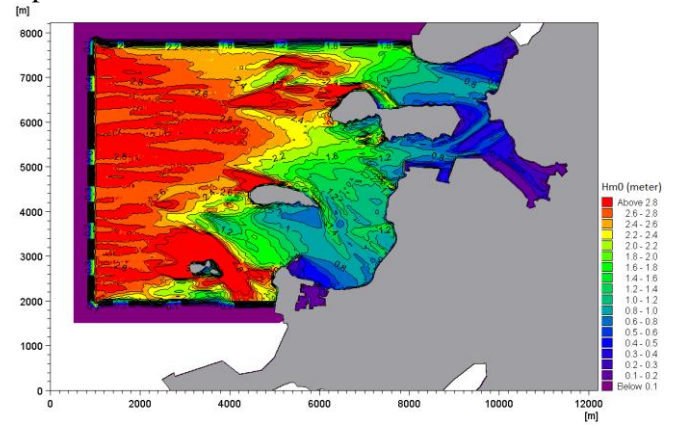


$H_{m0}$  3m

$T_p$  8s



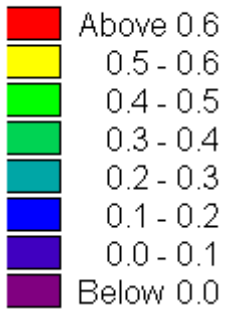
$T_p$  10s



**B.4  $H_{m0}$  at Hafnarbakki utan Klepps**

**Legend**

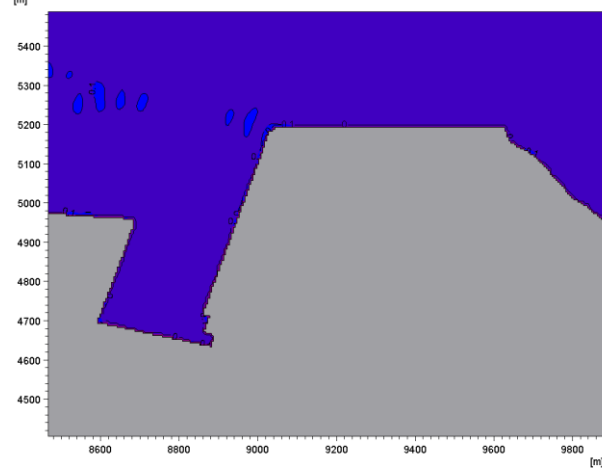
**Hm0 (meter)**



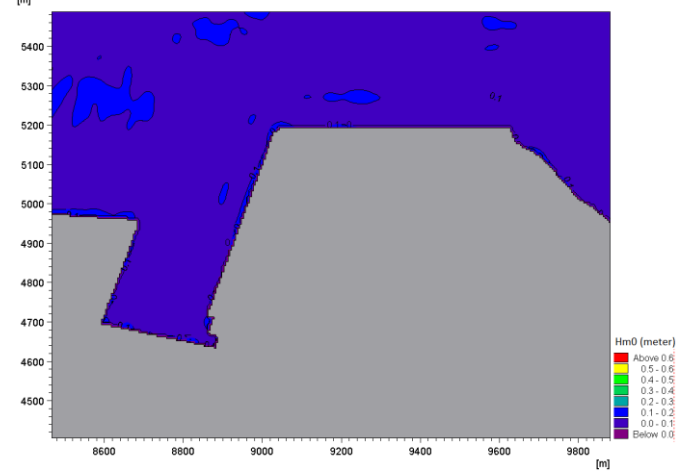
**MWD: 270 degrees**

**H<sub>m0</sub> 1m**

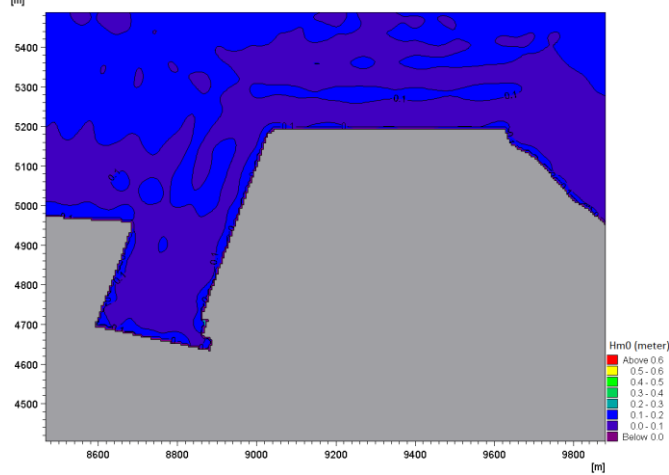
**Tp 10s**



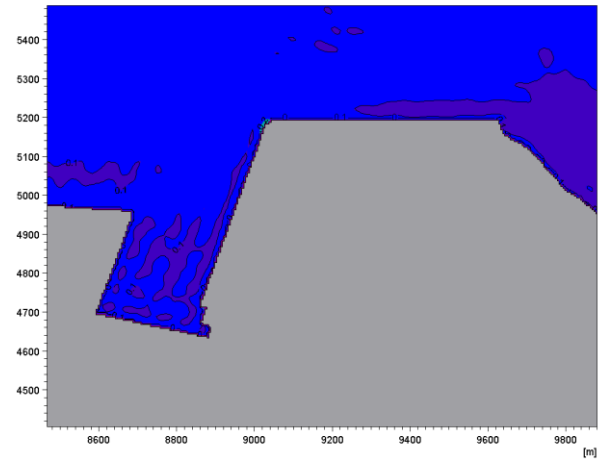
**Tp 12s**



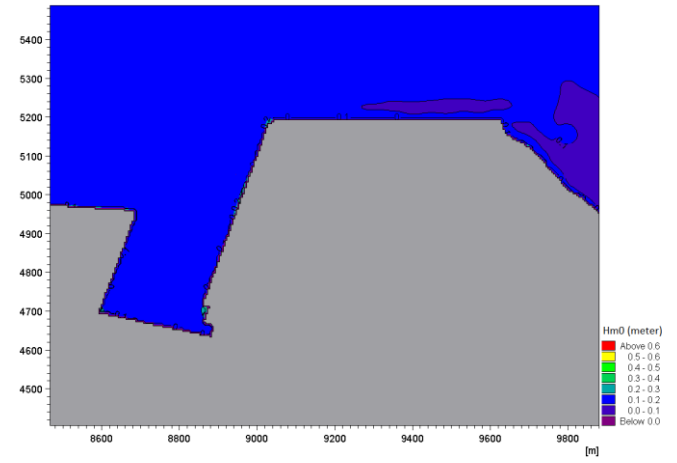
**Tp 15s**



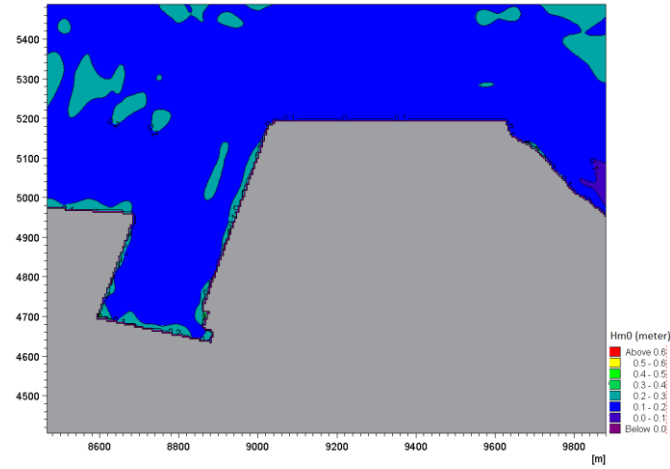
$H_{m0}$  2m  
Tp 10s



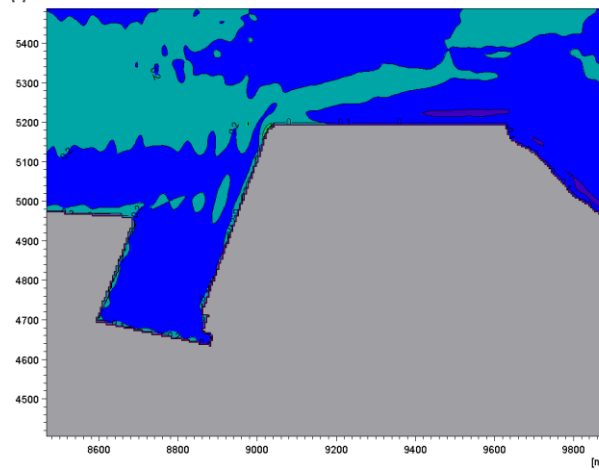
Tp 12s



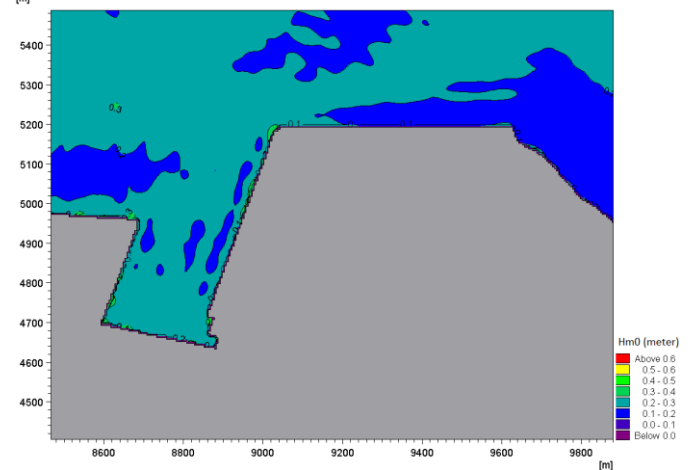
Tp 15s



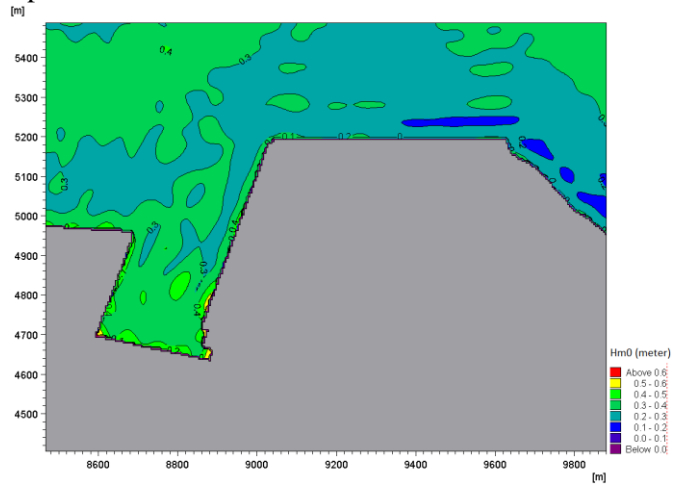
$H_{m0}$  3m  
Tp 10s



Tp 12s



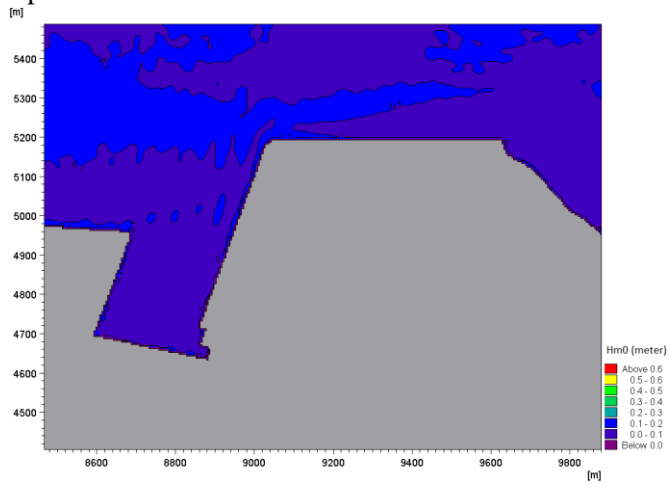
Tp 15s



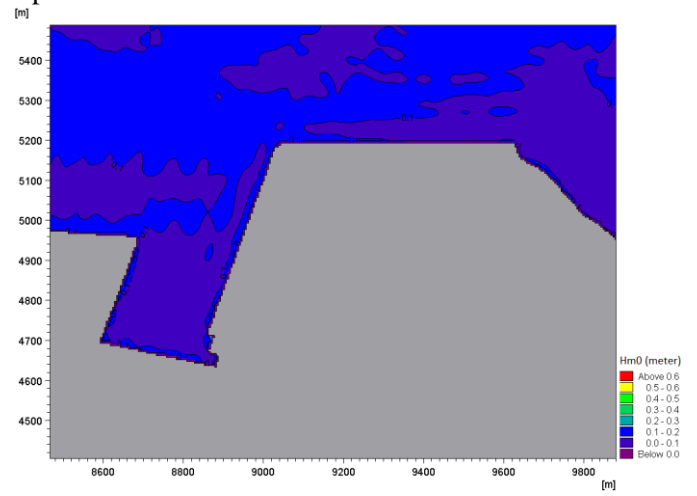
MWD: 280 degrees

Hm0 1m

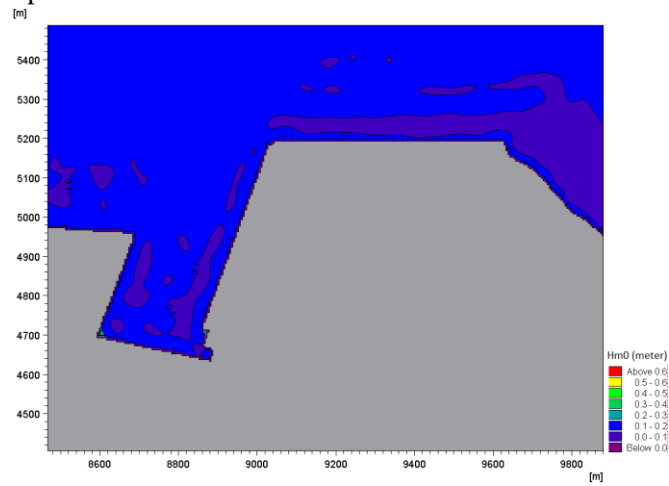
Tp 10s



Tp 12s

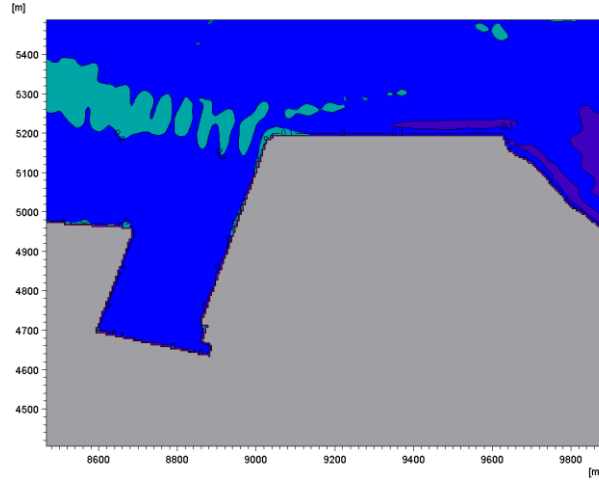


Tp 15s

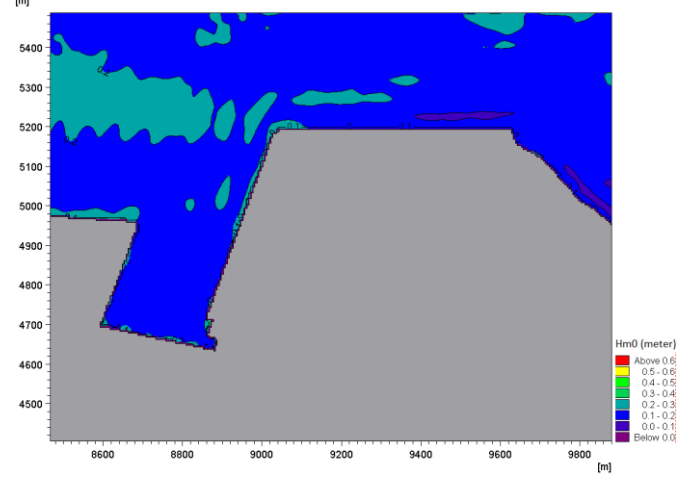


$H_{m0}$  2m

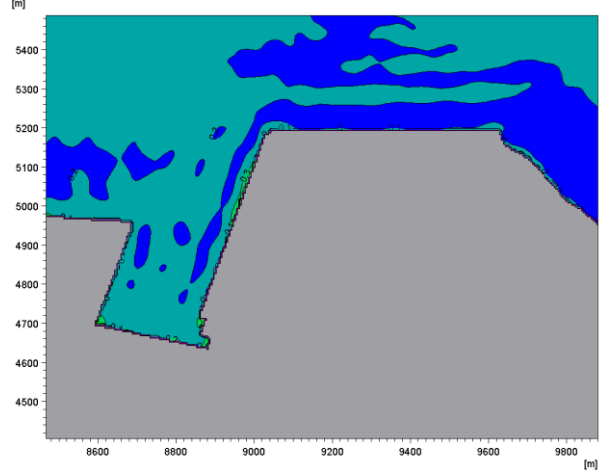
$T_p$  10s



$T_p$  12s

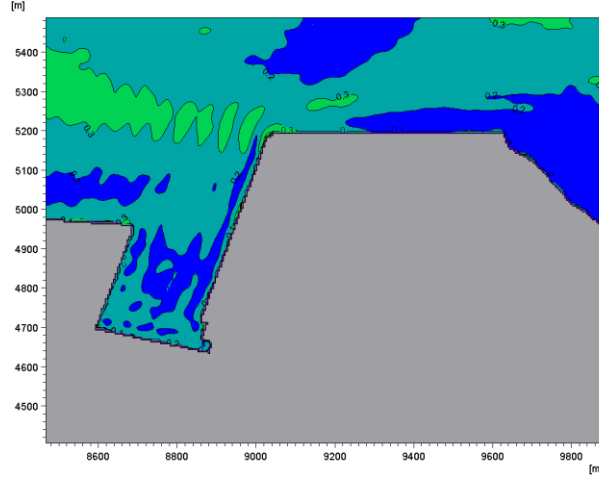


$T_p$  15s

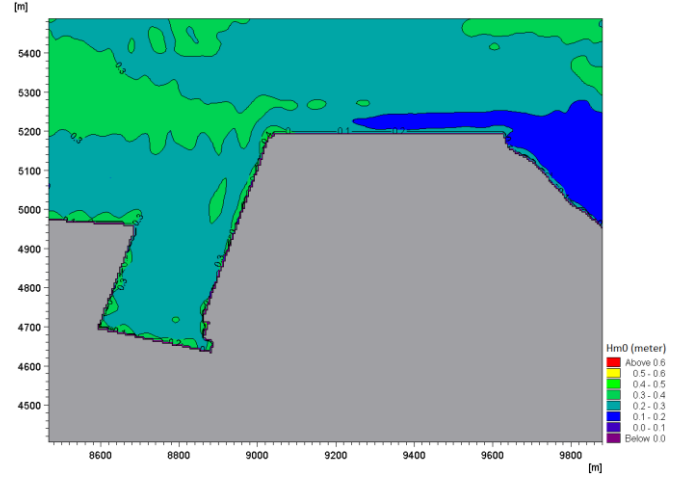


$H_{m0}$  3m

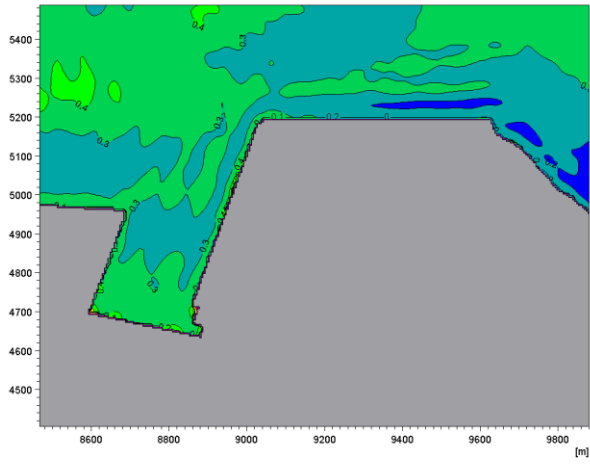
$T_p$  10s



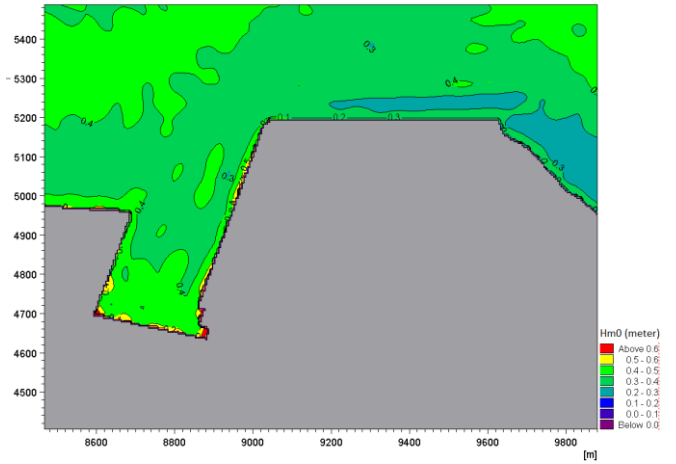
$T_p$  12s



Tp 13s  
 [m]

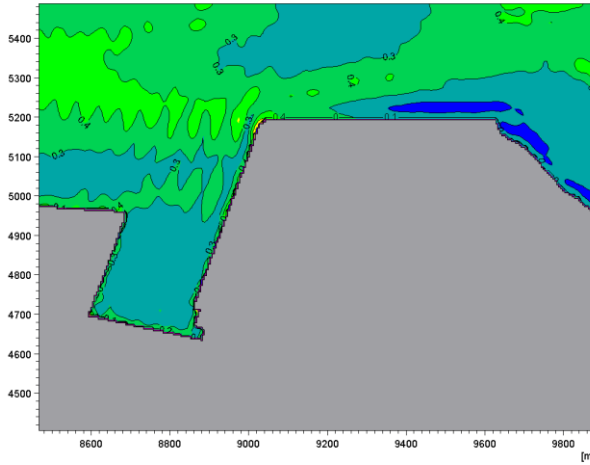


Tp 15s  
 [m]

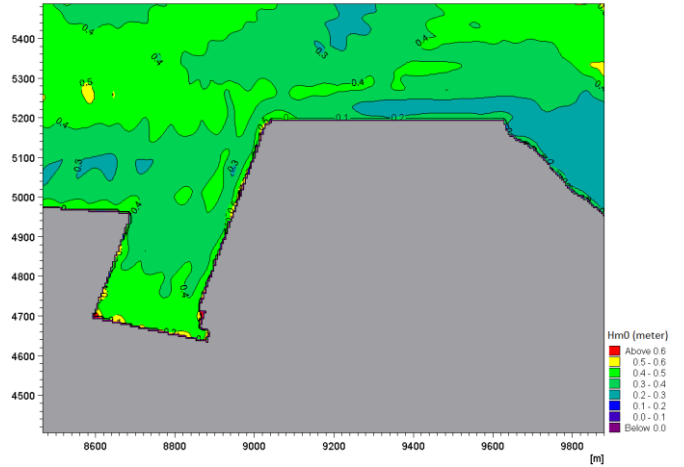


H<sub>m0</sub> 4m

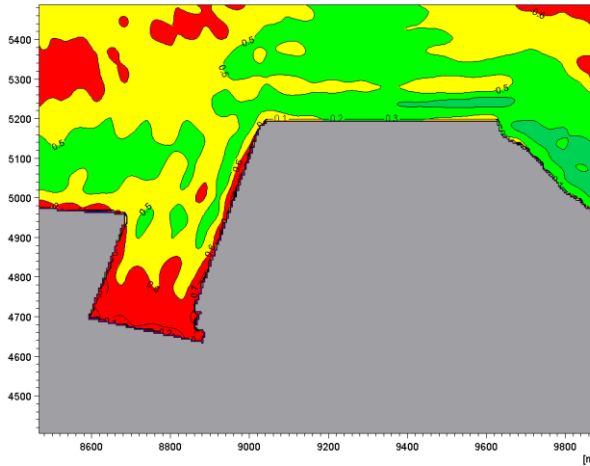
Tp 10s  
 [m]



Tp 12s  
 [m]



Tp 15s  
 [m]

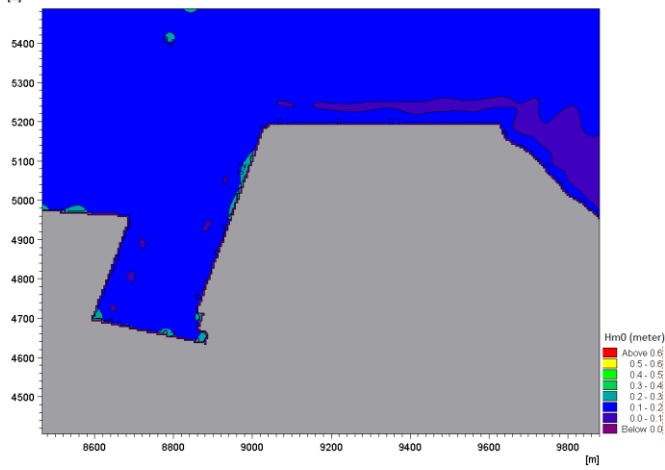




MWD: 285 degrees

$H_{m0}$  1m

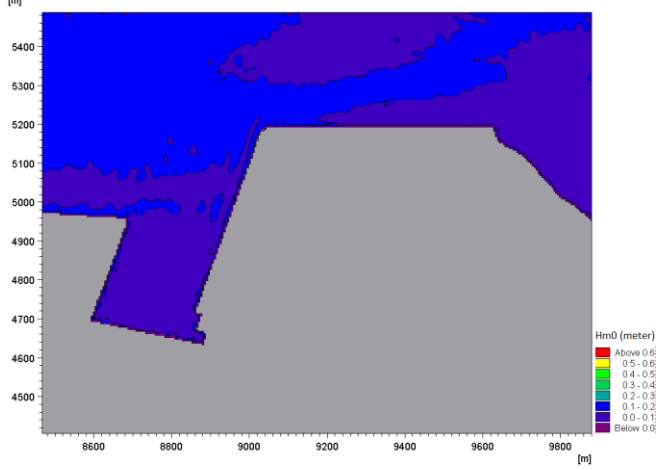
$T_p$  17s



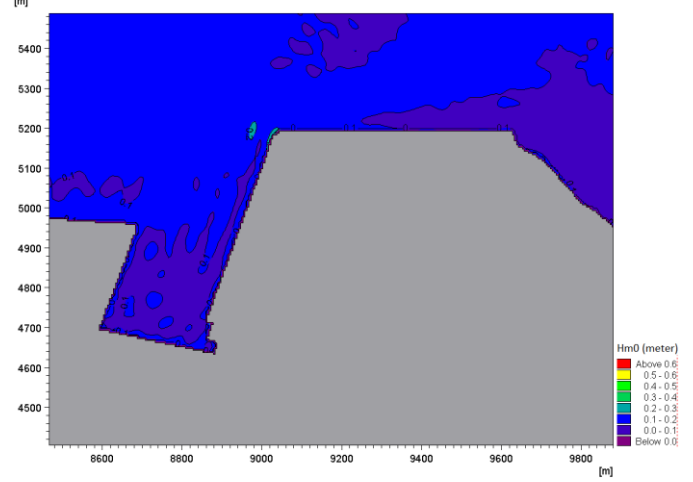
MWD: 290 degrees

$H_{m0}$  1m

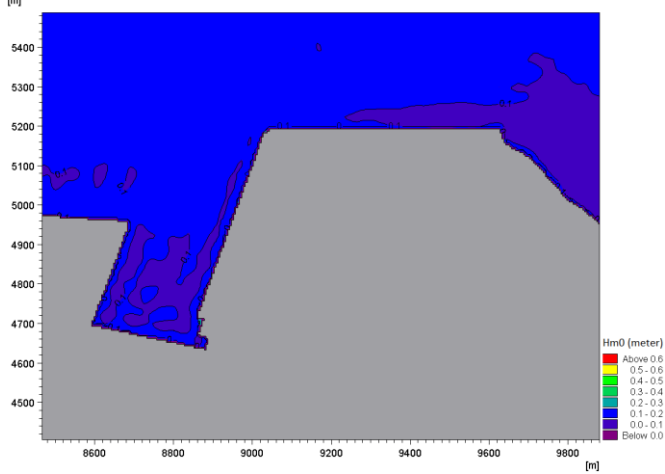
$T_p$  8s



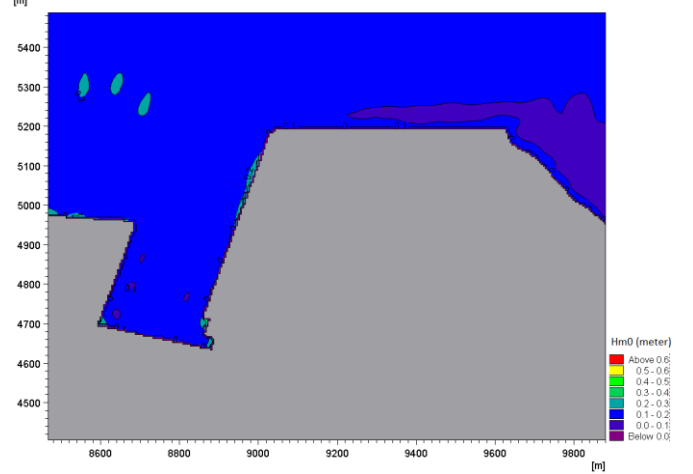
$T_p$  10s



$T_p$  12s

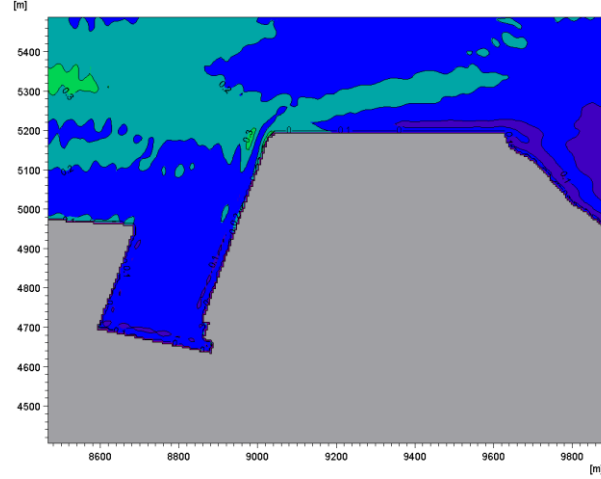


$T_p$  15s

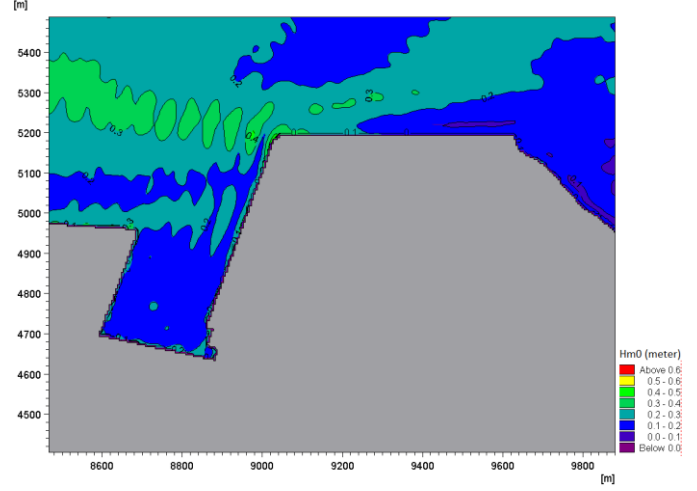


$H_{m0}$  2m

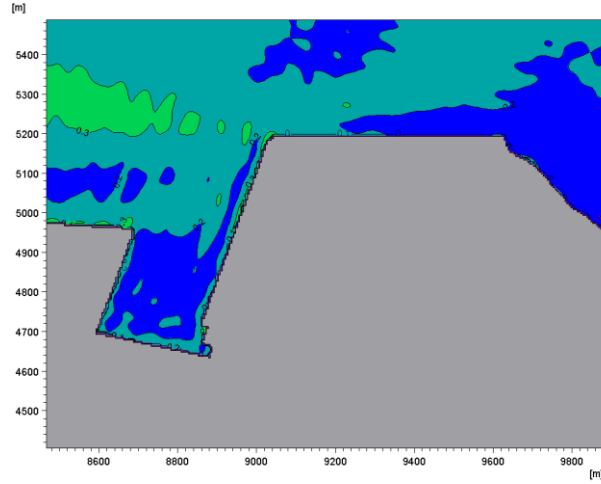
$T_p$  8s



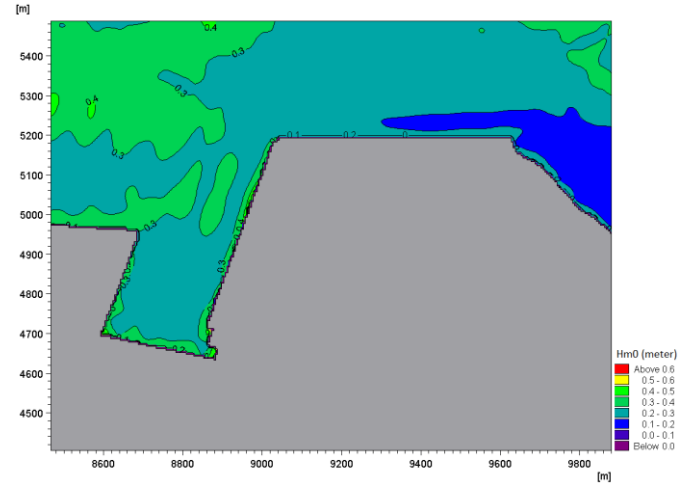
$T_p$  10s



$T_p$  12s

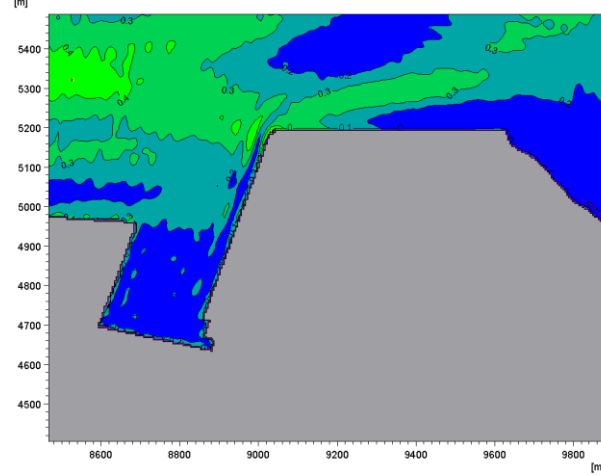


$T_p$  15s

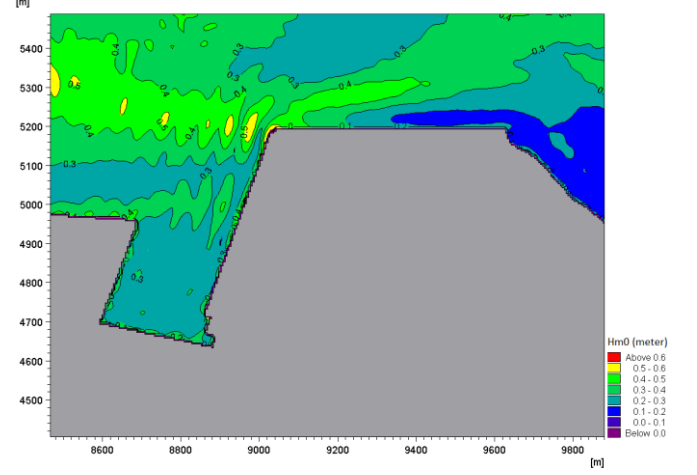


$H_{m0}$  3m

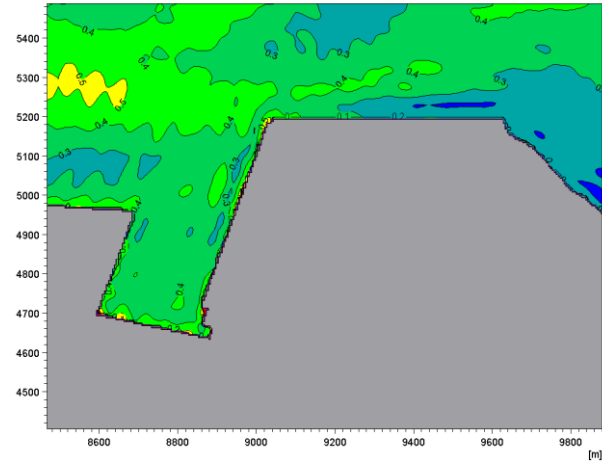
$T_p$  8s



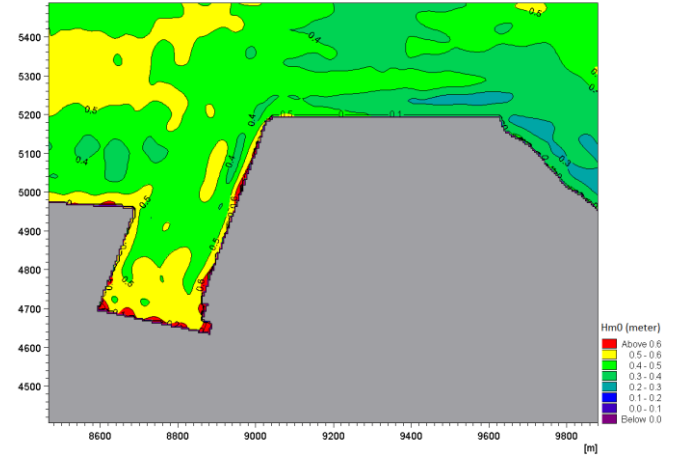
$T_p$  10s



Tp 12s

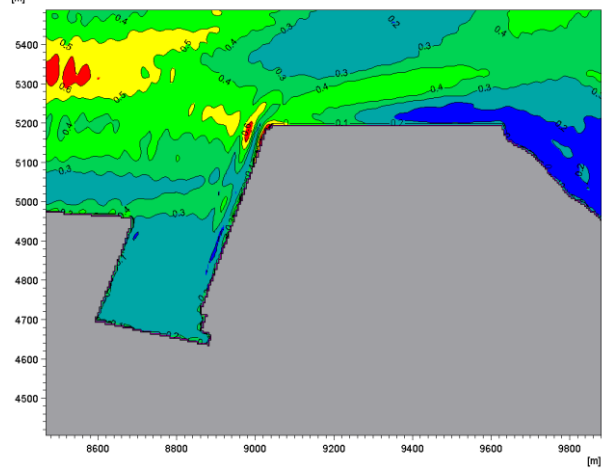


Tp 15s

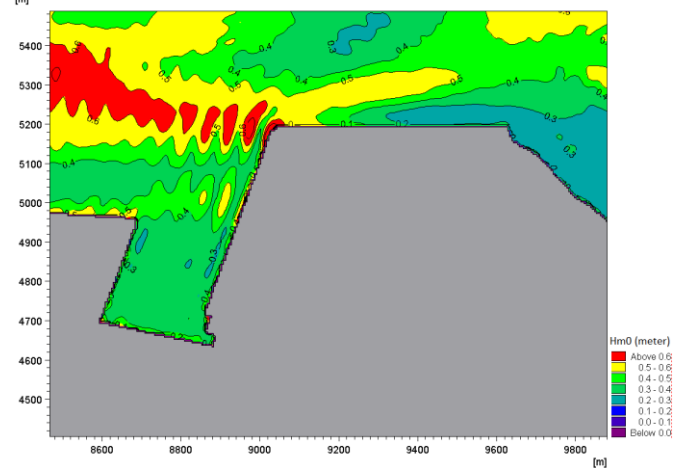


H<sub>m0</sub> 4m

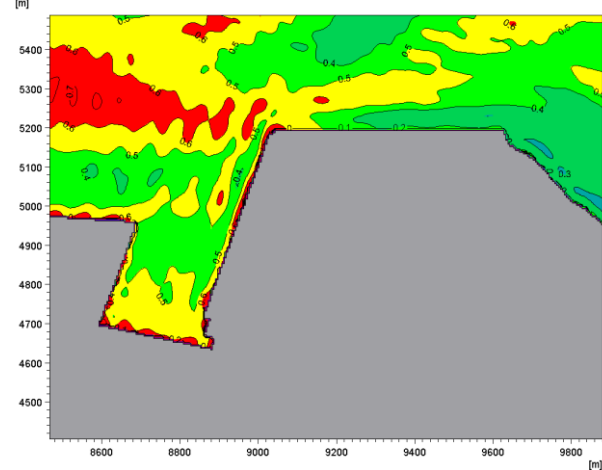
Tp 8s



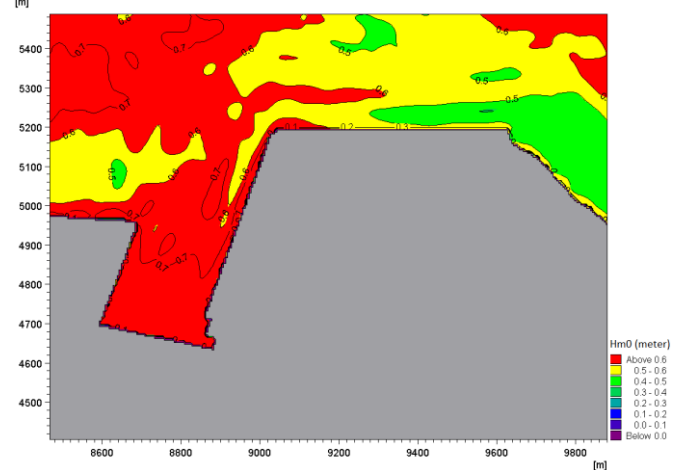
Tp 10s



Tp 12s



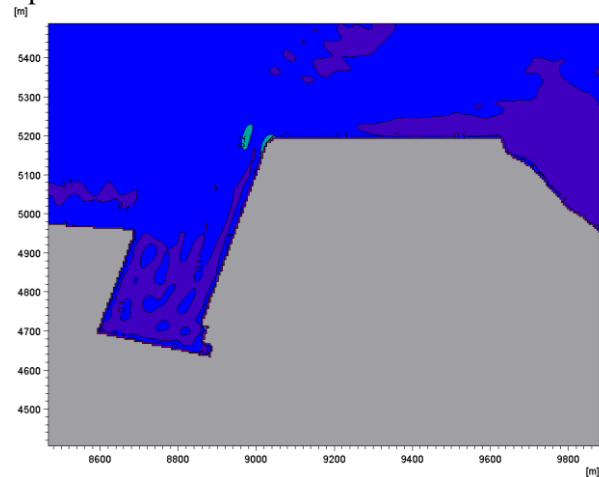
Tp 15s



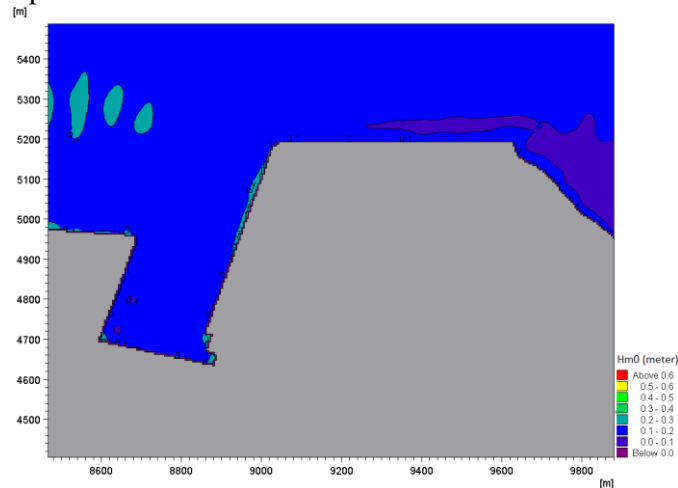
# MWD: 292.5 degrees

$H_{m0}$  1m

$T_p$  10s

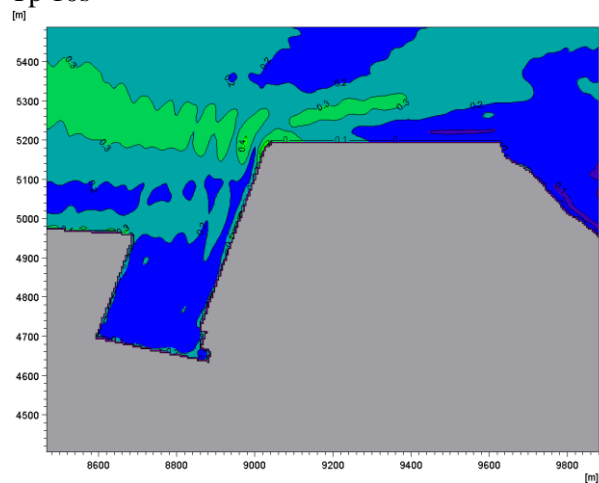


$T_p$  15s

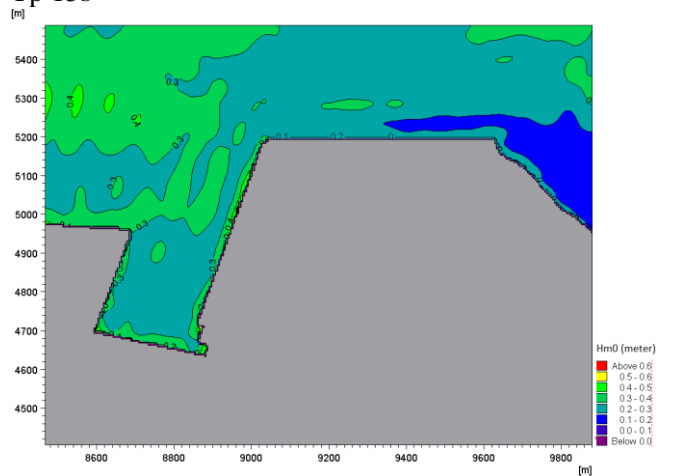


$H_{m0}$  2m

$T_p$  10s

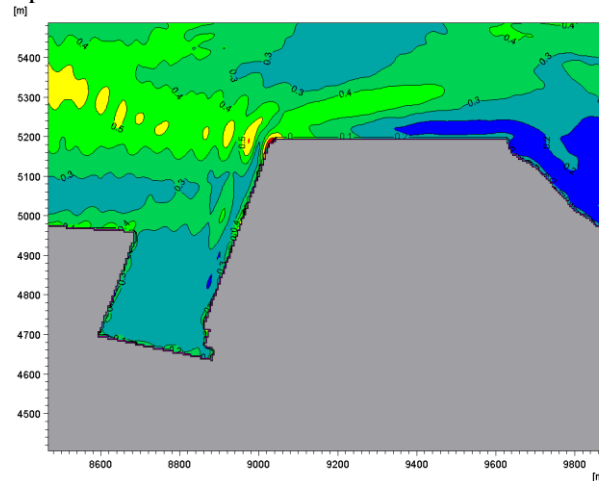


$T_p$  15s

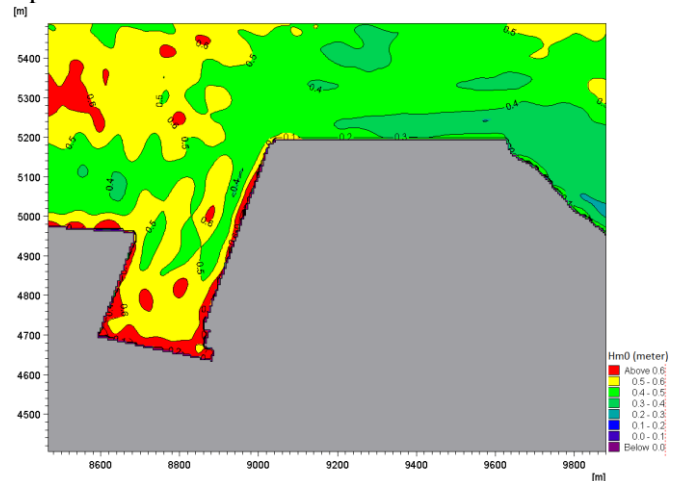


$H_{m0}$  3m

$T_p$  10s



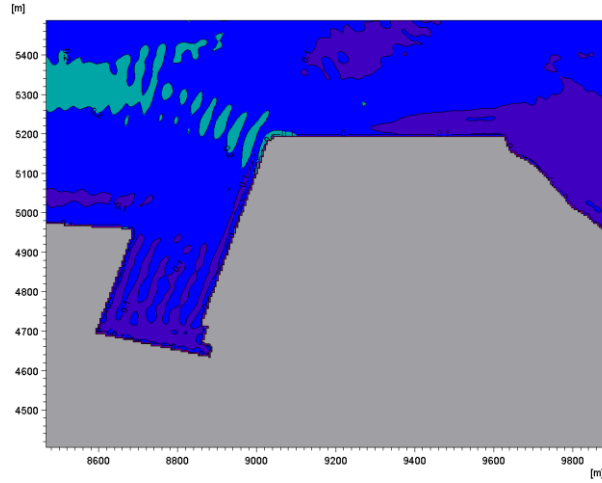
$T_p$  15s



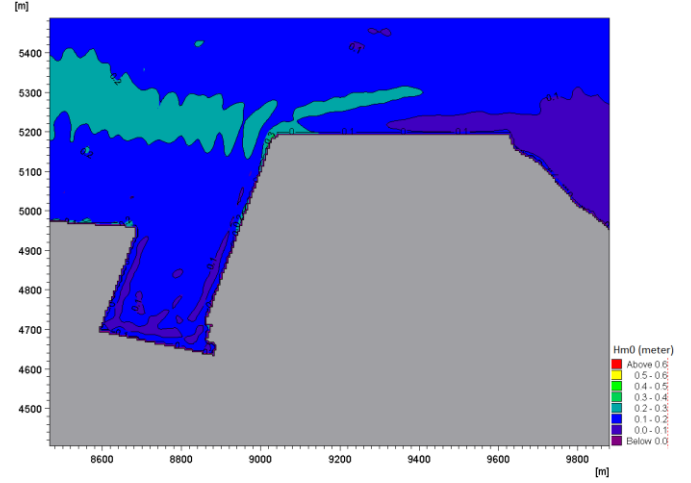
MWD: 300 degrees

$H_{m0}$  1m

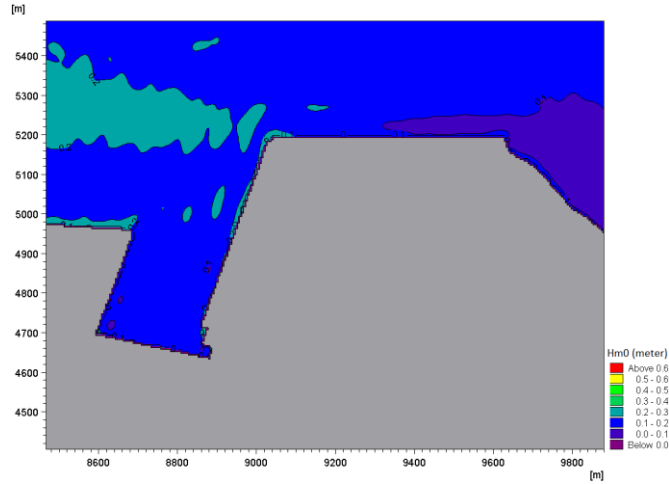
$T_p$  8s



$T_p$  10s

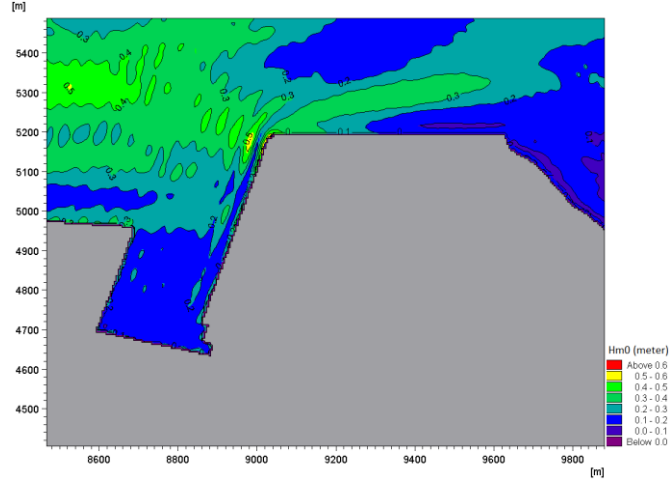


$T_p$  12s

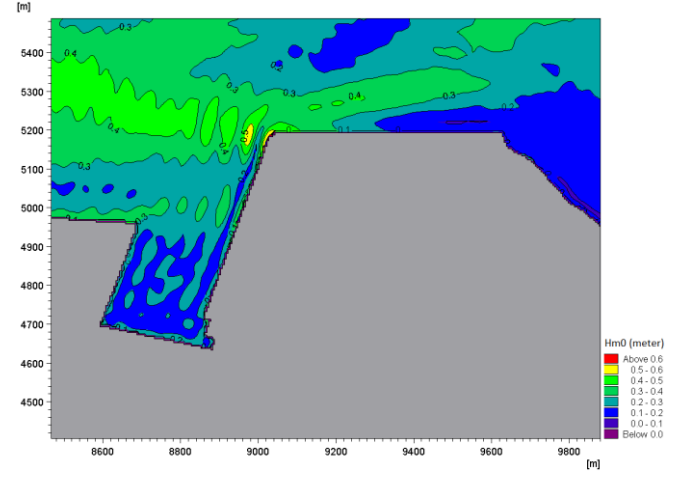


$H_{m0}$  2m

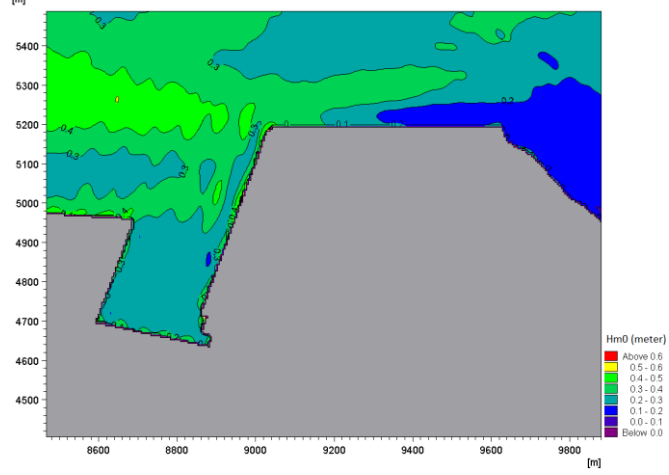
$T_p$  8s



$T_p$  10s

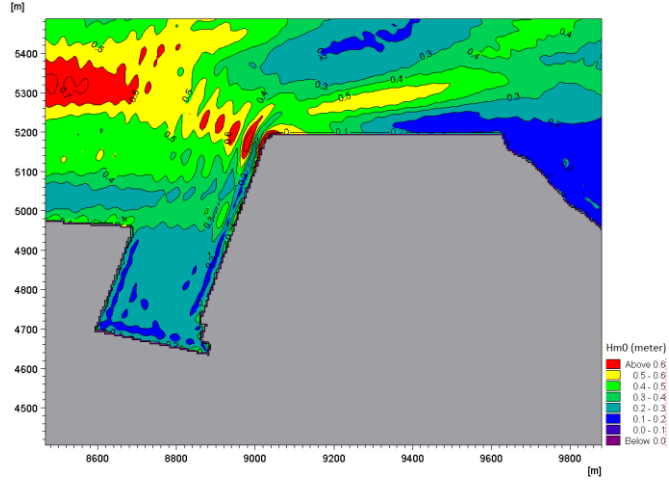


Tp 12s

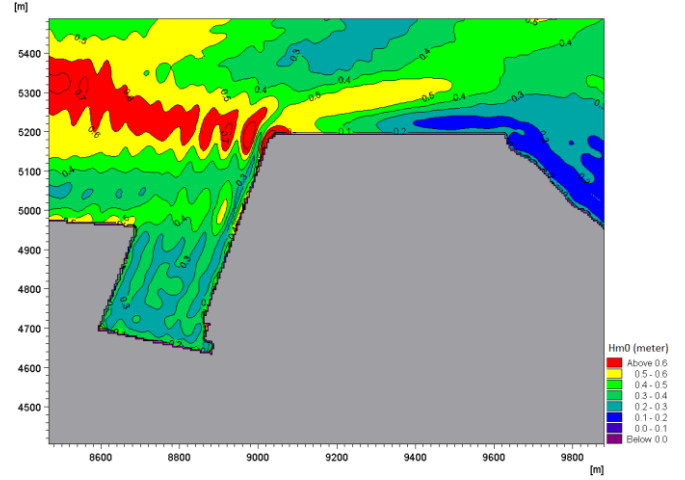


$H_{m0}$  3m

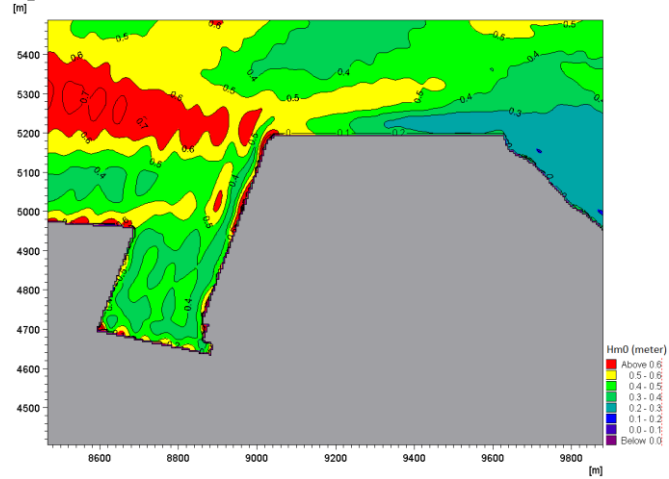
Tp 8s



Tp 10s

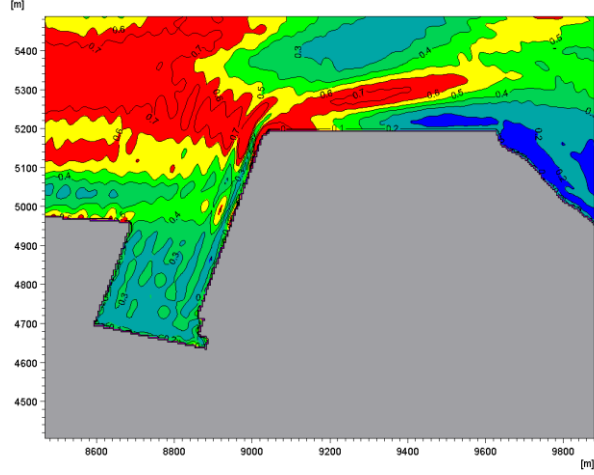


Tp 12s

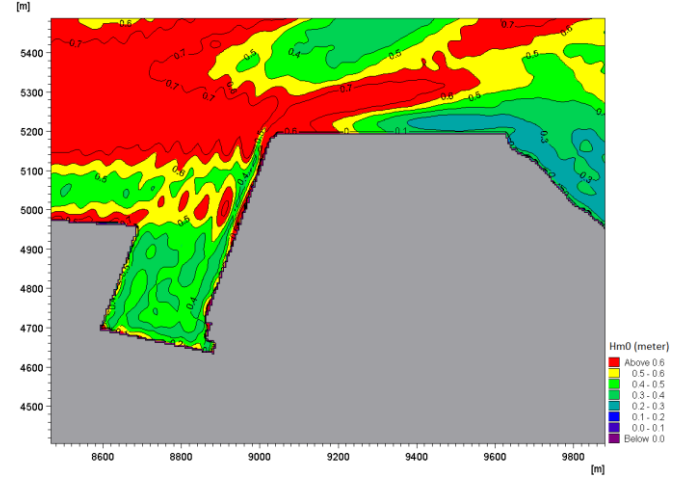


$H_{m0}$  4m

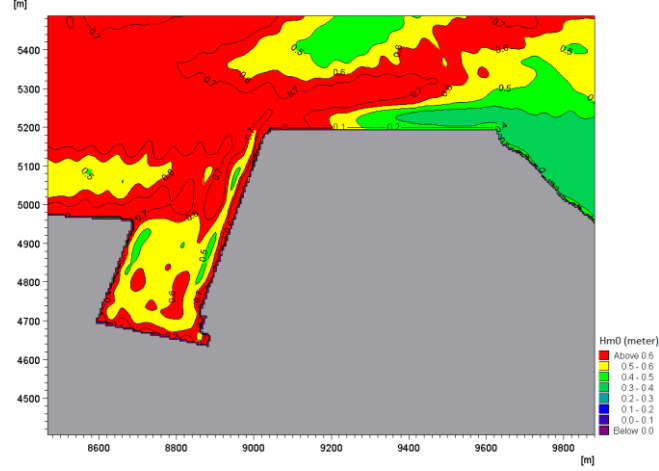
$T_p$  8s



$T_p$  10s



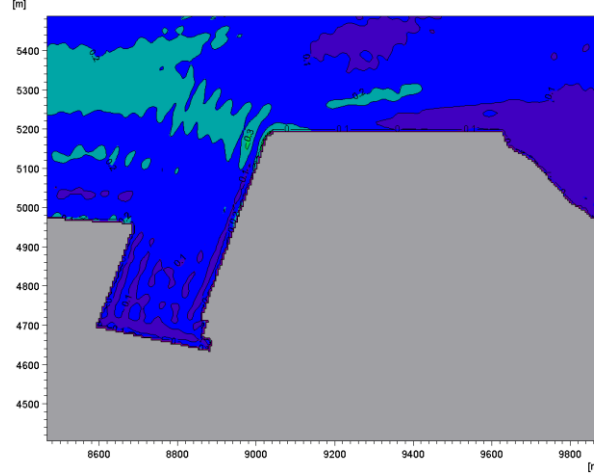
$T_p$  12s



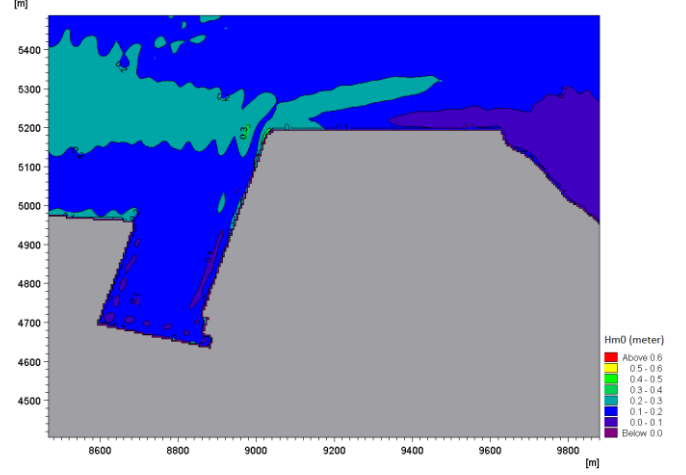
MWD: 305 degrees

$H_{m0}$  1m

$T_p$  8s

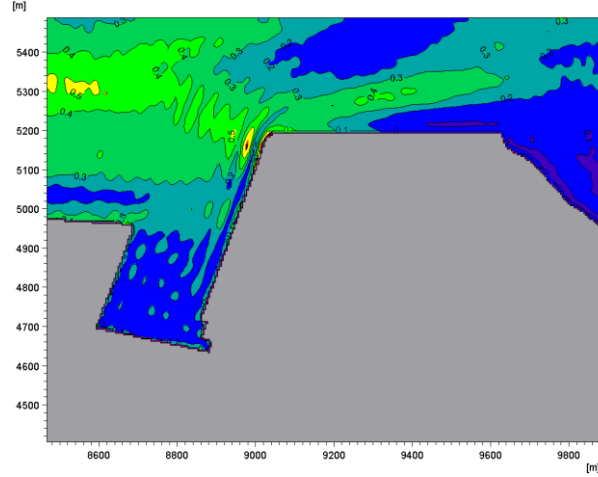


$T_p$  10s

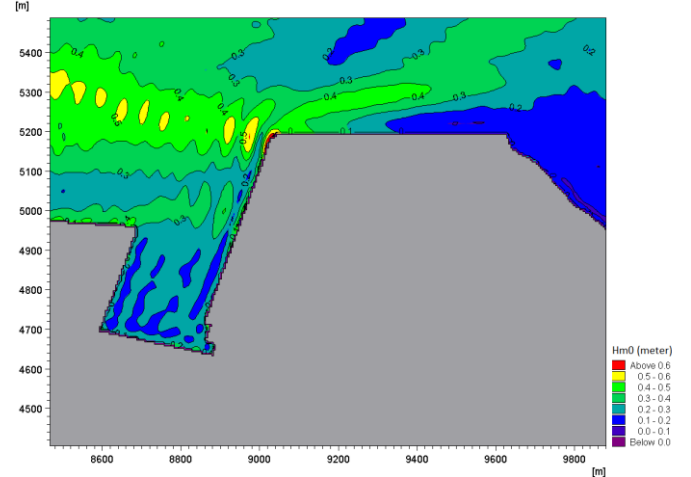


$H_{m0}$  2m

$T_p$  8s

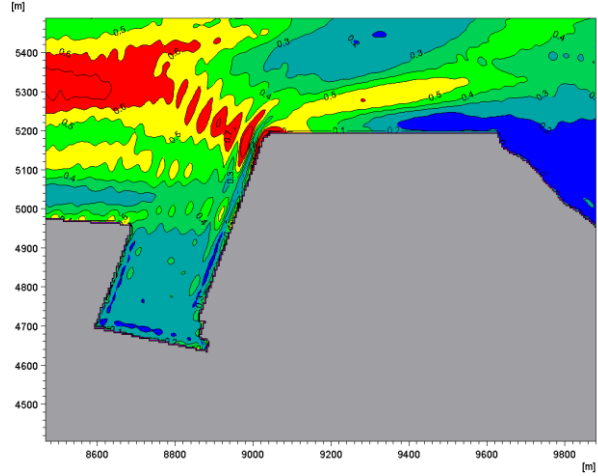


$T_p$  10s

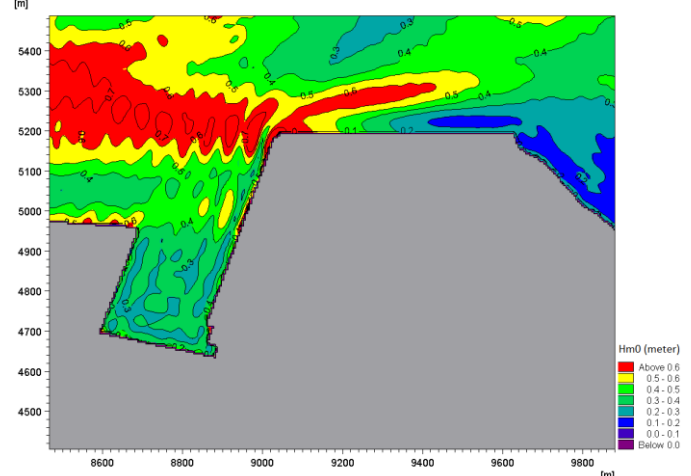


$H_{m0}$  3m

$T_p$  8s



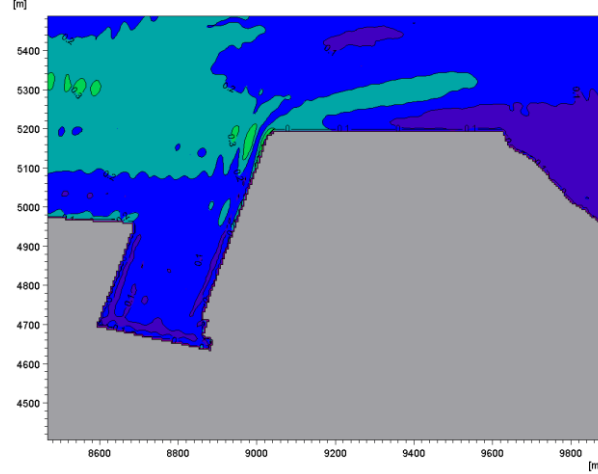
$T_p$  10s



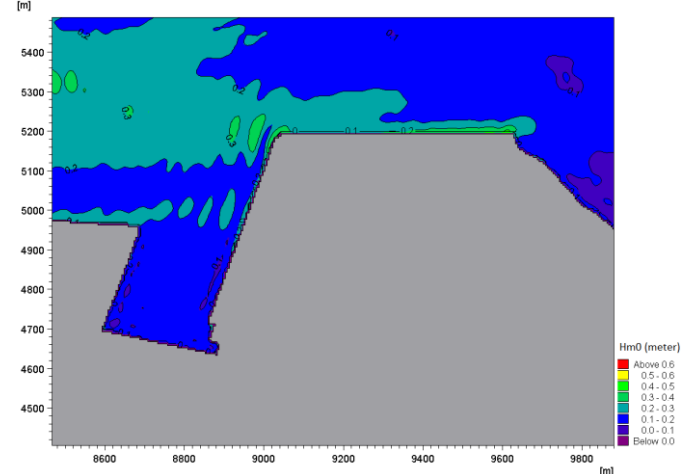
MWD: 315 degrees

$H_{m0}$  1m

$T_p$  8s

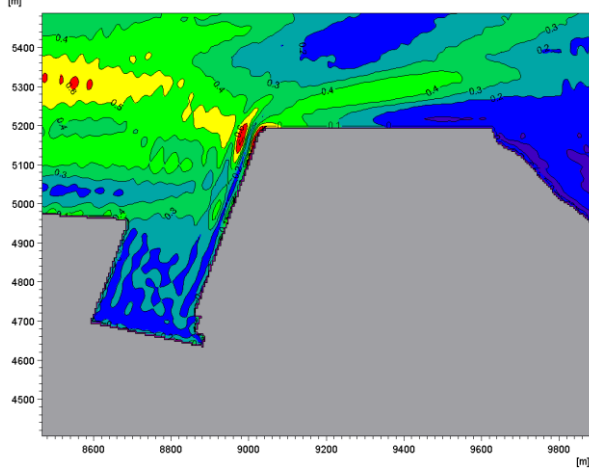


$T_p$  10s

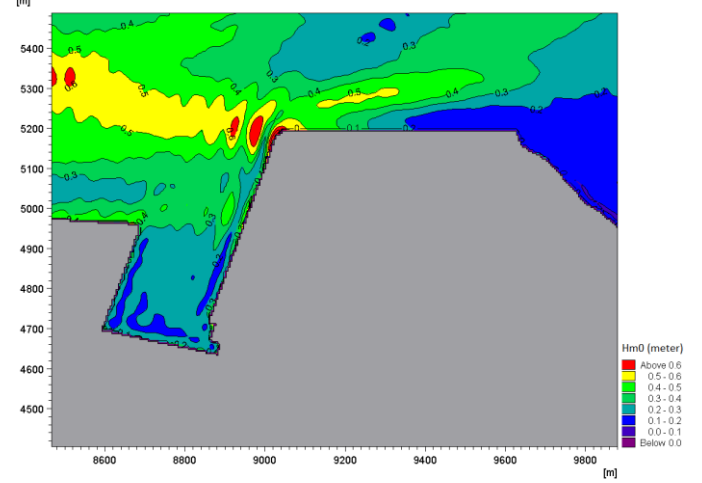




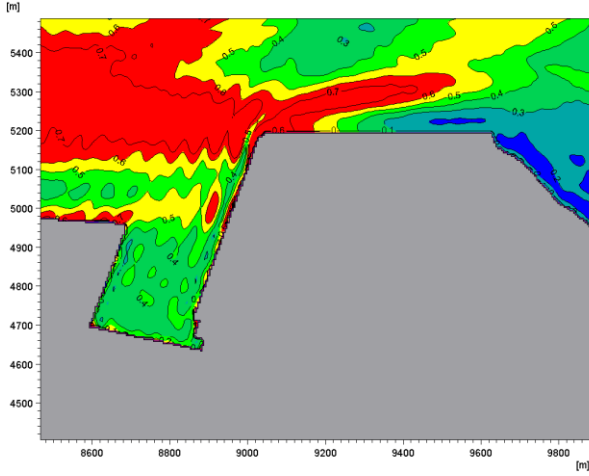
$H_{m0}$  2m  
 $T_p$  8s



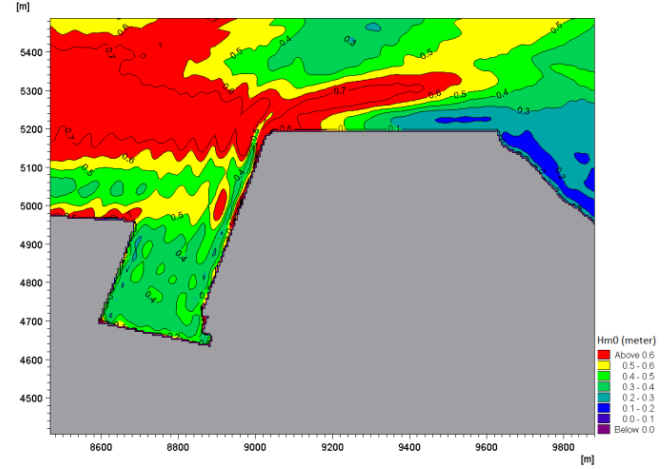
$T_p$  10s



$H_{m0}$  3m  
 $T_p$  8s



$T_p$  10s



## C Appendix - DVRS Figures

In this appendix all the data points and figures of the six degrees of motion for the different DVRS outputs are shown in tables and figures, along with the mooring line force figures.

### C.1 Polypropylene Line, Polyamide Tail, no wind

Table C.1: DVRS Datapoints for  $H_{m0}$  1m

	Hm0 1m																				
	Tp 8s				Tp 10s								Tp 12s				Tp 15s				Tp 17s
	290	300	305	315	270	280	290	292.5	300	305	315	270	280	290	300	270	280	290	292.5	285	
Surge (m)	0.016	0.028	0.027	0.028	0.032	0.035	0.040	0.060	0.062	0.071	0.071	0.059	0.067	0.083	0.100	0.079	0.093	0.098	0.110	0.128	
Sway (m)	0.053	0.056	0.053	0.048	0.066	0.069	0.072	0.082	0.077	0.075	0.078	0.096	0.099	0.114	0.103	0.092	0.107	0.106	0.111	0.139	
Heave (m)	0.027	0.032	0.033	0.032	0.040	0.043	0.046	0.053	0.050	0.051	0.052	0.056	0.061	0.057	0.058	0.070	0.076	0.076	0.084	0.091	
Roll (deg)	0.157	0.182	0.182	0.183	0.225	0.250	0.270	0.293	0.321	0.336	0.334	0.285	0.353	0.351	0.394	0.328	0.344	0.371	0.417	0.397	
Pitch (deg)	0.038	0.059	0.069	0.081	0.046	0.055	0.064	0.070	0.089	0.101	0.104	0.060	0.069	0.086	0.103	0.065	0.074	0.083	0.089	0.081	
Yaw (deg)	0.042	0.045	0.044	0.043	0.067	0.078	0.074	0.079	0.078	0.082	0.101	0.111	0.122	0.127	0.116	0.133	0.147	0.137	0.148	0.165	

Table C.2: DVRS Datapoints for  $H_{m0}$  2m

	Hm0 2m																			
	Tp 8s				Tp 10s								Tp 12s				Tp 15s			
	290	300	305	315	270	280	290	292.5	300	305	315	270	280	290	300	270	280	290	292.5	
Surge (m)	0.044	0.073	0.063	0.076	0.065	0.083	0.100	0.122	0.141	0.140	0.137	0.118	0.134	0.181	0.219	0.134	0.204	0.307	0.306	
Sway (m)	0.078	0.082	0.083	0.073	0.096	0.105	0.113	0.126	0.115	0.113	0.100	0.146	0.158	0.169	0.146	0.139	0.214	0.192	0.209	
Heave (m)	0.046	0.054	0.057	0.058	0.060	0.068	0.078	0.083	0.084	0.084	0.090	0.080	0.087	0.092	0.093	0.099	0.119	0.135	0.136	
Roll (deg)	0.244	0.262	0.278	0.264	0.351	0.403	0.416	0.467	0.469	0.504	0.494	0.461	0.532	0.567	0.658	0.481	0.560	0.627	0.708	
Pitch (deg)	0.078	0.119	0.143	0.159	0.077	0.089	0.116	0.127	0.160	0.184	0.197	0.093	0.106	0.139	0.177	0.095	0.113	0.157	0.150	
Yaw (deg)	0.057	0.059	0.060	0.061	0.090	0.106	0.105	0.111	0.108	0.106	0.107	0.156	0.183	0.177	0.169	0.186	0.238	0.246	0.230	

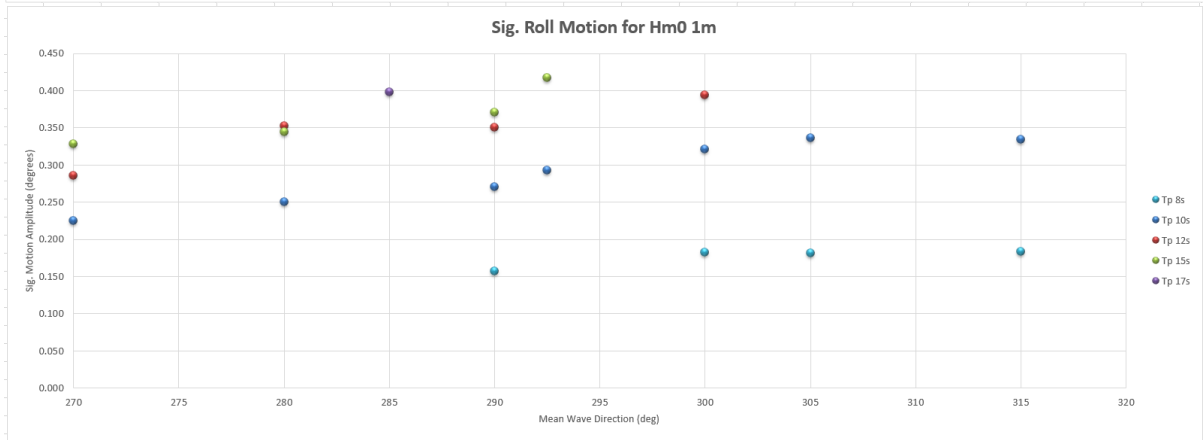
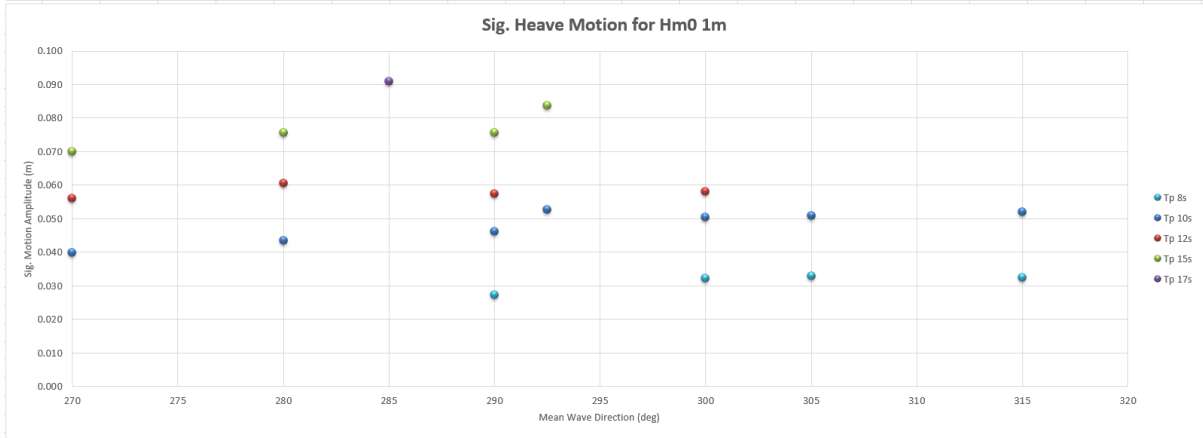
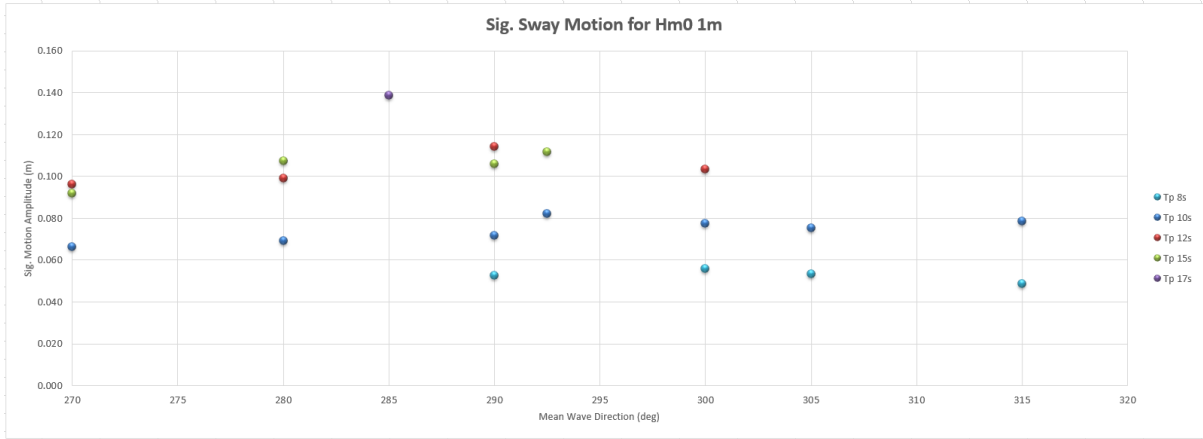
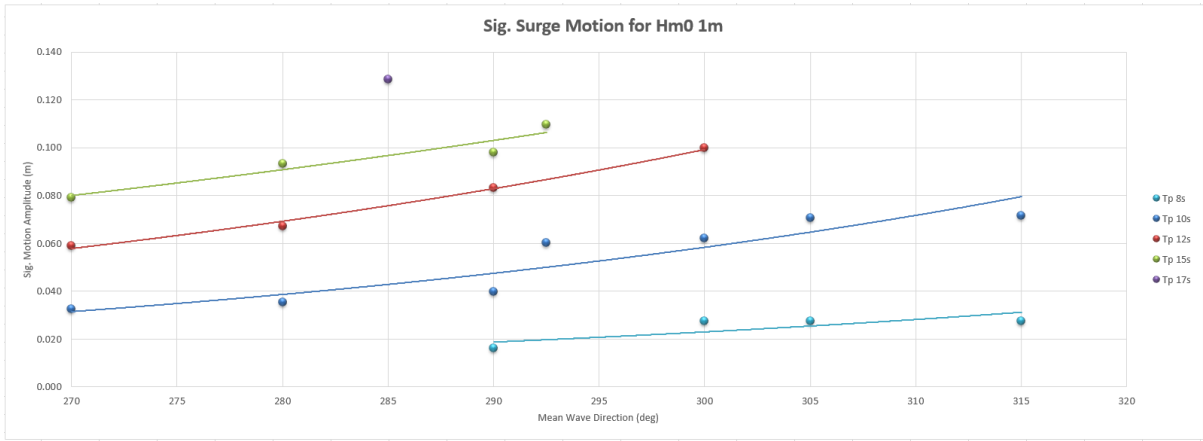
Table C.3: DVRS Datapoints for  $H_{m0}$  3m

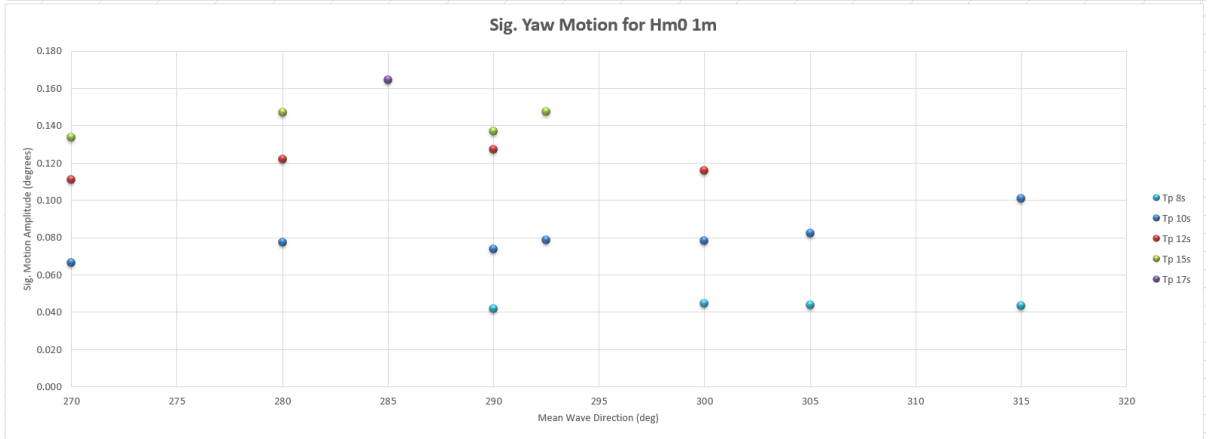
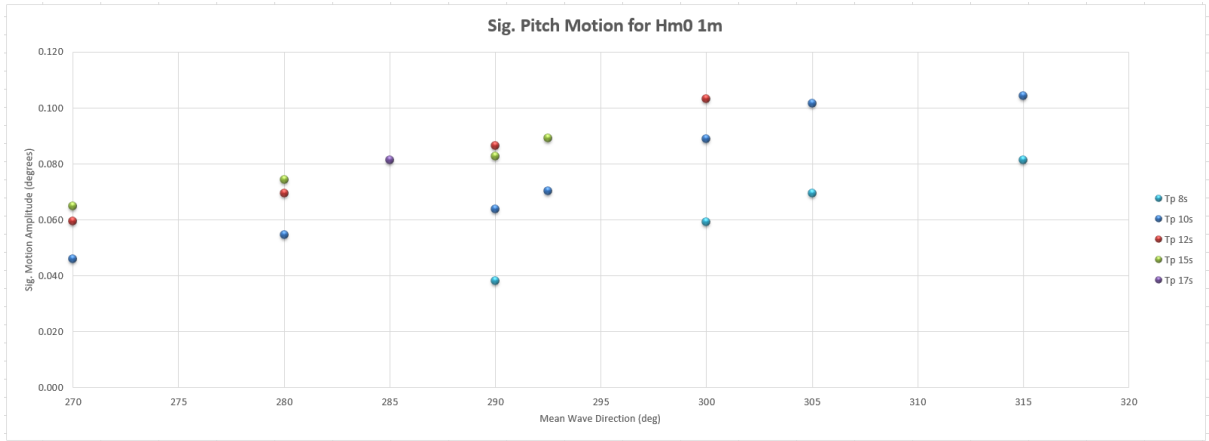
	Hm0 3m																				
	Tp 8s				Tp 10s								Tp 12s				Tp 13s	Tp 15s			
	290	300	305	315	270	280	290	292.5	300	305	315	270	280	290	300	280	270	280	290	292.5	
Surge (m)	0.092	0.123	0.163	0.160	0.085	0.140	0.201	0.204	0.301	0.367	0.456	0.145	0.262	0.332	0.502	0.389	0.531	0.970	0.819	0.995	
Sway (m)	0.086	0.083	0.083	0.082	0.090	0.112	0.136	0.135	0.138	0.134	0.128	0.160	0.185	0.241	0.255	0.234	0.388	0.417	0.513	0.488	
Heave (m)	0.057	0.069	0.074	0.086	0.065	0.085	0.102	0.111	0.119	0.117	0.137	0.103	0.108	0.131	0.166	0.150	0.172	0.211	0.248	0.260	
Roll (deg)	0.284	0.294	0.330	0.331	0.355	0.435	0.515	0.554	0.644	0.660	0.745	0.516	0.641	0.850	1.112	0.893	1.061	1.227	1.509	1.548	
Pitch (deg)	0.126	0.179	0.209	0.245	0.092	0.127	0.176	0.172	0.230	0.267	0.287	0.116	0.150	0.190	0.277	0.180	0.215	0.211	0.256	0.305	
Yaw (deg)	0.075	0.080	0.079	0.079	0.108	0.123	0.134	0.138	0.181	0.170	0.176	0.185	0.211	0.258	0.303	0.316	0.377	0.424	0.478	0.466	

Table C.4: DVRS Datapoints for  $H_{m0}$  4m

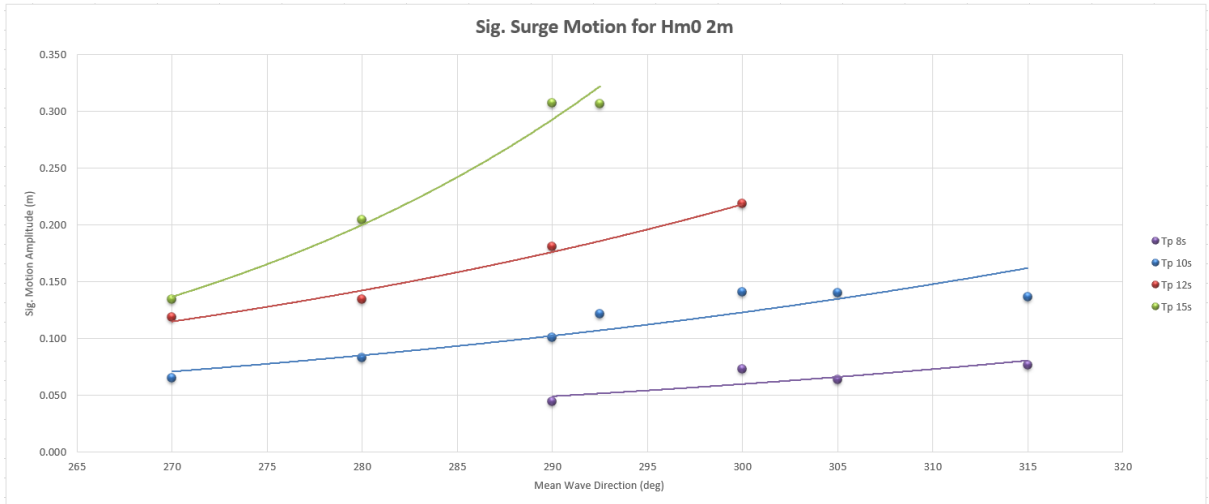
	Hm0 4m									
	Tp 8s		Tp 10s			Tp 12s			Tp 15s	
	290	300	280	290	300	280	290	300	280	290
Surge (m)	0.193	0.264	0.244	0.509	0.982	0.595	0.774	1.573	1.955	1.354
Sway (m)	0.091	0.091	0.180	0.189	0.228	0.266	0.311	0.375	0.614	0.609
Heave (m)	0.078	0.106	0.124	0.150	0.168	0.170	0.211	0.235	0.283	0.334
Roll (deg)	0.353	0.390	0.648	0.739	0.864	0.919	1.085	1.401	1.690	1.623
Pitch (deg)	0.170	0.234	0.182	0.235	0.326	0.210	0.268	0.404	0.285	0.328
Yaw (deg)	0.100	0.098	0.206	0.214	0.273	0.322	0.381	0.454	0.593	0.566

# H<sub>m0</sub> 1m

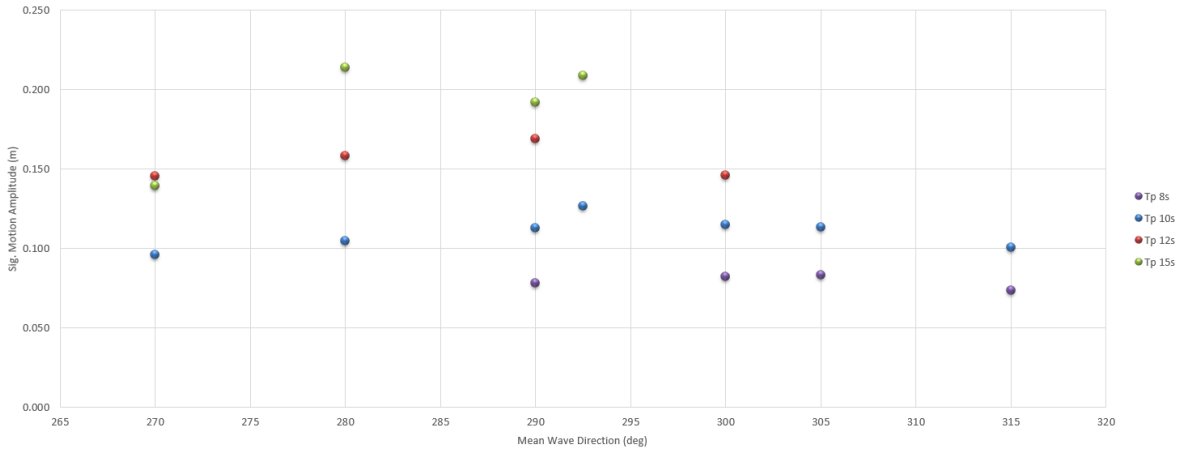




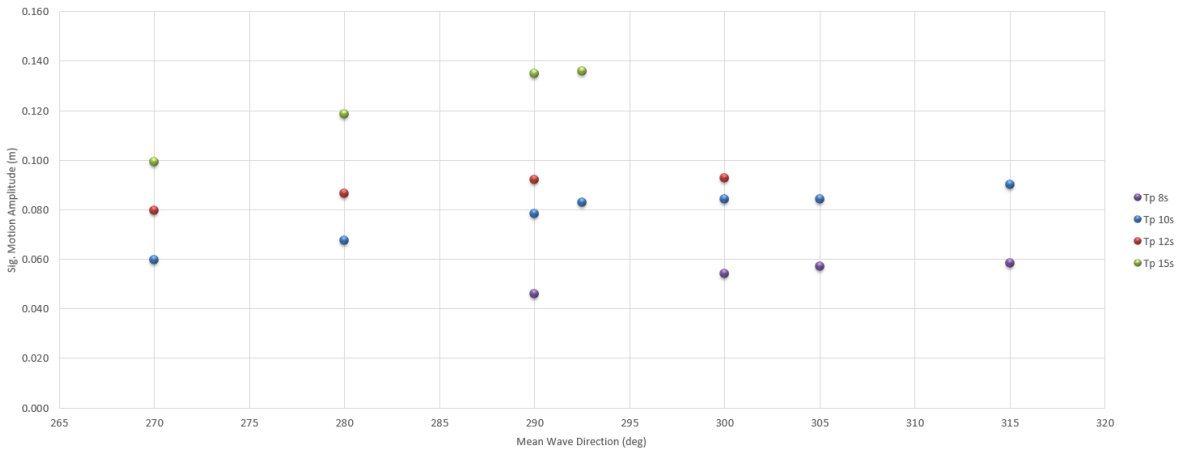
## Hm0 2m



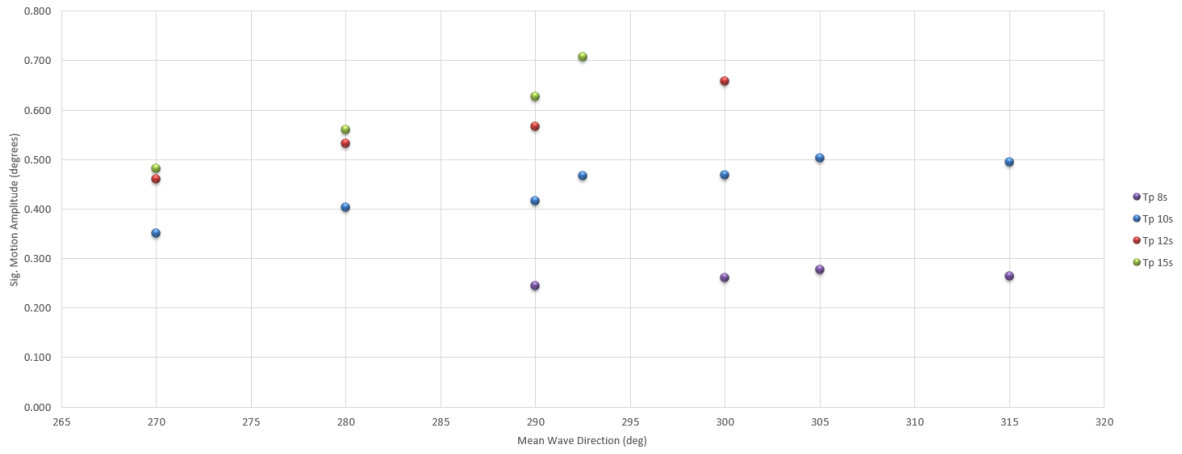
Sig. Sway Motion for Hm0 2m

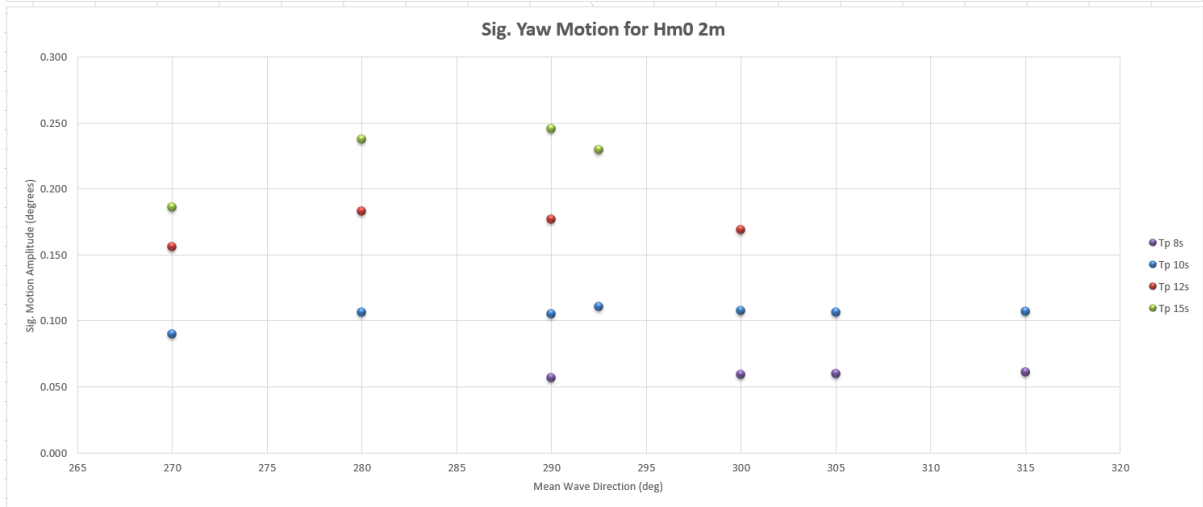
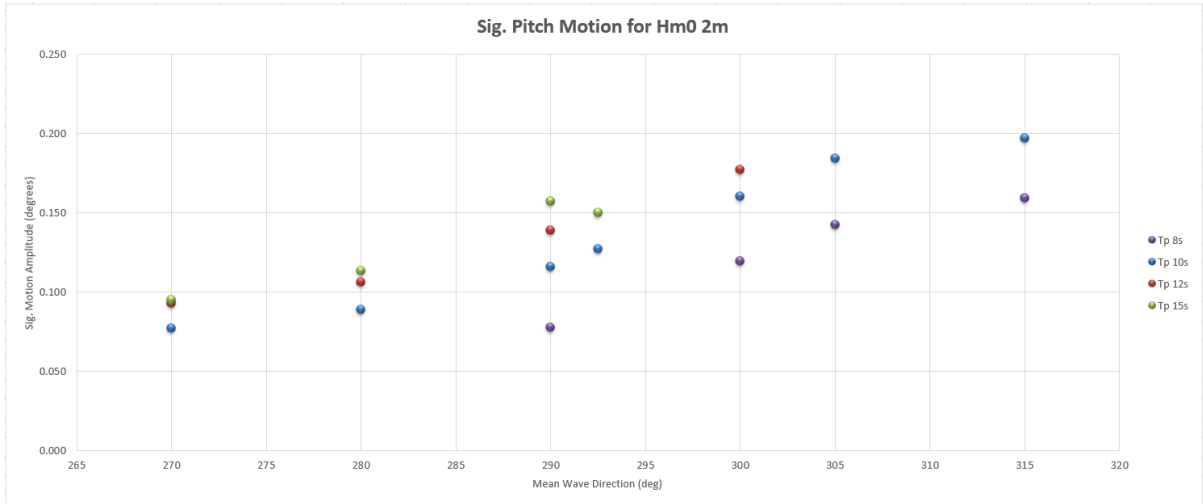


Sig. Heave Motion for Hm0 2m

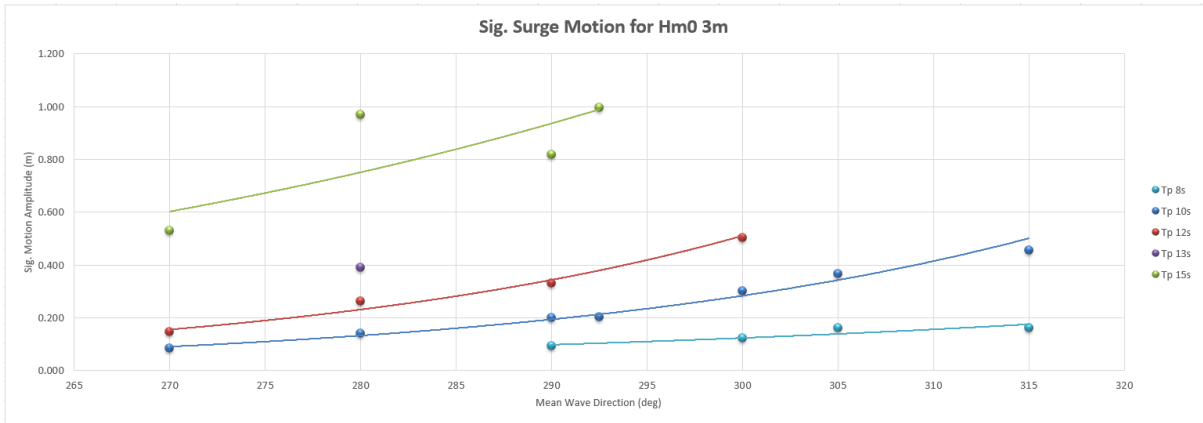


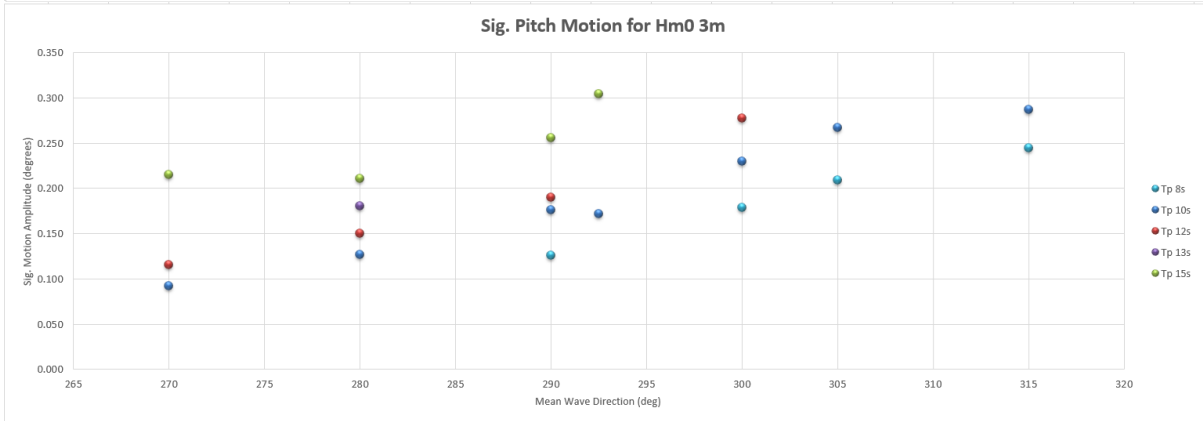
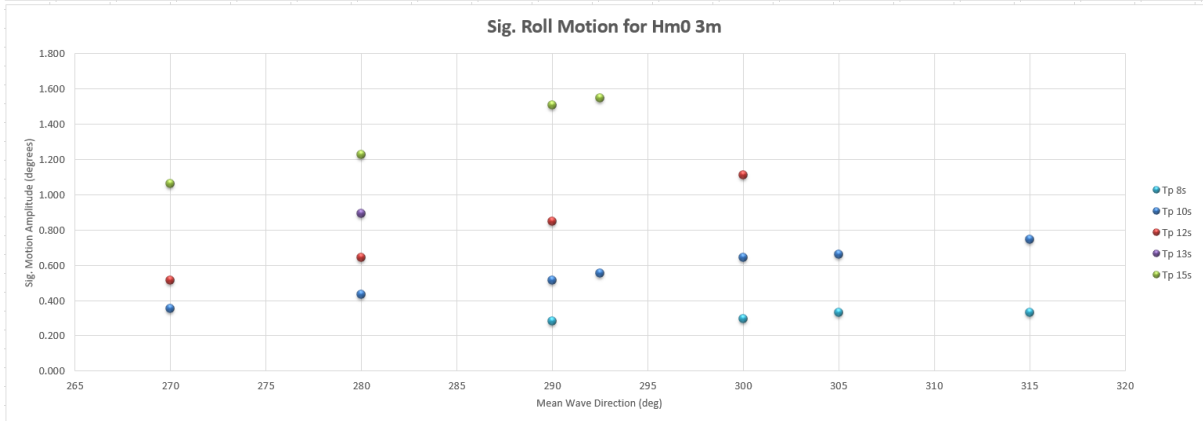
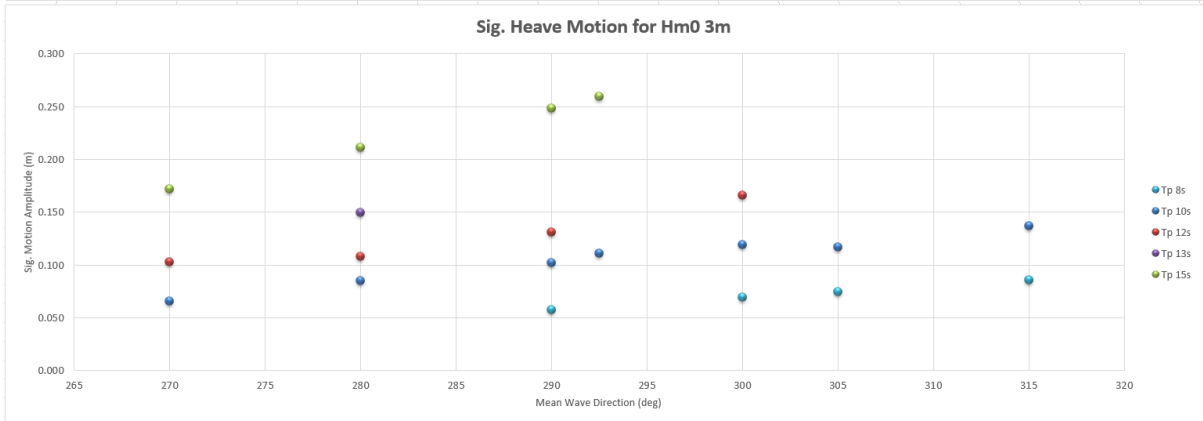
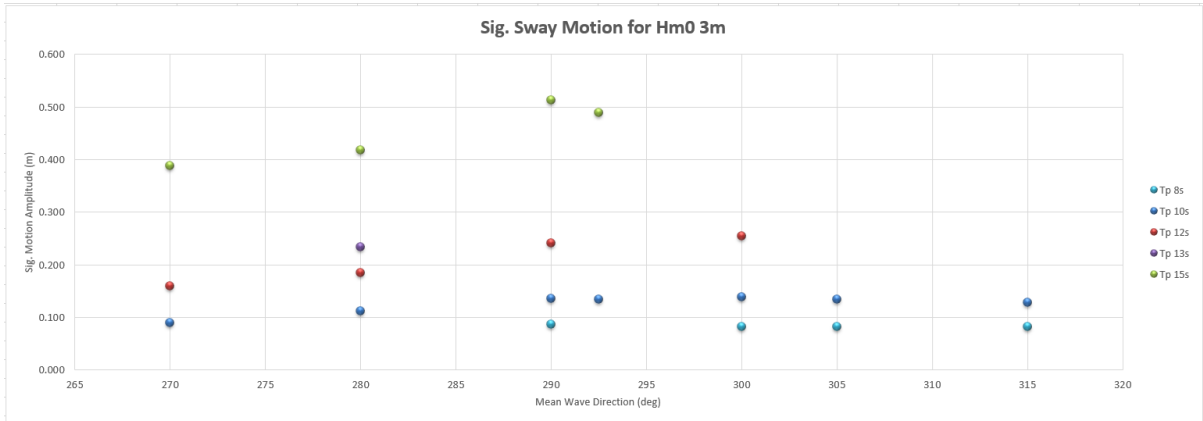
Sig. Roll Motion for Hm0 2m

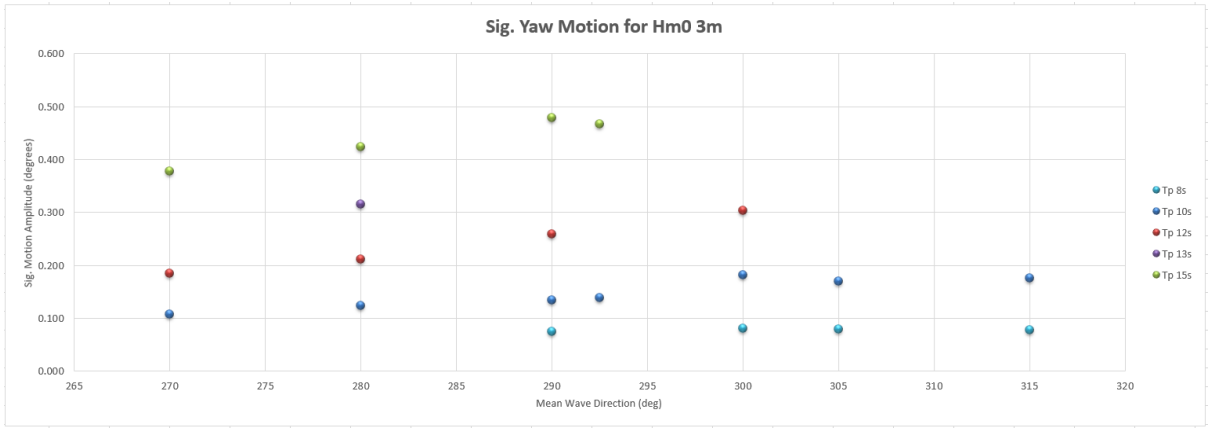




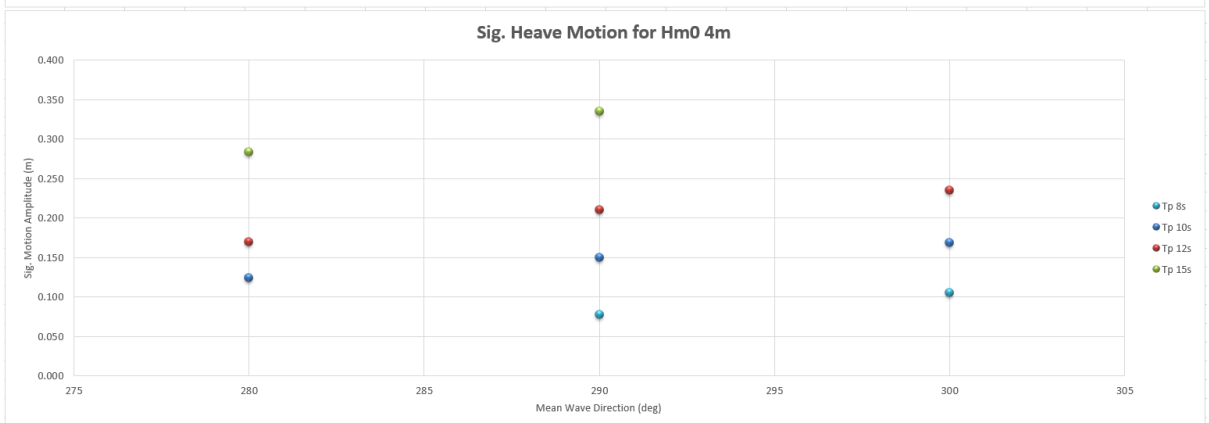
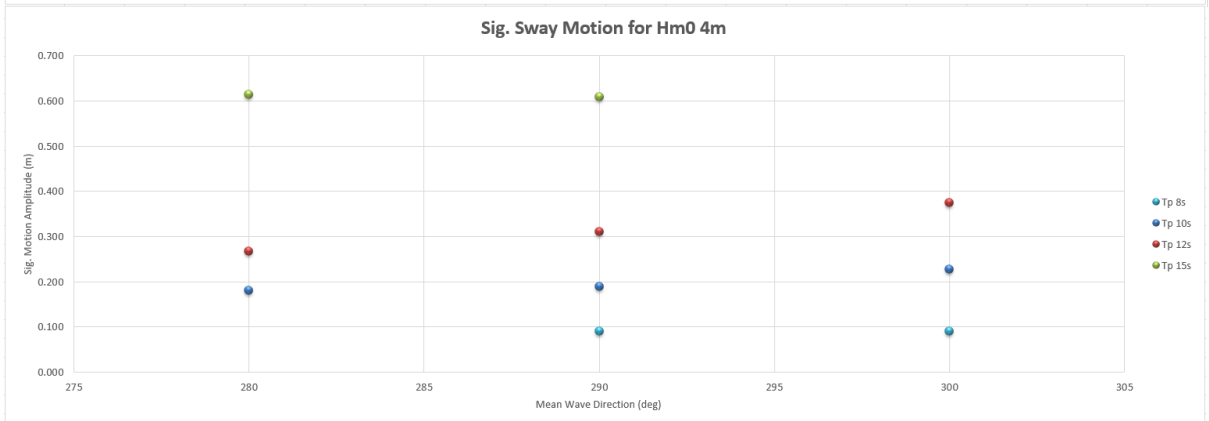
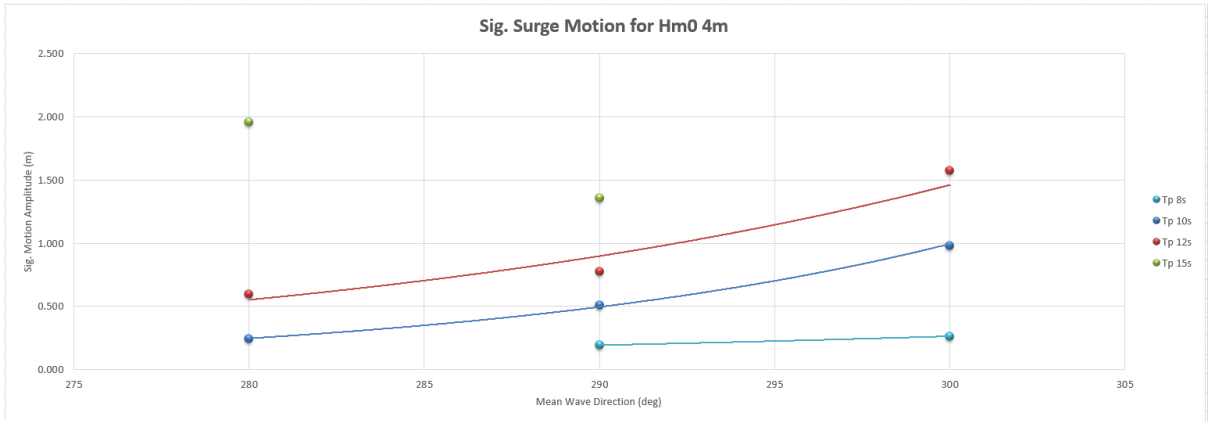
## Hm0 3m







## H<sub>m0</sub> 4m





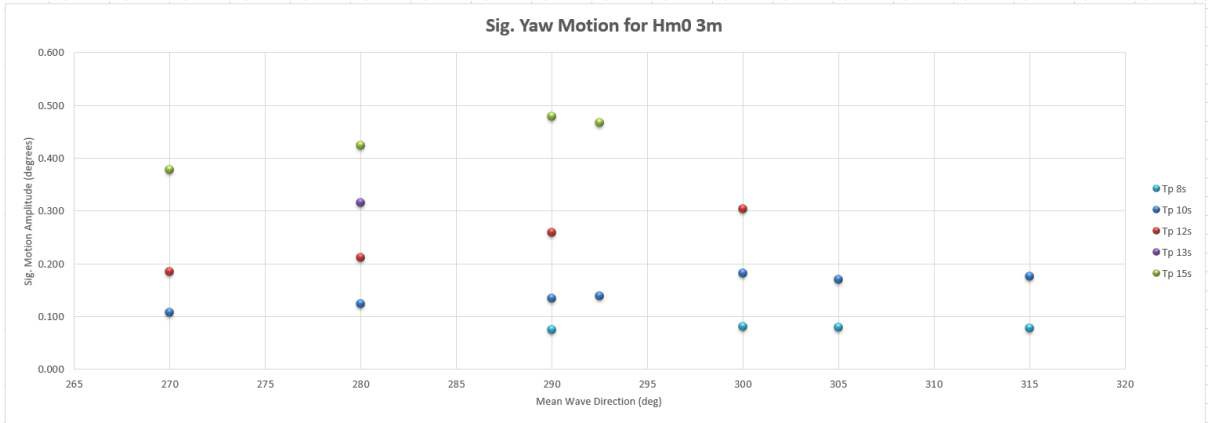
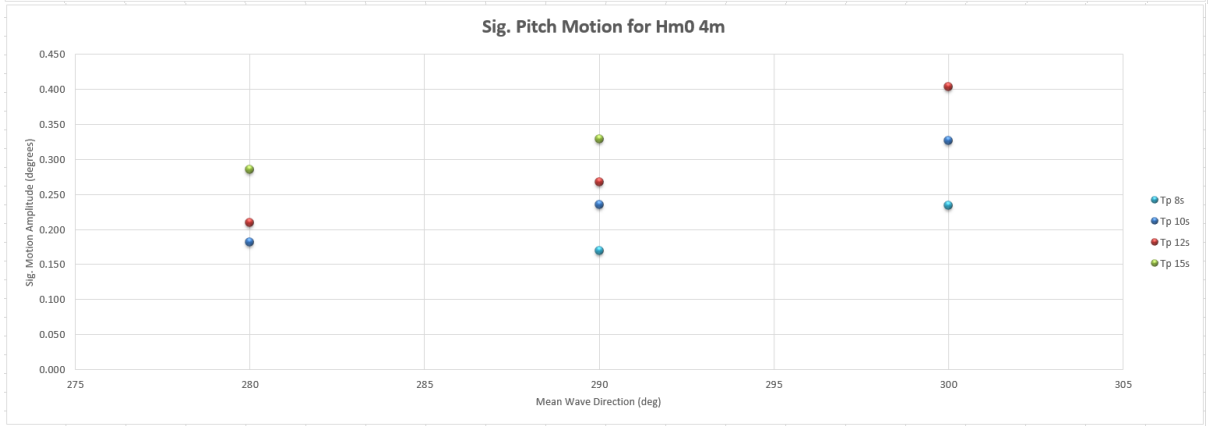
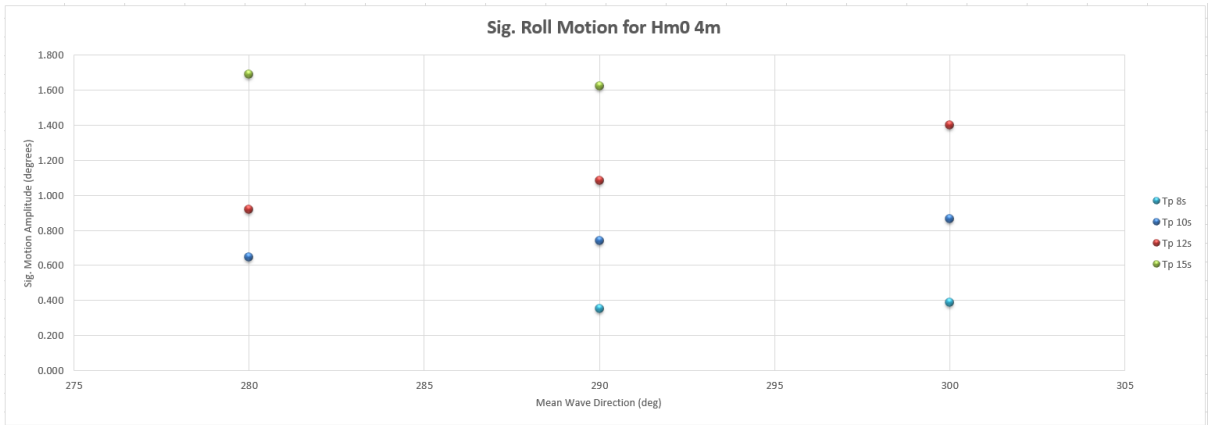


Table C.5: DVRS Datapoints for Mooring Line Forces

MWD		270	280	290	292.5	300	305	315
Hm0	1m							
Tp	8			61.628		62.031	61.957	62.046
	10	68.207	67.573	69.708	73.146	70.565	70.798	84.945
	12	72.449	90.424	74.661		74.695		
	15	73.33	87.32	74.23	81.819			
Hm0	2m							
Tp	8			64.665		67.023	70.225	68.218
	10	75.394	76.589	78.607	88.228	79.623	81.99	84.975
	12	91.644	107.756	97.528		87.73		
	15	89.878	114.467	114.836	131.384			
Hm0	3m							
Tp	8			72.932		69.184	79.852	72.194
	10	75.85	86.884	99.492	97.544	109.135	105.468	98.411
	12	98.191	106.775	114.152		140.277		
	15	143.661	175.187	228.821	222.039			
Hm0	4m							
Tp	8			79.614		82.897		
	10		107.852	136.797		153.738		
	12		190.167	187.579		212.697		
	15		259.87	253.429				

C.2 Ultraline Dyneema Line, Polyamide Tail, no wind

Table C.6: DVRS Datapoints for  $H_{m0}$  1m

	Hm0 1m																				
	Tp 8s				Tp 10s								Tp 12s				Tp 15s				Tp 17s
	290	300	305	315	270	280	290	292.5	300	305	315	270	280	290	300	270	280	290	292.5	285	
Surge (m)	0.023	0.028	0.028	0.031	0.035	0.039	0.045	0.050	0.056	0.061	0.072	0.064	0.067	0.079	0.095	0.097	0.130	0.121	0.125	0.169	
Sway (m)	0.049	0.052	0.049	0.045	0.063	0.068	0.073	0.080	0.074	0.073	0.081	0.108	0.107	0.104	0.104	0.110	0.141	0.120	0.123	0.150	
Heave (m)	0.026	0.031	0.032	0.031	0.038	0.042	0.045	0.051	0.049	0.049	0.050	0.055	0.060	0.057	0.057	0.070	0.076	0.076	0.084	0.091	
Roll (deg)	0.135	0.151	0.158	0.152	0.206	0.243	0.239	0.255	0.264	0.283	0.304	0.304	0.353	0.341	0.398	0.355	0.387	0.387	0.447	0.417	
Pitch (deg)	0.046	0.068	0.078	0.090	0.049	0.058	0.068	0.074	0.093	0.106	0.110	0.063	0.072	0.090	0.107	0.067	0.076	0.085	0.091	0.082	
Yaw (deg)	0.043	0.046	0.046	0.045	0.066	0.080	0.076	0.081	0.077	0.084	0.107	0.111	0.126	0.118	0.116	0.132	0.148	0.134	0.141	0.146	

Table C.7: DVRS Datapoints for  $H_{m0}$  2m

	Hm0 2m																			
	Tp 8s				Tp 10s								Tp 12s				Tp 15s			
	290	300	305	315	270	280	290	292.5	300	305	315	270	280	290	300	270	280	290	292.5	
Surge (m)	0.050	0.063	0.066	0.084	0.057	0.079	0.112	0.133	0.149	0.157	0.161	0.098	0.141	0.168	0.254	0.187	0.278	0.362	0.324	
Sway (m)	0.072	0.075	0.076	0.067	0.094	0.107	0.112	0.123	0.117	0.121	0.108	0.133	0.158	0.161	0.141	0.181	0.199	0.207	0.222	
Heave (m)	0.045	0.054	0.057	0.059	0.058	0.066	0.077	0.082	0.083	0.083	0.090	0.079	0.086	0.091	0.092	0.099	0.119	0.135	0.137	
Roll (deg)	0.201	0.205	0.225	0.220	0.304	0.351	0.349	0.391	0.406	0.440	0.436	0.430	0.515	0.524	0.612	0.501	0.582	0.601	0.694	
Pitch (deg)	0.085	0.128	0.152	0.168	0.080	0.091	0.120	0.132	0.166	0.189	0.203	0.095	0.108	0.142	0.181	0.097	0.116	0.161	0.152	
Yaw (deg)	0.057	0.059	0.060	0.061	0.090	0.110	0.108	0.113	0.110	0.122	0.120	0.151	0.177	0.172	0.167	0.191	0.205	0.213	0.215	

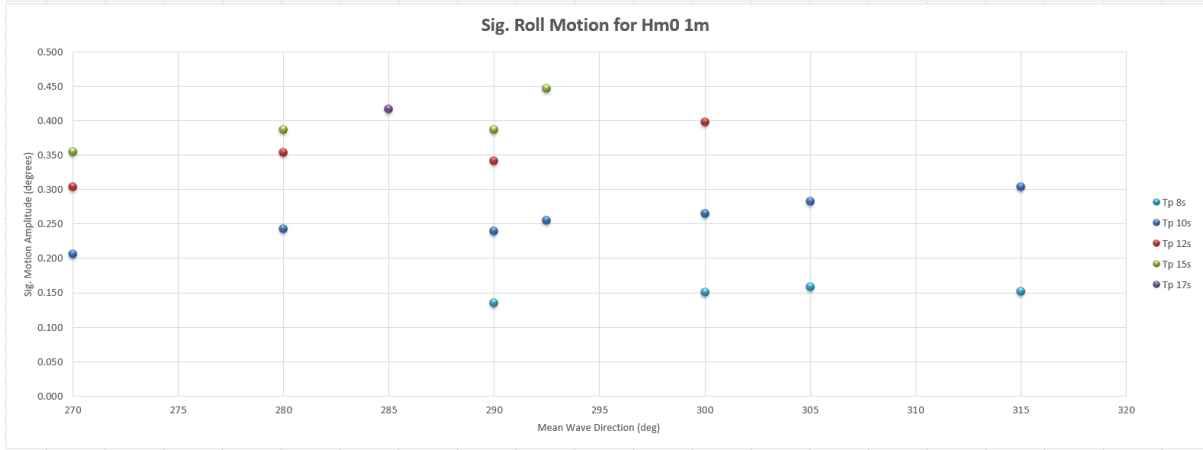
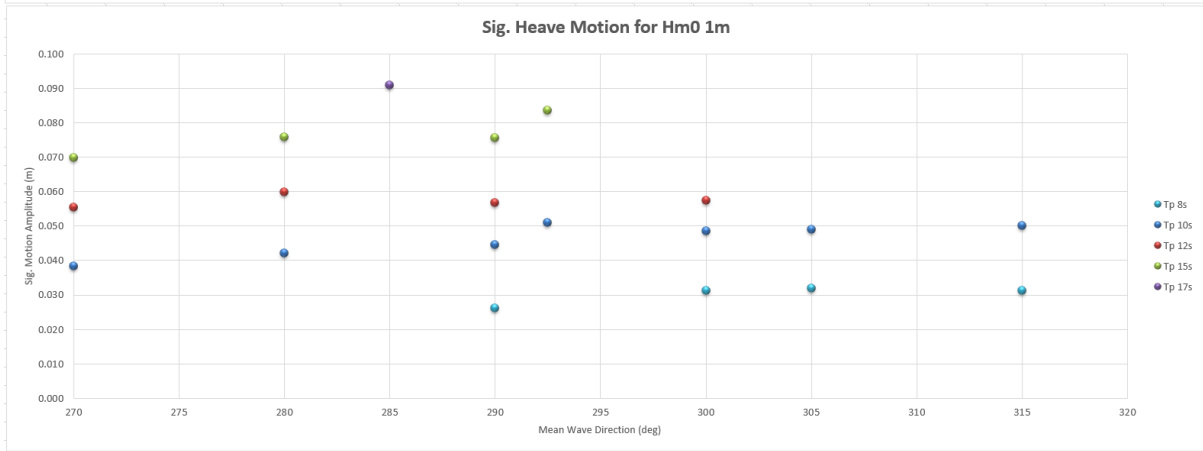
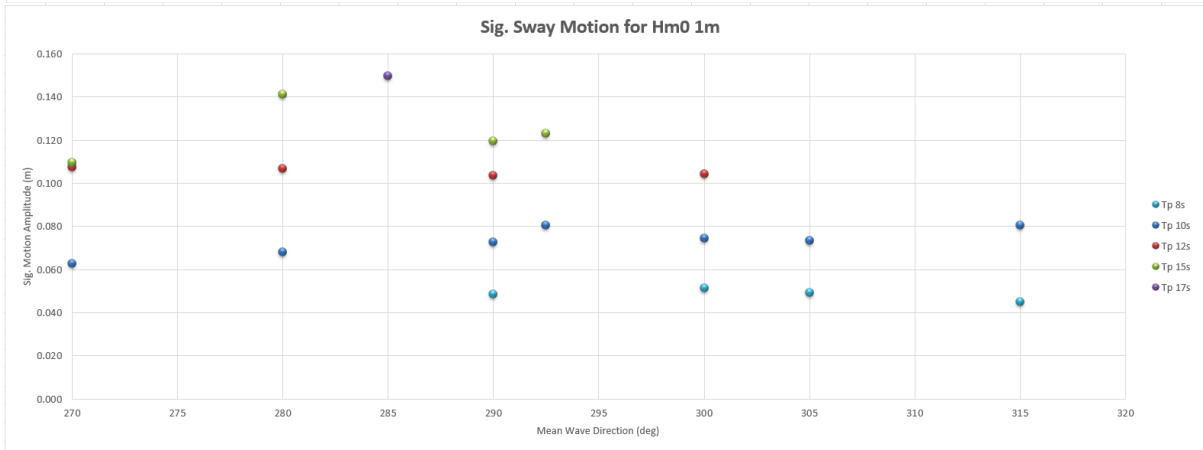
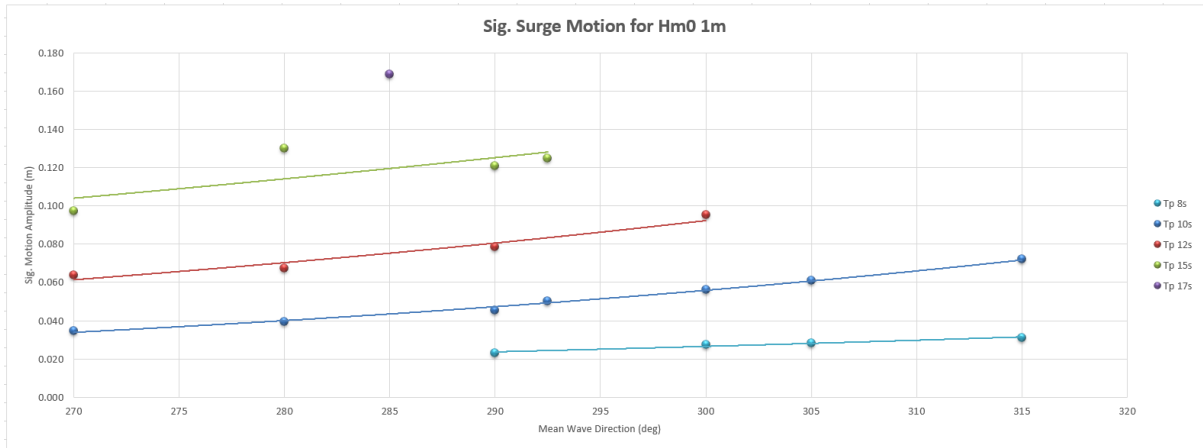
Table C.8: DVRS Datapoints for  $H_{m0}$  3m

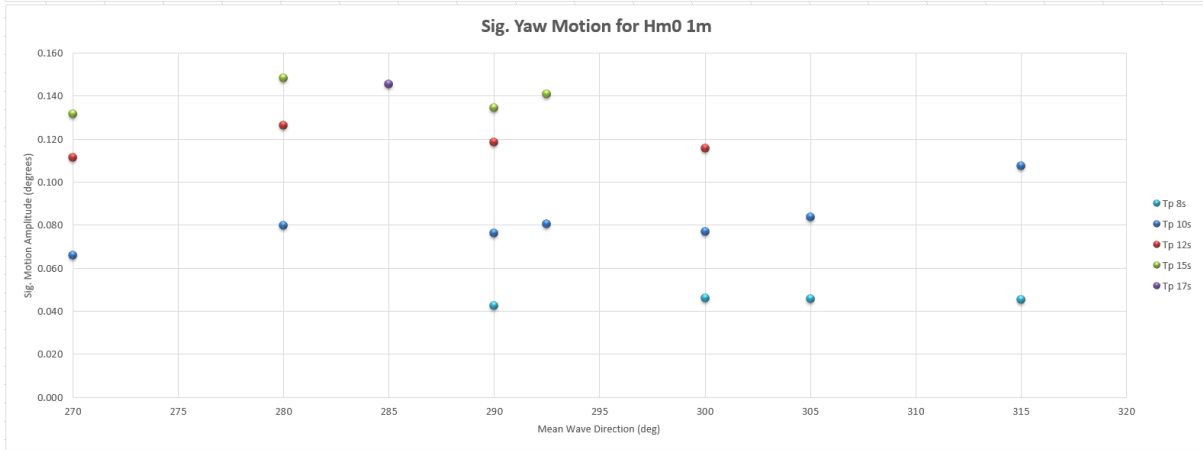
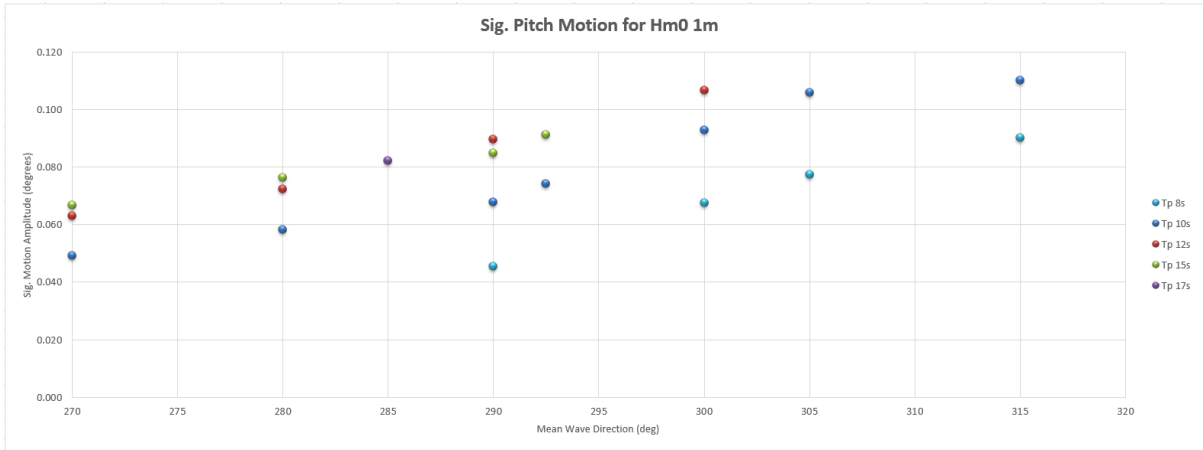
	Hm0 3m																				
	Tp 8s				Tp 10s								Tp 12s				Tp 13s	Tp 15s			
	290	300	305	315	270	280	290	292.5	300	305	315	270	280	290	300	280	270	280	290	292.5	
Surge (m)	0.109	0.161	0.182	0.203	0.094	0.170	0.243	0.269	0.347	0.409	0.482	0.191	0.314	0.387	0.493	0.388	0.421	0.724	0.699	0.730	
Sway (m)	0.083	0.079	0.080	0.079	0.091	0.116	0.138	0.140	0.149	0.137	0.143	0.152	0.169	0.242	0.230	0.238	0.288	0.367	0.366	0.347	
Heave (m)	0.057	0.070	0.076	0.088	0.064	0.083	0.102	0.110	0.120	0.117	0.138	0.103	0.107	0.130	0.165	0.148	0.172	0.211	0.249	0.261	
Roll (deg)	0.248	0.255	0.292	0.325	0.327	0.375	0.437	0.455	0.578	0.609	0.686	0.477	0.533	0.757	1.017	0.832	1.000	1.162	1.319	1.325	
Pitch (deg)	0.134	0.188	0.218	0.254	0.096	0.132	0.180	0.177	0.235	0.273	0.292	0.119	0.153	0.194	0.279	0.182	0.215	0.212	0.257	0.304	
Yaw (deg)	0.077	0.081	0.081	0.083	0.110	0.131	0.140	0.141	0.198	0.185	0.212	0.177	0.195	0.267	0.332	0.335	0.322	0.378	0.396	0.389	

Table C.9: DVRS Datapoints for  $H_{m0}$  4m

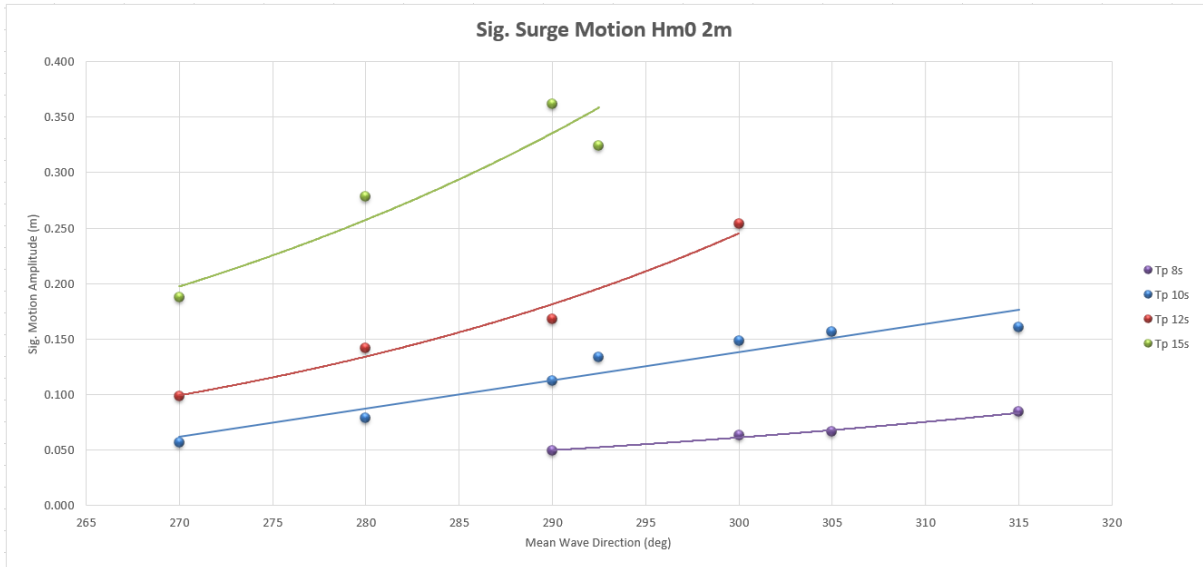
	Hm0 4m									
	Tp 8s		Tp 10s			Tp 12s			Tp 15s	
	290	300	280	290	300	280	290	300	280	290
Surge (m)	0.214	0.301	0.285	0.451	0.740	0.533	0.667	0.880	0.932	0.985
Sway (m)	0.095	0.095	0.162	0.199	0.219	0.251	0.287	0.296	0.452	0.482
Heave (m)	0.079	0.108	0.123	0.149	0.168	0.170	0.213	0.234	0.288	0.337
Roll (deg)	0.309	0.363	0.541	0.656	0.754	0.870	1.078	1.355	1.568	1.518
Pitch (deg)	0.178	0.242	0.186	0.240	0.332	0.212	0.270	0.406	0.281	0.327
Yaw (deg)	0.108	0.110	0.205	0.237	0.299	0.348	0.406	0.465	0.440	0.460

# Hm0 1m

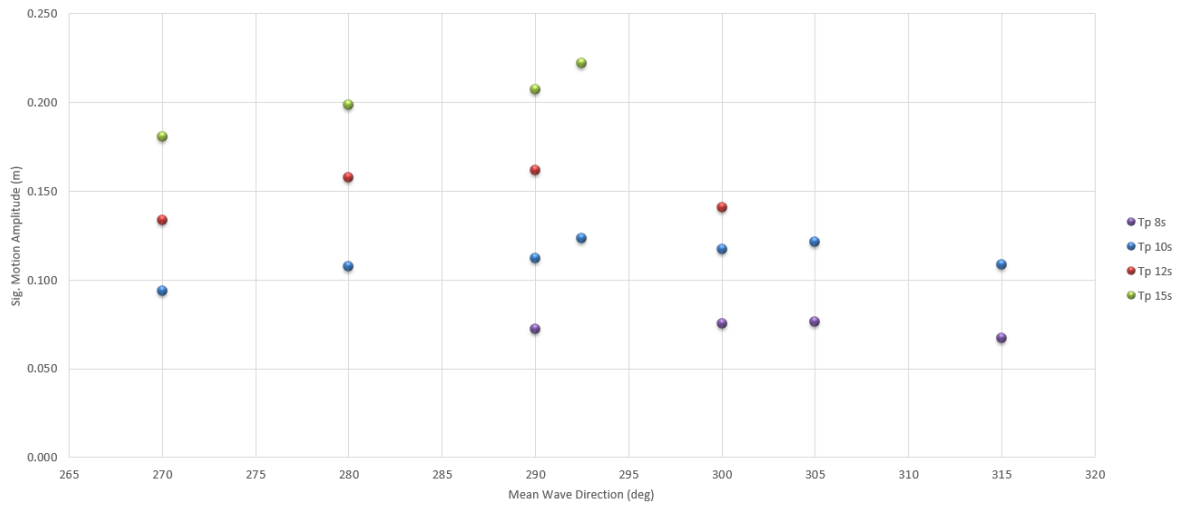




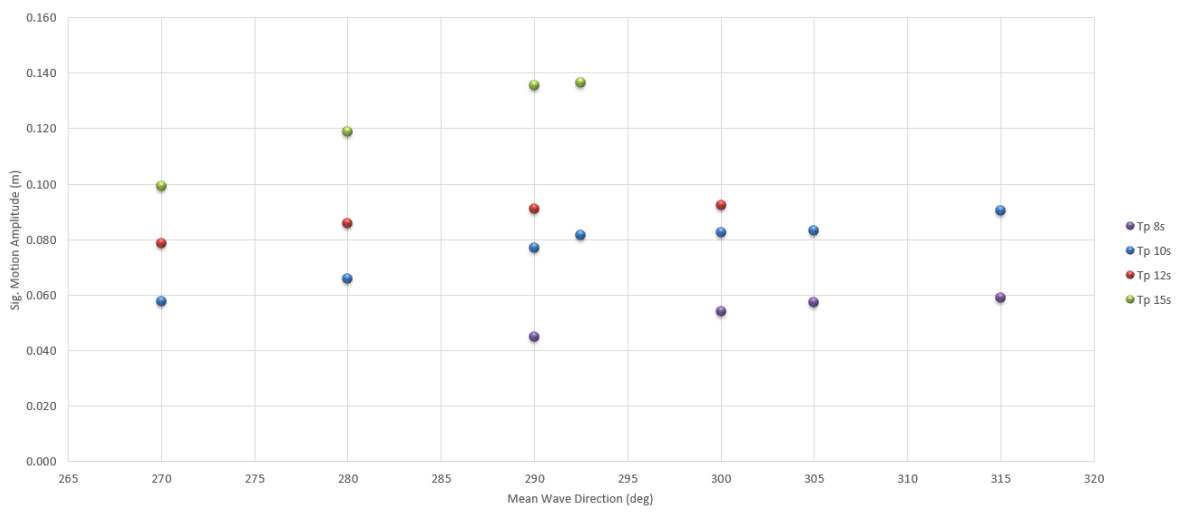
## Hm0 2m



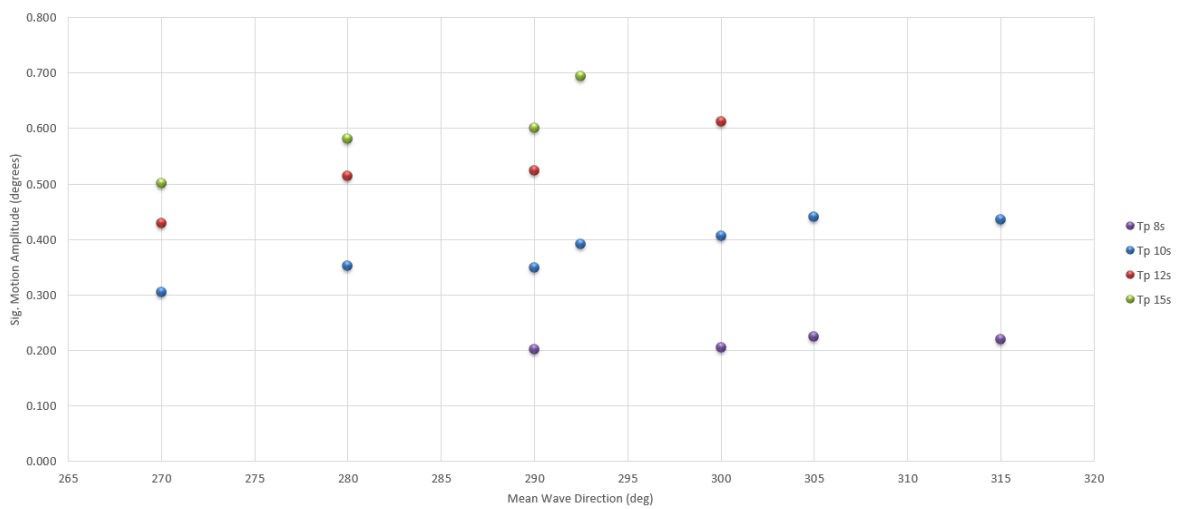
Sig. Sway Motion Hm0 2m

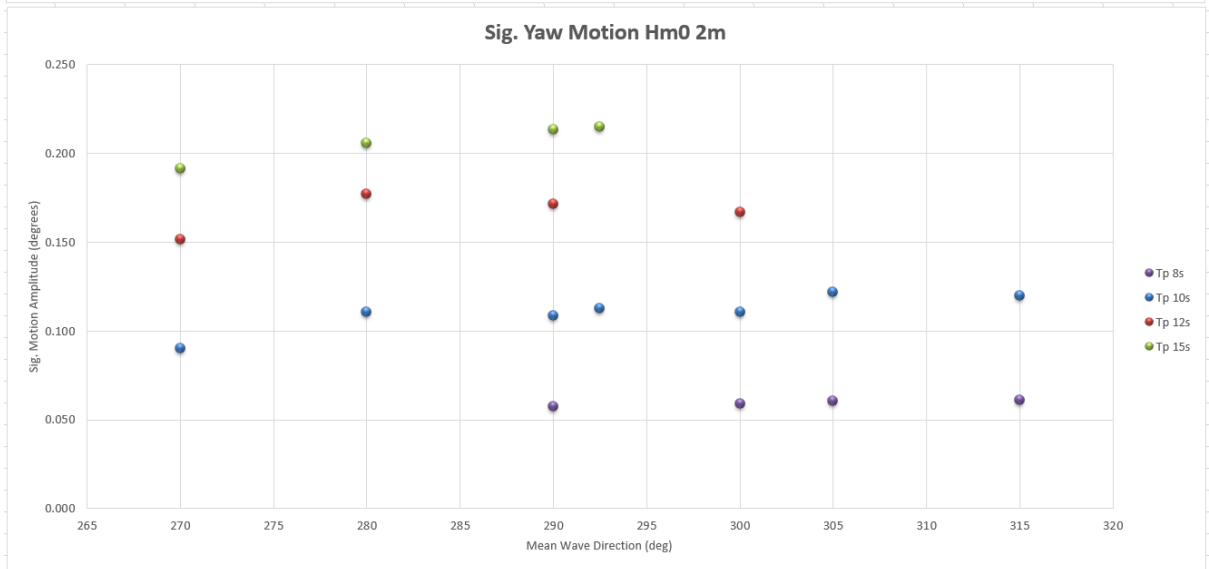
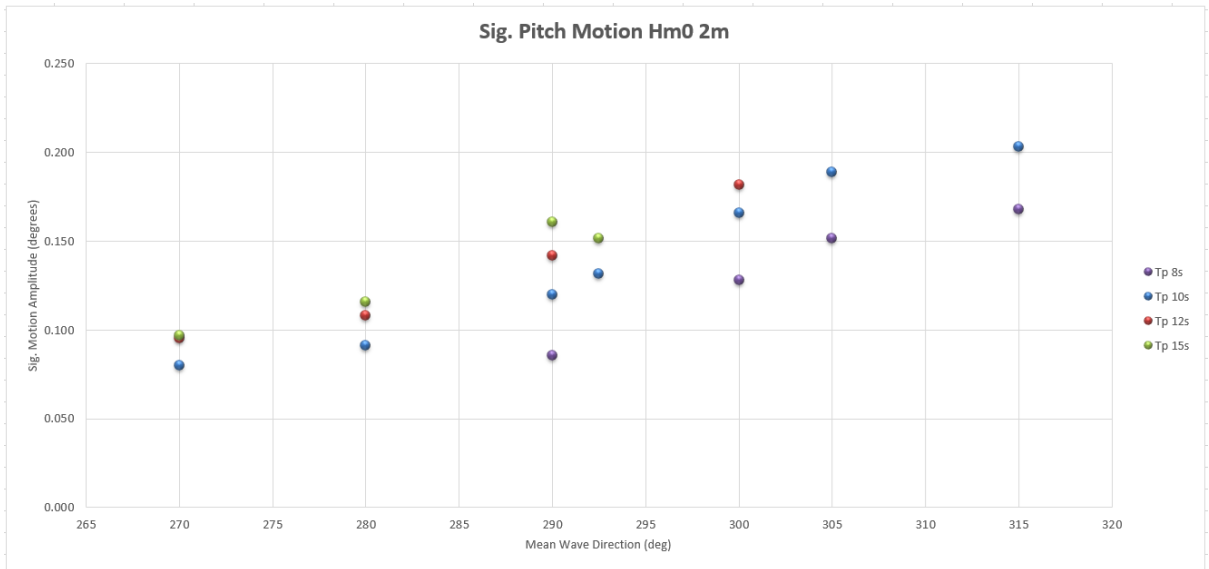


Sig. Heave Motion Hm0 2m

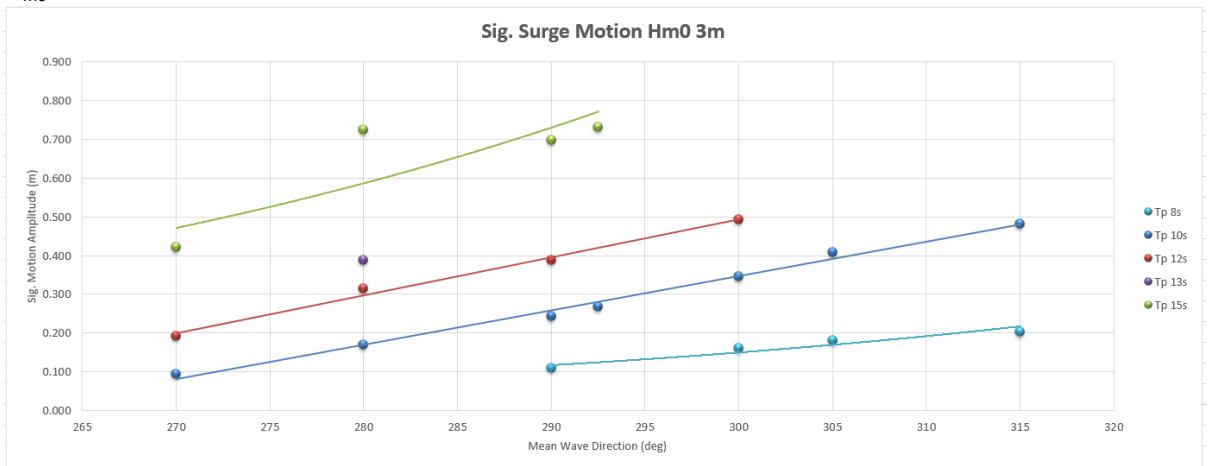


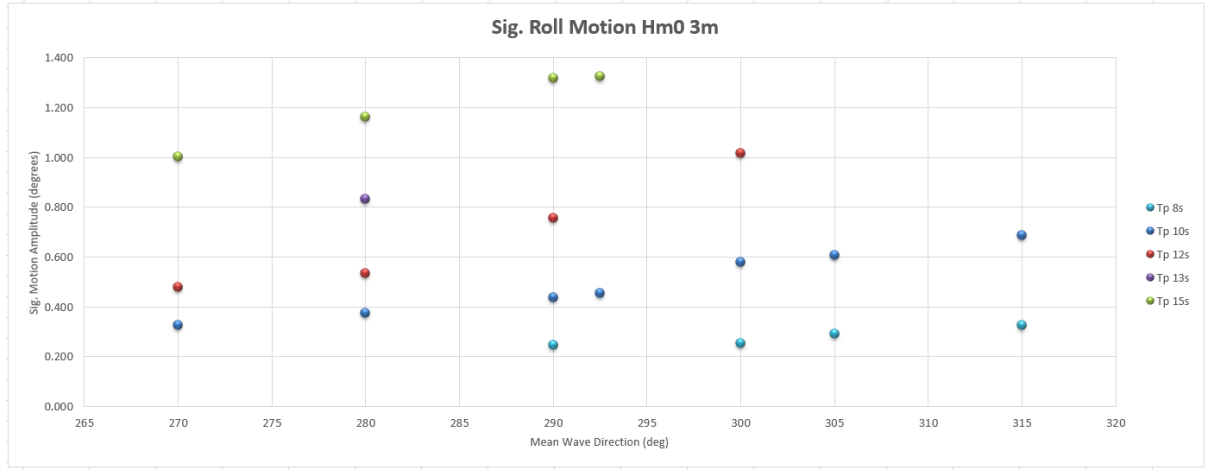
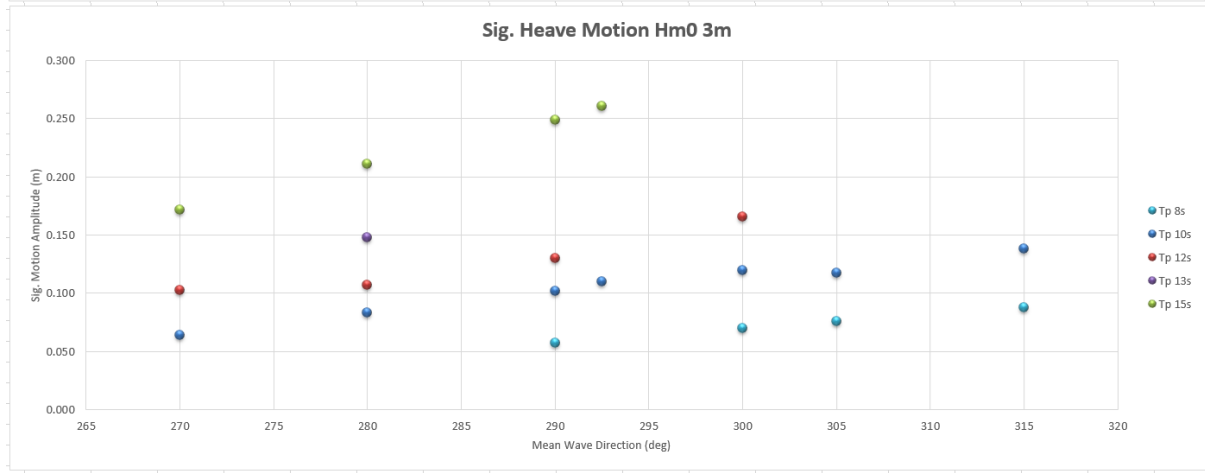
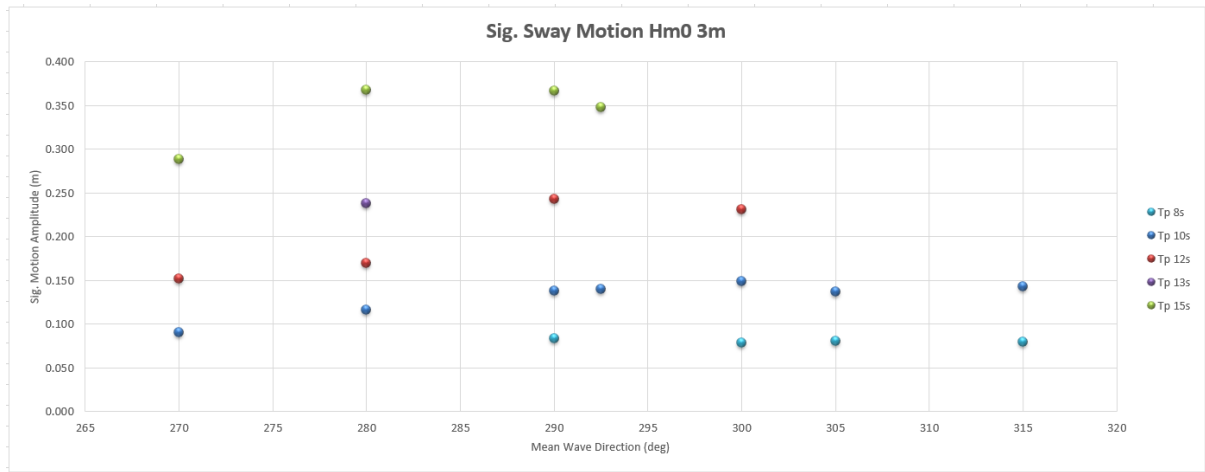
Sig. Roll Motion Hm0 2m



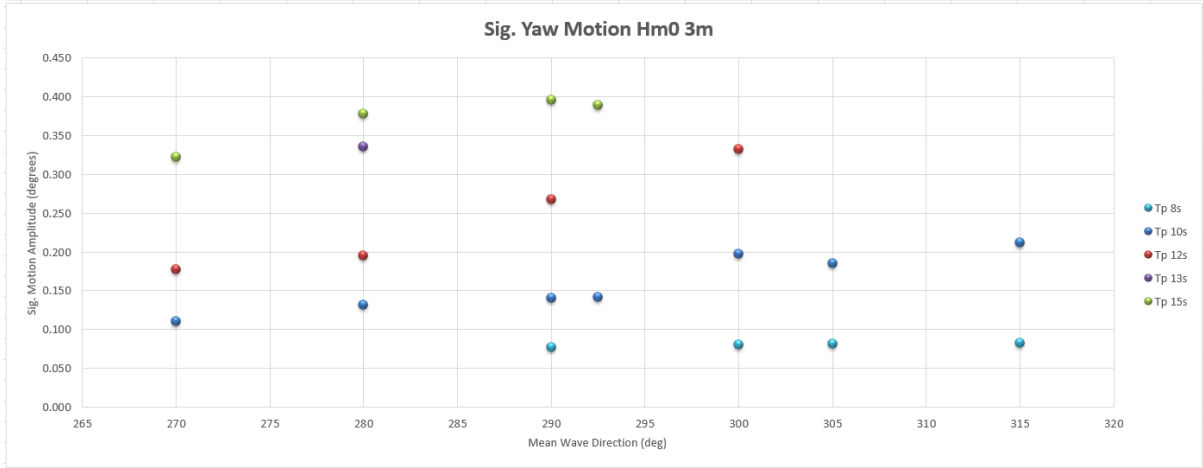
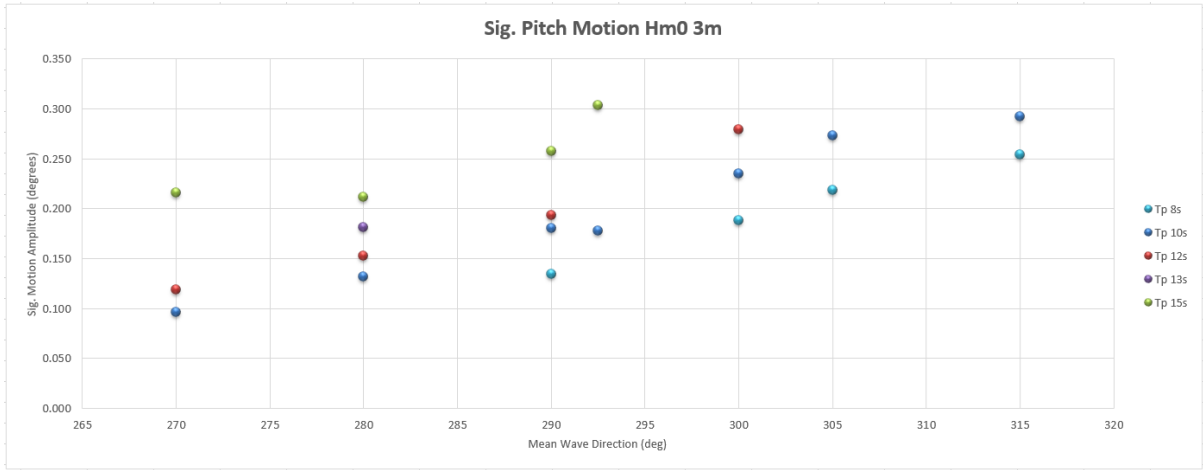


## H<sub>m0</sub> 3m

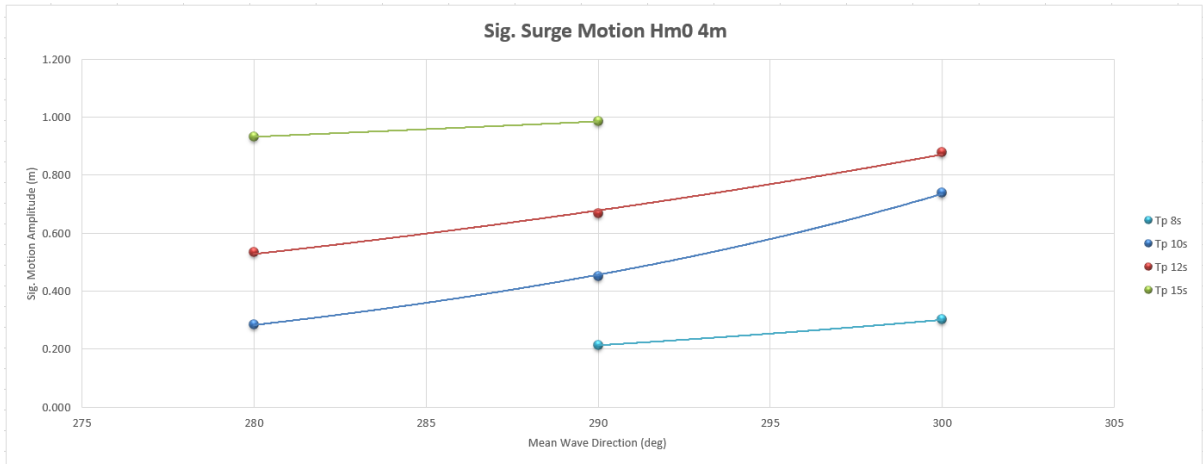


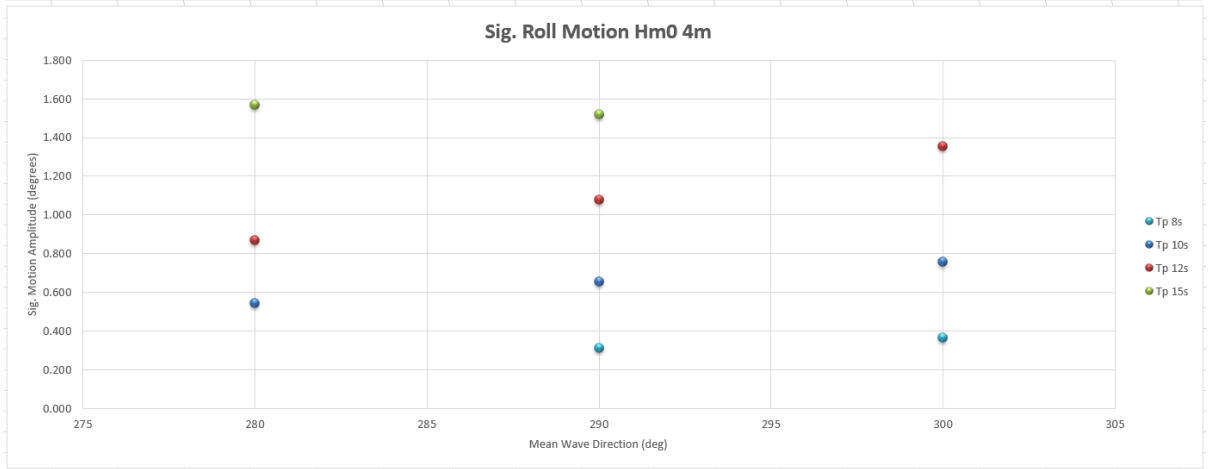
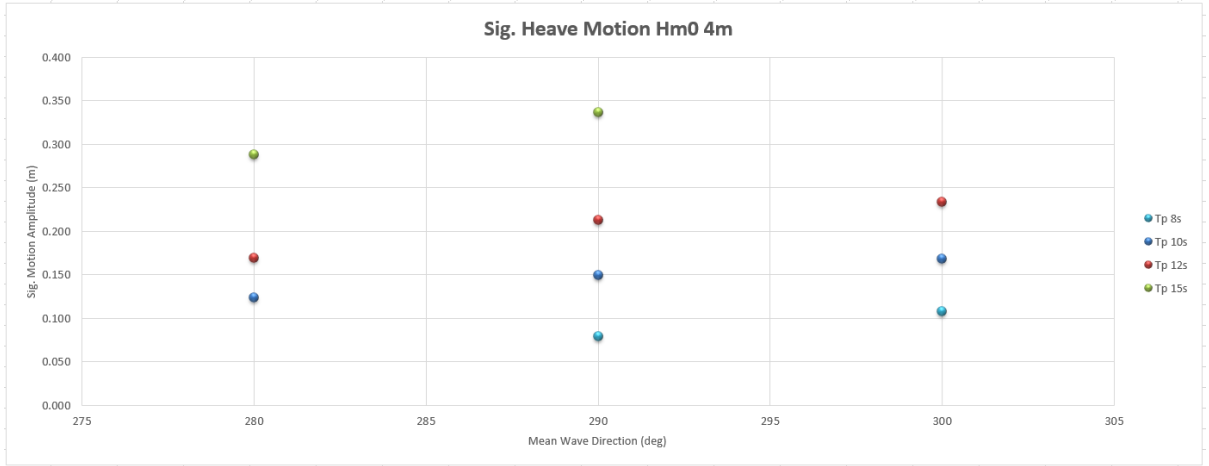
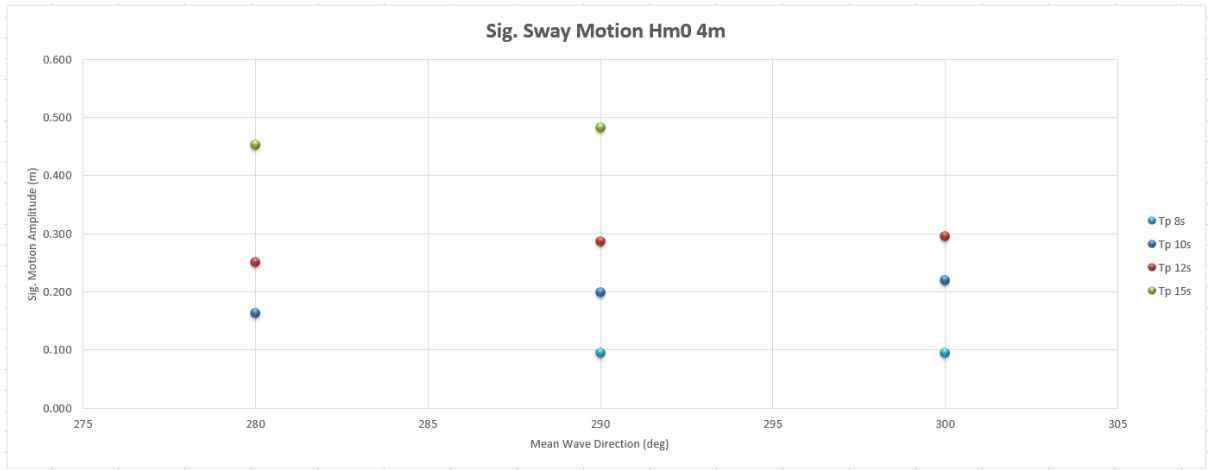






## H<sub>m0</sub> 4m





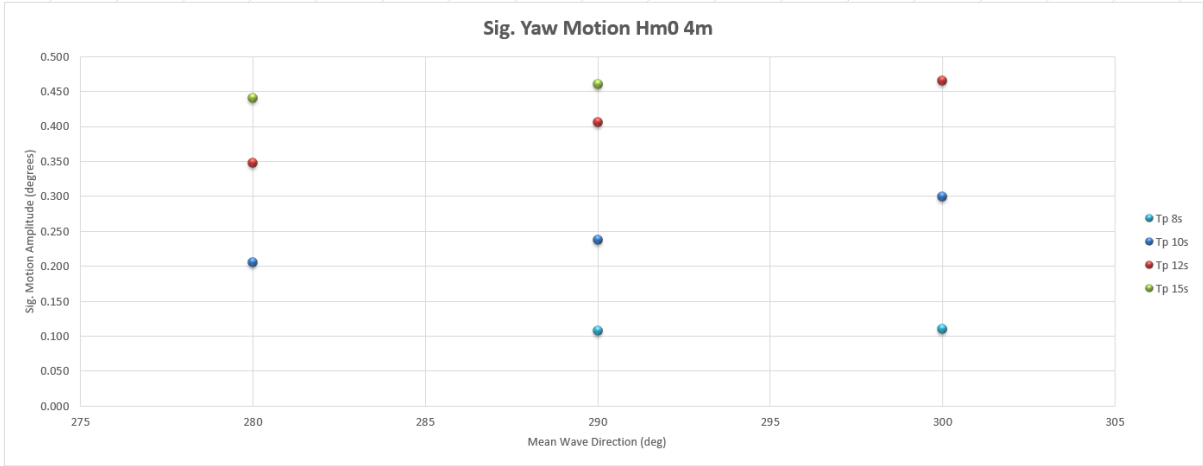
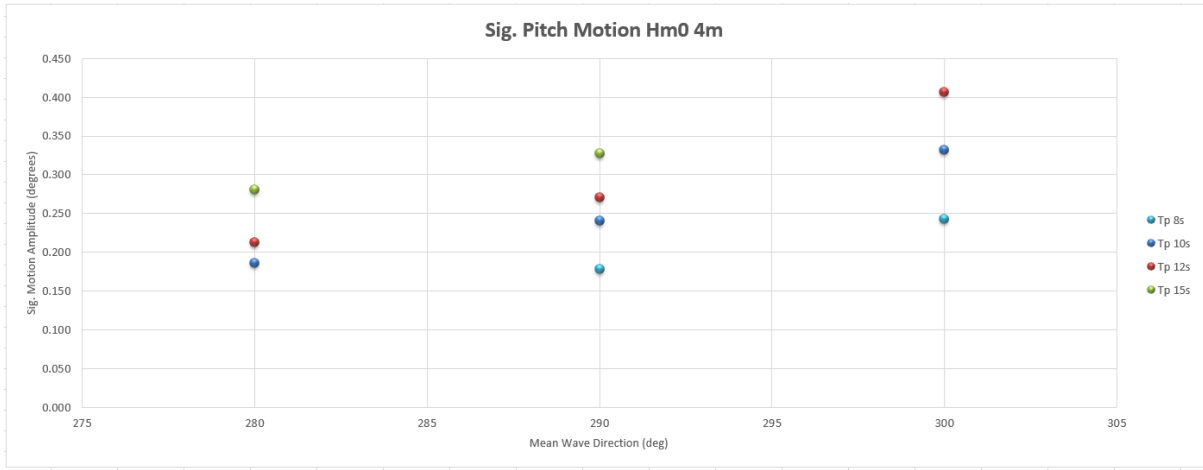


Table C.10: DVRS Datapoints for Mooring Line Forces

MWD		270	280	290	292.5	300	305	315
Hm0	1m							
Tp	8			48.409		46.548	48.375	49.422
	10	53.157	58.279	58.433	64.92	62.65	62.918	80.467
	12	67.604	85.717	72.961		73.824		
	15	76.508	113.388	86.688	83.198			
Hm0	2m							
Tp	8			52.366		55.573	63.943	58.862
	10	65.548	85.409	69.312	84.24	79.143	87.856	94.661
	12	107.618	138.335	108.403		130.446		
	15	154.062	154.205	298.289	284.131			
Hm0	3m							
Tp	8			75.449		61.317	82.087	69.449
	10	70.013	86.522	102.524	109.001	147.843	197.032	237.864
	12	117.594	141.958	184.094		252.702		
	15	281.98	551.716	456.85	580.952			
Hm0	4m							
Tp	8			88.03		105.642		
	10		157.995	193.883		374.933		
	12		288.62	380.67		609.197		
	15		701.312	1020.56				

C.3 Polypropylene Line, Polyamide Tail, Wind 10  $\frac{m}{s}$ , 0 degrees

Table C.11: DVRS Datapoints for  $H_{m0}$  1m

	Hm0 1m																			
	Tp 8s				Tp 10s					Tp 12s				Tp 15s				Tp 17s		
	290	300	305	315	270	280	290	292.5	300	305	315	270	280	290	300	270	280	290	292.5	285
Surge (m)	0.016	0.028	0.026	0.026	0.035	0.036	0.039	0.062	0.061	0.071	0.070	0.064	0.077	0.073	0.090	0.070	0.087	0.091	0.107	0.110
Sway (m)	0.051	0.054	0.052	0.047	0.064	0.069	0.074	0.080	0.075	0.073	0.081	0.091	0.092	0.097	0.094	0.085	0.142	0.100	0.119	0.127
Heave (m)	0.027	0.032	0.033	0.032	0.040	0.043	0.046	0.052	0.050	0.051	0.052	0.056	0.060	0.058	0.058	0.070	0.075	0.076	0.084	0.091
Roll (deg)	0.170	0.205	0.208	0.209	0.242	0.272	0.296	0.321	0.352	0.379	0.367	0.296	0.373	0.370	0.424	0.337	0.371	0.397	0.437	0.418
Pitch (deg)	0.039	0.060	0.070	0.081	0.047	0.056	0.065	0.072	0.090	0.103	0.105	0.061	0.070	0.087	0.104	0.065	0.074	0.083	0.090	0.081
Yaw (deg)	0.042	0.044	0.044	0.043	0.066	0.077	0.079	0.081	0.078	0.082	0.103	0.107	0.117	0.111	0.109	0.125	0.162	0.132	0.153	0.156

Table C.12: DVRS Datapoints for  $H_{m0}$  2m

	Hm0 2m																		
	Tp 8s				Tp 10s					Tp 12s				Tp 15s					
	290	300	305	315	270	280	290	292.5	300	305	315	270	280	290	300	270	280	290	292.5
Surge (m)	0.042	0.068	0.063	0.071	0.071	0.088	0.099	0.129	0.135	0.158	0.133	0.114	0.129	0.171	0.215	0.147	0.217	0.313	0.291
Sway (m)	0.077	0.081	0.081	0.072	0.093	0.106	0.111	0.126	0.114	0.118	0.105	0.131	0.135	0.150	0.139	0.174	0.243	0.241	0.287
Heave (m)	0.046	0.054	0.057	0.058	0.059	0.067	0.078	0.083	0.084	0.084	0.090	0.080	0.086	0.092	0.092	0.099	0.119	0.136	0.136
Roll (deg)	0.263	0.287	0.304	0.292	0.373	0.427	0.443	0.508	0.508	0.565	0.529	0.459	0.554	0.605	0.695	0.500	0.584	0.665	0.744
Pitch (deg)	0.078	0.119	0.142	0.158	0.079	0.090	0.117	0.128	0.161	0.184	0.197	0.093	0.106	0.138	0.178	0.095	0.113	0.158	0.150
Yaw (deg)	0.059	0.062	0.062	0.062	0.091	0.107	0.107	0.120	0.110	0.121	0.115	0.149	0.162	0.156	0.156	0.202	0.247	0.258	0.277

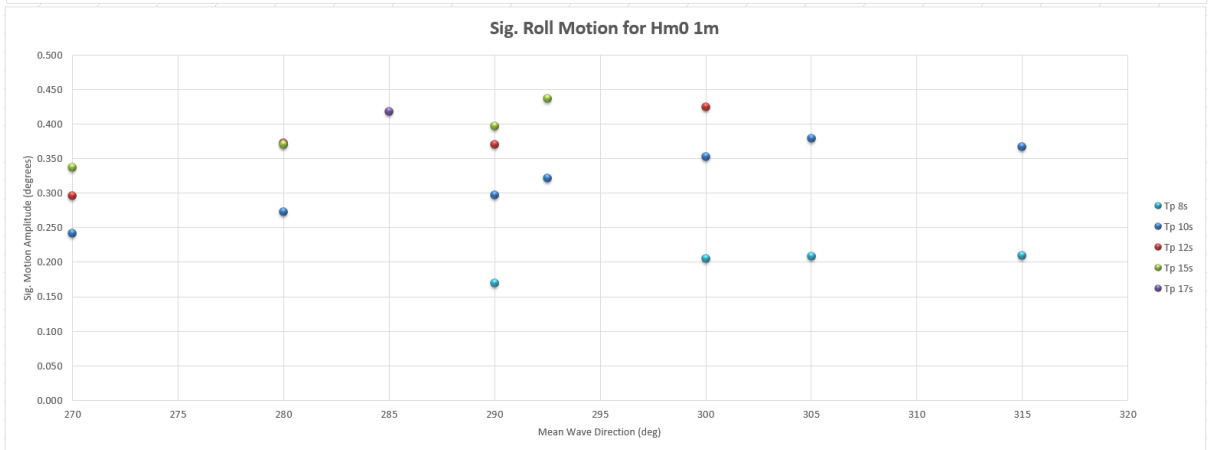
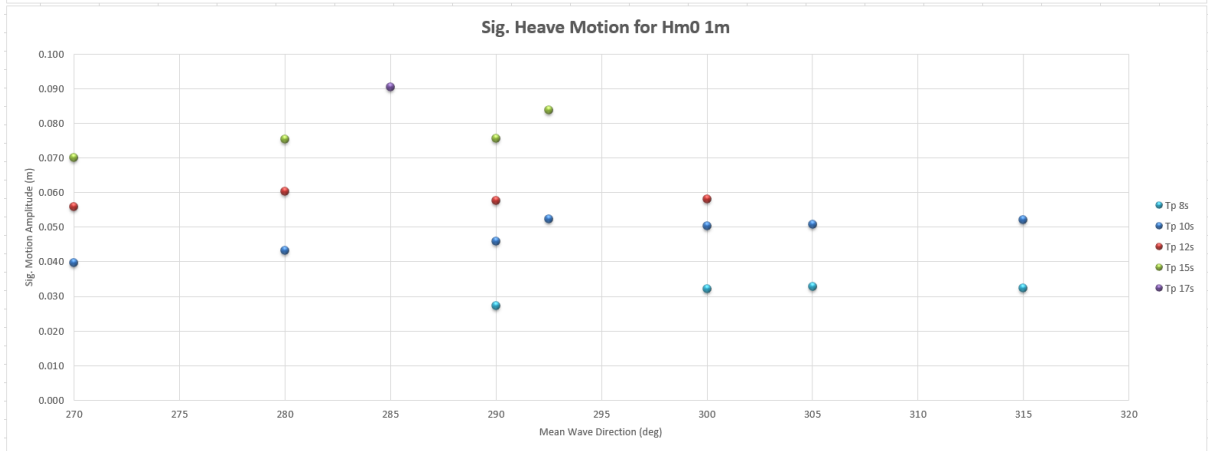
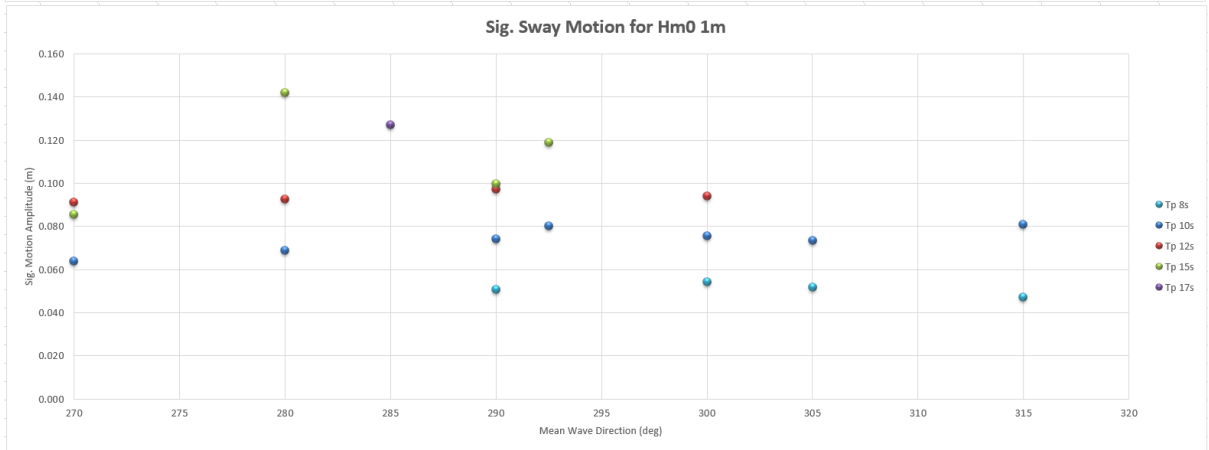
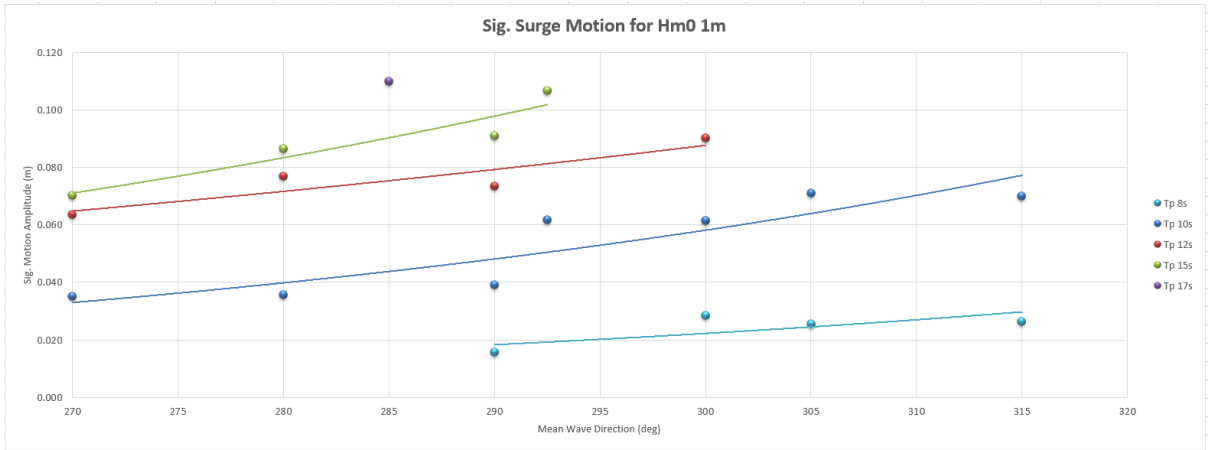
Table C.13: DVRS Datapoints for  $H_{m0}$  3m

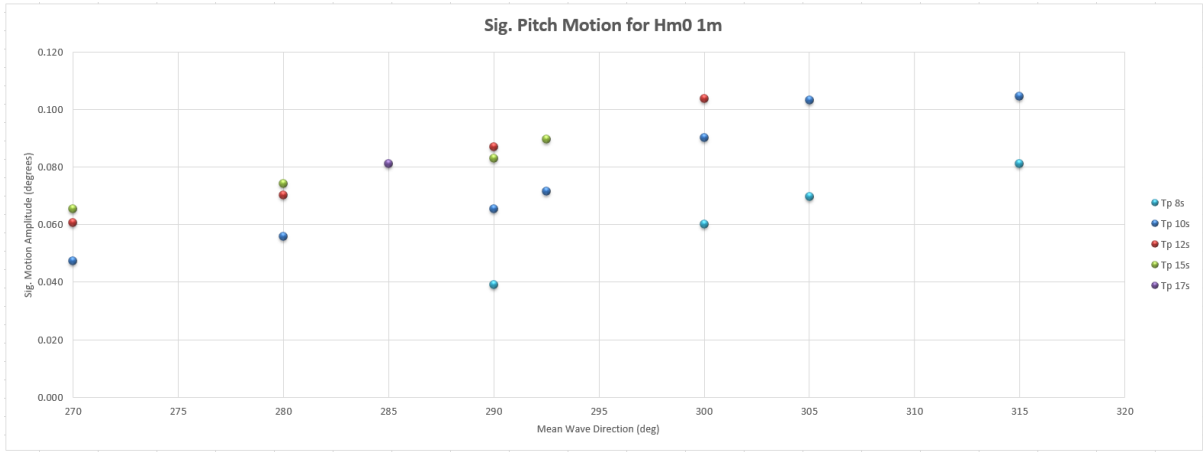
	Hm0 3m																			
	Tp 8s				Tp 10s					Tp 12s				Tp 13s	Tp 15s					
	290	300	305	315	270	280	290	292.5	300	305	315	270	280	290	300	280	270	280	290	292.5
Surge (m)	0.091	0.127	0.154	0.160	0.090	0.138	0.207	0.216	0.296	0.407	0.464	0.149	0.261	0.359	0.485	0.375	0.468	0.892	0.829	0.936
Sway (m)	0.087	0.083	0.083	0.082	0.086	0.121	0.161	0.151	0.140	0.146	0.134	0.145	0.174	0.180	0.258	0.198	0.352	0.402	0.507	0.447
Heave (m)	0.057	0.069	0.074	0.086	0.065	0.085	0.102	0.110	0.119	0.117	0.137	0.104	0.108	0.131	0.165	0.149	0.172	0.211	0.249	0.260
Roll (deg)	0.307	0.316	0.354	0.361	0.384	0.473	0.561	0.598	0.664	0.723	0.799	0.537	0.653	0.881	1.188	0.918	1.056	1.229	1.448	1.555
Pitch (deg)	0.125	0.178	0.208	0.244	0.094	0.128	0.176	0.172	0.231	0.267	0.286	0.117	0.151	0.191	0.277	0.180	0.214	0.211	0.257	0.303
Yaw (deg)	0.078	0.083	0.082	0.083	0.106	0.132	0.159	0.151	0.179	0.180	0.185	0.181	0.202	0.238	0.313	0.295	0.353	0.415	0.472	0.449

Table C.14: DVRS Datapoints for  $H_{m0}$  4m

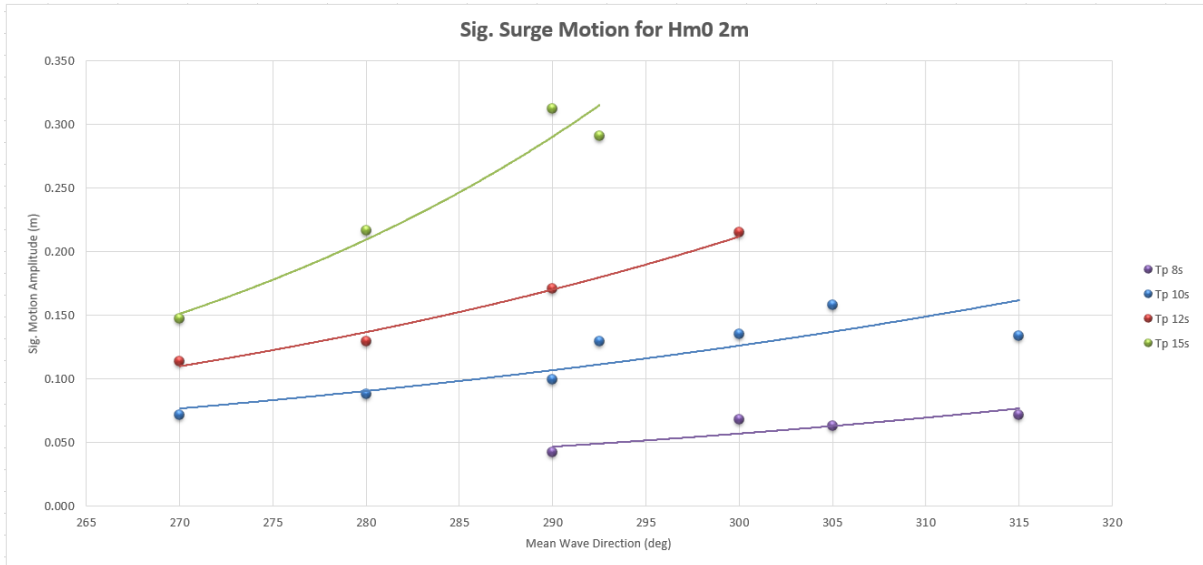
	Hm0 4m									
	Tp 8s		Tp 10s			Tp 12s			Tp 15s	
	290	300	280	290	300	280	290	300	280	290
Surge (m)	0.197	0.272	0.251	0.515	0.955	0.618	0.813	1.576	1.966	1.500
Sway (m)	0.096	0.095	0.176	0.234	0.247	0.288	0.356	0.366	0.603	0.570
Heave (m)	0.078	0.106	0.123	0.149	0.169	0.169	0.211	0.233	0.285	0.337
Roll (deg)	0.382	0.409	0.706	0.842	0.945	1.006	1.194	1.509	1.726	1.609
Pitch (deg)	0.169	0.232	0.183	0.235	0.325	0.210	0.266	0.405	0.286	0.329
Yaw (deg)	0.106	0.104	0.213	0.260	0.300	0.344	0.405	0.454	0.604	0.535

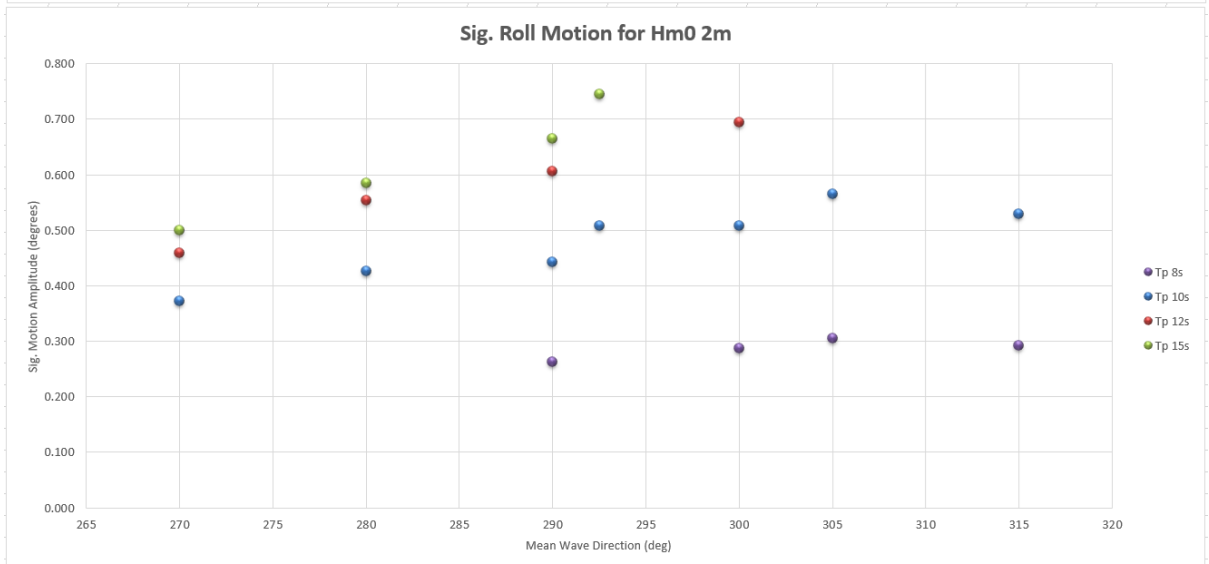
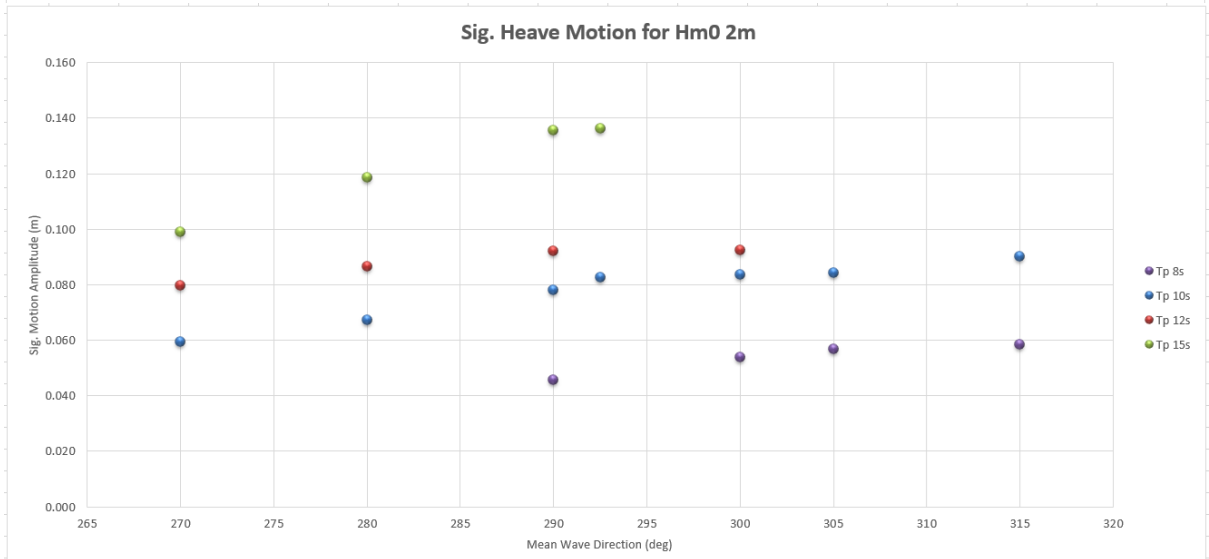
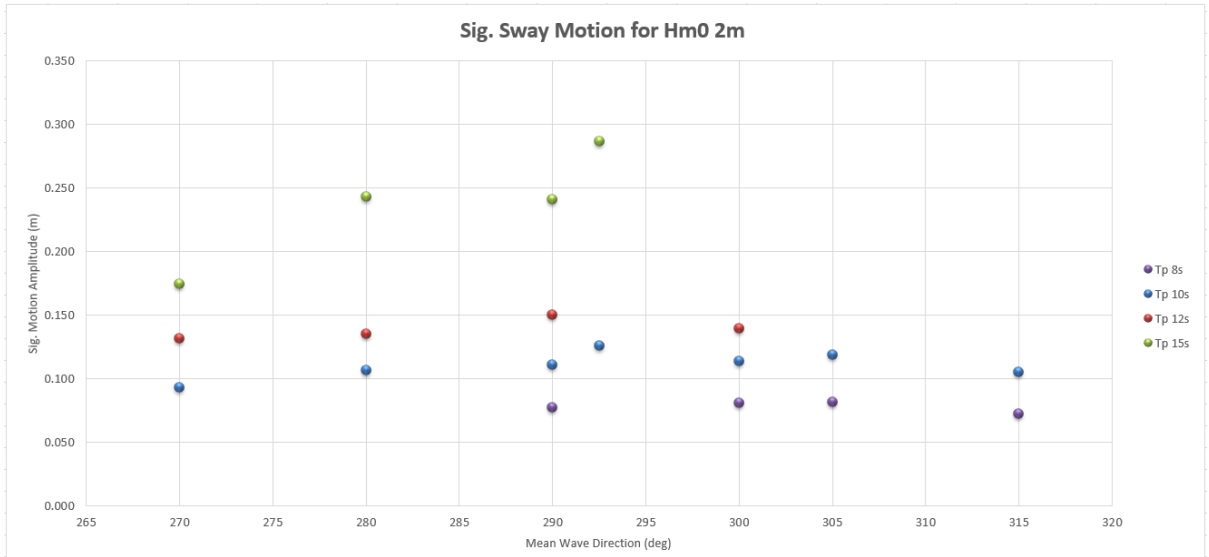
# H<sub>m0</sub> 1m



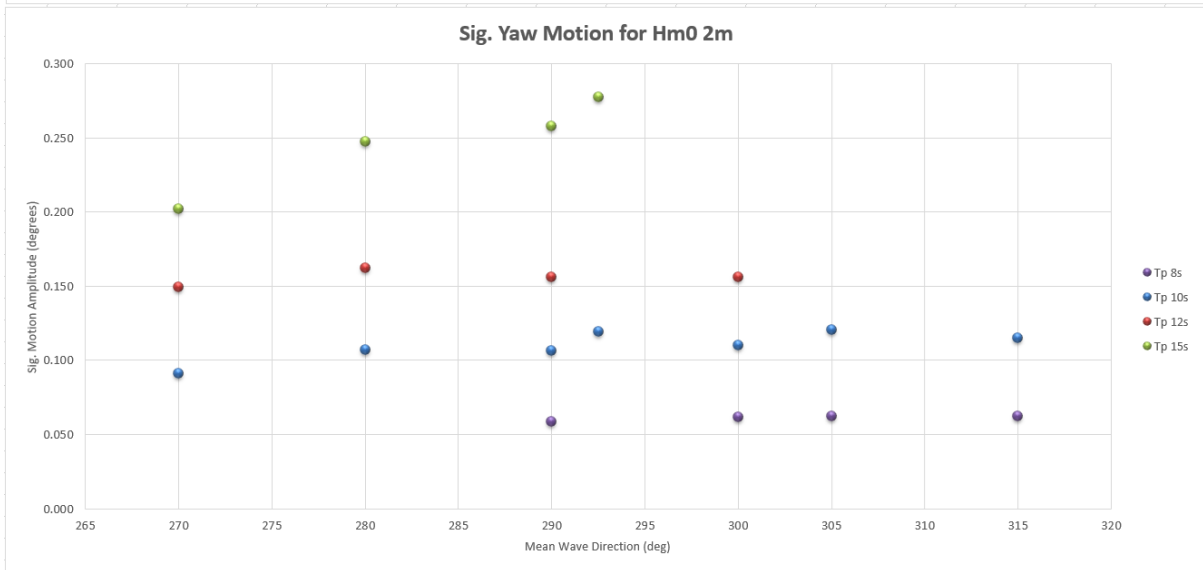
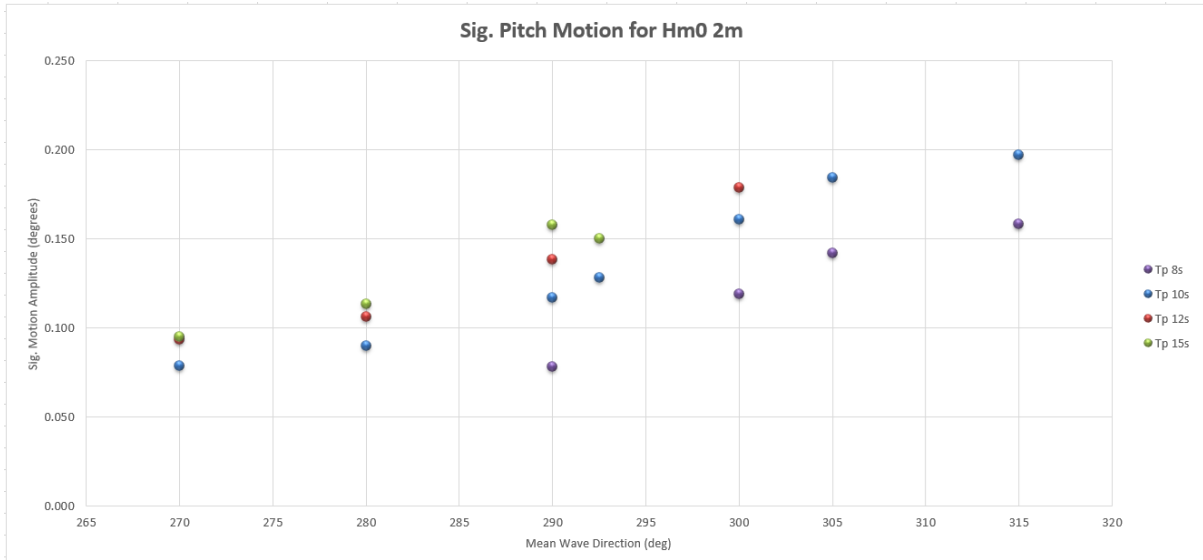


## Hm0 2m

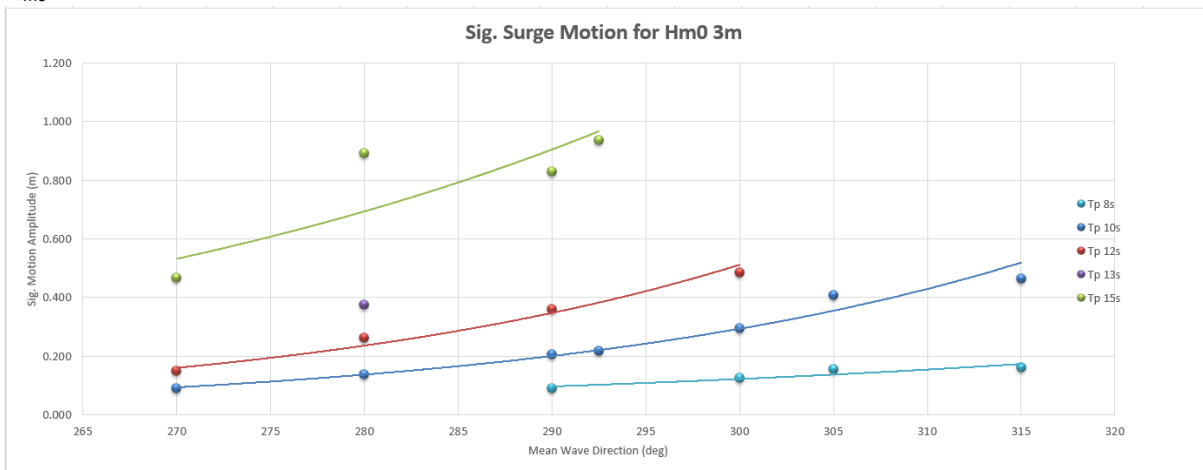


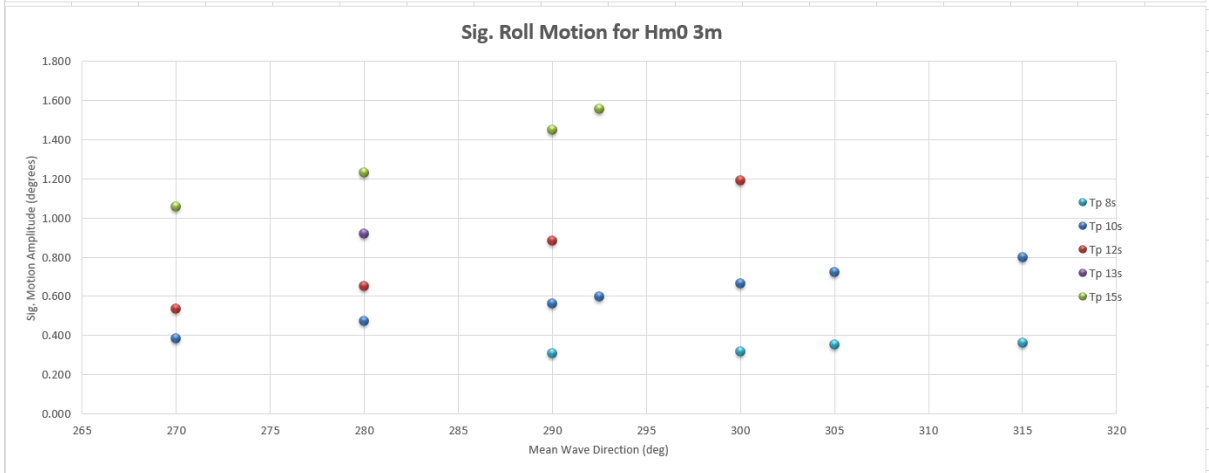
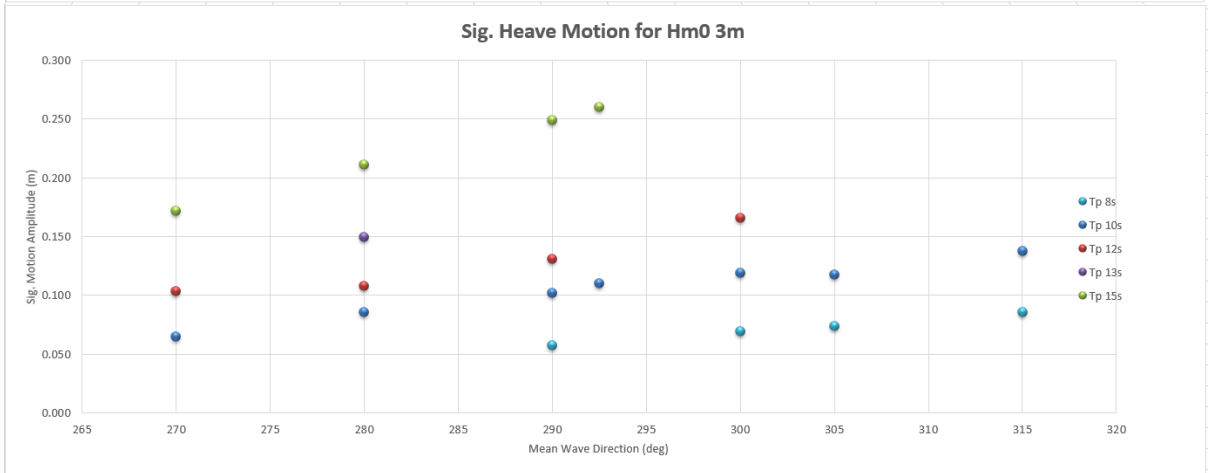
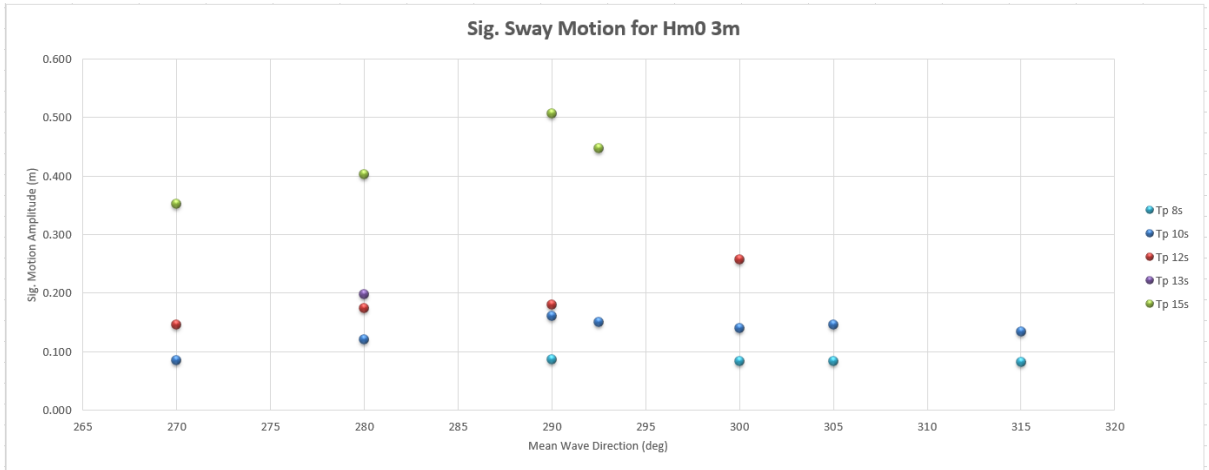


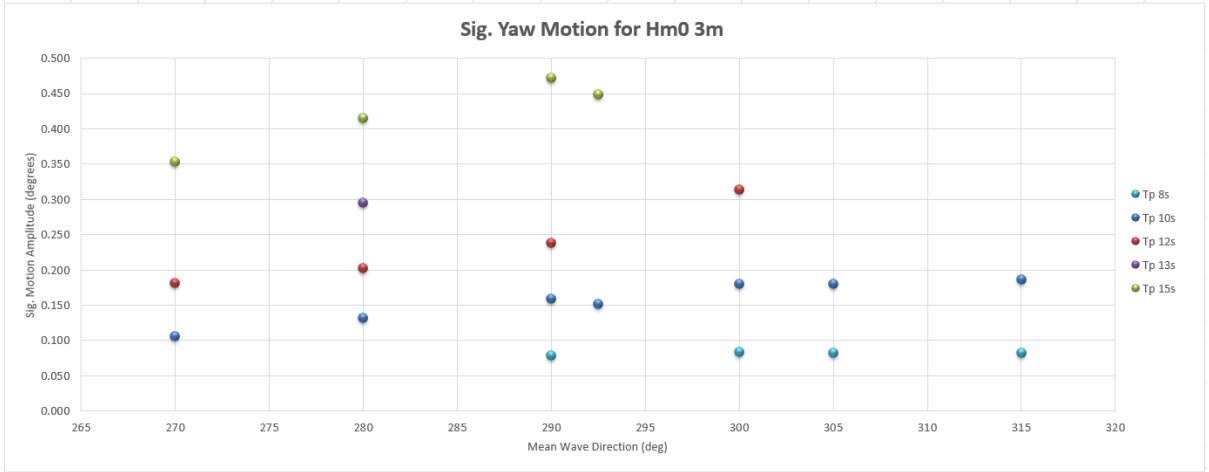
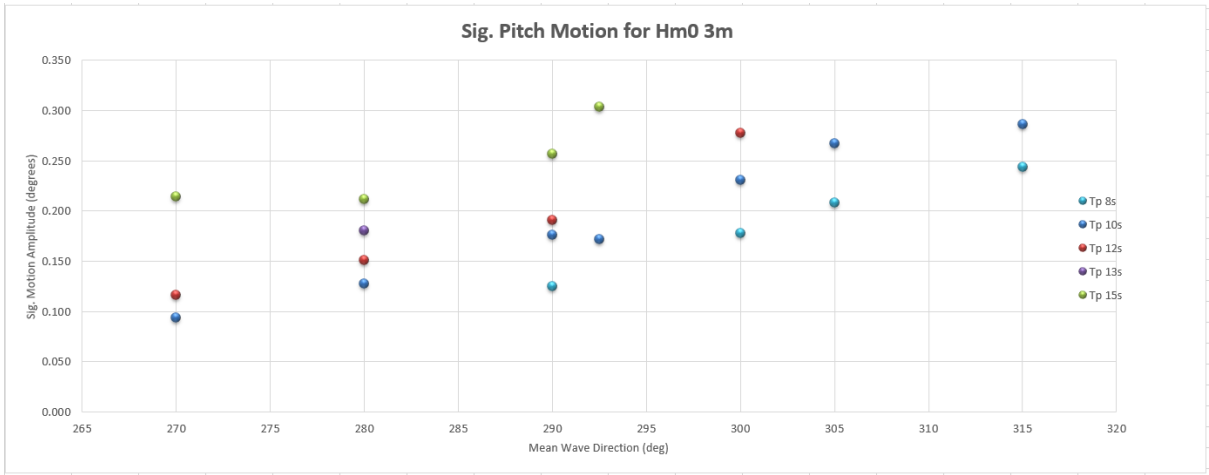




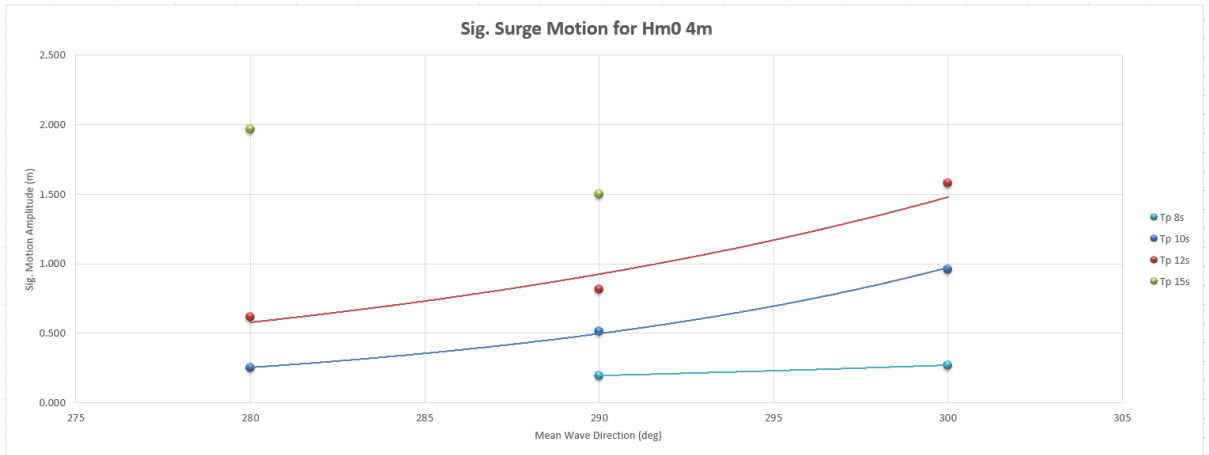
## Hm0 3m

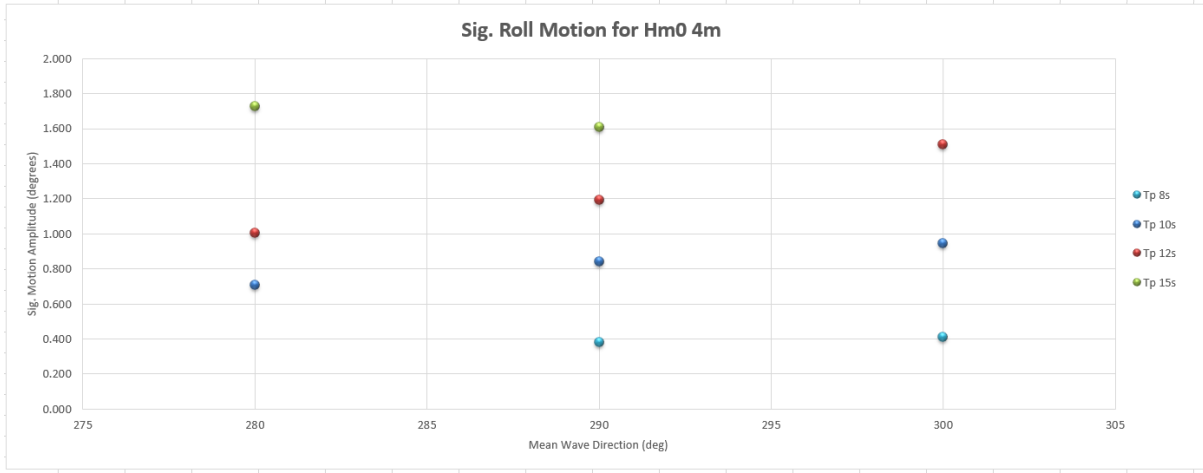
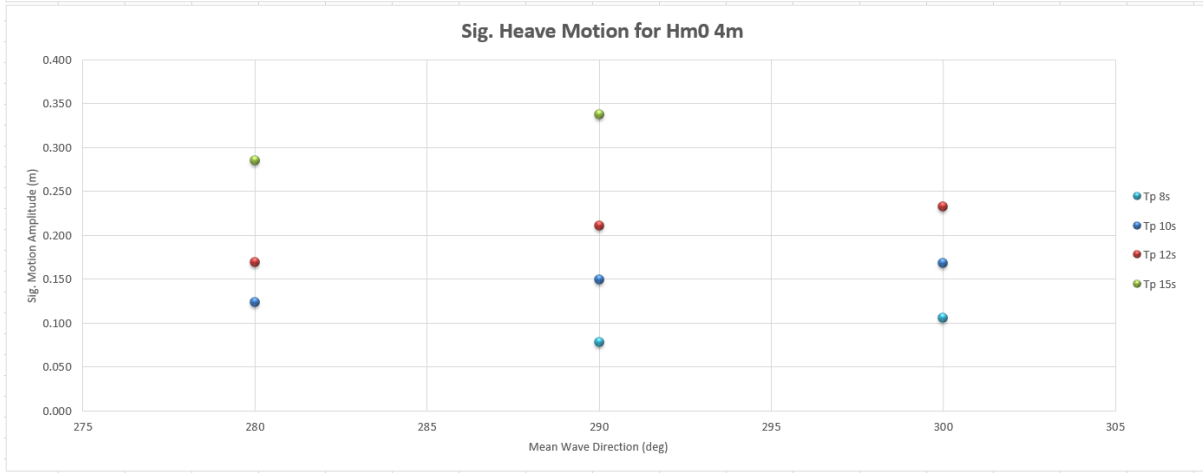
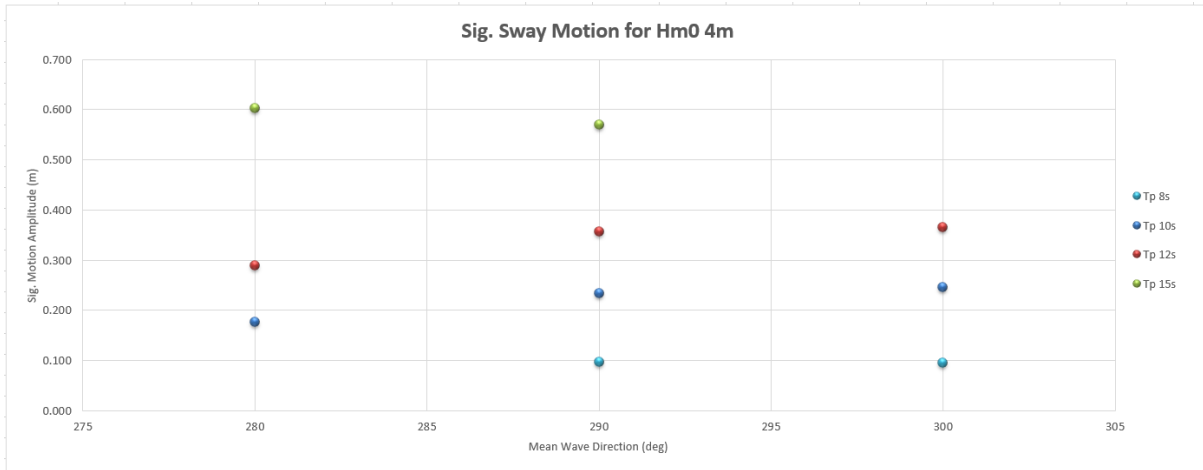






## H<sub>m0</sub> 4m





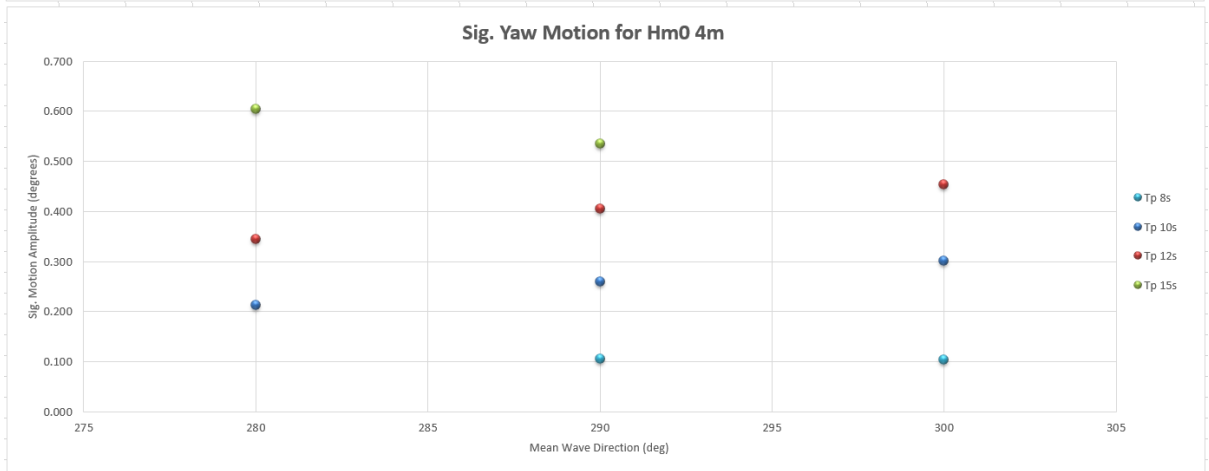
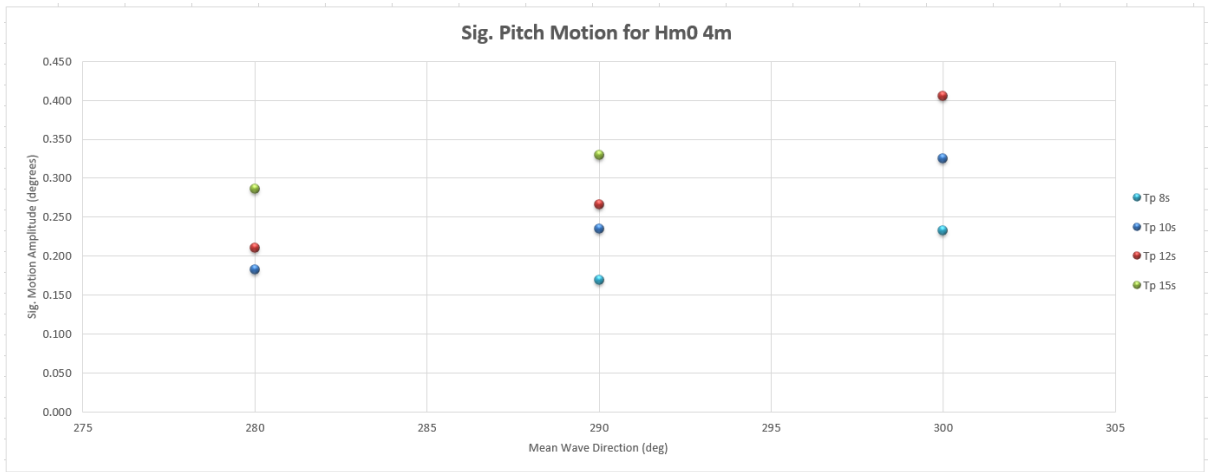


Table C.15: DVRS Datapoints for Mooring Line Forces

MWD		270	280	290	292.5	300	305	315
Hm0	1m							
Tp	8			71.583		72.228	71.88	70.28
	10	77.939	78.132	81.587	86.663	80.603	82.646	93.764
	12	82.691	91.306	88.873		83.184		
	15	80.814	87.261	82.877	96.686			
Hm0	2m							
Tp	8			75.23		77.767	80.655	78.817
	10	88.141	92.759	91.09	103.119	88.048	92.963	96.027
	12	107.998	113.36	101.191		101.184		
	15	96.13	119.256	111.314	114.803			
Hm0	3m							
Tp	8			83.978		78.418	88.997	81.066
	10	87.427	97.954	110.192	110.063	126.293	118.376	113.647
	12	109.238	123.182	127.43		149.952		
	15	140.873	180.678	219.799	198.742			
Hm0	4m							
Tp	8			91.682		91.693		
	10		120.673	150.382		160.975		
	12		166.874	223.431		242.708		
	15		233.733	241.237				

C.4 Ultraline Dyneema Line, Polyamide Tail, Wind 10  $\frac{m}{s}$ , 0 degrees

Table C.16: DVRS Datapoints for  $H_{m0}$  1m

	Hm0 1m																				
	Tp 8s				Tp 10s								Tp 12s				Tp 15s				Tp 17s
	290	300	305	315	270	280	290	292.5	300	305	315	270	280	290	300	270	280	290	292.5	285	
Surge (m)	0.024	0.028	0.029	0.032	0.036	0.041	0.045	0.051	0.055	0.062	0.071	0.058	0.066	0.072	0.088	0.087	0.105	0.116	0.129	0.147	
Sway (m)	0.048	0.051	0.049	0.044	0.061	0.070	0.068	0.080	0.073	0.071	0.082	0.080	0.093	0.089	0.084	0.116	0.126	0.118	0.128	0.139	
Heave (m)	0.026	0.031	0.032	0.031	0.038	0.042	0.045	0.051	0.049	0.049	0.050	0.055	0.060	0.057	0.057	0.070	0.076	0.076	0.084	0.091	
Roll (deg)	0.150	0.174	0.179	0.172	0.228	0.265	0.261	0.291	0.297	0.325	0.336	0.306	0.368	0.365	0.414	0.370	0.381	0.408	0.456	0.425	
Pitch (deg)	0.045	0.067	0.076	0.089	0.050	0.058	0.068	0.074	0.093	0.106	0.110	0.063	0.072	0.089	0.107	0.066	0.076	0.084	0.091	0.081	
Yaw (deg)	0.045	0.049	0.048	0.048	0.070	0.084	0.079	0.086	0.082	0.086	0.109	0.096	0.118	0.105	0.106	0.117	0.130	0.120	0.134	0.137	

Table C.17: DVRS Datapoints for  $H_{m0}$  2m

	Hm0 2m																			
	Tp 8s				Tp 10s								Tp 12s				Tp 15s			
	290	300	305	315	270	280	290	292.5	300	305	315	270	280	290	300	270	280	290	292.5	
Surge (m)	0.050	0.067	0.069	0.078	0.062	0.083	0.110	0.121	0.150	0.158	0.150	0.095	0.140	0.149	0.237	0.176	0.240	0.355	0.320	
Sway (m)	0.074	0.077	0.080	0.069	0.094	0.110	0.111	0.131	0.118	0.116	0.106	0.126	0.143	0.152	0.142	0.189	0.163	0.183	0.195	
Heave (m)	0.045	0.054	0.057	0.059	0.058	0.066	0.077	0.082	0.083	0.083	0.090	0.079	0.085	0.091	0.092	0.099	0.119	0.135	0.136	
Roll (deg)	0.229	0.232	0.262	0.239	0.330	0.391	0.381	0.445	0.453	0.499	0.478	0.453	0.542	0.581	0.679	0.503	0.572	0.609	0.707	
Pitch (deg)	0.084	0.126	0.150	0.166	0.080	0.091	0.119	0.131	0.165	0.188	0.202	0.094	0.108	0.140	0.181	0.096	0.115	0.160	0.151	
Yaw (deg)	0.064	0.067	0.068	0.067	0.094	0.120	0.110	0.125	0.119	0.120	0.122	0.140	0.173	0.166	0.167	0.179	0.191	0.203	0.203	

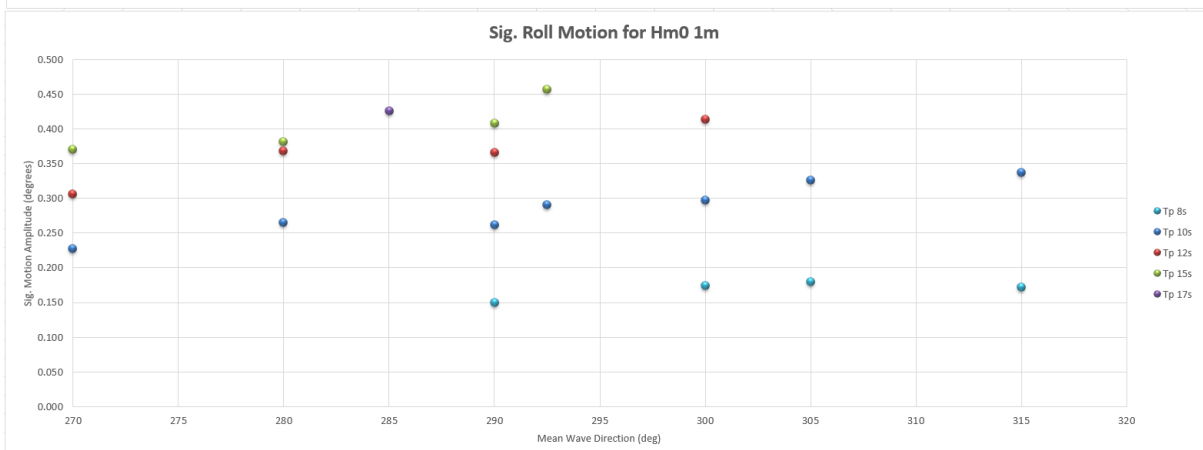
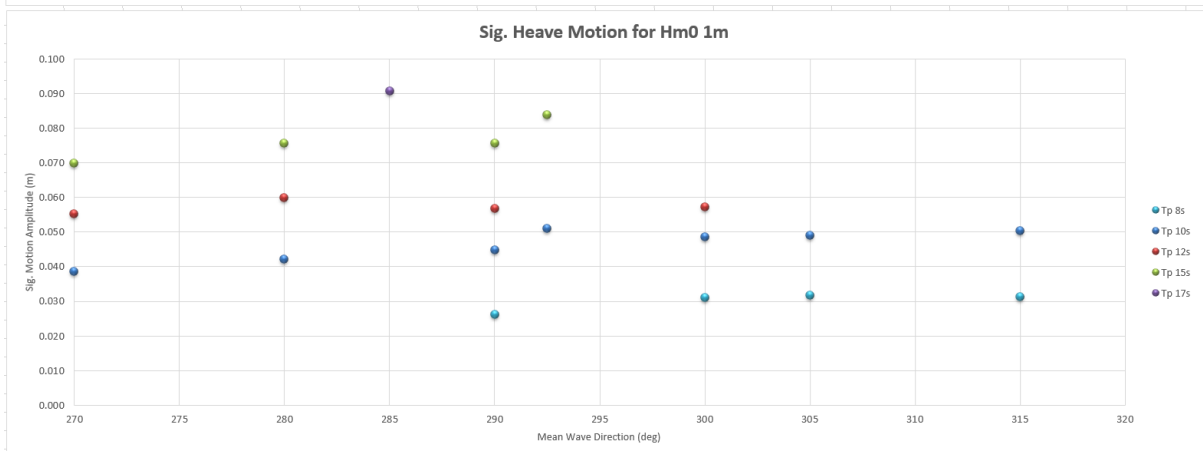
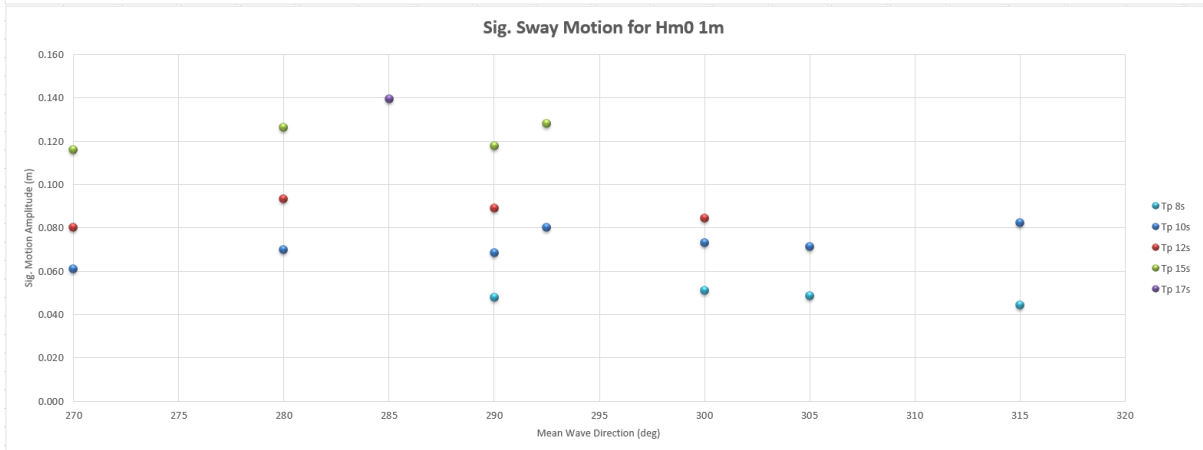
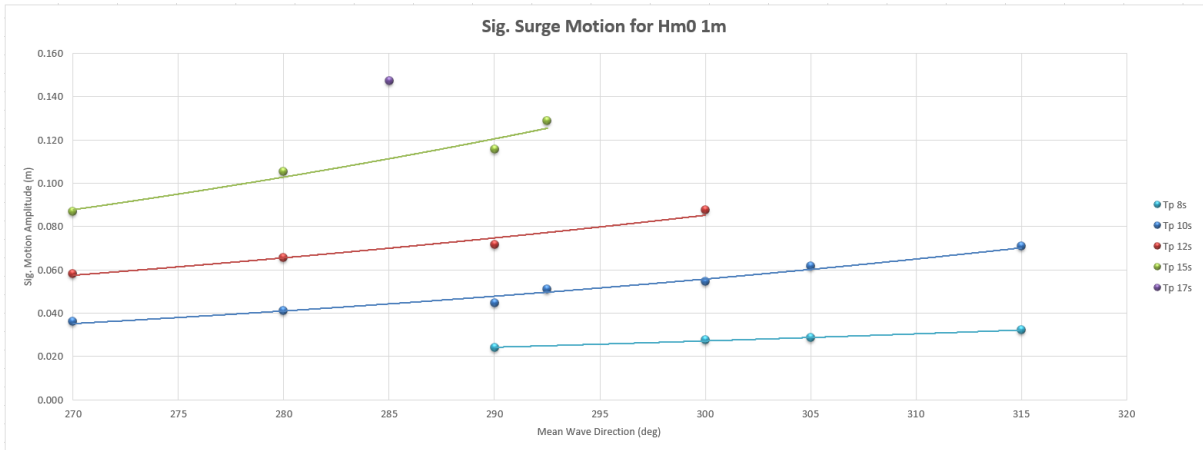
Table C.18: DVRS Datapoints for  $H_{m0}$  3m

	Hm0 3m																				
	Tp 8s				Tp 10s								Tp 12s				Tp 13s	Tp 15s			
	290	300	305	315	270	280	290	292.5	300	305	315	270	280	290	300	280	270	280	290	292.5	
Surge (m)	0.120	0.160	0.182	0.207	0.095	0.172	0.239	0.248	0.329	0.384	0.470	0.175	0.319	0.358	0.480	0.362	0.413	0.641	0.628	0.730	
Sway (m)	0.088	0.083	0.089	0.087	0.090	0.117	0.145	0.147	0.144	0.137	0.152	0.127	0.178	0.202	0.231	0.199	0.258	0.334	0.335	0.355	
Heave (m)	0.057	0.070	0.076	0.087	0.064	0.083	0.102	0.110	0.119	0.117	0.139	0.103	0.108	0.129	0.165	0.148	0.172	0.211	0.249	0.260	
Roll (deg)	0.267	0.282	0.314	0.333	0.343	0.426	0.481	0.515	0.613	0.658	0.759	0.515	0.620	0.821	1.064	0.847	0.984	1.173	1.260	1.351	
Pitch (deg)	0.133	0.186	0.217	0.253	0.096	0.131	0.179	0.177	0.234	0.272	0.291	0.119	0.153	0.193	0.278	0.182	0.214	0.210	0.256	0.302	
Yaw (deg)	0.085	0.089	0.093	0.093	0.111	0.132	0.149	0.149	0.202	0.189	0.217	0.172	0.201	0.268	0.338	0.326	0.318	0.366	0.382	0.388	

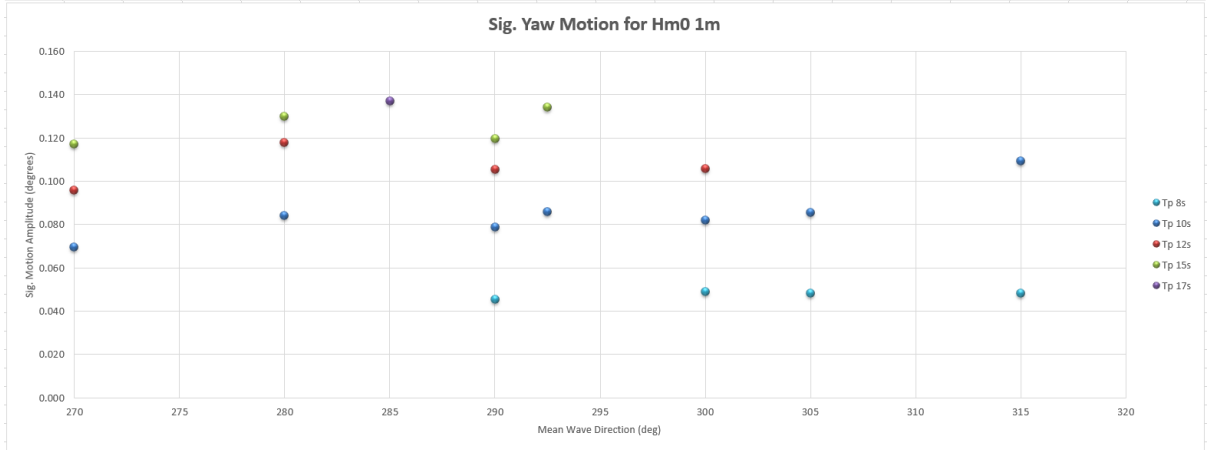
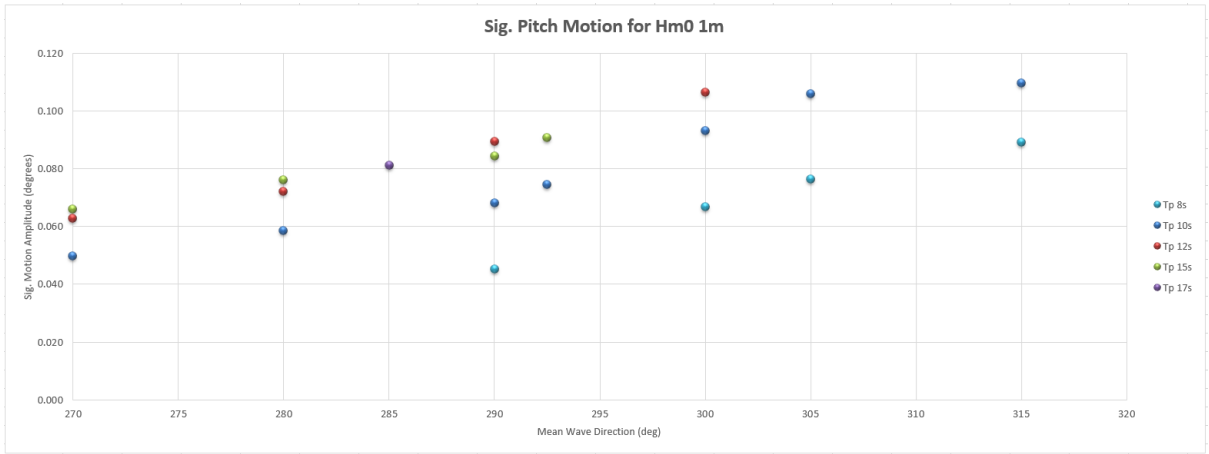
Table C.19: DVRS Datapoints for  $H_{m0}$  4m

	Hm0 4m									
	Tp 8s		Tp 10s			Tp 12s			Tp 15s	
	290	300	280	290	300	280	290	300	280	290
Surge (m)	0.215	0.307	0.295	0.413	0.725	0.498	0.637	0.901	0.865	0.950
Sway (m)	0.100	0.100	0.155	0.222	0.226	0.248	0.275	0.301	0.427	0.476
Heave (m)	0.078	0.107	0.123	0.148	0.168	0.169	0.214	0.232	0.288	0.335
Roll (deg)	0.347	0.377	0.585	0.733	0.830	0.913	1.134	1.412	1.591	1.545
Pitch (deg)	0.176	0.241	0.186	0.239	0.331	0.212	0.270	0.406	0.280	0.328
Yaw (deg)	0.114	0.119	0.216	0.251	0.316	0.342	0.409	0.464	0.428	0.456

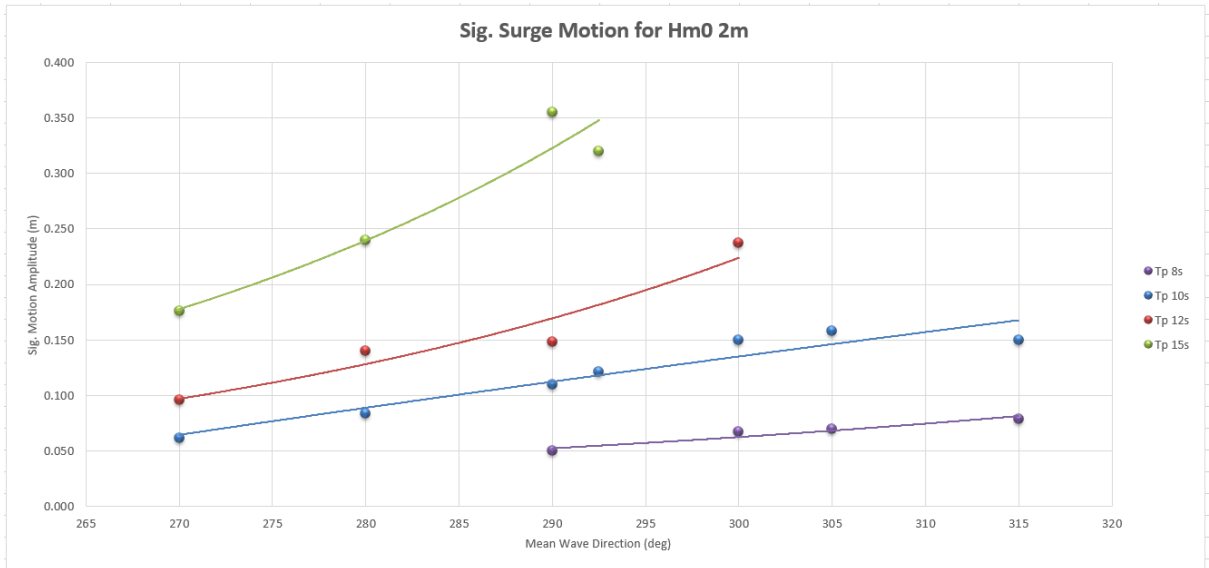
# H<sub>m0</sub> 1m



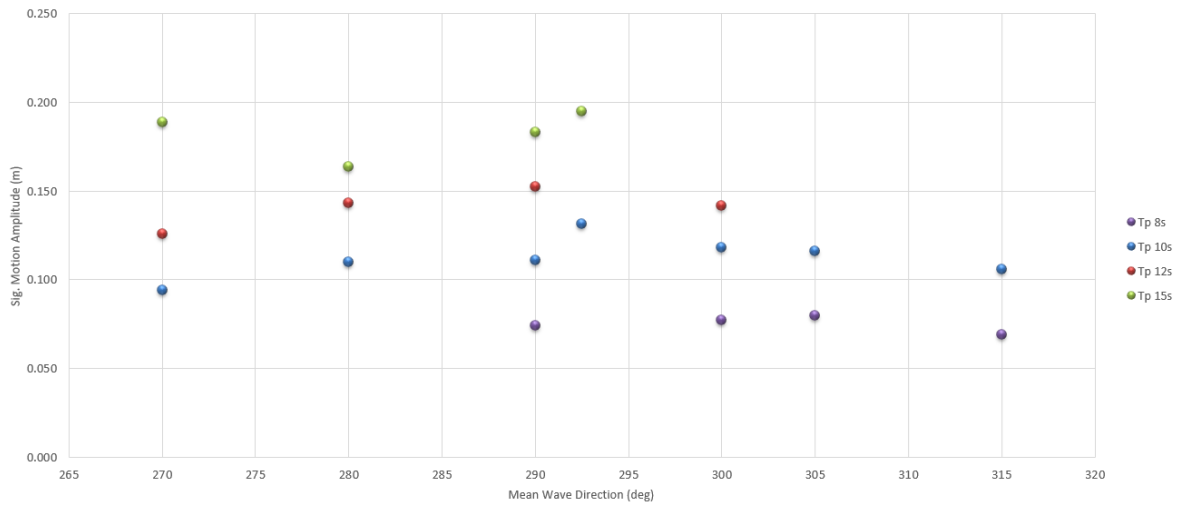




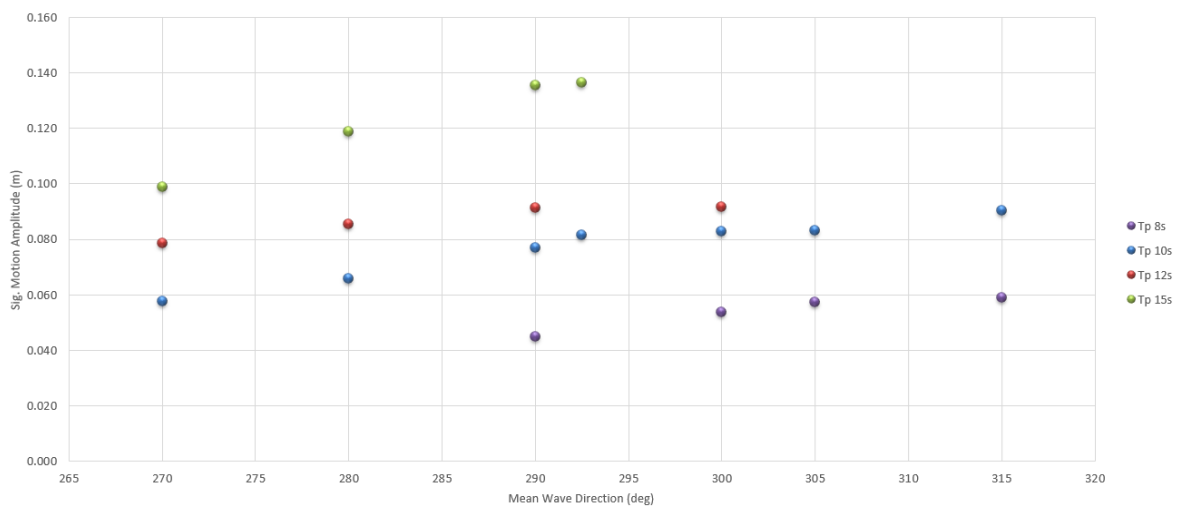
## H<sub>m0</sub> 2m



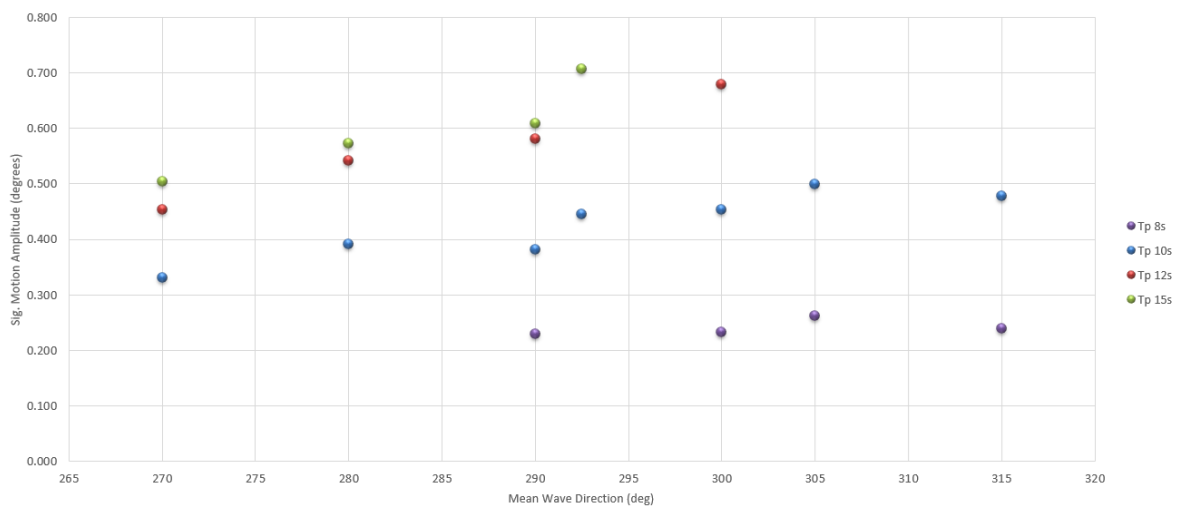
**Sig. Sway Motion for Hm0 2m**

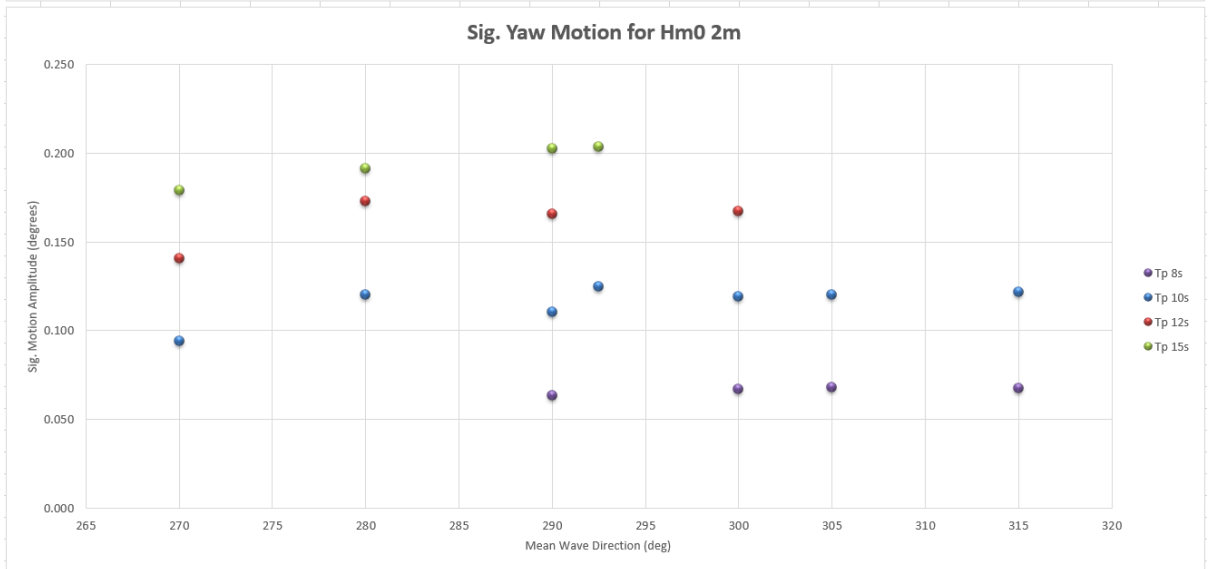
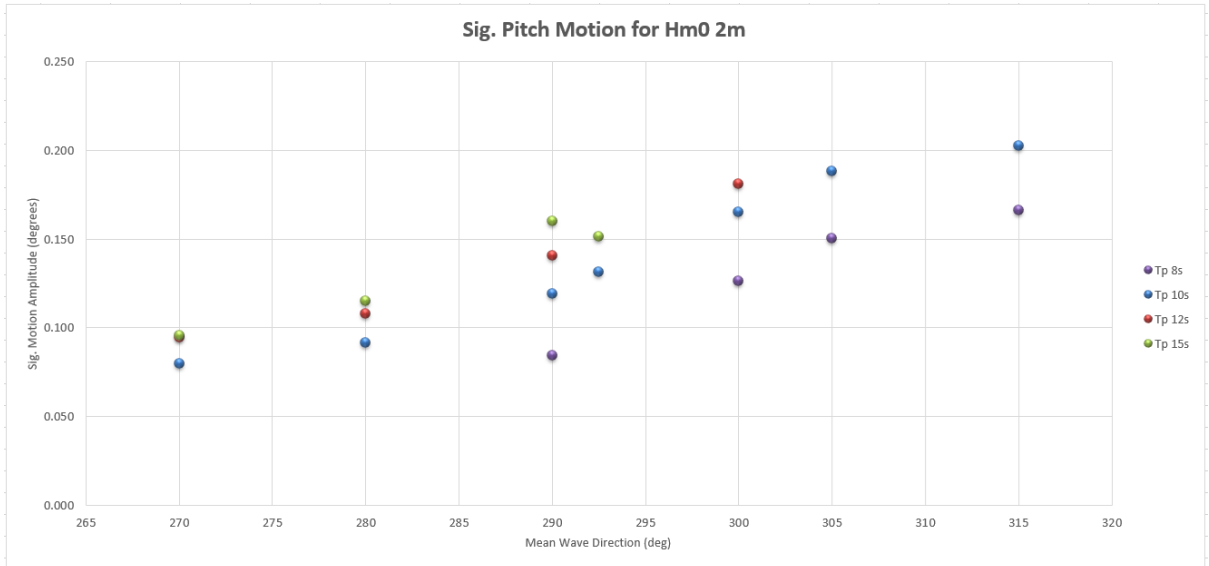


**Sig. Heave Motion for Hm0 2m**

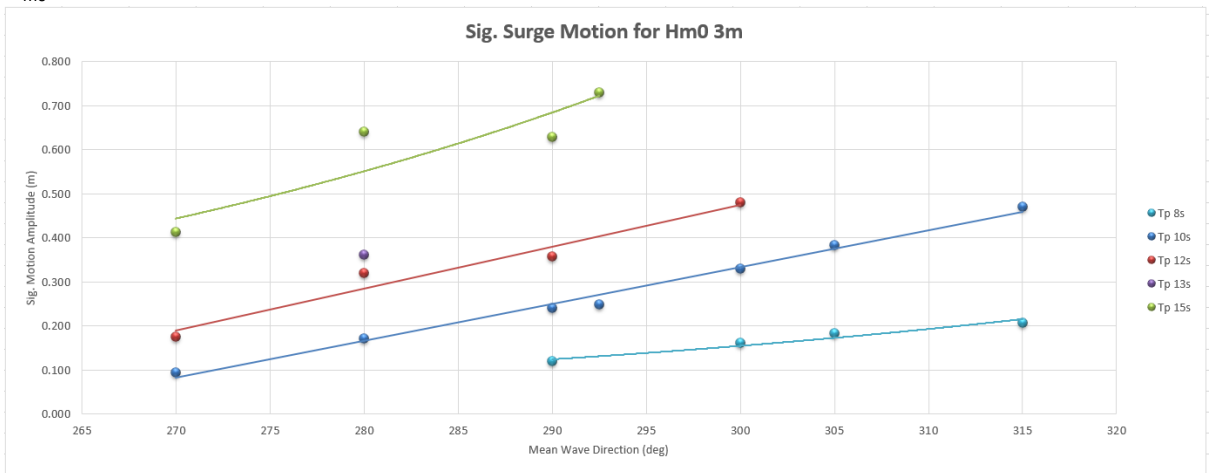


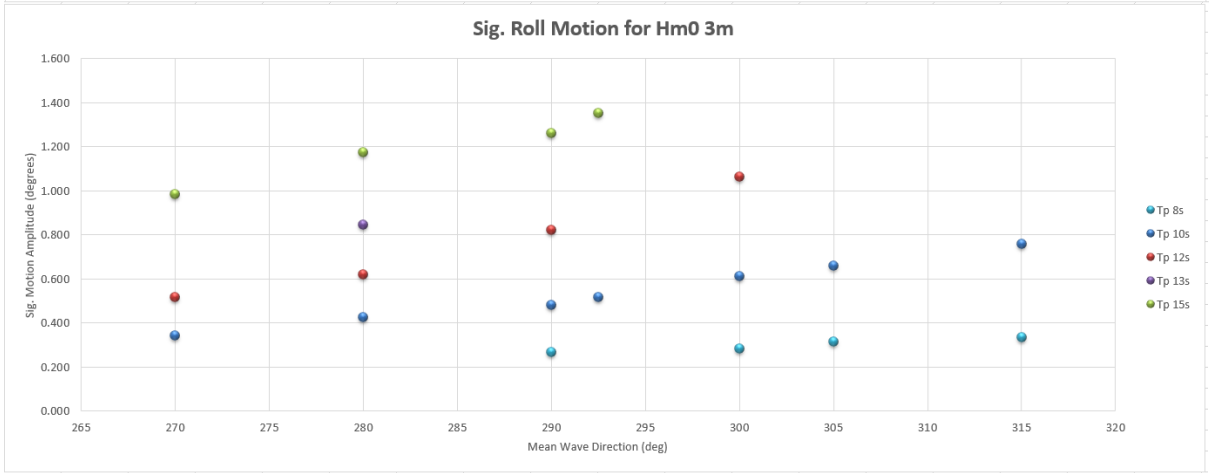
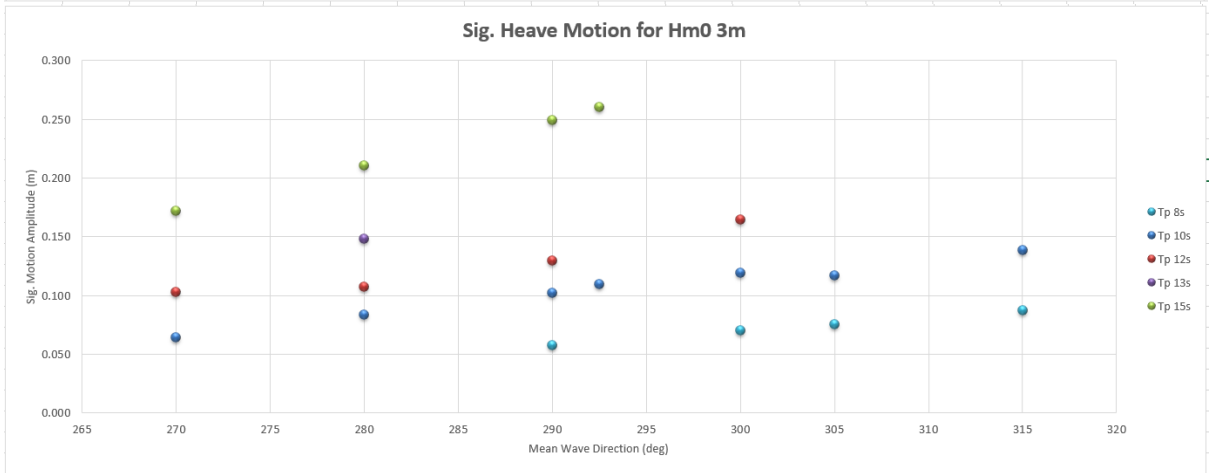
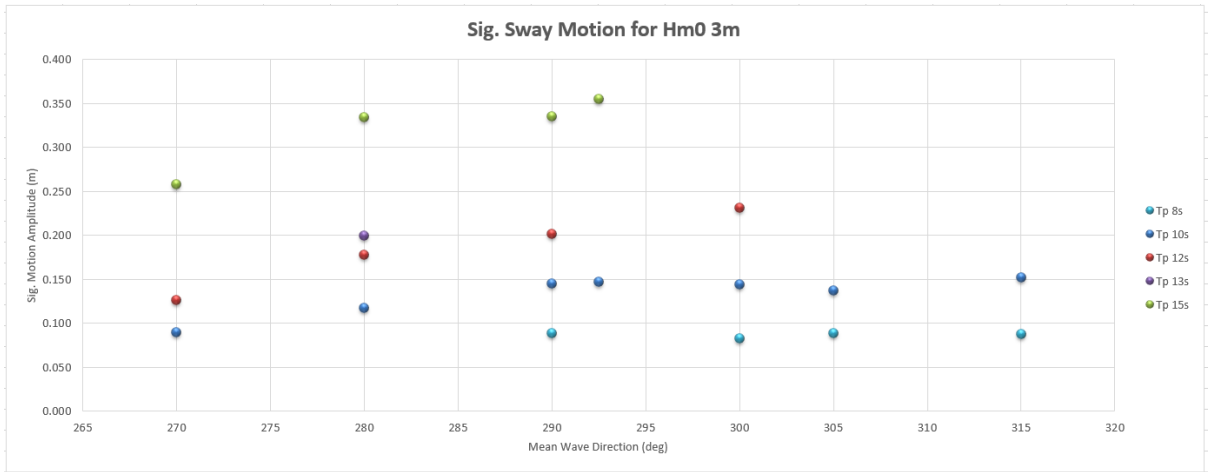
**Sig. Roll Motion for Hm0 2m**

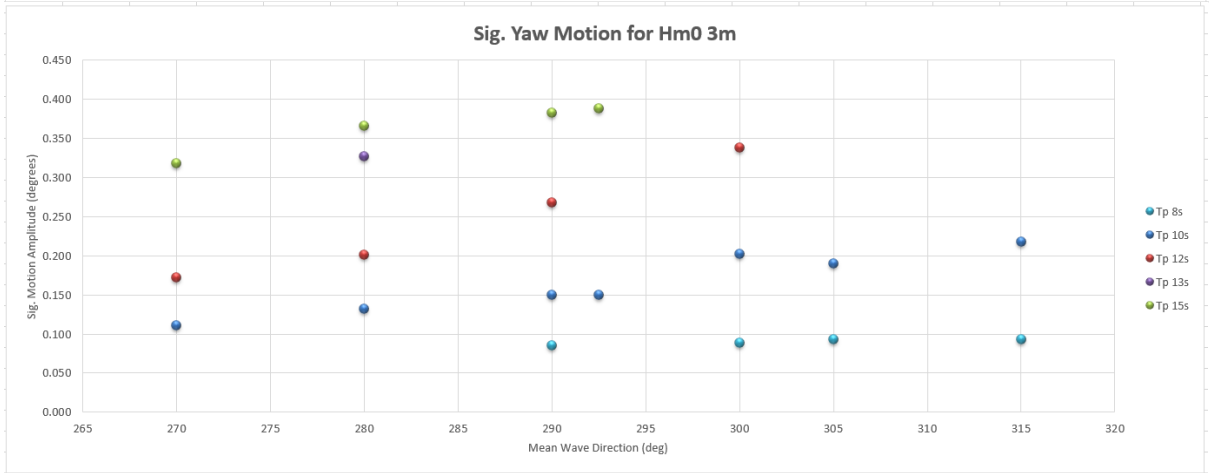
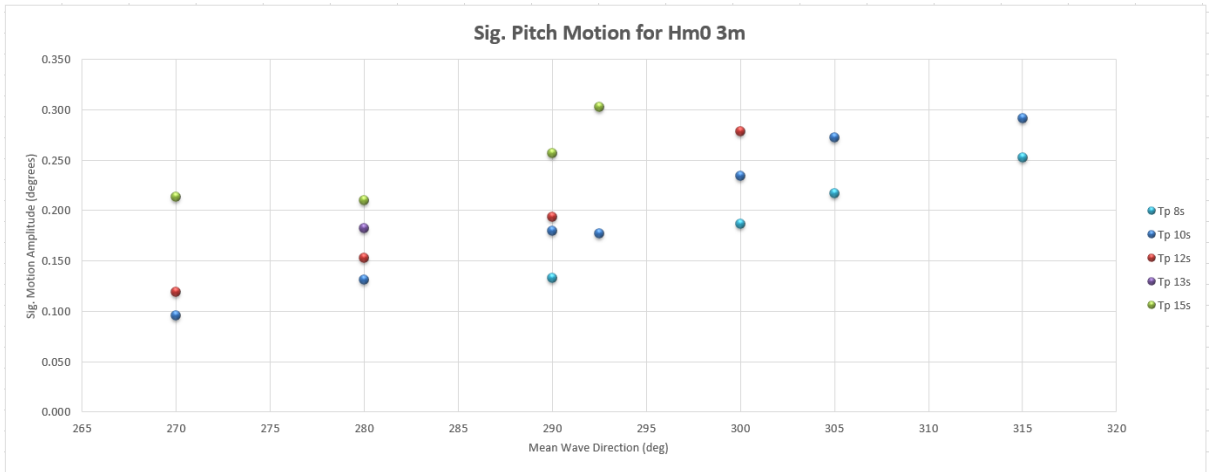




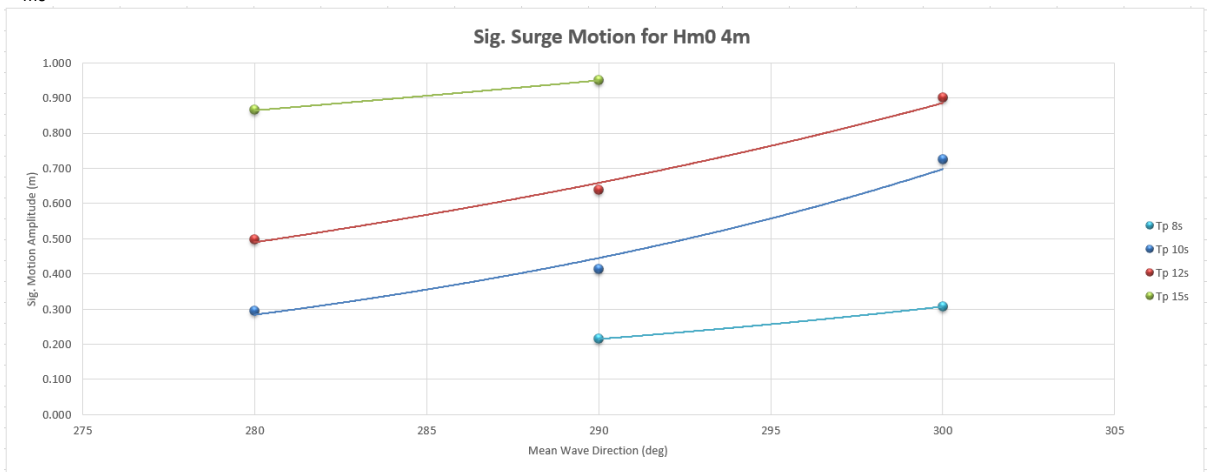
## H<sub>m0</sub> 3m

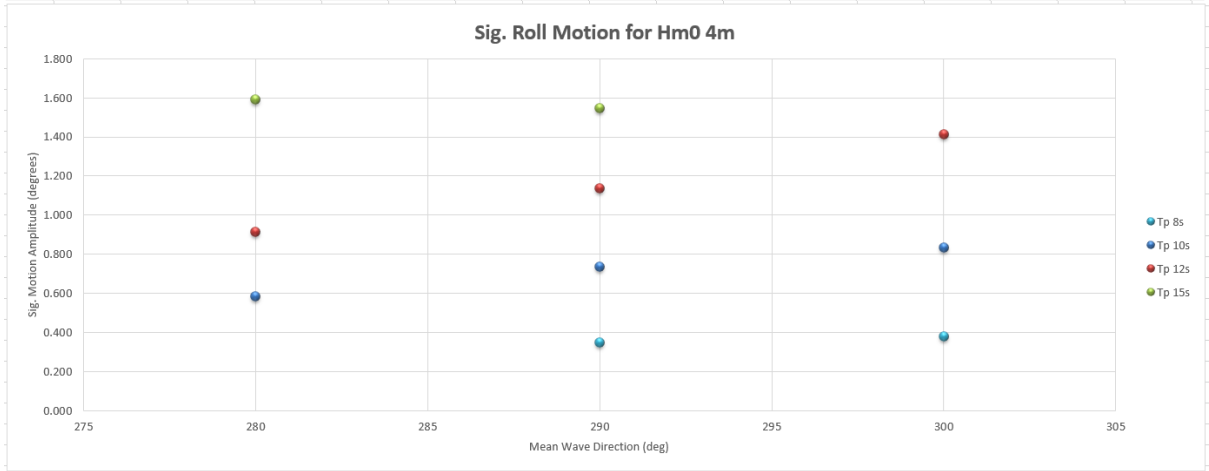
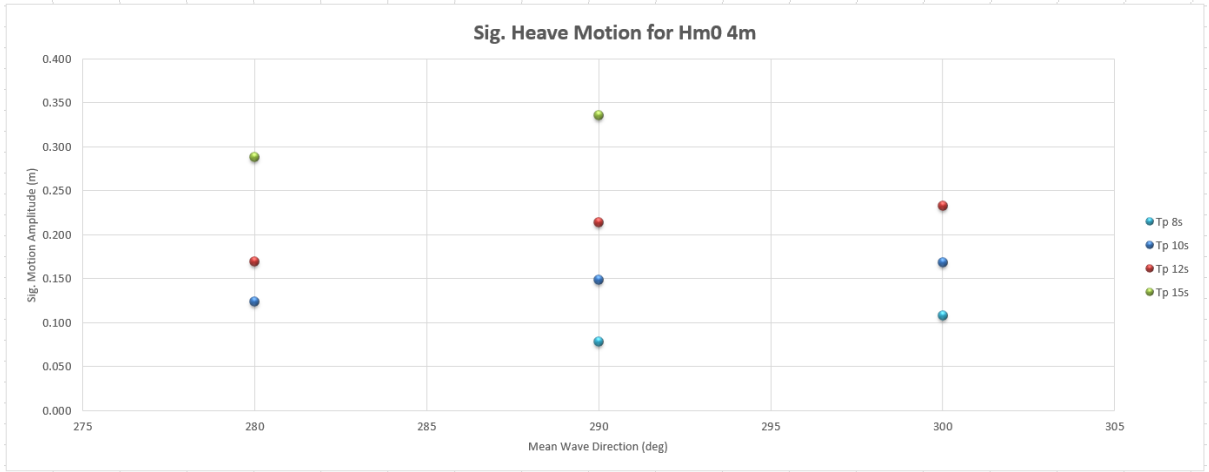
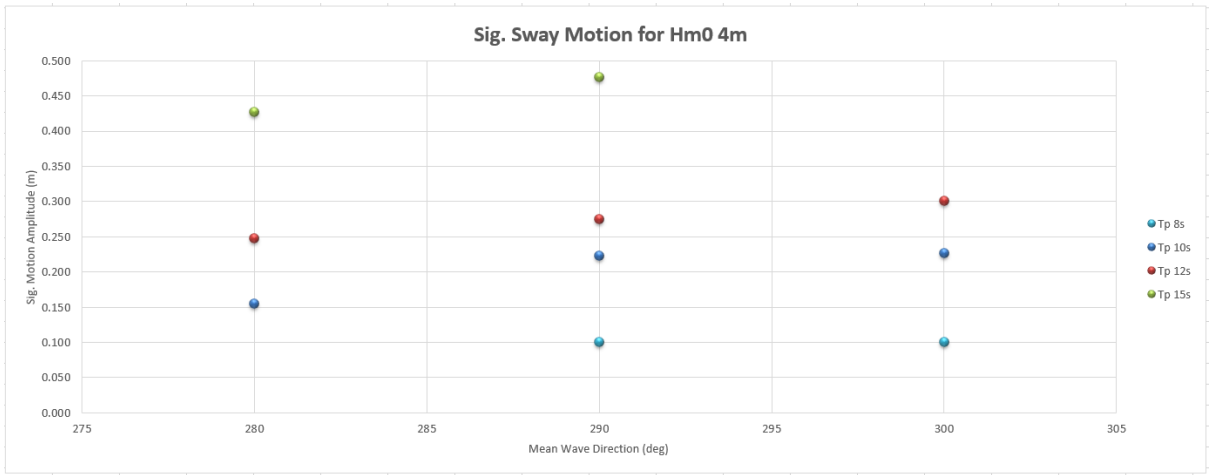




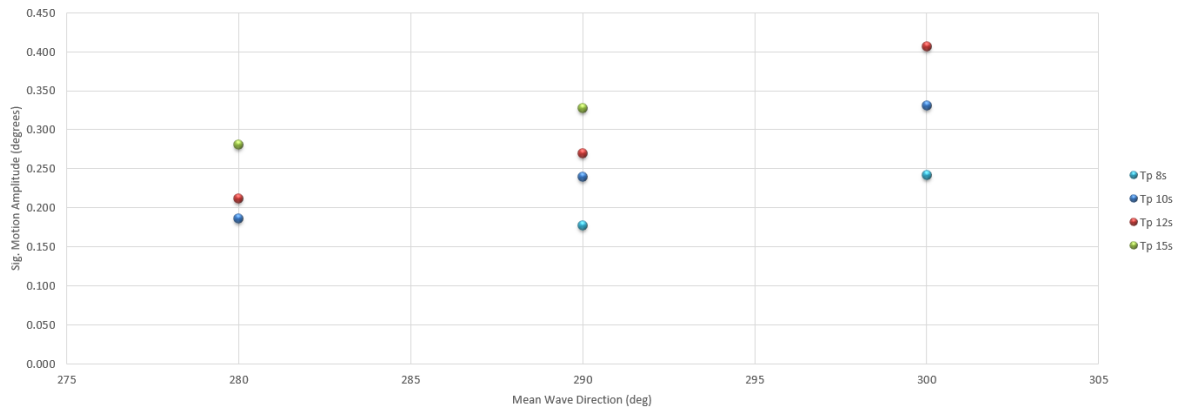


## Hm0 4m





**Sig. Pitch Motion for Hm0 4m**



**Sig. Yaw Motion for Hm0 4m**

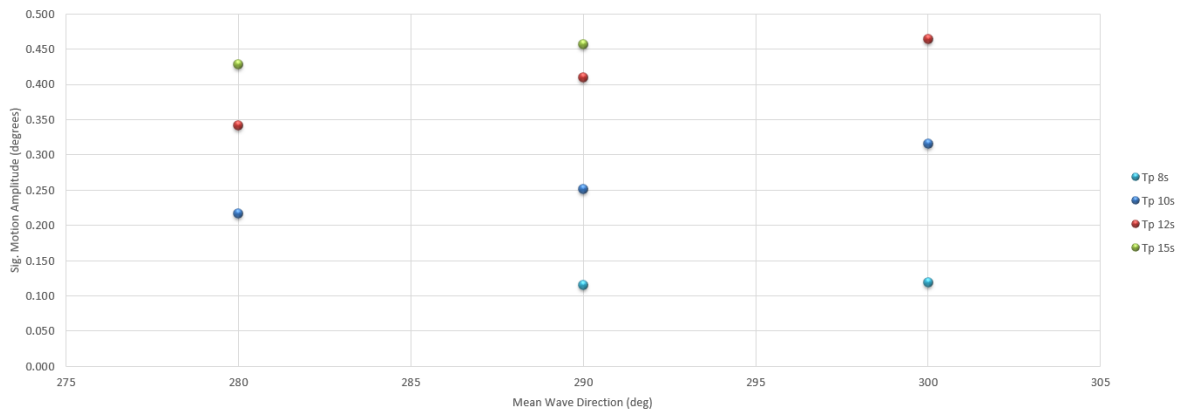


Table C.20: DVRS Datapoints for Mooring Line Forces

MWD		270	280	290	292.5	300	305	315
Hm0	1m							
Tp	8			58.521		56.439	56.686	58.585
	10	65.586	69.606	68.864	77.763	71.667	74.623	93.147
	12	74.279	93.201	84.261		87.995		
	15	98.845	98.358	119.173	100.071			
Hm0	2m							
Tp	8			63.016		67.412	76.951	69.022
	10	80.961	92.224	87.984	101.681	104.69	111.092	105.643
	12	107.843	128.235	111.437		182.85		
	15	141.377	188.22	294.708	331.928			
Hm0	3m							
Tp	8			86.677		89.88	117.724	105.854
	10	83.81	102.101	171.818	169.225	178.427	238.899	290.245
	12	126.836	172.189	183.725		286.869		
	15	279.476	466.078	512.393	655.589			
Hm0	4m							
Tp	8			117.293		150.372		
	10		206.436	262.676		458.478		
	12		298.356	340.557		724.875		
	15		754.611	924.647				



C.5 Polypropylene Line, Polyamide Tail, Wind 15  $\frac{m}{s}$ , 0 degrees

Table C.21: DVRS Datapoints for  $H_{m0}$  1m

	Hm0 1m																				
	Tp 8s				Tp 10s								Tp 12s				Tp 15s				Tp 17s
	290	300	305	315	270	280	290	292.5	300	305	315	270	280	290	300	270	280	290	292.5	285	
Surge (m)	0.014	0.021	0.025	0.025	0.027	0.031	0.037	0.059	0.052	0.071	0.068	0.058	0.067	0.067	0.095	0.063	0.078	0.094	0.101	0.133	
Sway (m)	0.048	0.051	0.049	0.044	0.060	0.063	0.068	0.076	0.073	0.071	0.075	0.067	0.075	0.076	0.076	0.070	0.089	0.117	0.128	0.247	
Heave (m)	0.027	0.032	0.033	0.032	0.039	0.043	0.046	0.052	0.050	0.050	0.052	0.056	0.060	0.057	0.058	0.070	0.075	0.075	0.084	0.090	
Roll (deg)	0.193	0.239	0.245	0.251	0.265	0.302	0.324	0.360	0.402	0.435	0.425	0.308	0.391	0.393	0.461	0.354	0.378	0.431	0.468	0.465	
Pitch (deg)	0.041	0.060	0.070	0.081	0.049	0.058	0.068	0.073	0.093	0.105	0.106	0.062	0.072	0.089	0.106	0.066	0.075	0.084	0.091	0.081	
Yaw (deg)	0.042	0.045	0.044	0.043	0.064	0.076	0.072	0.079	0.081	0.084	0.101	0.089	0.105	0.093	0.095	0.110	0.126	0.133	0.149	0.233	

Table C.22: DVRS Datapoints for  $H_{m0}$  2m

	Hm0 2m																			
	Tp 8s				Tp 10s								Tp 12s				Tp 15s			
	290	300	305	315	270	280	290	292.5	300	305	315	270	280	290	300	270	280	290	292.5	
Surge (m)	0.039	0.055	0.063	0.061	0.065	0.079	0.104	0.138	0.137	0.157	0.141	0.097	0.119	0.205	0.211	0.140	0.199	0.291	0.272	
Sway (m)	0.077	0.079	0.084	0.071	0.089	0.103	0.113	0.133	0.116	0.120	0.110	0.103	0.131	0.196	0.130	0.140	0.196	0.267	0.228	
Heave (m)	0.046	0.054	0.056	0.058	0.059	0.067	0.078	0.082	0.083	0.084	0.090	0.079	0.086	0.092	0.093	0.099	0.118	0.136	0.136	
Roll (deg)	0.296	0.323	0.341	0.338	0.417	0.462	0.490	0.558	0.559	0.625	0.601	0.474	0.568	0.656	0.745	0.521	0.591	0.714	0.762	
Pitch (deg)	0.078	0.117	0.140	0.156	0.081	0.092	0.118	0.130	0.162	0.185	0.197	0.094	0.107	0.139	0.179	0.094	0.114	0.158	0.150	
Yaw (deg)	0.063	0.067	0.072	0.067	0.089	0.110	0.111	0.124	0.119	0.126	0.123	0.129	0.156	0.192	0.153	0.171	0.208	0.269	0.242	

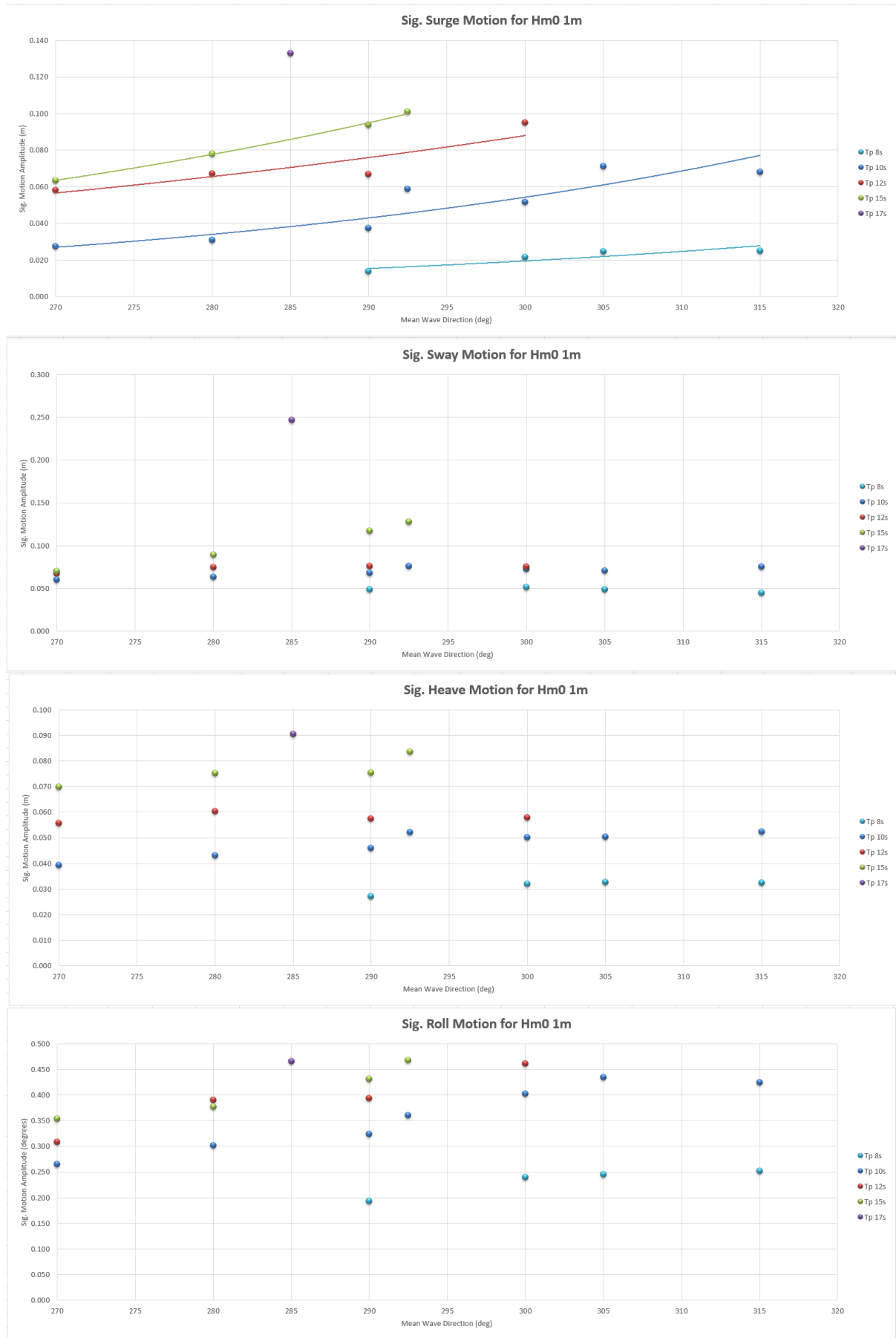
Table C.23: DVRS Datapoints for  $H_{m0}$  3m

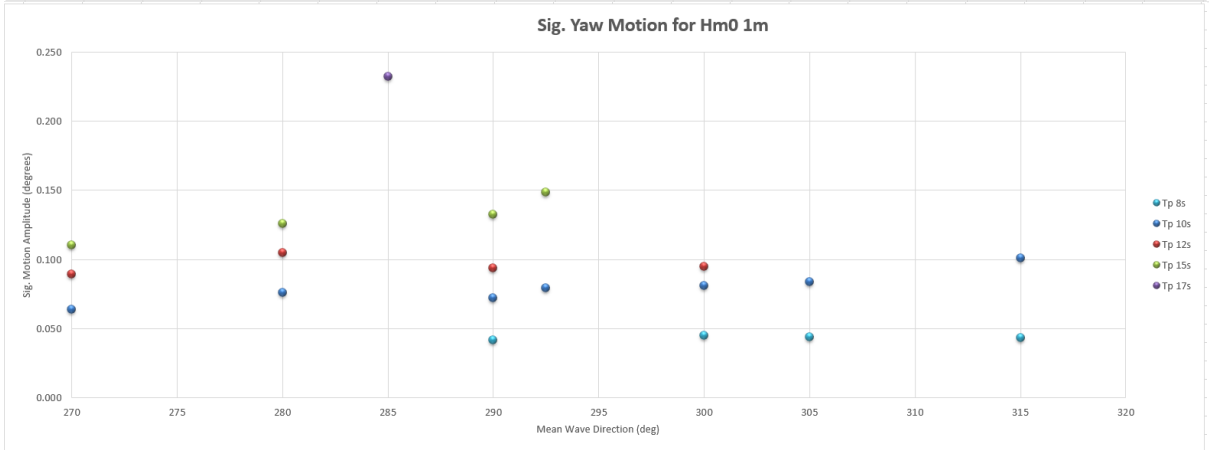
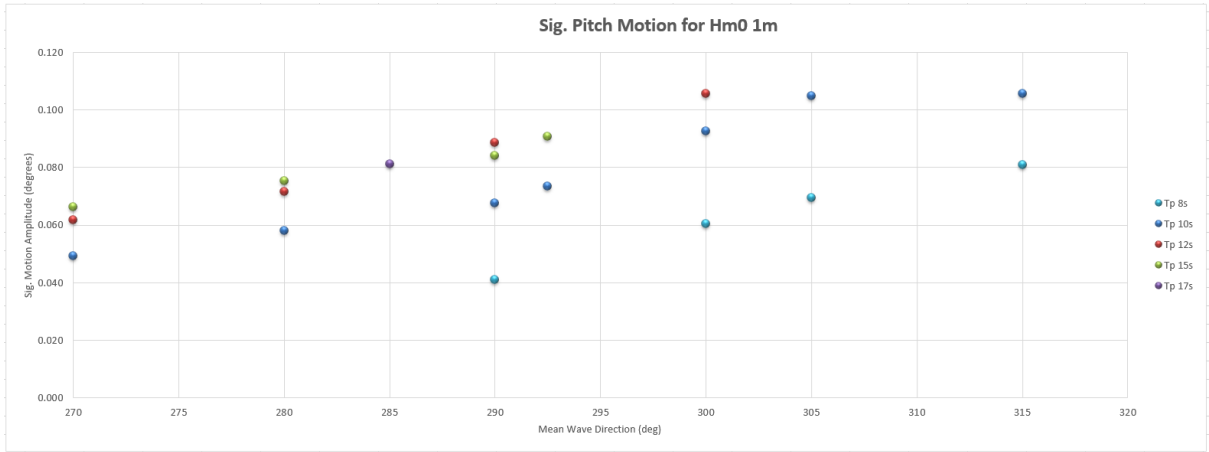
	Hm0 3m																				
	Tp 8s				Tp 10s								Tp 12s				Tp 13s	Tp 15s			
	290	300	305	315	270	280	290	292.5	300	305	315	270	280	290	300	280	270	280	290	292.5	
Surge (m)	0.090	0.115	0.159	0.161	0.089	0.154	0.202	0.222	0.316	0.396	0.515	0.151	0.275	0.346	0.478	0.372	0.480	0.889	0.766	0.884	
Sway (m)	0.094	0.086	0.101	0.089	0.089	0.126	0.133	0.165	0.148	0.145	0.160	0.135	0.208	0.185	0.222	0.210	0.231	0.286	0.426	0.383	
Heave (m)	0.058	0.069	0.074	0.085	0.065	0.085	0.102	0.110	0.118	0.117	0.136	0.103	0.108	0.131	0.165	0.147	0.171	0.211	0.249	0.262	
Roll (deg)	0.344	0.351	0.404	0.409	0.426	0.518	0.596	0.624	0.730	0.795	0.876	0.582	0.714	0.921	1.228	0.980	1.082	1.211	1.380	1.501	
Pitch (deg)	0.123	0.175	0.205	0.241	0.096	0.129	0.176	0.172	0.230	0.267	0.284	0.118	0.151	0.192	0.277	0.181	0.215	0.211	0.254	0.303	
Yaw (deg)	0.090	0.089	0.103	0.094	0.110	0.135	0.141	0.172	0.189	0.176	0.210	0.176	0.233	0.242	0.286	0.277	0.284	0.358	0.423	0.417	

Table C.24: DVRS Datapoints for  $H_{m0}$  4m

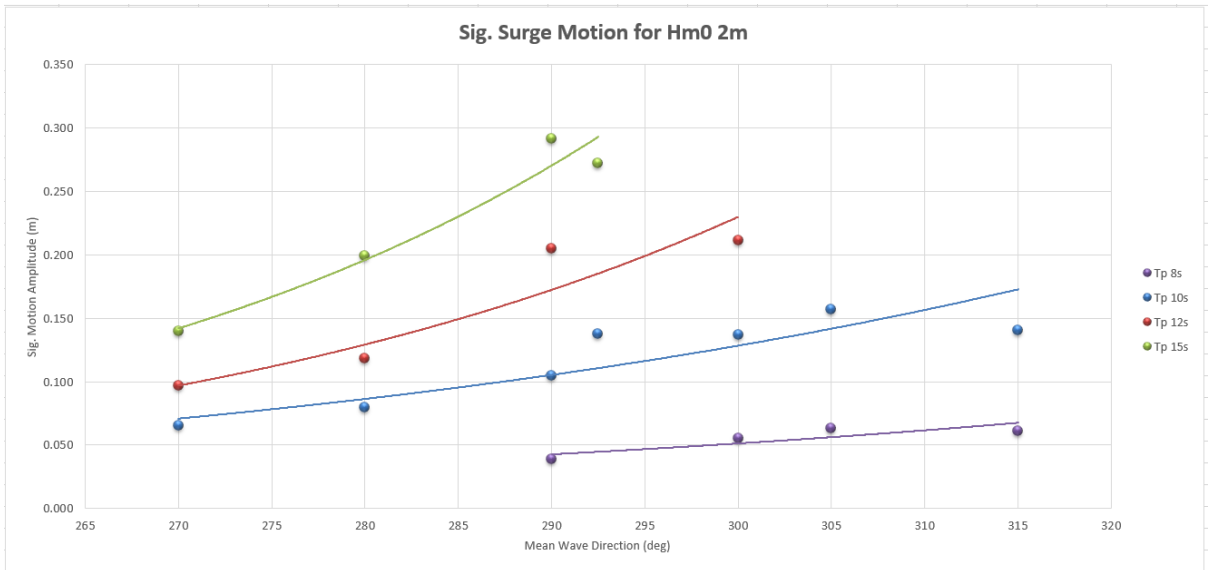
	Hm0 4m										
	Tp 8s		Tp 10s				Tp 12s			Tp 15s	
	290	300	280	290	300	280	290	300	280	290	
Surge (m)	0.200	0.267	0.248	0.496	1.014	0.571	0.924	1.674	1.723	1.305	
Sway (m)	0.114	0.115	0.191	0.222	0.278	0.236	0.367	0.390	0.506	0.589	
Heave (m)	0.078	0.106	0.123	0.149	0.170	0.169	0.211	0.232	0.285	0.339	
Roll (deg)	0.418	0.436	0.750	0.894	0.992	1.048	1.267	1.608	1.657	1.629	
Pitch (deg)	0.167	0.230	0.184	0.235	0.324	0.212	0.267	0.406	0.284	0.327	
Yaw (deg)	0.123	0.127	0.226	0.246	0.325	0.307	0.397	0.436	0.536	0.540	

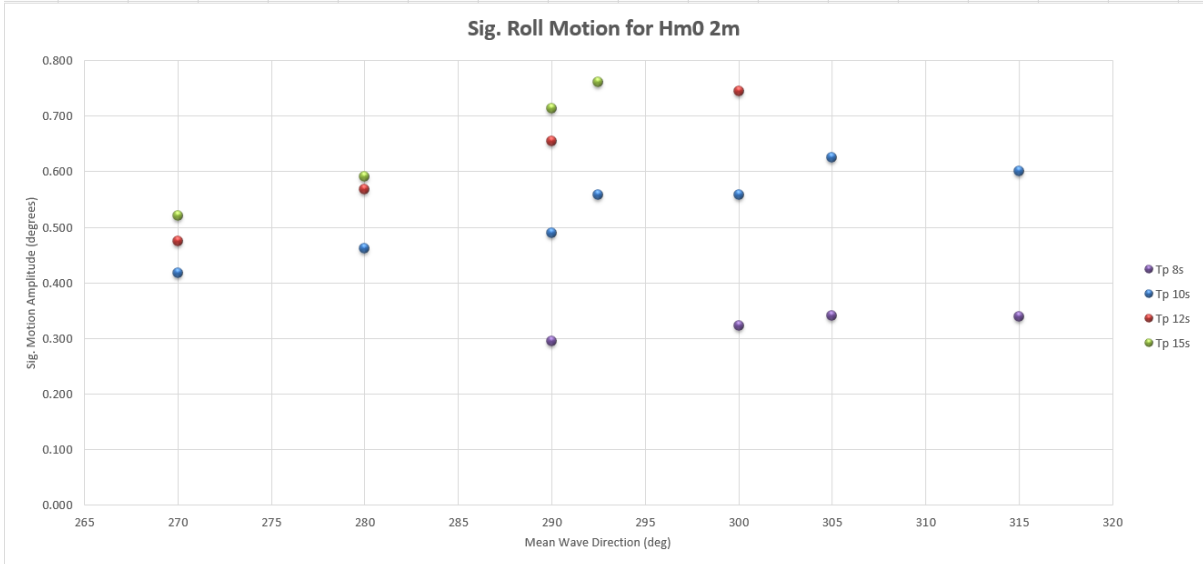
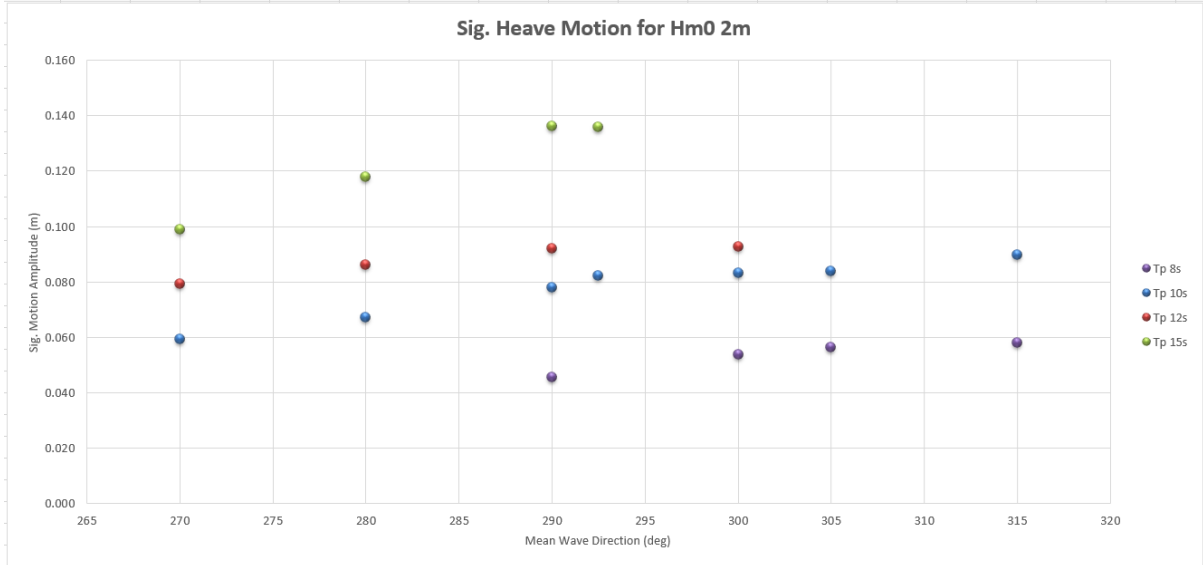
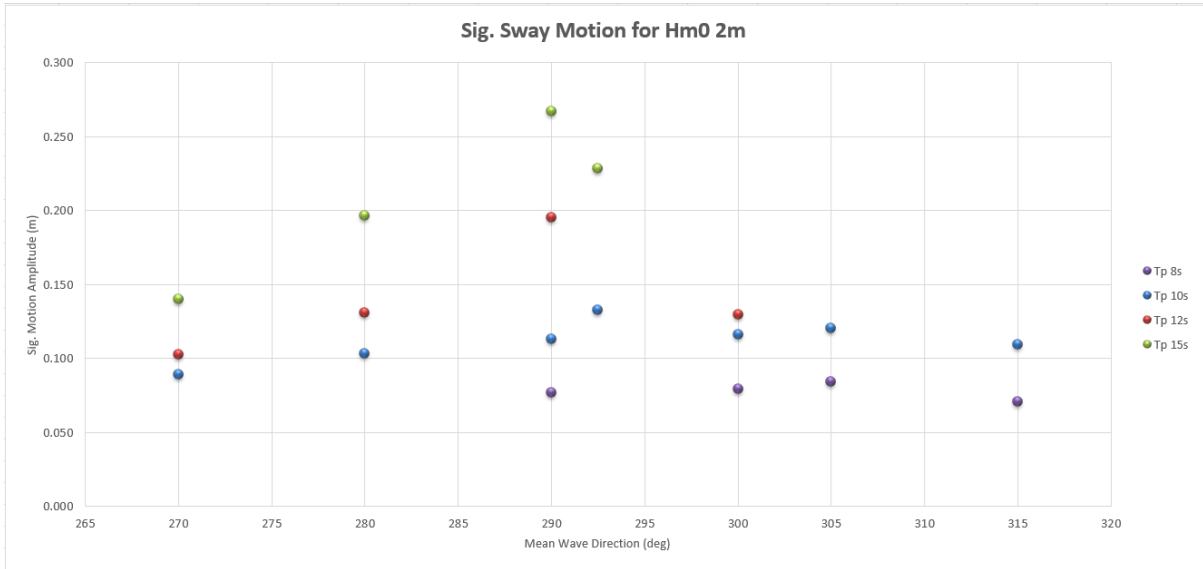
# H<sub>m0</sub> 1m

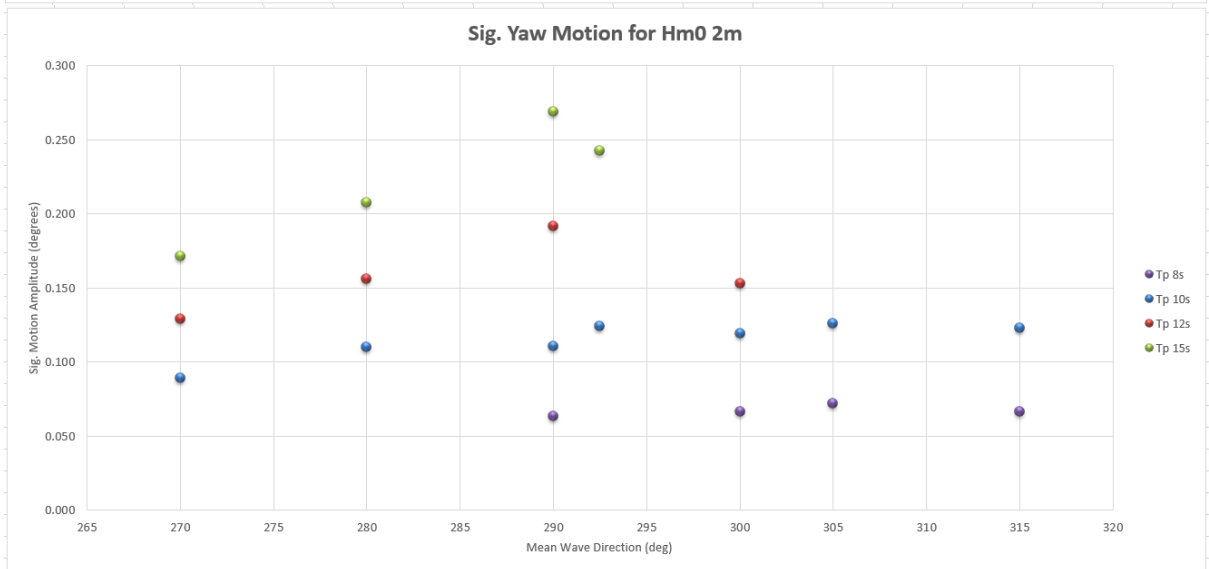
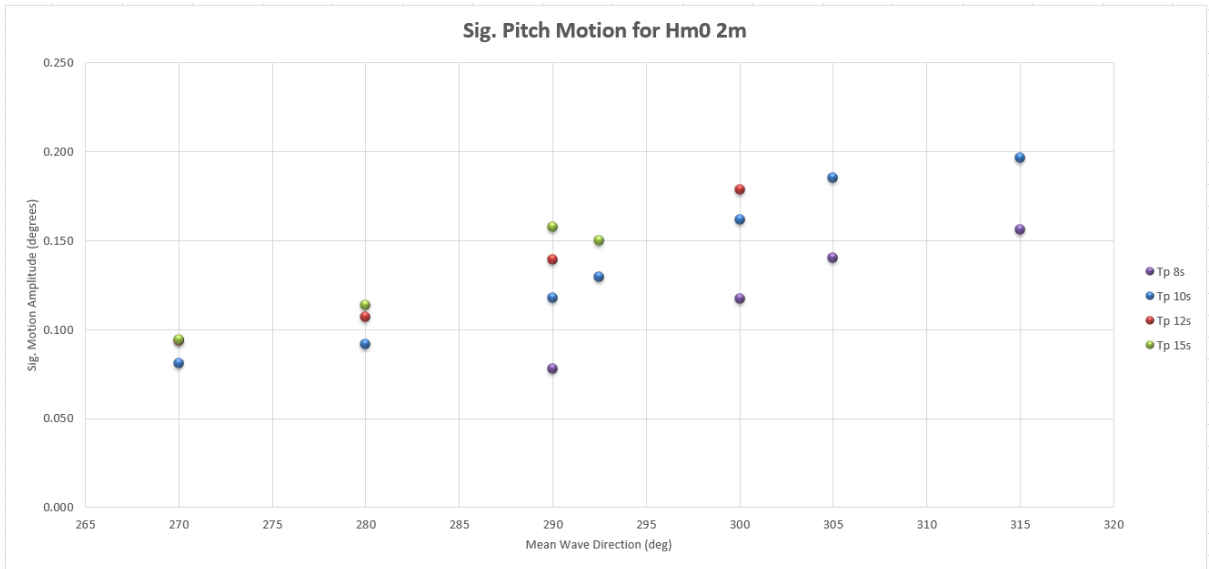




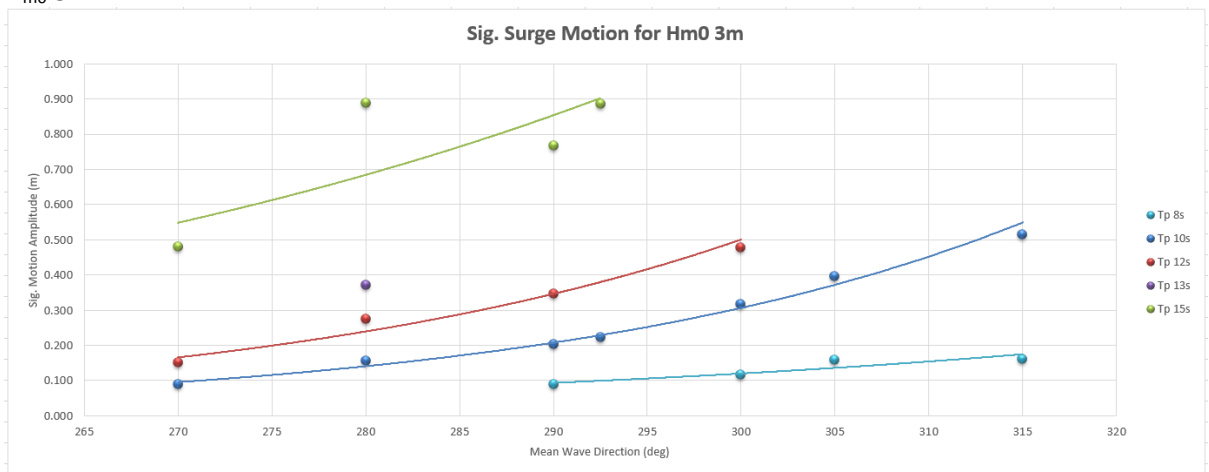
## Hm0 2m

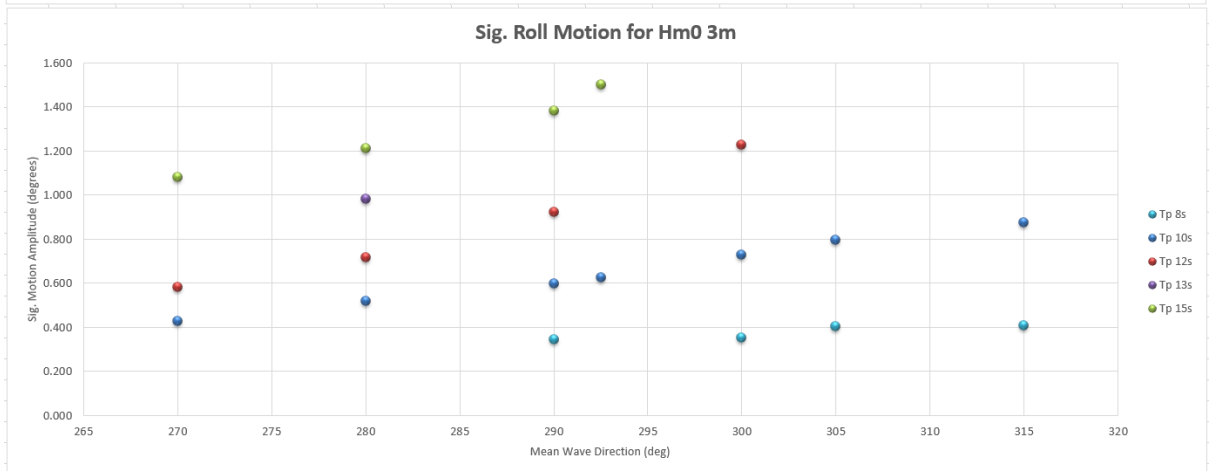
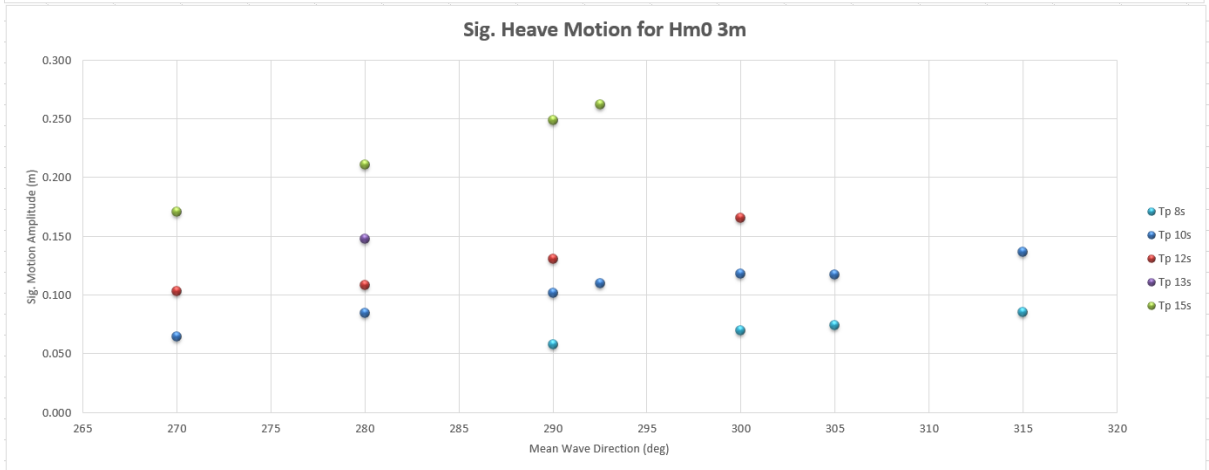
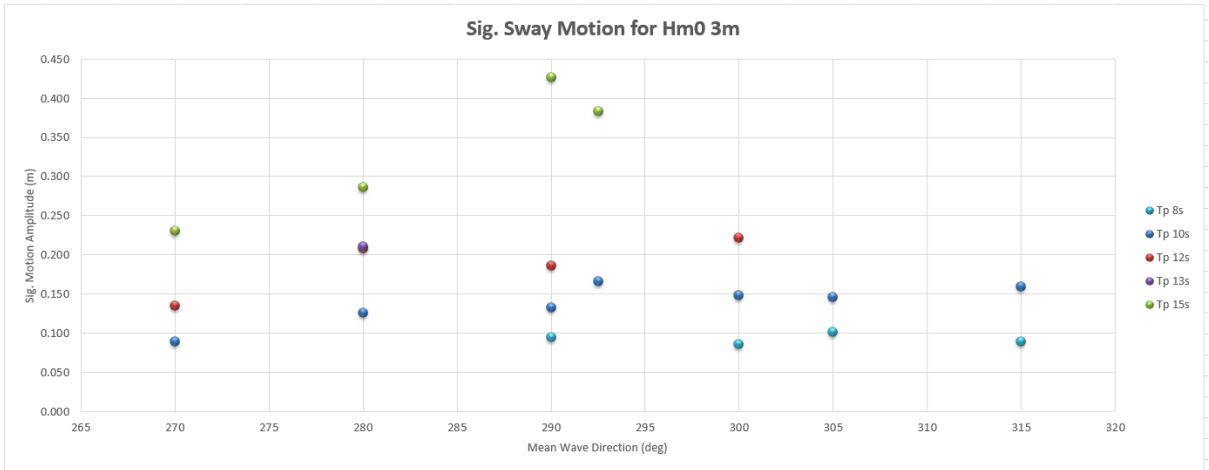


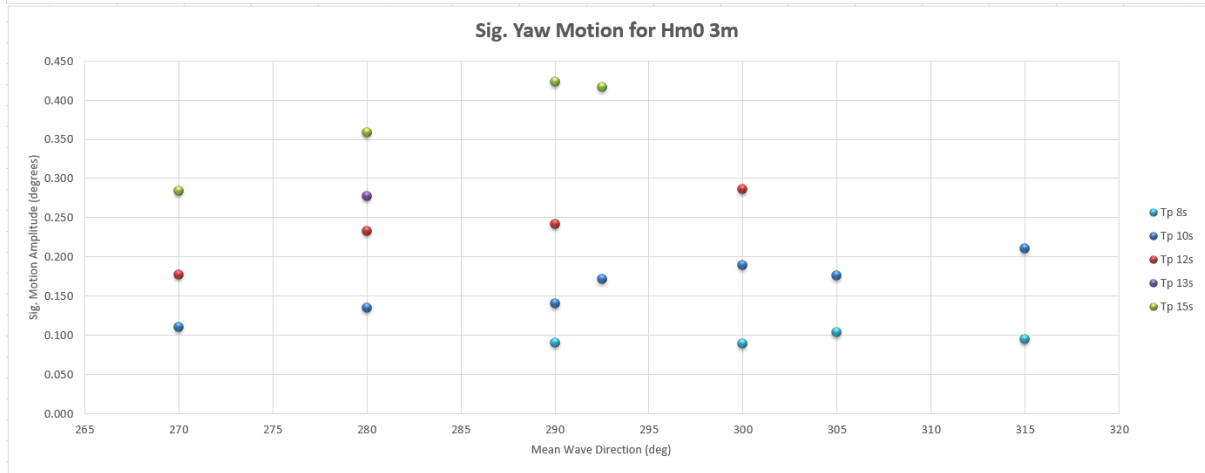
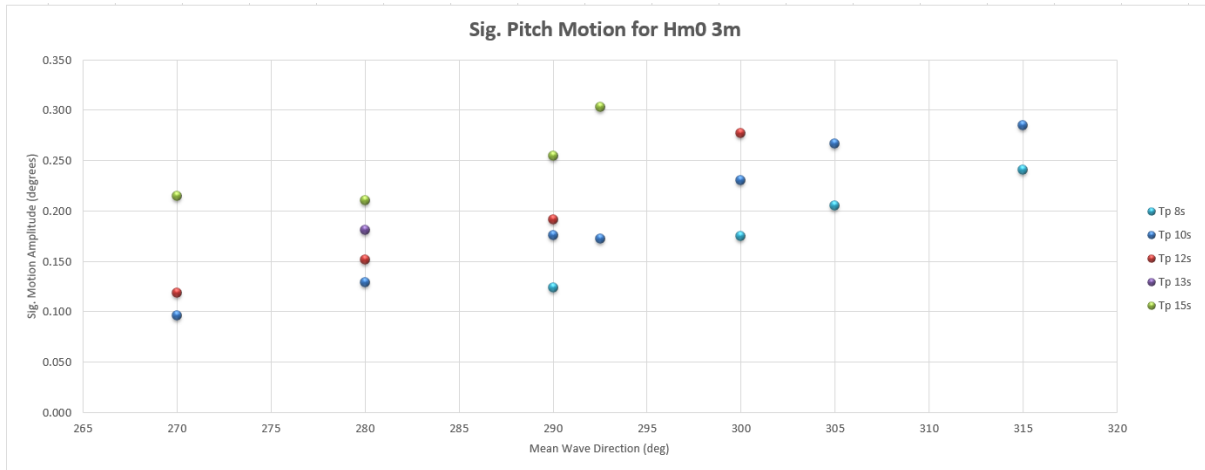




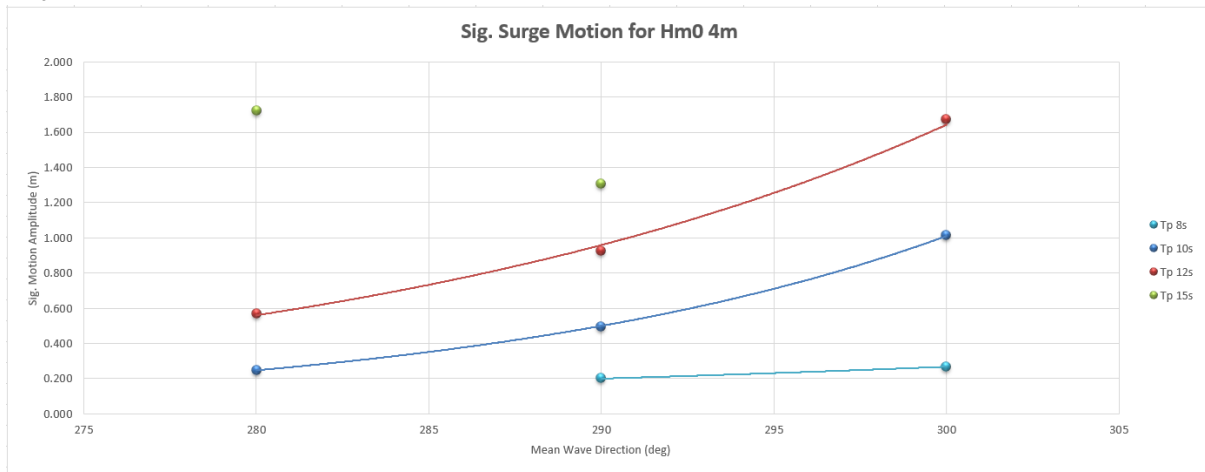
## H<sub>m0</sub> 3m



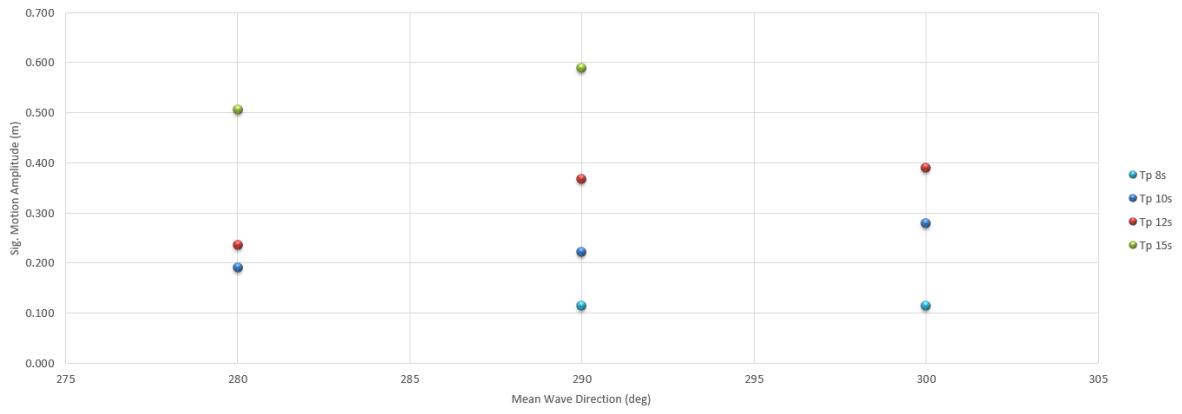




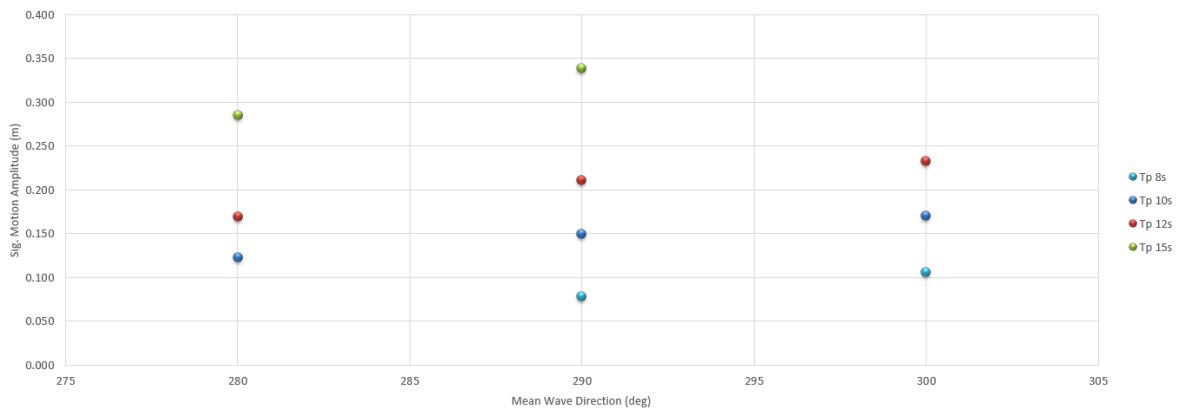
## Hm0 4m



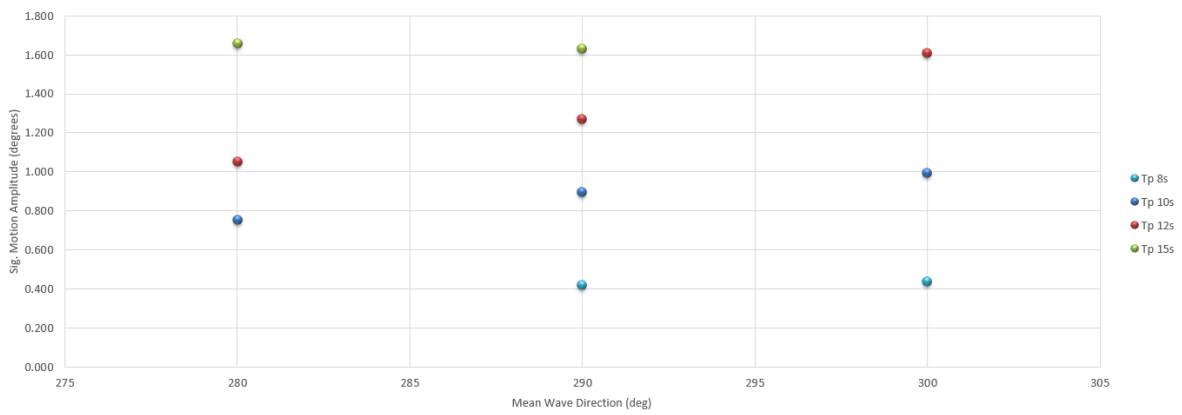
**Sig. Sway Motion for Hm0 4m**



**Sig. Heave Motion for Hm0 4m**

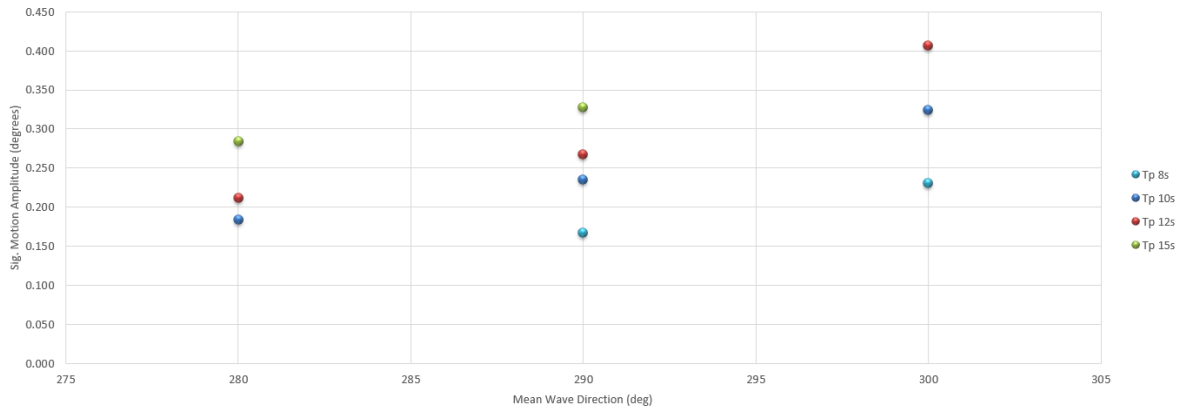


**Sig. Roll Motion for Hm0 4m**





**Sig. Pitch Motion for Hm0 4m**



**Sig. Yaw Motion for Hm0 4m**

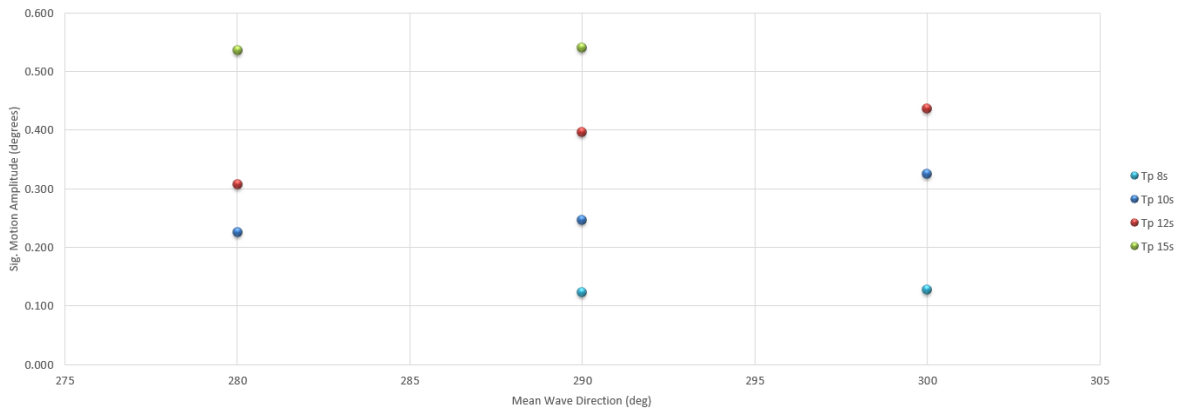


Table C.25: DVRS Datapoints for Mooring Line Forces

MWD		270	280	290	292.5	300	305	315
Hm0	1m							
Tp	8			91.509		90.861	91.035	90.134
	10	95.472	96.043	95.795	101.346	100.284	99.969	107.928
	12	101.164	109.505	101.407		104.373		
	15	101.05	102.775	101.139	105.902			
Hm0	2m							
Tp	8			94.872		95.444	97.554	94.61
	10	104.604	112.011	105.156	119.928	106.68	117.703	109.741
	12	120.345	125.171	117.377		118.233		
	15	112.712	119.996	123.468	120.094			
Hm0	3m							
Tp	8			99.055		94.986	103.898	99.553
	10	105.04	115.965	127.148	126.654	142.671	131.159	166.167
	12	129.253	142.721	151.806		168.423		
	15	145.517	166.188	185.178	199.439			
Hm0	4m							
Tp	8			107.717		110.782		
	10		146.776	171.372		195.385		
	12		172.017	205.307		328.93		
	15		281.422	252.299				

C.6 Ultraline Dyneema Line, Polyamide Tail, Wind 15  $\frac{m}{s}$ , 0 degrees

Table C.26: DVRS Datapoints for  $H_{m0}$  1m

	Hm0 1m																				
	Tp 8s				Tp 10s								Tp 12s				Tp 15s				Tp 17s
	290	300	305	315	270	280	290	292.5	300	305	315	270	280	290	300	270	280	290	292.5	285	
Surge (m)	0.023	0.024	0.029	0.030	0.032	0.038	0.043	0.047	0.052	0.056	0.063	0.051	0.058	0.062	0.082	0.072	0.085	0.102	0.109	0.139	
Sway (m)	0.053	0.055	0.051	0.047	0.062	0.067	0.076	0.091	0.086	0.076	0.100	0.067	0.079	0.082	0.084	0.071	0.095	0.104	0.101	0.193	
Heave (m)	0.026	0.031	0.032	0.031	0.038	0.042	0.045	0.051	0.049	0.049	0.050	0.055	0.060	0.057	0.057	0.070	0.075	0.075	0.083	0.091	
Roll (deg)	0.166	0.190	0.191	0.194	0.244	0.278	0.284	0.312	0.322	0.356	0.355	0.306	0.375	0.377	0.424	0.362	0.381	0.417	0.462	0.430	
Pitch (deg)	0.044	0.065	0.075	0.087	0.050	0.059	0.068	0.074	0.093	0.105	0.108	0.063	0.072	0.089	0.107	0.066	0.076	0.084	0.091	0.081	
Yaw (deg)	0.051	0.055	0.052	0.052	0.072	0.083	0.081	0.094	0.093	0.094	0.118	0.087	0.107	0.098	0.102	0.097	0.112	0.110	0.117	0.167	

Table C.27: DVRS Datapoints for  $H_{m0}$  2m

	Hm0 2m																			
	Tp 8s				Tp 10s								Tp 12s				Tp 15s			
	290	300	305	315	270	280	290	292.5	300	305	315	270	280	290	300	270	280	290	292.5	
Surge (m)	0.048	0.061	0.064	0.073	0.060	0.073	0.096	0.111	0.151	0.141	0.141	0.088	0.116	0.137	0.212	0.141	0.207	0.299	0.280	
Sway (m)	0.088	0.088	0.092	0.085	0.097	0.122	0.136	0.146	0.140	0.132	0.126	0.119	0.152	0.162	0.163	0.128	0.179	0.207	0.202	
Heave (m)	0.045	0.054	0.057	0.059	0.058	0.066	0.077	0.081	0.082	0.083	0.090	0.078	0.085	0.091	0.092	0.099	0.119	0.136	0.137	
Roll (deg)	0.236	0.246	0.276	0.261	0.352	0.410	0.409	0.453	0.467	0.519	0.509	0.453	0.536	0.612	0.663	0.507	0.562	0.633	0.703	
Pitch (deg)	0.083	0.125	0.148	0.164	0.080	0.091	0.119	0.130	0.164	0.187	0.201	0.094	0.108	0.140	0.180	0.095	0.114	0.159	0.151	
Yaw (deg)	0.076	0.080	0.080	0.081	0.099	0.123	0.124	0.132	0.134	0.132	0.136	0.135	0.170	0.165	0.174	0.148	0.182	0.202	0.196	

Table C.28: DVRS Datapoints for  $H_{m0}$  3m

	Hm0 3m																				
	Tp 8s				Tp 10s								Tp 12s				Tp 13s	Tp 15s			
	290	300	305	315	270	280	290	292.5	300	305	315	270	280	290	300	280	270	280	290	292.5	
Surge (m)	0.100	0.146	0.158	0.185	0.077	0.141	0.209	0.214	0.280	0.315	0.433	0.140	0.266	0.321	0.443	0.331	0.374	0.556	0.583	0.698	
Sway (m)	0.095	0.109	0.128	0.115	0.098	0.142	0.138	0.183	0.167	0.164	0.190	0.149	0.167	0.187	0.226	0.215	0.222	0.338	0.344	0.325	
Heave (m)	0.057	0.070	0.075	0.087	0.064	0.083	0.102	0.109	0.119	0.117	0.139	0.103	0.107	0.129	0.166	0.148	0.171	0.209	0.248	0.262	
Roll (deg)	0.281	0.290	0.349	0.345	0.366	0.450	0.498	0.543	0.620	0.667	0.736	0.554	0.659	0.816	1.071	0.856	1.002	1.137	1.275	1.300	
Pitch (deg)	0.131	0.184	0.214	0.250	0.096	0.130	0.178	0.175	0.234	0.271	0.290	0.118	0.152	0.193	0.277	0.181	0.214	0.210	0.255	0.302	
Yaw (deg)	0.093	0.103	0.117	0.111	0.116	0.147	0.150	0.169	0.209	0.194	0.218	0.174	0.203	0.264	0.322	0.305	0.282	0.358	0.369	0.356	

Table C.29: DVRS Datapoints for  $H_{m0}$  4m

	Hm0 4m										
	Tp 8s		Tp 10s				Tp 12s			Tp 15s	
	290	300	280	290	300	280	290	300	280	290	
Surge (m)	0.188	0.263	0.235	0.347	0.630	0.423	0.563	0.809	0.784	0.881	
Sway (m)	0.134	0.147	0.177	0.225	0.246	0.239	0.291	0.288	0.399	0.455	
Heave (m)	0.079	0.107	0.123	0.148	0.167	0.170	0.211	0.233	0.286	0.335	
Roll (deg)	0.376	0.385	0.624	0.752	0.861	0.893	1.109	1.430	1.547	1.460	
Pitch (deg)	0.175	0.239	0.186	0.238	0.329	0.212	0.268	0.405	0.281	0.326	
Yaw (deg)	0.134	0.147	0.224	0.258	0.314	0.320	0.397	0.445	0.419	0.441	

# Hm0 1m

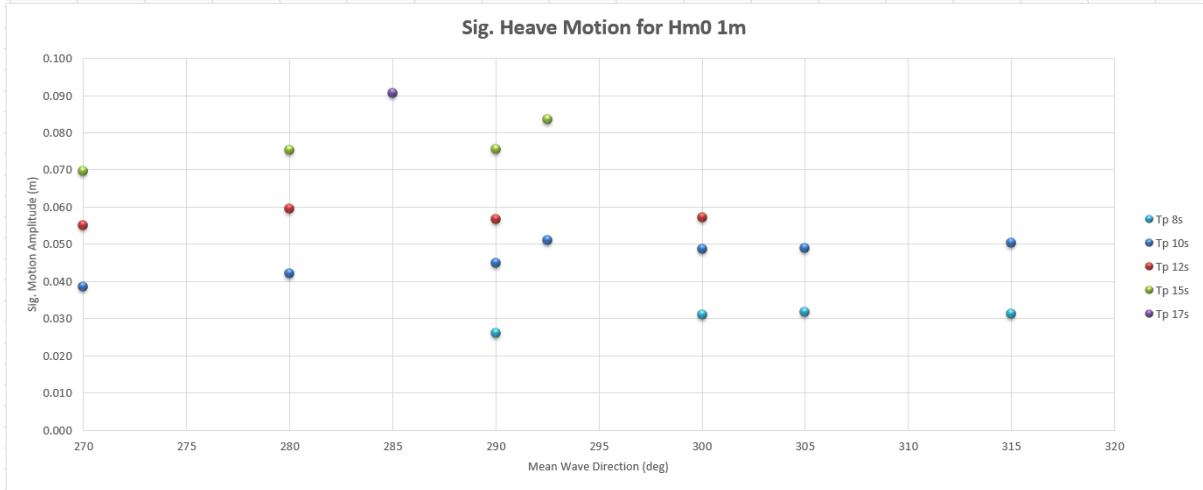
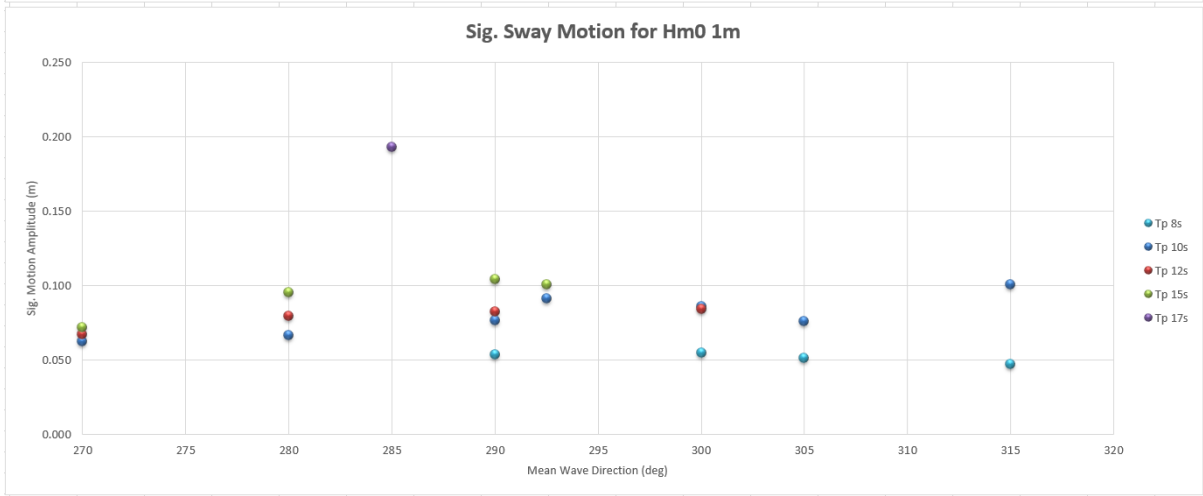
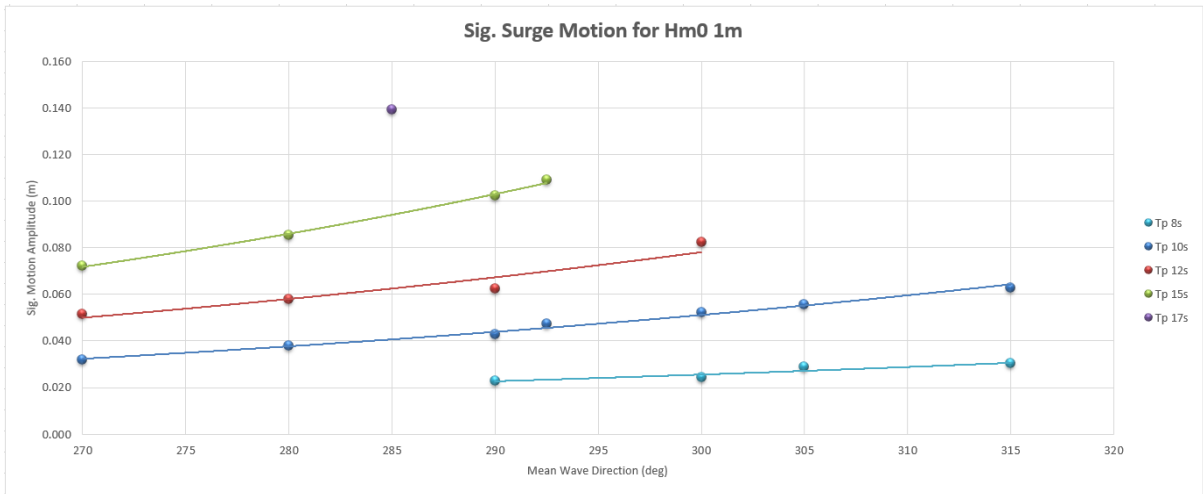


Fig. Roll Motion for Hm0 1m

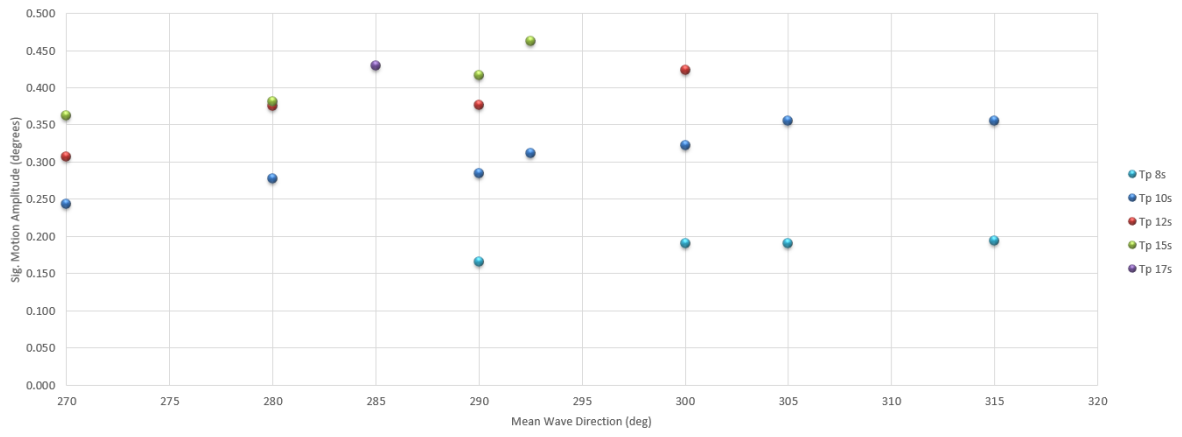


Fig. Pitch Motion for Hm0 1m

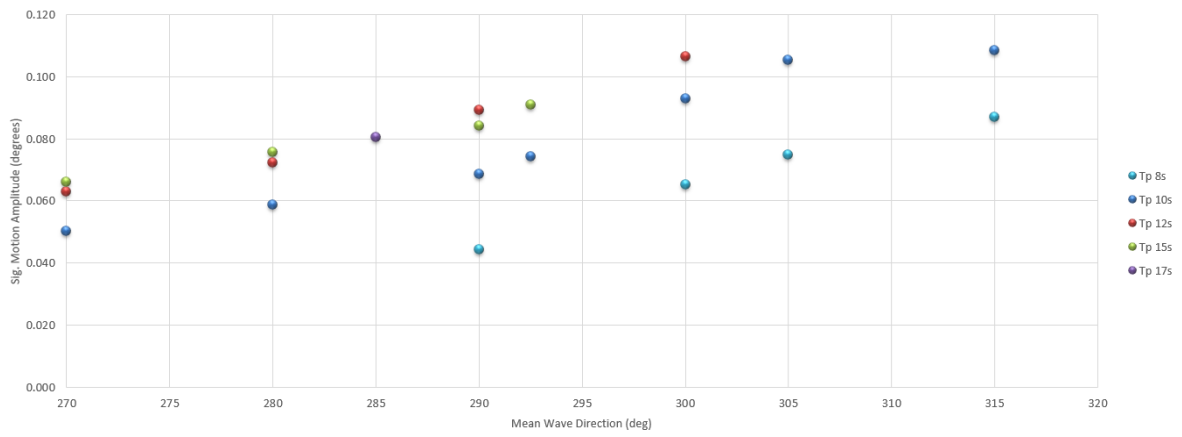
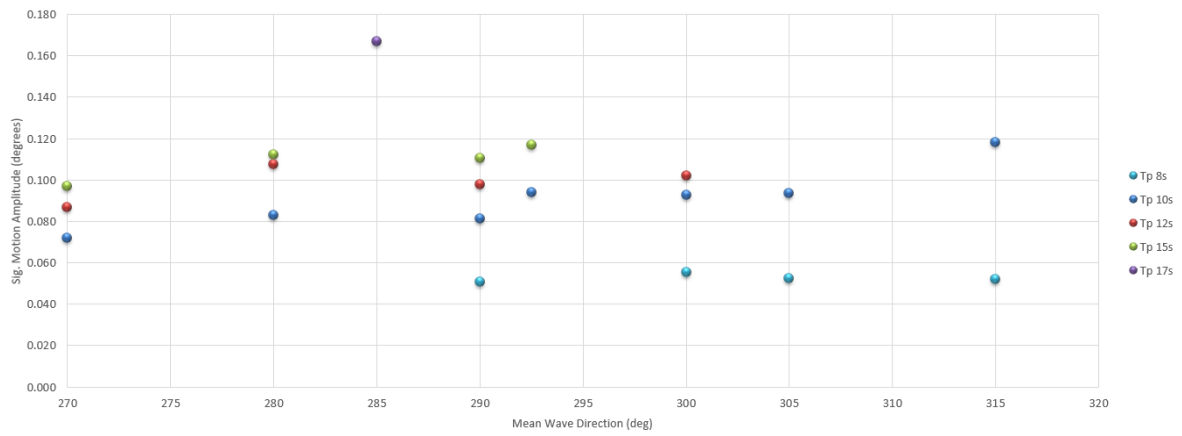
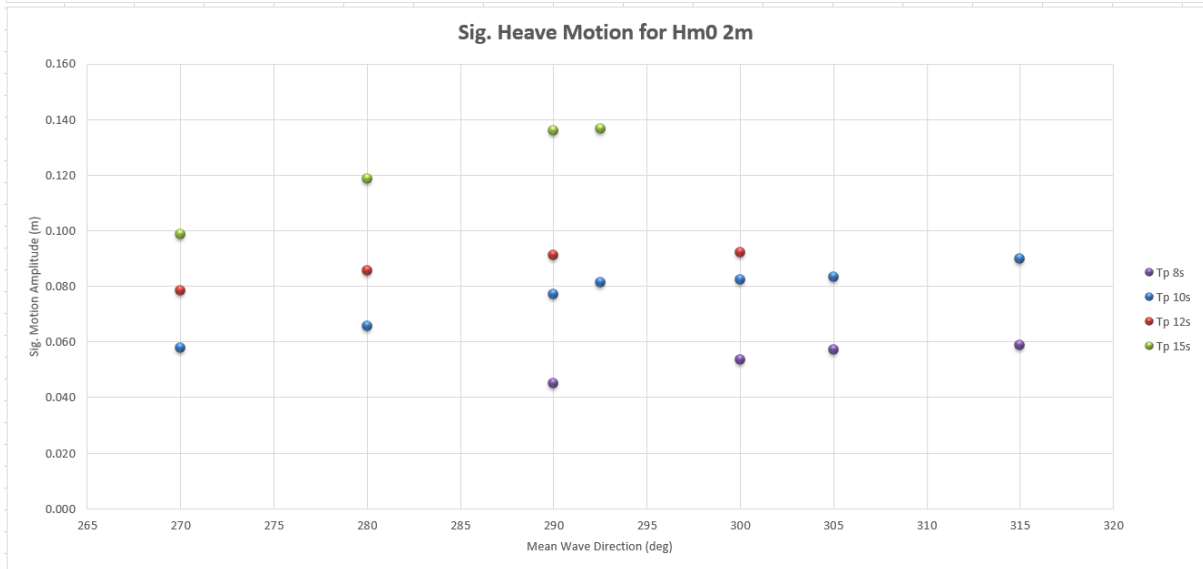
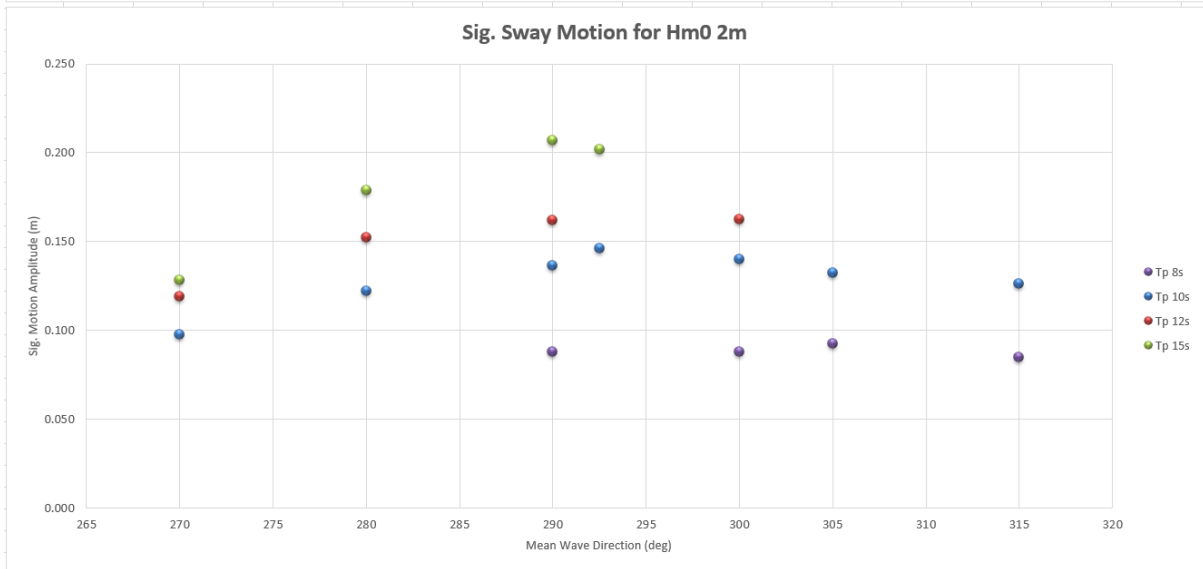
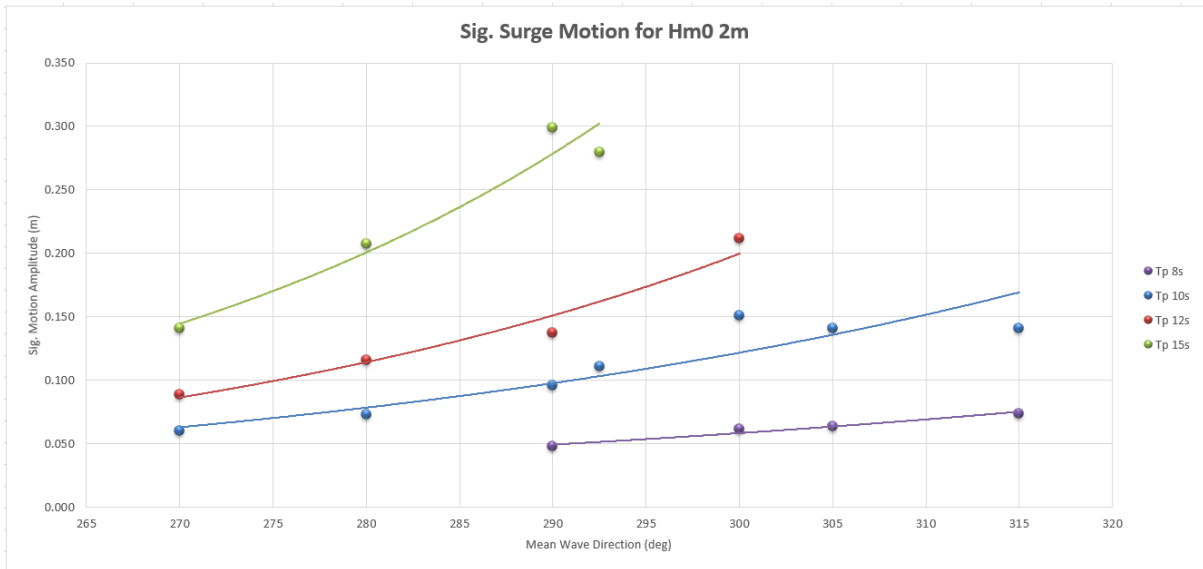
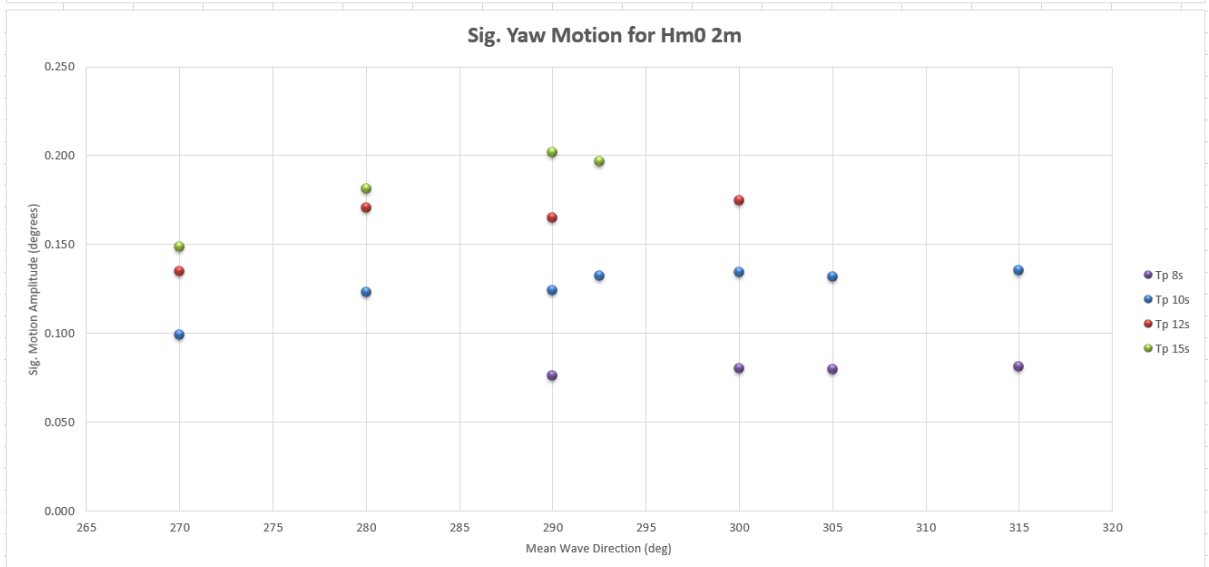
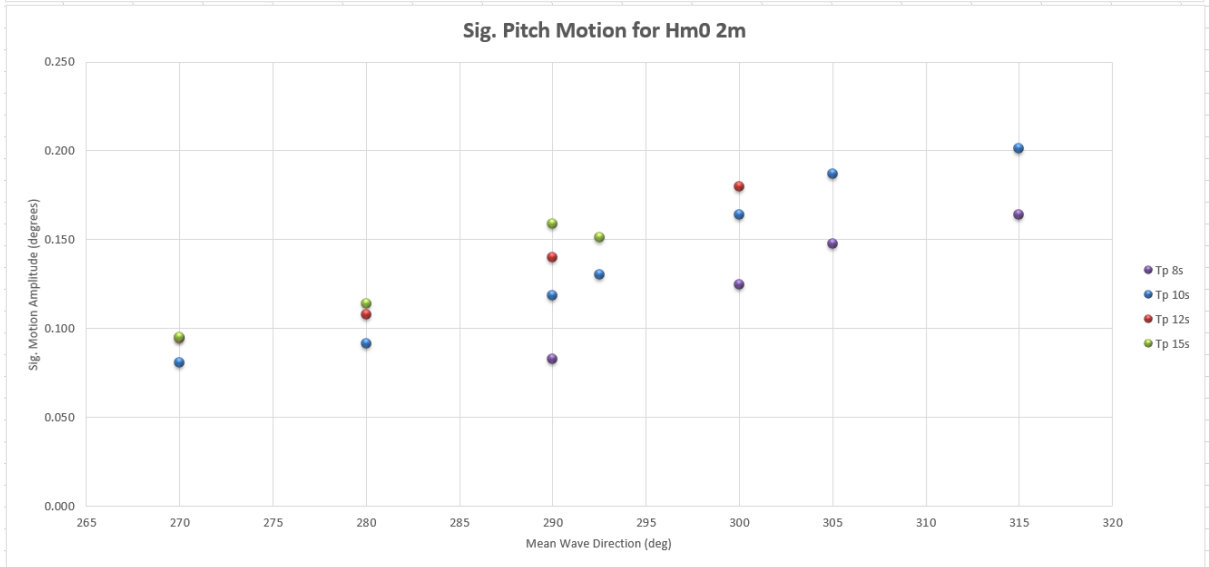
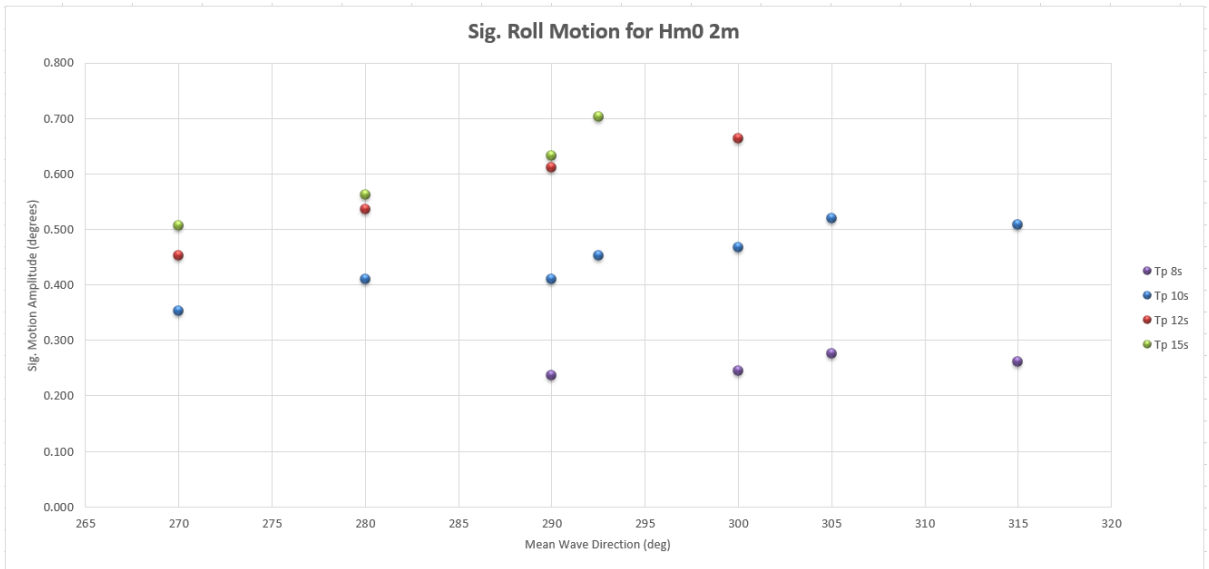


Fig. Yaw Motion for Hm0 1m

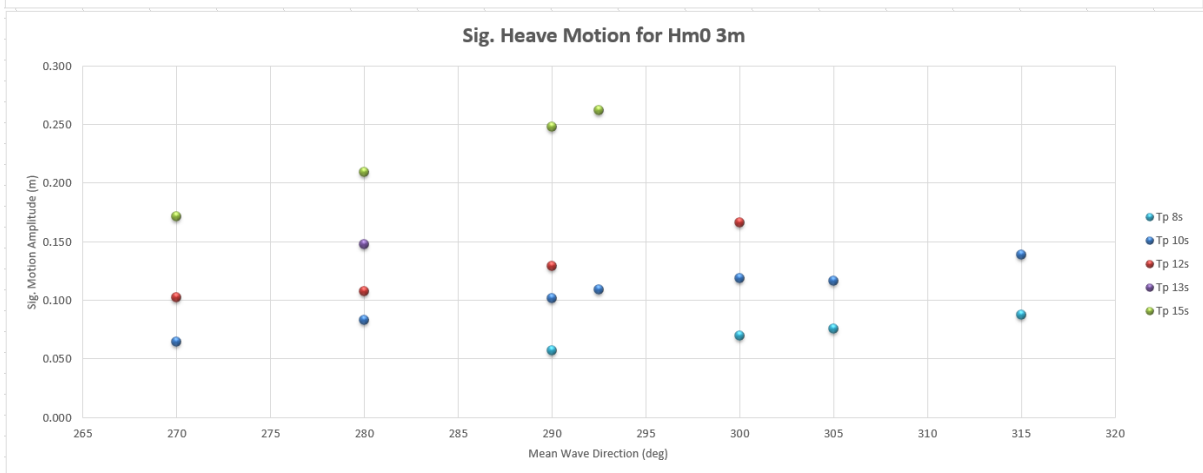
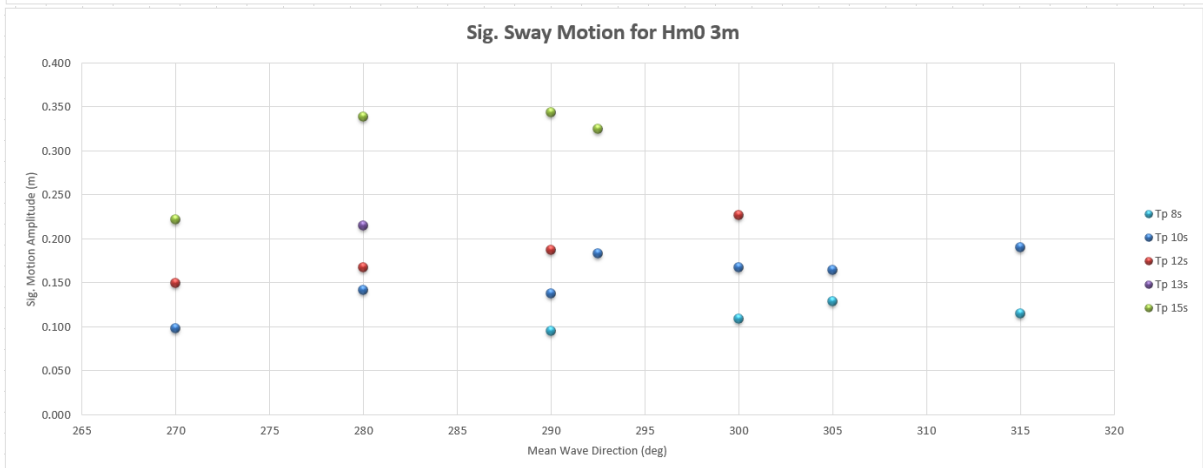
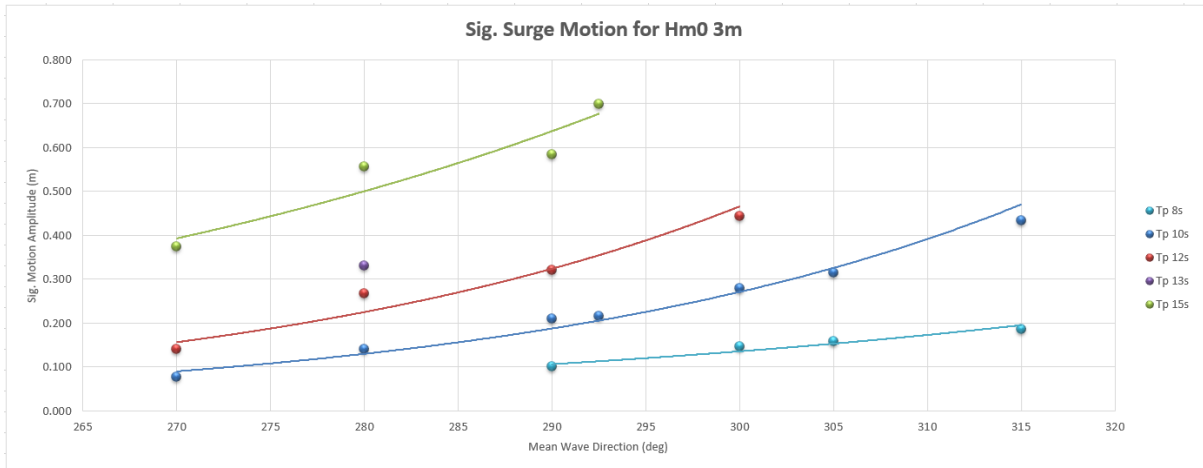


# H<sub>m0</sub> 2m

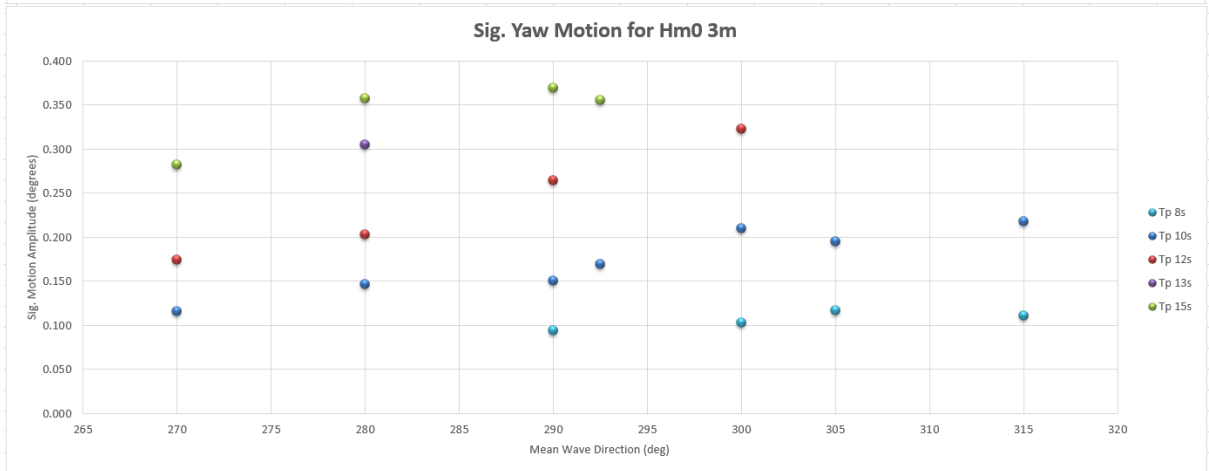
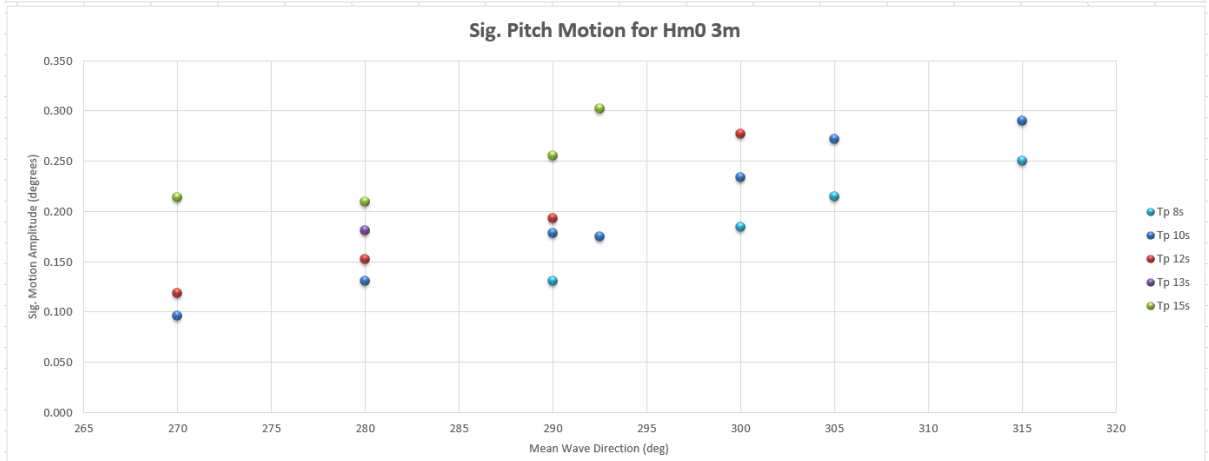
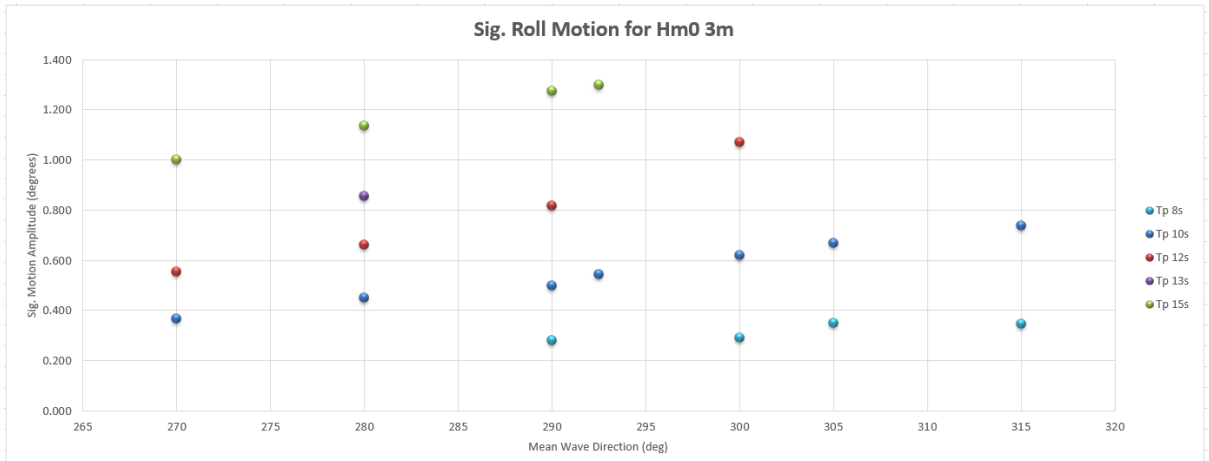




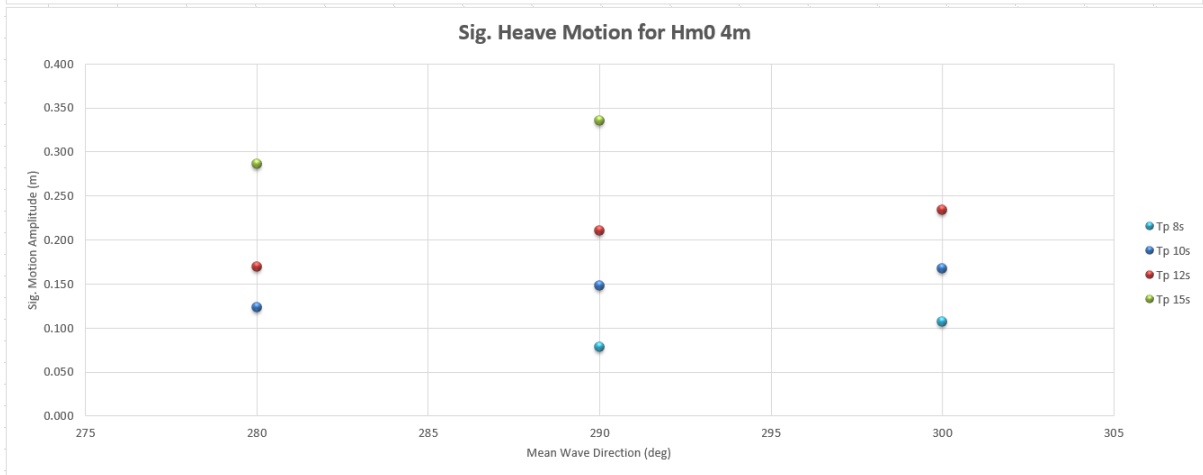
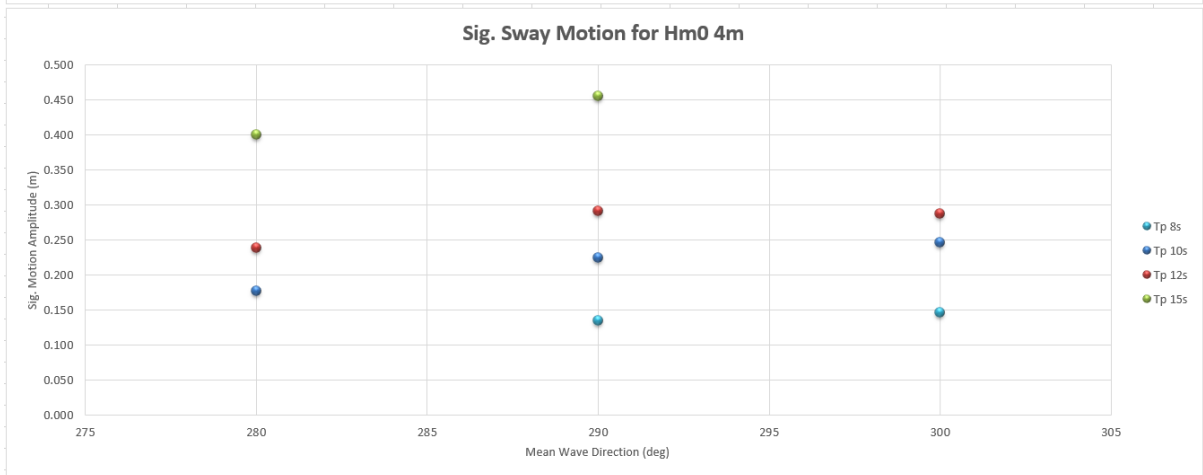
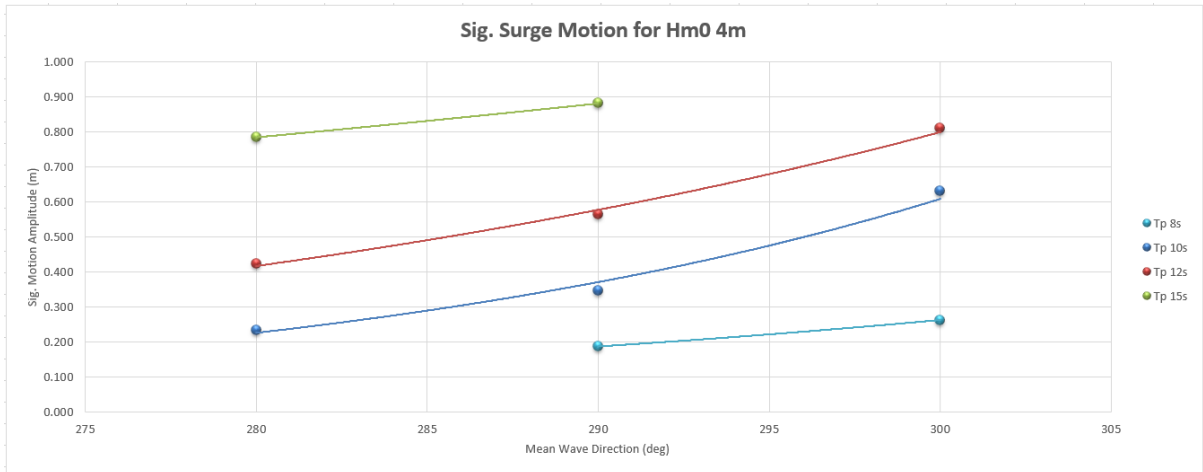
# Hm0 3m



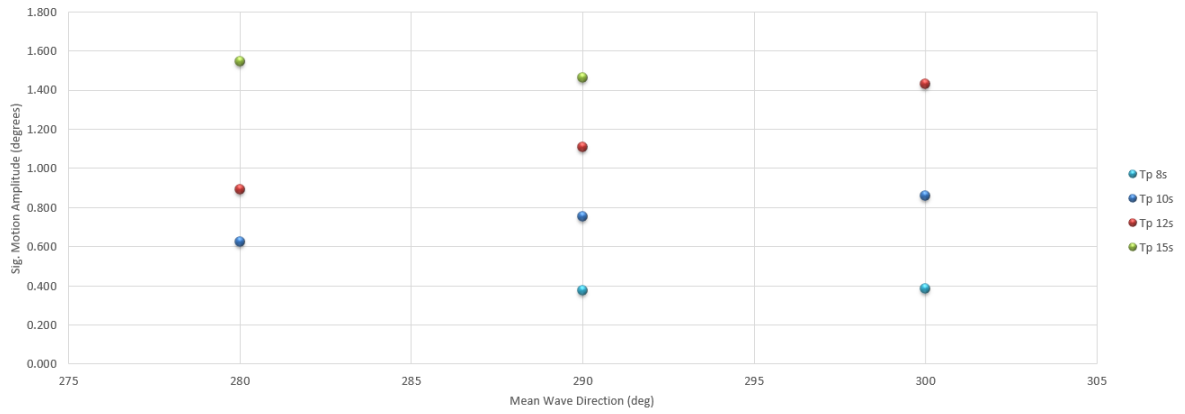




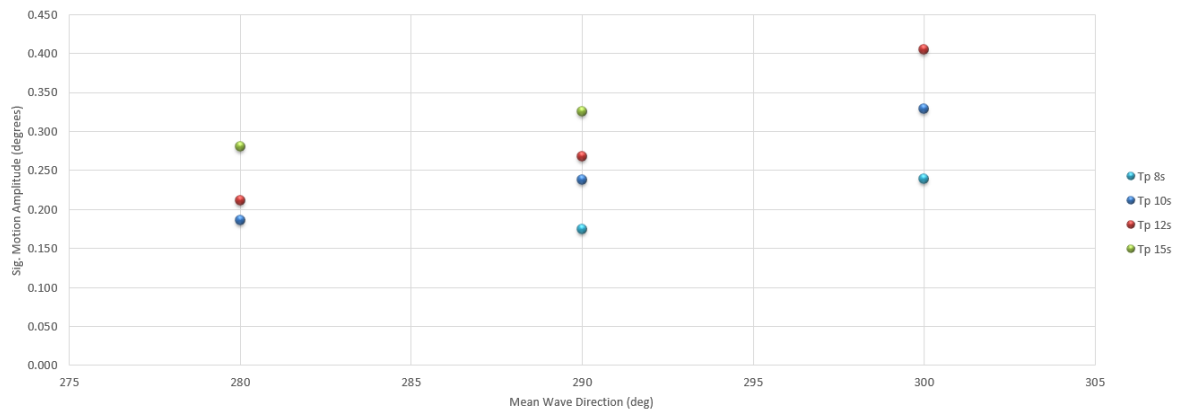
H<sub>m0</sub> 4m



**Sig. Roll Motion for Hm0 4m**



**Sig. Pitch Motion for Hm0 4m**



**Sig. Yaw Motion for Hm0 4m**

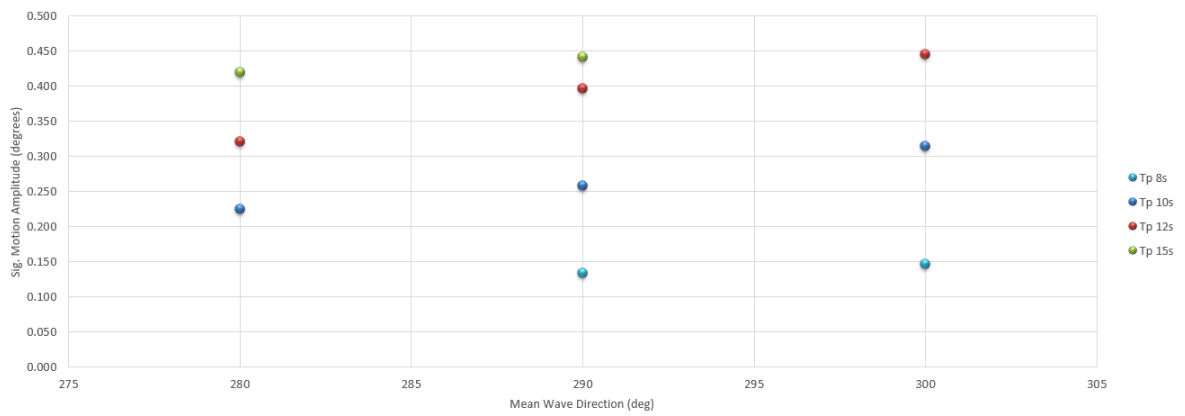


Table C.30: DVRS Datapoints for Mooring Line Forces

MWD		270	280	290	292.5	300	305	315
Hm0	1m							
Tp	8			122.962		123.774	125.094	121.038
	10	140.533	133.125	140.73	145.376	143.944	142.128	143.865
	12	145.346	150.804	151.532		162.636		
	15	151.368	183.421	178.641	192.156			
Hm0	2m							
Tp	8			124.265		133.523	135.034	143.672
	10	155.779	163.202	160.251	177.19	180.947	191.665	183.85
	12	186.836	195.426	194.97		264.793		
	15	196.625	257.434	295.567	412.738			
Hm0	3m							
Tp	8			162.317		179.135	200.179	207.941
	10	149.553	182.932	238.091	225.556	270.559	331.773	407.056
	12	224.238	247.131	339.98		450.441		
	15	411.804	684.154	710.817	963.05			
Hm0	4m							
Tp	8			200.168		243.382		
	10		279.367	342.127		520.982		
	12		378.517	489.809		921.74		
	15		993.676	771.266				

C.7 Polypropylene Line, Polyamide Tail, Wind 15  $\frac{m}{s}$ , 250 degrees

Table C.31: DVRS Datapoints for  $H_{m0}$  1m

	Hm0 1m																			
	Tp 8s				Tp 10s					Tp 12s				Tp 15s				Tp 17s		
	290	300	305	315	270	280	290	292.5	300	305	315	270	280	290	300	270	280	290	292.5	285
Surge (m)	0.013	0.021	0.022	0.022	0.025	0.030	0.030	0.043	0.045	0.055	0.067	0.050	0.056	0.064	0.093	0.073	0.093	0.101	0.126	0.149
Sway (m)	0.054	0.057	0.055	0.049	0.071	0.075	0.077	0.087	0.082	0.080	0.083	0.090	0.098	0.097	0.093	0.109	0.119	0.127	0.132	0.163
Heave (m)	0.028	0.033	0.033	0.033	0.040	0.044	0.046	0.053	0.051	0.052	0.052	0.056	0.061	0.058	0.059	0.071	0.076	0.076	0.084	0.091
Roll (deg)	0.132	0.151	0.146	0.146	0.199	0.212	0.233	0.259	0.261	0.268	0.269	0.268	0.305	0.300	0.322	0.324	0.341	0.353	0.400	0.398
Pitch (deg)	0.034	0.057	0.067	0.079	0.041	0.050	0.060	0.067	0.085	0.098	0.102	0.057	0.067	0.084	0.101	0.064	0.073	0.082	0.089	0.081
Yaw (deg)	0.041	0.044	0.043	0.043	0.067	0.079	0.075	0.076	0.076	0.082	0.102	0.106	0.116	0.113	0.109	0.154	0.160	0.157	0.170	0.190

Table C.32: DVRS Datapoints for  $H_{m0}$  2m

	Hm0 2m																		
	Tp 8s				Tp 10s					Tp 12s				Tp 15s					
	290	300	305	315	270	280	290	292.5	300	305	315	270	280	290	300	270	280	290	292.5
Surge (m)	0.037	0.061	0.055	0.065	0.049	0.074	0.081	0.102	0.115	0.127	0.127	0.092	0.115	0.189	0.196	0.142	0.221	0.291	0.304
Sway (m)	0.081	0.085	0.086	0.075	0.103	0.112	0.116	0.130	0.121	0.119	0.105	0.133	0.141	0.150	0.135	0.148	0.170	0.186	0.198
Heave (m)	0.046	0.055	0.058	0.059	0.061	0.068	0.079	0.084	0.085	0.085	0.091	0.080	0.087	0.093	0.094	0.100	0.119	0.136	0.136
Roll (deg)	0.210	0.227	0.250	0.233	0.309	0.340	0.352	0.395	0.383	0.409	0.403	0.404	0.467	0.476	0.529	0.443	0.522	0.555	0.615
Pitch (deg)	0.075	0.118	0.142	0.158	0.072	0.084	0.113	0.125	0.158	0.182	0.196	0.091	0.104	0.137	0.175	0.094	0.113	0.157	0.149
Yaw (deg)	0.055	0.056	0.057	0.059	0.088	0.102	0.099	0.102	0.098	0.102	0.105	0.152	0.156	0.161	0.146	0.204	0.228	0.263	0.253

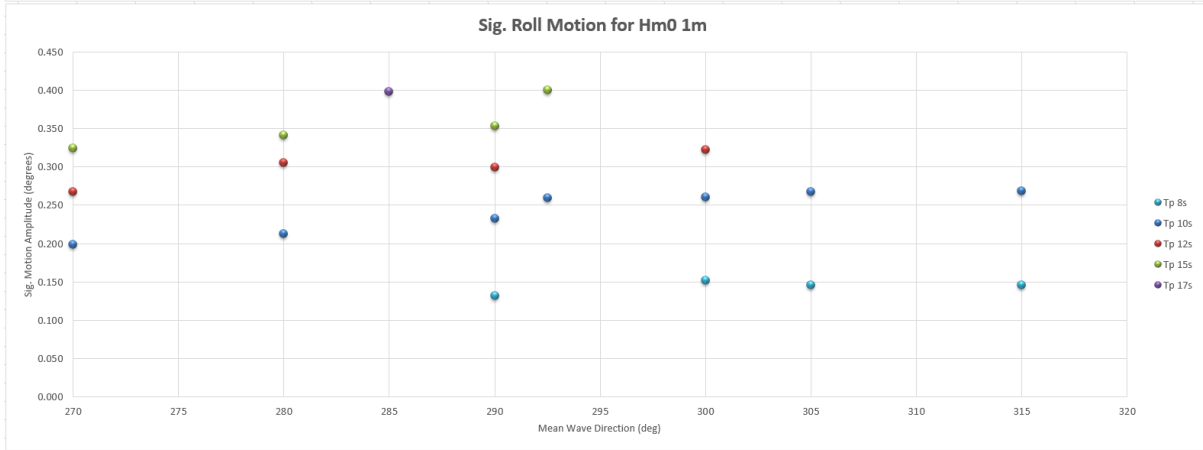
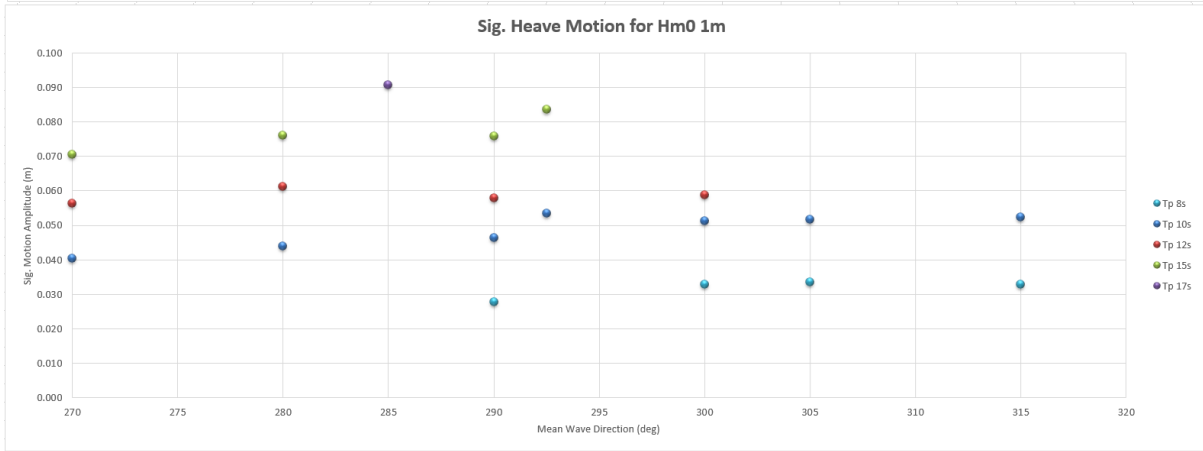
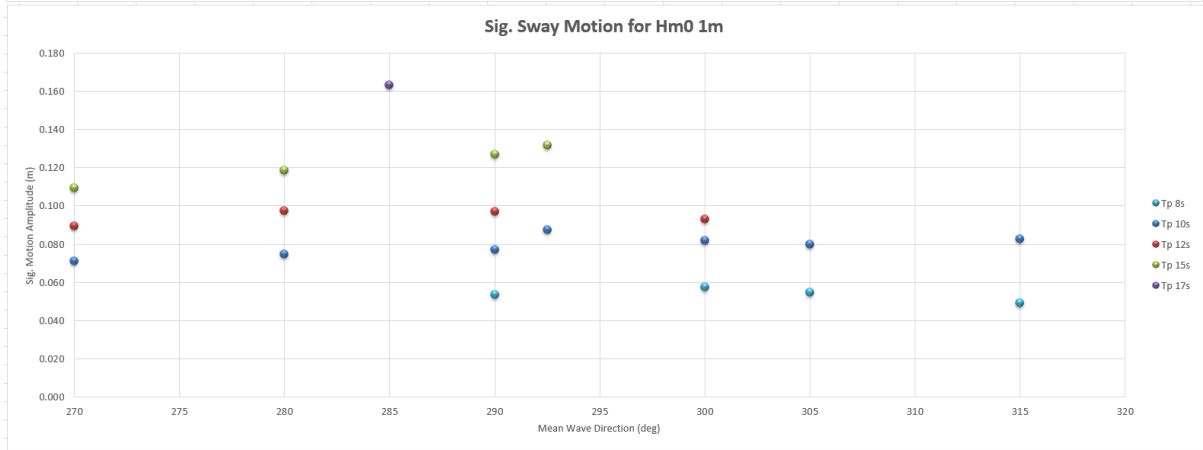
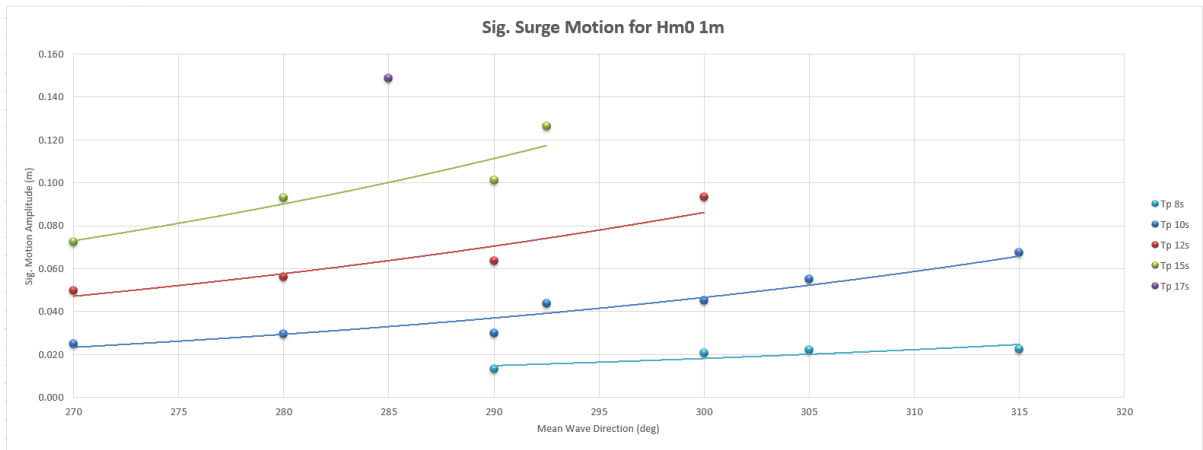
Table C.33: DVRS Datapoints for  $H_{m0}$  3m

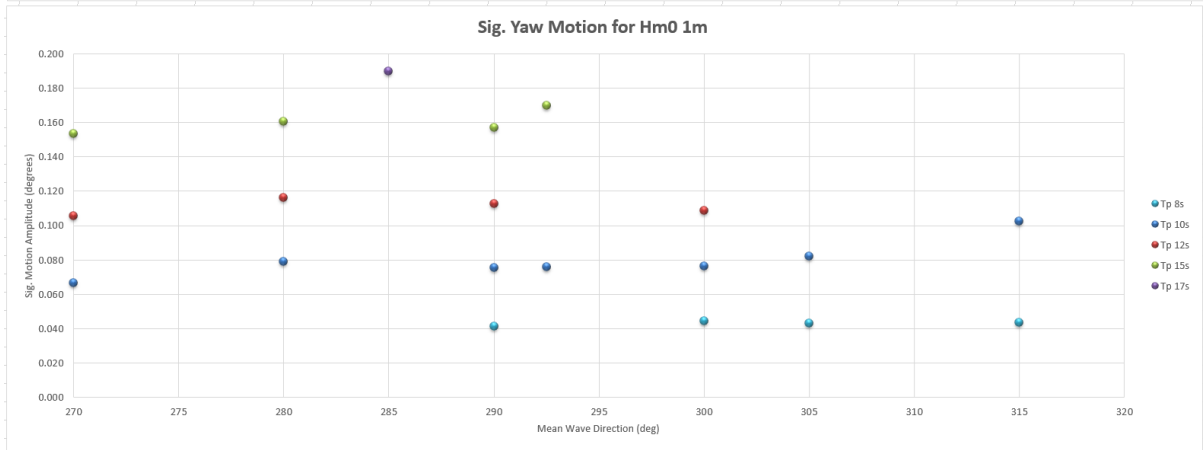
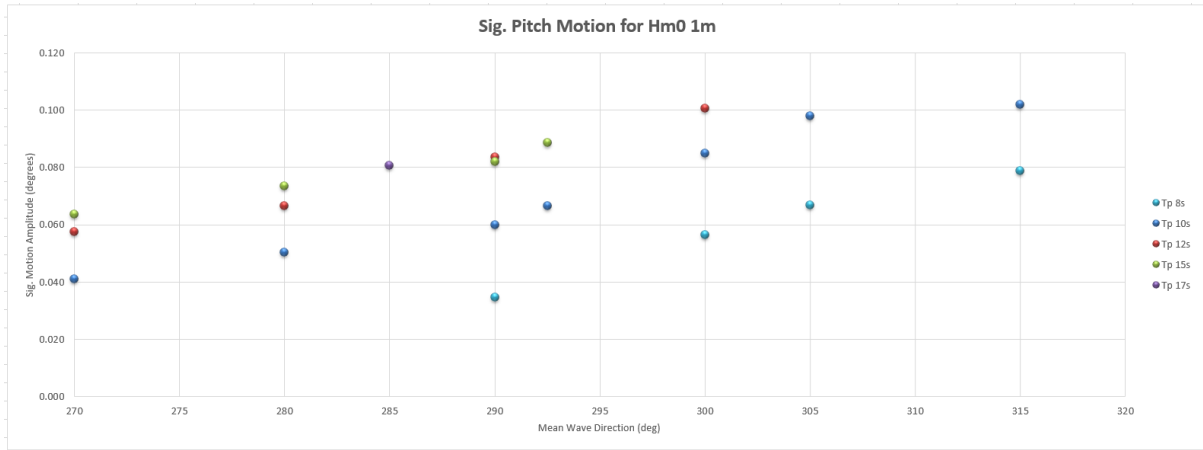
	Hm0 3m																			
	Tp 8s				Tp 10s					Tp 12s				Tp 13s	Tp 15s					
	290	300	305	315	270	280	290	292.5	300	305	315	270	280	290	300	280	270	280	290	292.5
Surge (m)	0.085	0.103	0.133	0.139	0.064	0.103	0.186	0.175	0.246	0.287	0.383	0.155	0.205	0.321	0.446	0.335	0.451	0.763	0.800	0.942
Sway (m)	0.089	0.085	0.085	0.084	0.094	0.115	0.132	0.133	0.125	0.123	0.123	0.141	0.160	0.191	0.241	0.247	0.308	0.347	0.416	0.369
Heave (m)	0.057	0.069	0.074	0.086	0.066	0.085	0.103	0.111	0.120	0.117	0.138	0.104	0.108	0.131	0.165	0.150	0.172	0.210	0.248	0.261
Roll (deg)	0.253	0.269	0.298	0.295	0.300	0.386	0.441	0.458	0.536	0.529	0.622	0.446	0.521	0.695	0.890	0.741	0.875	1.054	1.296	1.364
Pitch (deg)	0.125	0.178	0.208	0.245	0.088	0.125	0.174	0.170	0.229	0.266	0.285	0.114	0.148	0.189	0.275	0.179	0.216	0.212	0.257	0.305
Yaw (deg)	0.072	0.077	0.075	0.076	0.109	0.121	0.125	0.128	0.172	0.158	0.166	0.184	0.193	0.246	0.290	0.318	0.373	0.417	0.486	0.460

Table C.34: DVRS Datapoints for  $H_{m0}$  4m

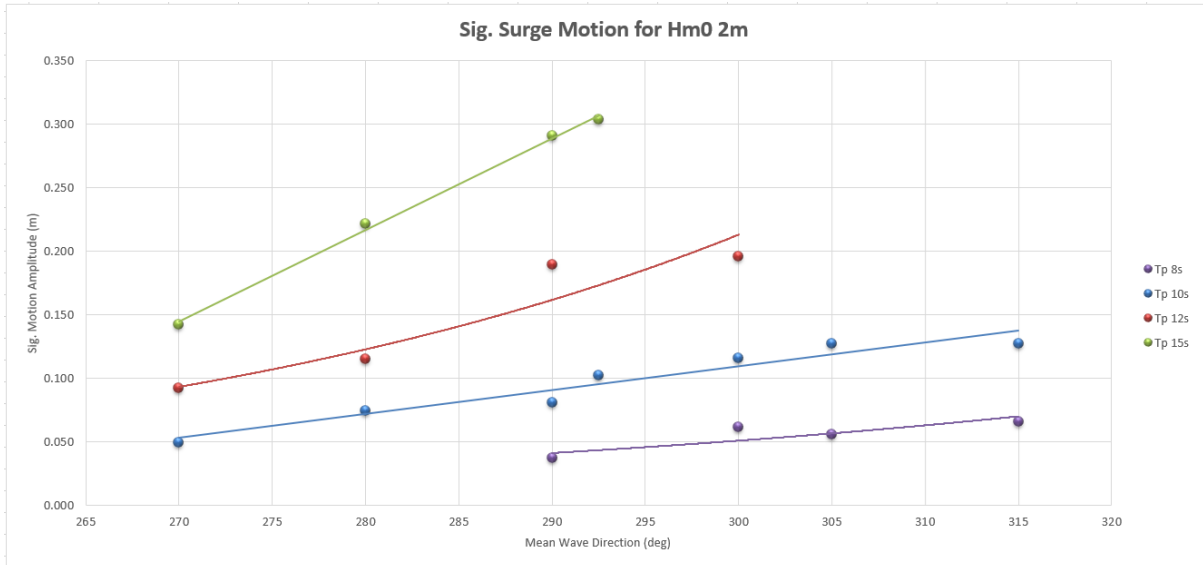
	Hm0 4m									
	Tp 8s		Tp 10s			Tp 12s		Tp 15s		
	290	300	280	290	300	280	290	300	280	290
Surge (m)	0.163	0.211	0.190	0.382	0.742	0.549	0.709	1.152	1.452	1.184
Sway (m)	0.092	0.092	0.154	0.184	0.185	0.263	0.290	0.300	0.504	0.541
Heave (m)	0.078	0.105	0.125	0.150	0.169	0.170	0.213	0.234	0.285	0.336
Roll (deg)	0.299	0.359	0.550	0.647	0.679	0.785	0.960	1.119	1.465	1.568
Pitch (deg)	0.168	0.234	0.179	0.233	0.325	0.208	0.266	0.404	0.286	0.330
Yaw (deg)	0.095	0.093	0.189	0.202	0.232	0.325	0.375	0.409	0.538	0.548

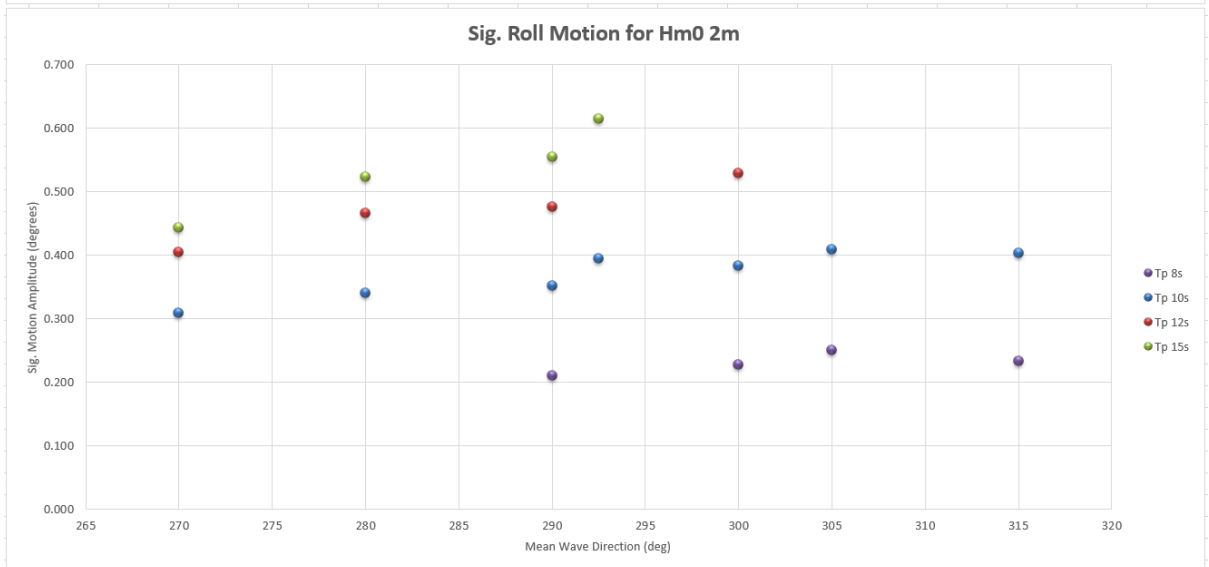
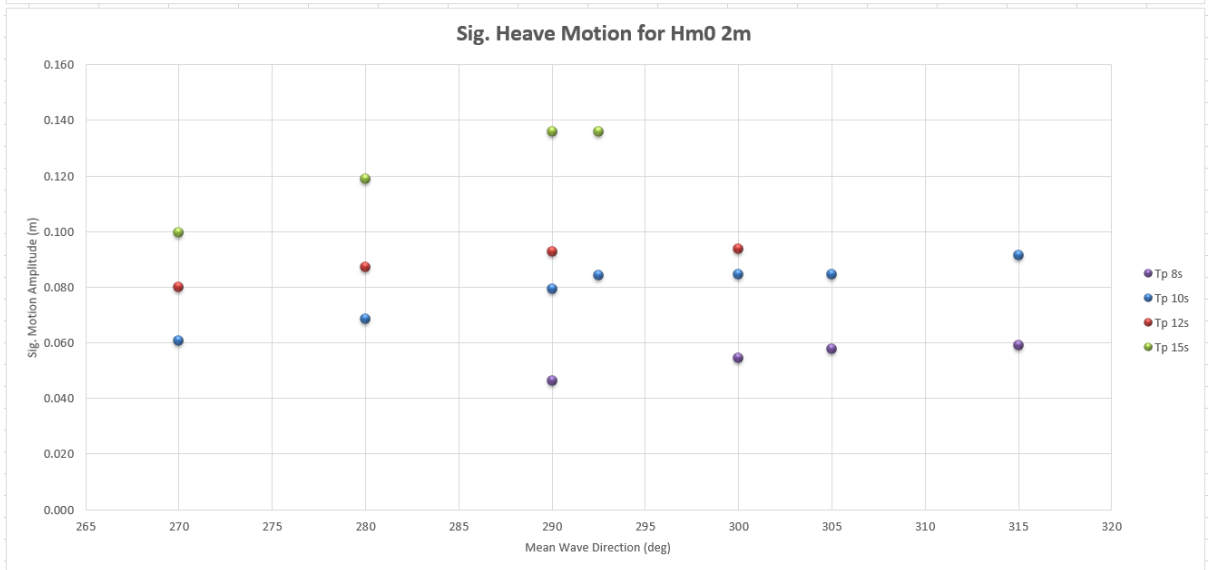
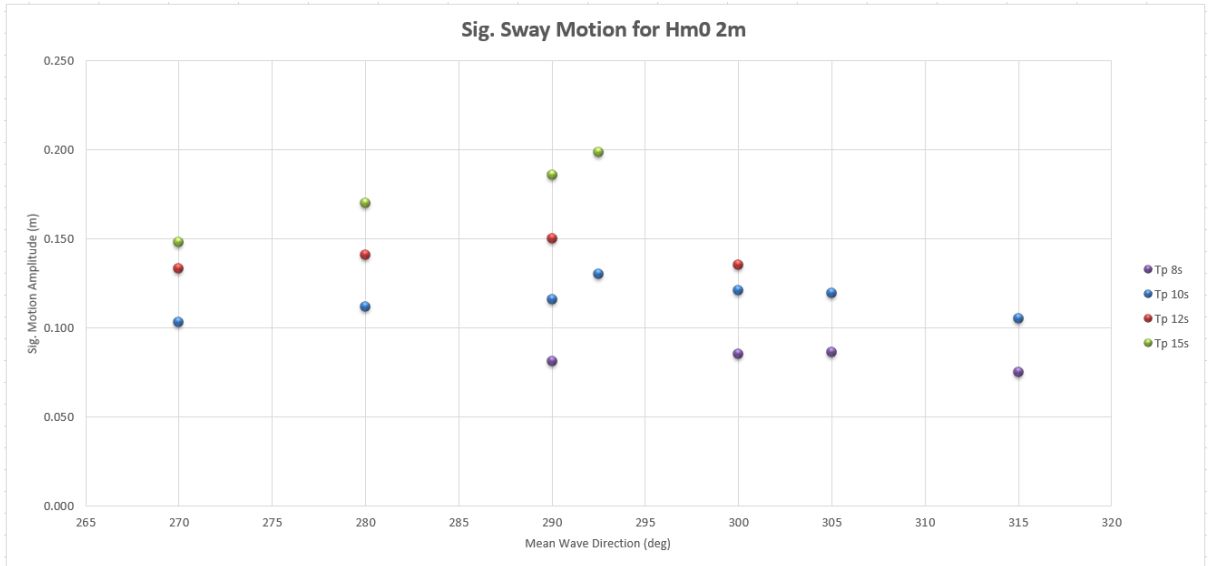
# Hm0 1m



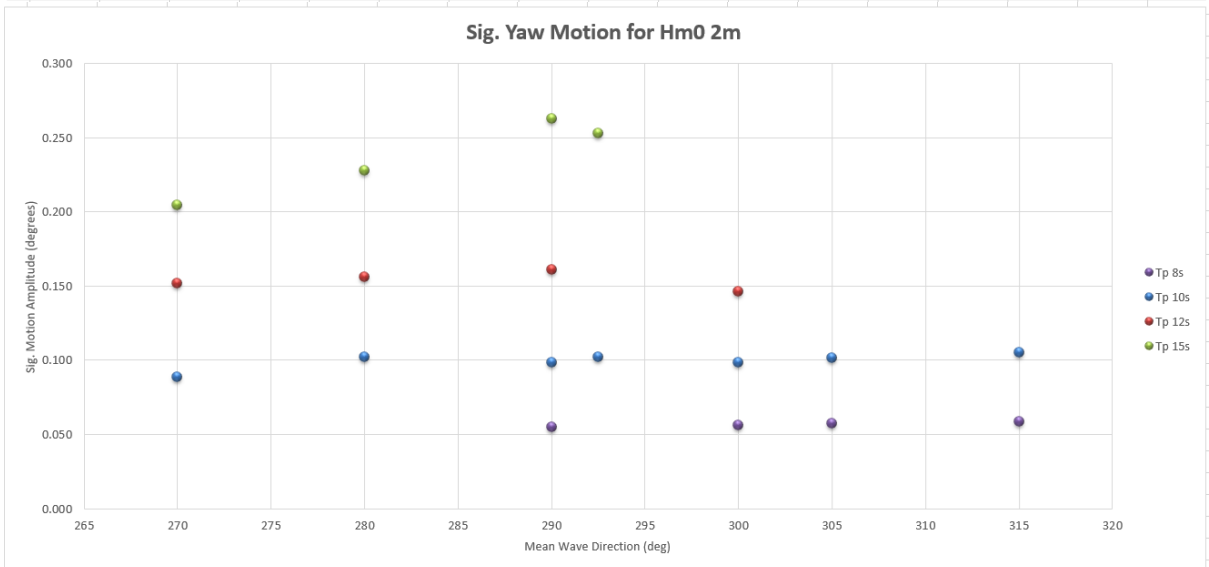
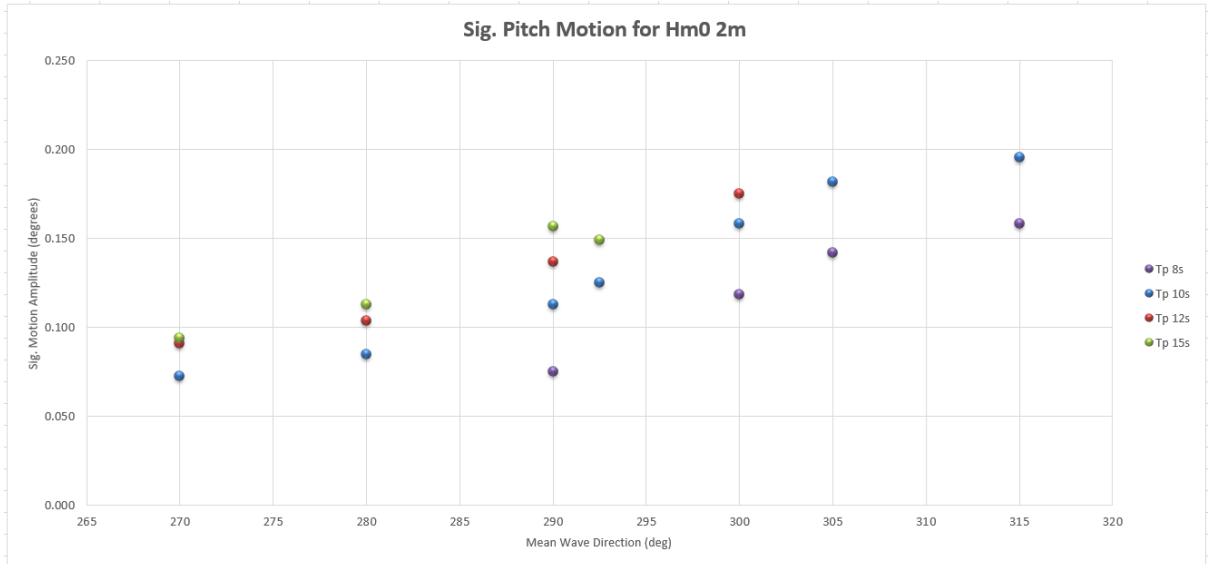


## Hm0 2m

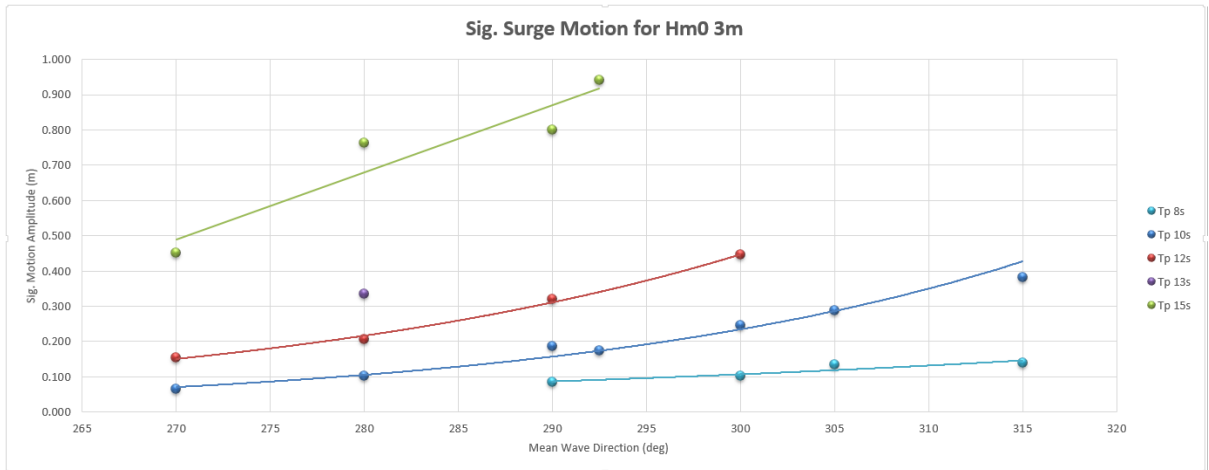


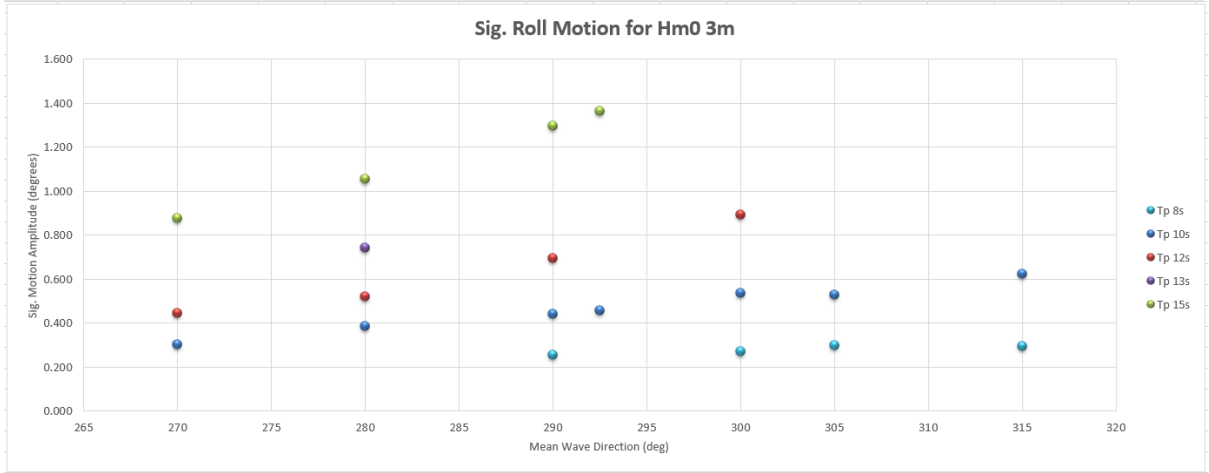
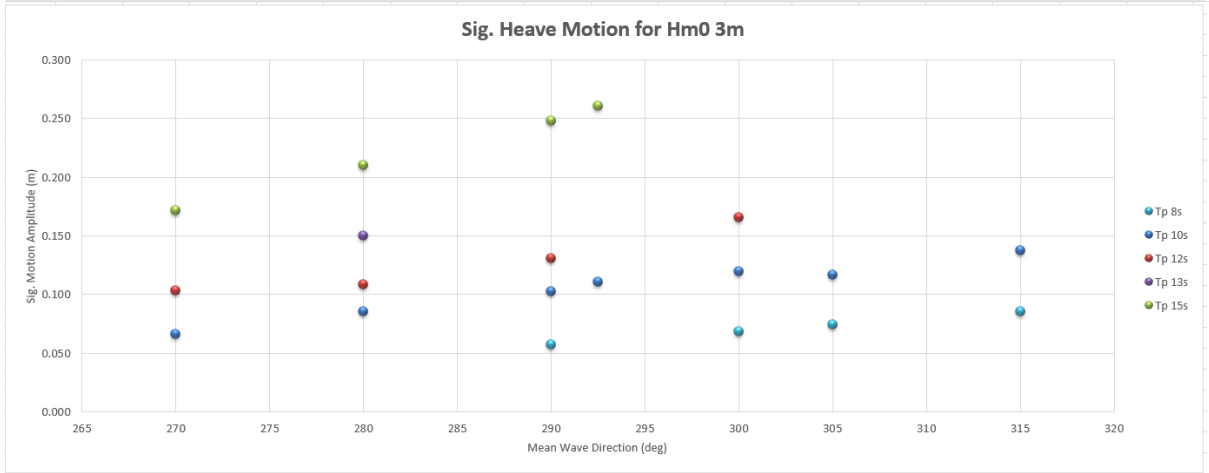
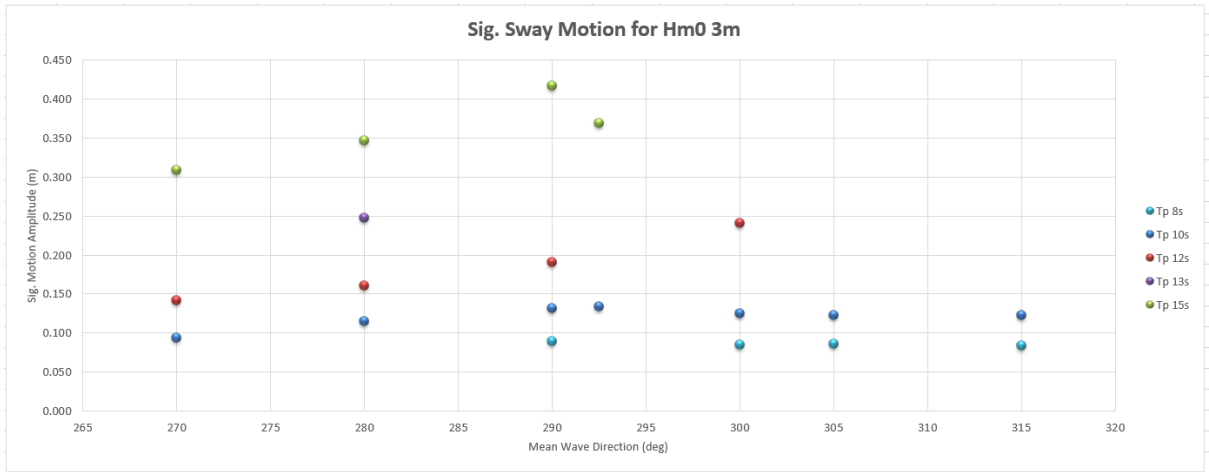


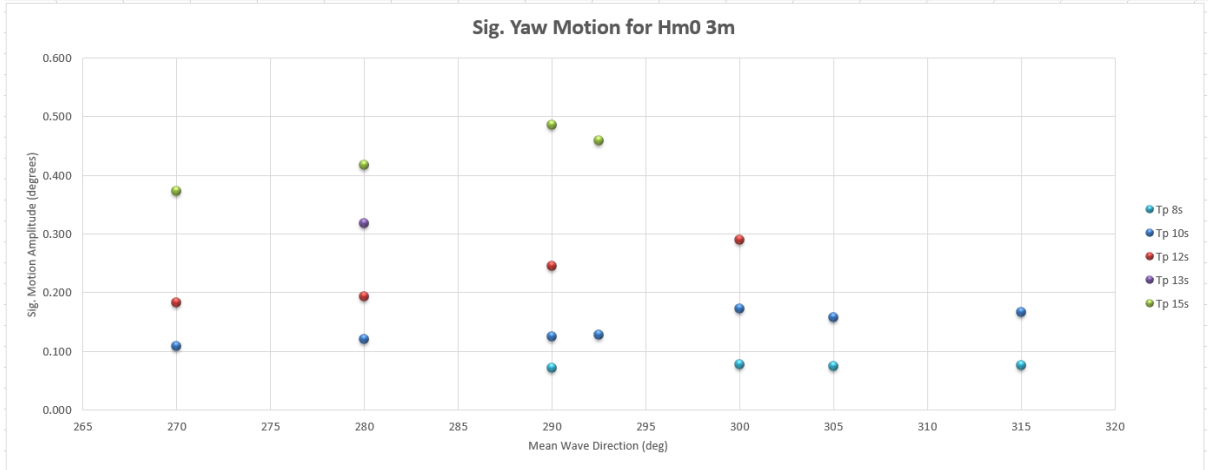
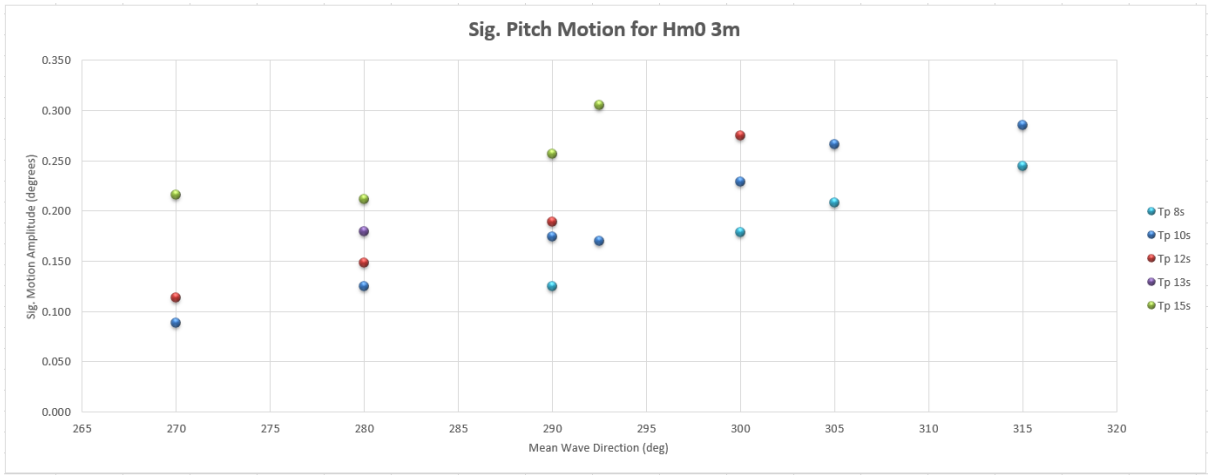




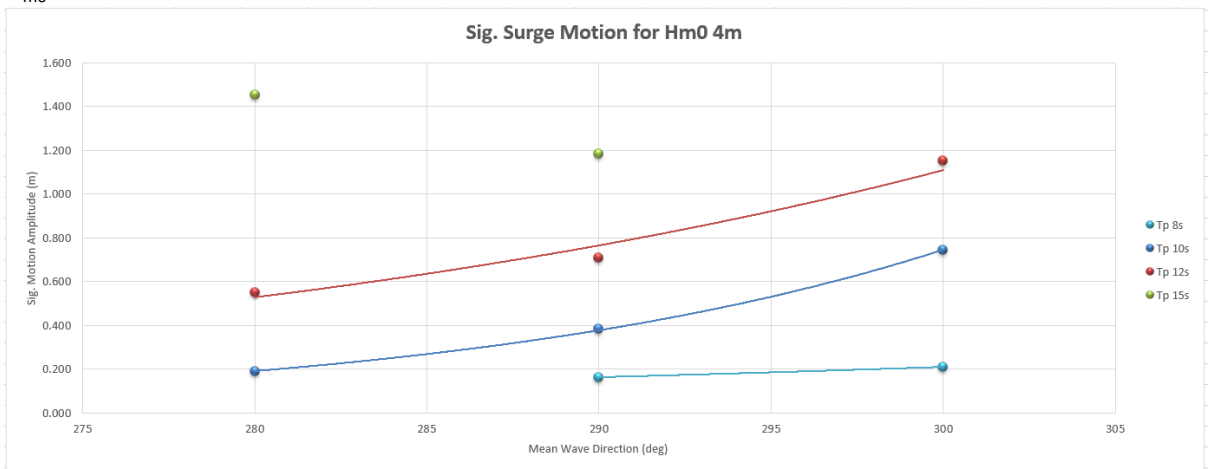
## Hm0 3m

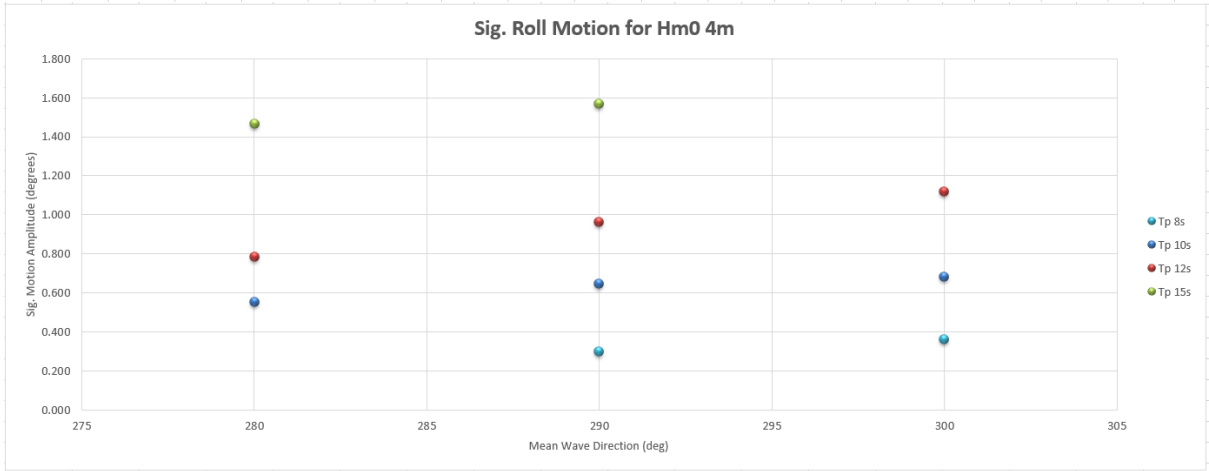
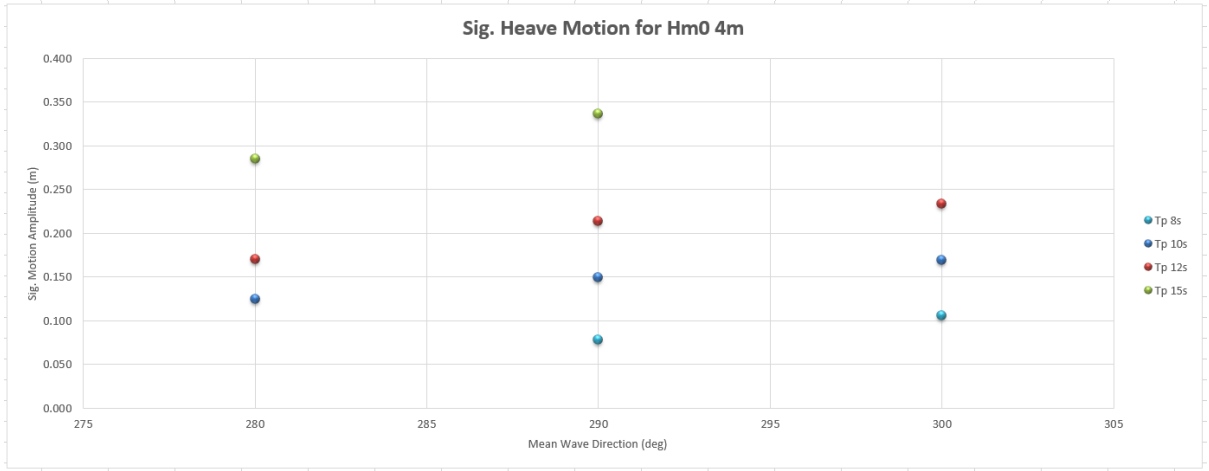
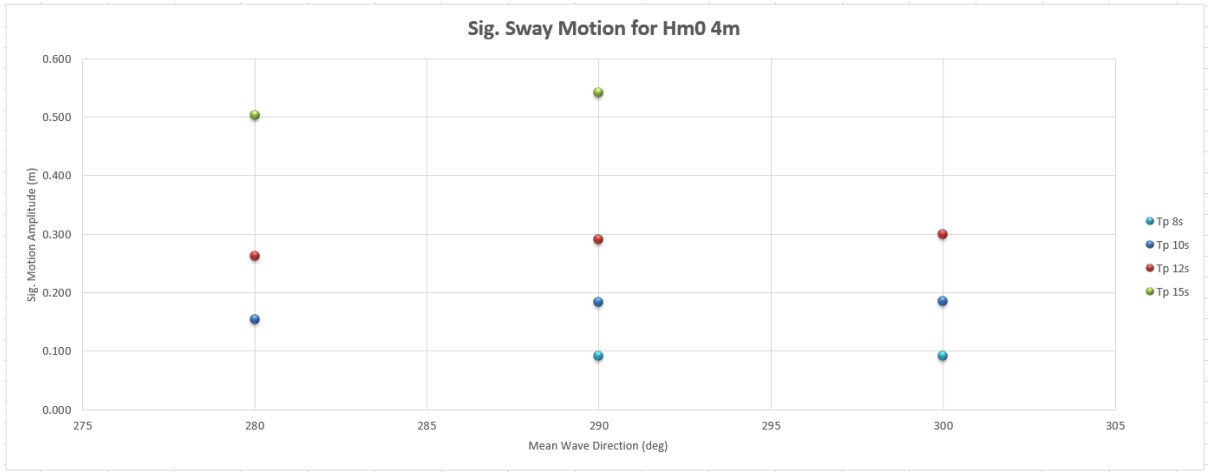




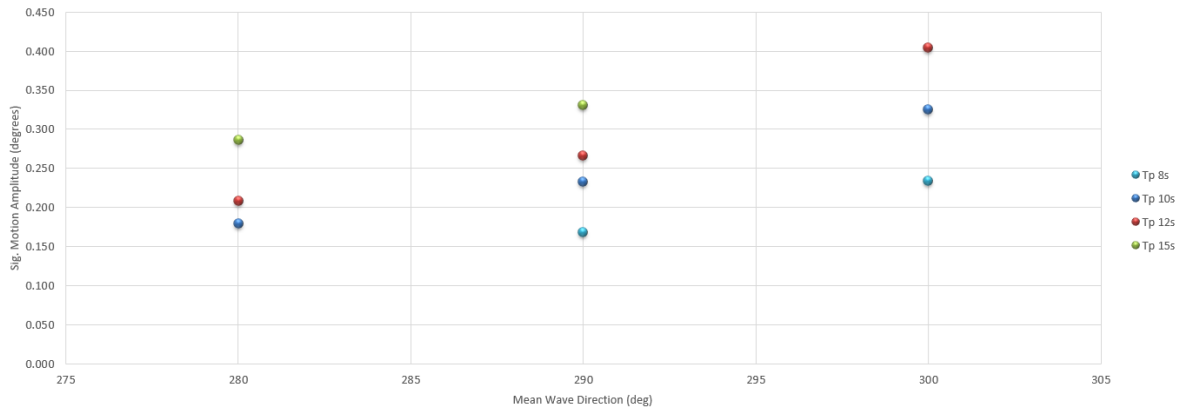


## H<sub>m0</sub> 4m





**Sig. Pitch Motion for Hm0 4m**



**Sig. Yaw Motion for Hm0 4m**

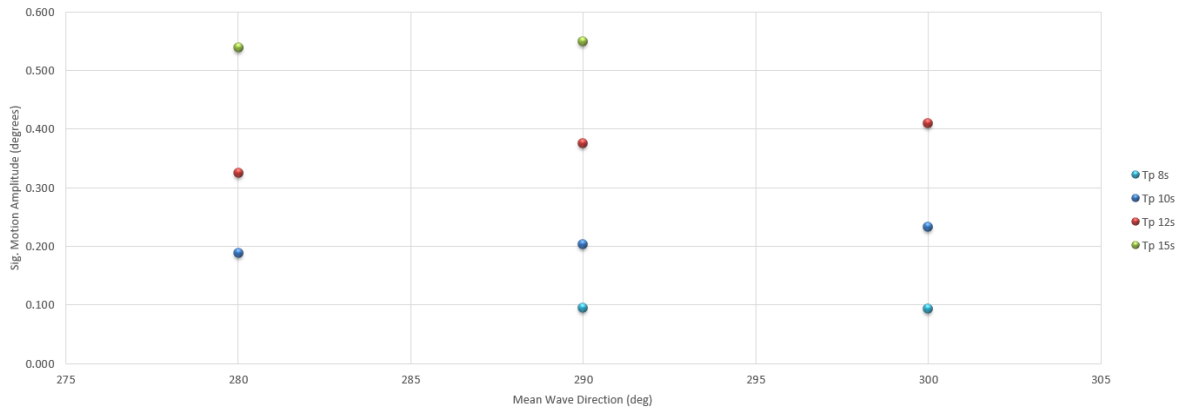


Table C.35: DVRS Datapoints for Mooring Line Forces

MWD		270	280	290	292.5	300	305	315
Hm0	1m							
Tp	8			72.648		73.46	74.832	74.335
	10	74.75	74.393	75.819	75.932	77.089	75.025	78.613
	12	80.013	78.153	83.891		84.063		
	15	91.392	92.5	95.317	99.31			
Hm0	2m							
Tp	8			75.304		79.585	80.928	81.196
	10	79.251	80.41	81.949	89.11	87.753	82.137	84.522
	12	91.602	95.551	95.287		93.634		
	15	102.908	109.675	136.794	114.957			
Hm0	3m							
Tp	8			78.872		84.702	84.598	86.846
	10	78.57	83.999	92.408	88.093	96.835	101.928	111.838
	12	95.554	103.191	128.539		154.1		
	15	176.222	178.261	212.417	189.992			
Hm0	4m							
Tp	8			84.234		92.833		
	10		96.688	128.147		137.803		
	12		161.702	174.584		208.708		
	15		254.678	277.551				

C.8 Ultraline Dyneema Line, Polyamide Tail, Wind 15  $\frac{m}{s}$ , 250 degrees

Table C.36: DURS Datapoints for  $H_{m0}$  1m

	Hm0 1m																			
	Tp 8s				Tp 10s					Tp 12s				Tp 15s				Tp 17s		
	290	300	305	315	270	280	290	292.5	300	305	315	270	280	290	300	270	280	290	292.5	285
Surge (m)	0.017	0.025	0.024	0.025	0.028	0.035	0.038	0.044	0.054	0.055	0.067	0.055	0.063	0.079	0.093	0.098	0.110	0.122	0.126	0.167
Sway (m)	0.051	0.055	0.052	0.047	0.070	0.075	0.074	0.084	0.078	0.077	0.080	0.096	0.105	0.101	0.099	0.124	0.135	0.140	0.147	0.180
Heave (m)	0.026	0.031	0.032	0.031	0.039	0.043	0.045	0.052	0.049	0.050	0.050	0.056	0.060	0.057	0.058	0.070	0.076	0.076	0.084	0.091
Roll (deg)	0.117	0.129	0.132	0.128	0.180	0.192	0.187	0.210	0.207	0.218	0.219	0.258	0.275	0.265	0.301	0.318	0.348	0.344	0.385	0.377
Pitch (deg)	0.044	0.066	0.076	0.089	0.046	0.056	0.066	0.072	0.091	0.104	0.109	0.062	0.071	0.089	0.105	0.066	0.076	0.084	0.091	0.082
Yaw (deg)	0.040	0.041	0.041	0.042	0.067	0.078	0.077	0.075	0.073	0.082	0.107	0.117	0.128	0.127	0.116	0.160	0.165	0.156	0.166	0.166

Table C.37: DURS Datapoints for  $H_{m0}$  2m

	Hm0 2m																		
	Tp 8s				Tp 10s					Tp 12s				Tp 15s					
	290	300	305	315	270	280	290	292.5	300	305	315	270	280	290	300	270	280	290	292.5
Surge (m)	0.041	0.056	0.055	0.064	0.052	0.068	0.090	0.106	0.121	0.125	0.134	0.098	0.124	0.148	0.175	0.166	0.244	0.342	0.290
Sway (m)	0.075	0.079	0.079	0.069	0.098	0.108	0.109	0.123	0.113	0.112	0.099	0.137	0.146	0.153	0.144	0.173	0.191	0.223	0.221
Heave (m)	0.045	0.054	0.058	0.059	0.059	0.067	0.077	0.082	0.083	0.083	0.090	0.079	0.086	0.091	0.093	0.099	0.119	0.135	0.137
Roll (deg)	0.172	0.189	0.203	0.207	0.261	0.284	0.275	0.310	0.308	0.332	0.348	0.368	0.400	0.394	0.432	0.443	0.489	0.529	0.577
Pitch (deg)	0.084	0.127	0.151	0.167	0.077	0.089	0.118	0.130	0.165	0.188	0.203	0.094	0.107	0.141	0.180	0.096	0.115	0.159	0.151
Yaw (deg)	0.052	0.053	0.054	0.055	0.094	0.104	0.104	0.102	0.096	0.107	0.107	0.162	0.177	0.175	0.156	0.206	0.226	0.235	0.224

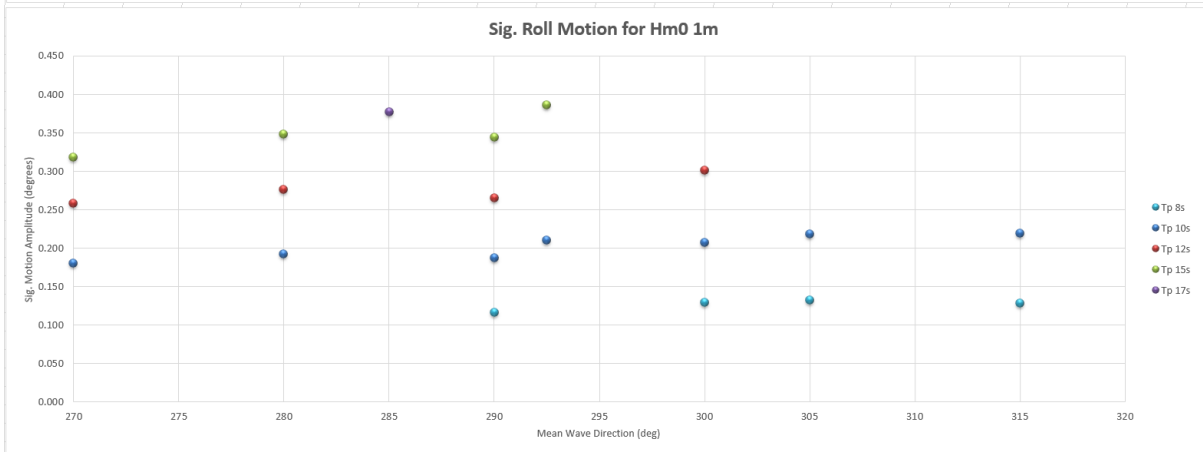
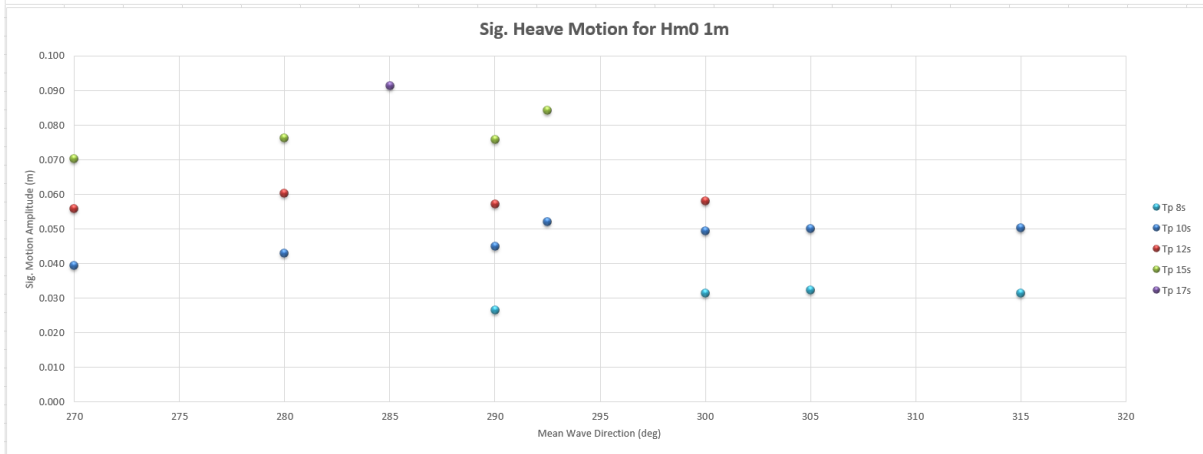
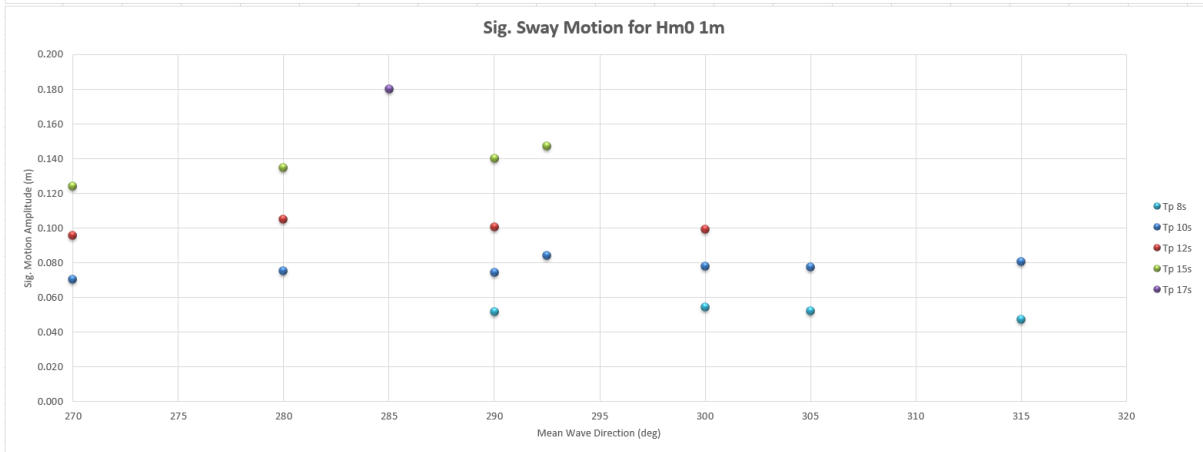
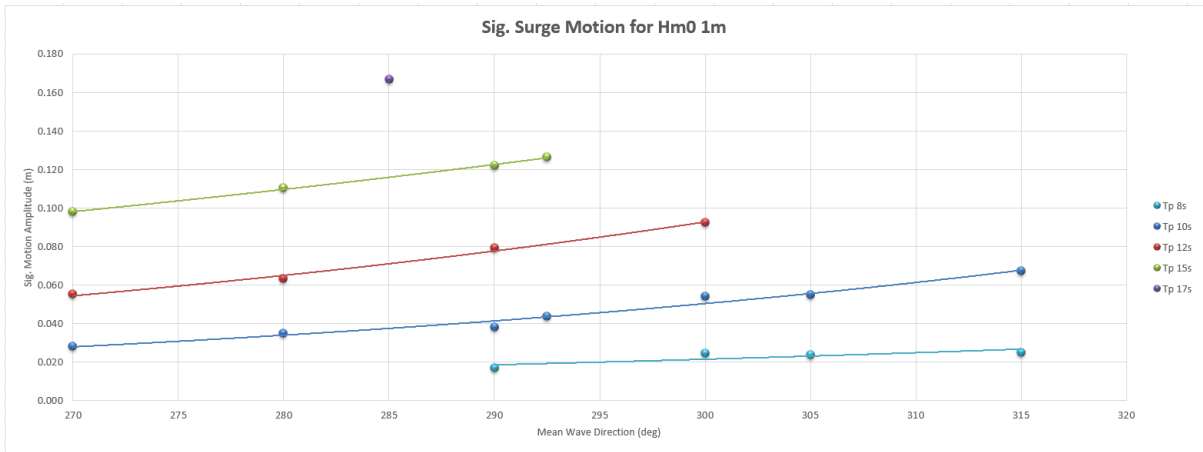
Table C.38: DURS Datapoints for  $H_{m0}$  3m

	Hm0 3m																			
	Tp 8s				Tp 10s					Tp 12s				Tp 13s	Tp 15s					
	290	300	305	315	270	280	290	292.5	300	305	315	270	280	290	300	280	270	280	290	292.5
Surge (m)	0.089	0.112	0.140	0.161	0.074	0.113	0.189	0.181	0.239	0.305	0.380	0.155	0.232	0.312	0.421	0.303	0.423	0.623	0.647	0.687
Sway (m)	0.082	0.078	0.080	0.077	0.093	0.112	0.131	0.132	0.129	0.124	0.128	0.150	0.170	0.195	0.216	0.214	0.297	0.338	0.398	0.399
Heave (m)	0.057	0.069	0.075	0.087	0.065	0.084	0.102	0.110	0.119	0.116	0.137	0.103	0.108	0.131	0.165	0.149	0.172	0.211	0.249	0.260
Roll (deg)	0.223	0.243	0.266	0.279	0.257	0.321	0.378	0.390	0.476	0.486	0.575	0.386	0.440	0.618	0.872	0.704	0.904	0.970	1.144	1.129
Pitch (deg)	0.134	0.188	0.217	0.253	0.095	0.131	0.180	0.177	0.234	0.272	0.292	0.117	0.152	0.192	0.278	0.181	0.214	0.211	0.256	0.303
Yaw (deg)	0.068	0.073	0.071	0.073	0.108	0.127	0.126	0.129	0.186	0.172	0.180	0.178	0.200	0.253	0.317	0.340	0.350	0.381	0.427	0.418

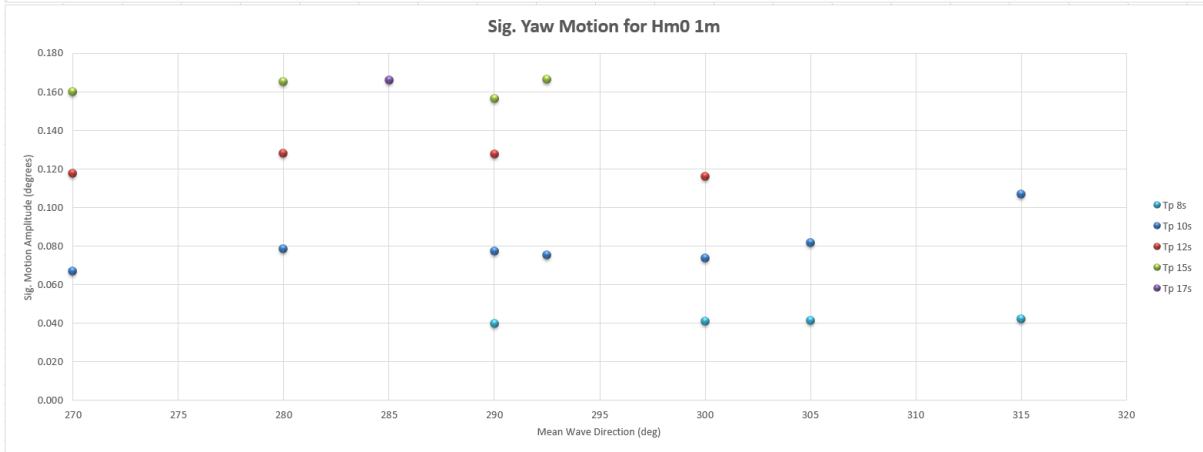
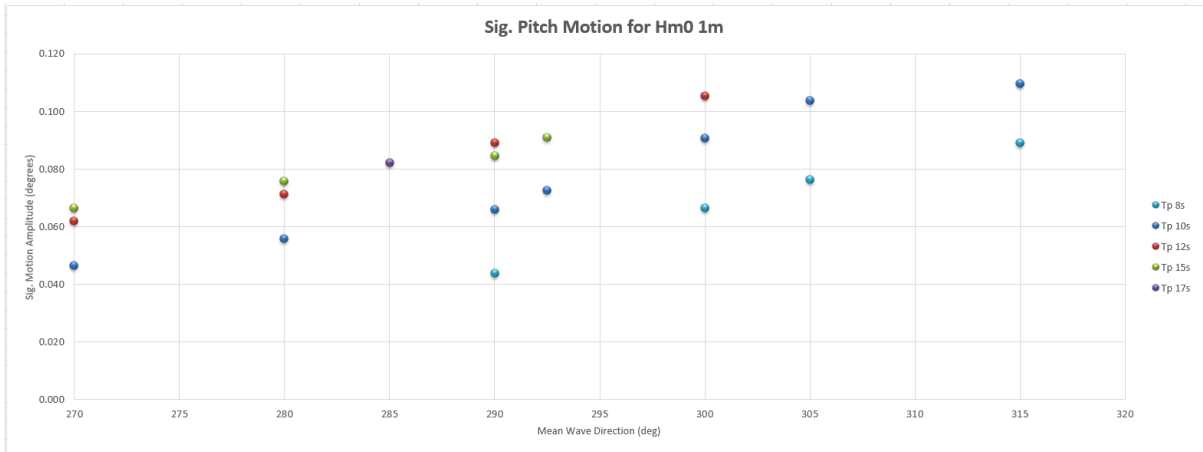
Table C.39: DURS Datapoints for  $H_{m0}$  4m

	Hm0 4m									
	Tp 8s		Tp 10s			Tp 12s			Tp 15s	
	290	300	280	290	300	280	290	300	280	290
Surge (m)	0.170	0.233	0.226	0.368	0.617	0.414	0.593	0.748	0.921	0.890
Sway (m)	0.084	0.084	0.151	0.184	0.187	0.231	0.304	0.268	0.452	0.512
Heave (m)	0.079	0.107	0.124	0.149	0.168	0.170	0.214	0.234	0.286	0.336
Roll (deg)	0.261	0.324	0.448	0.584	0.664	0.718	0.974	1.203	1.404	1.451
Pitch (deg)	0.177	0.242	0.184	0.239	0.330	0.211	0.269	0.405	0.283	0.328
Yaw (deg)	0.096	0.095	0.192	0.220	0.266	0.342	0.409	0.443	0.449	0.479

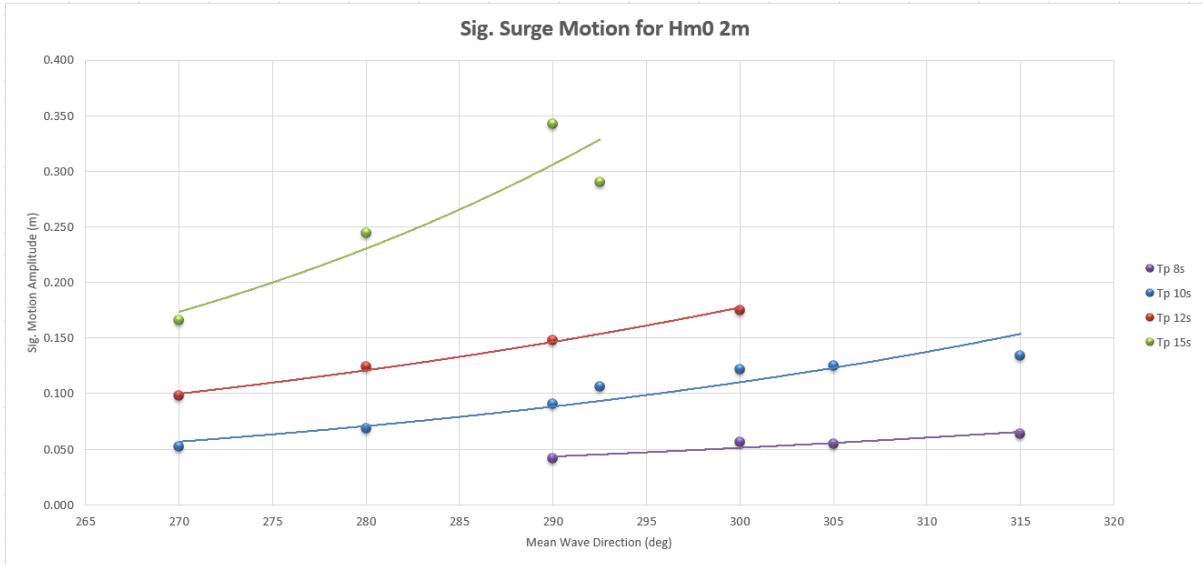
# H<sub>m0</sub> 1m

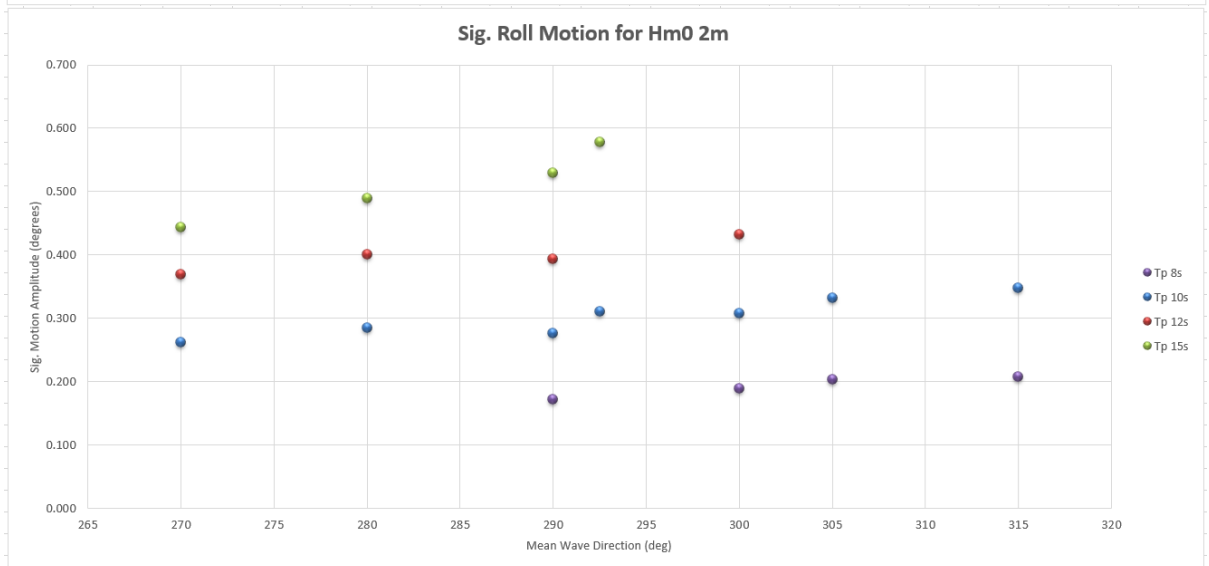
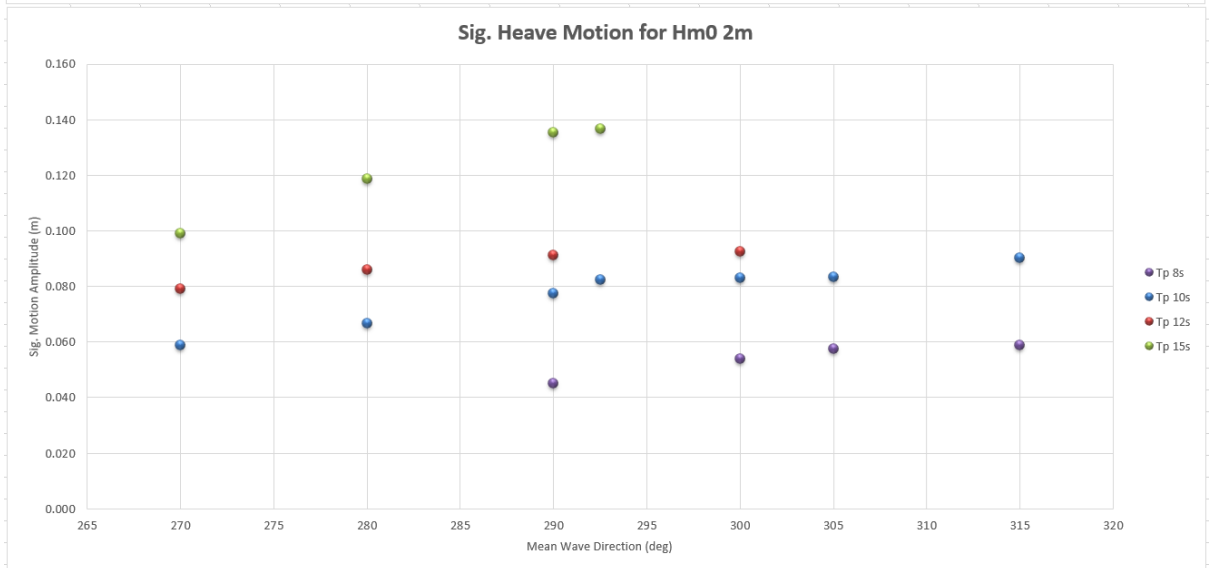
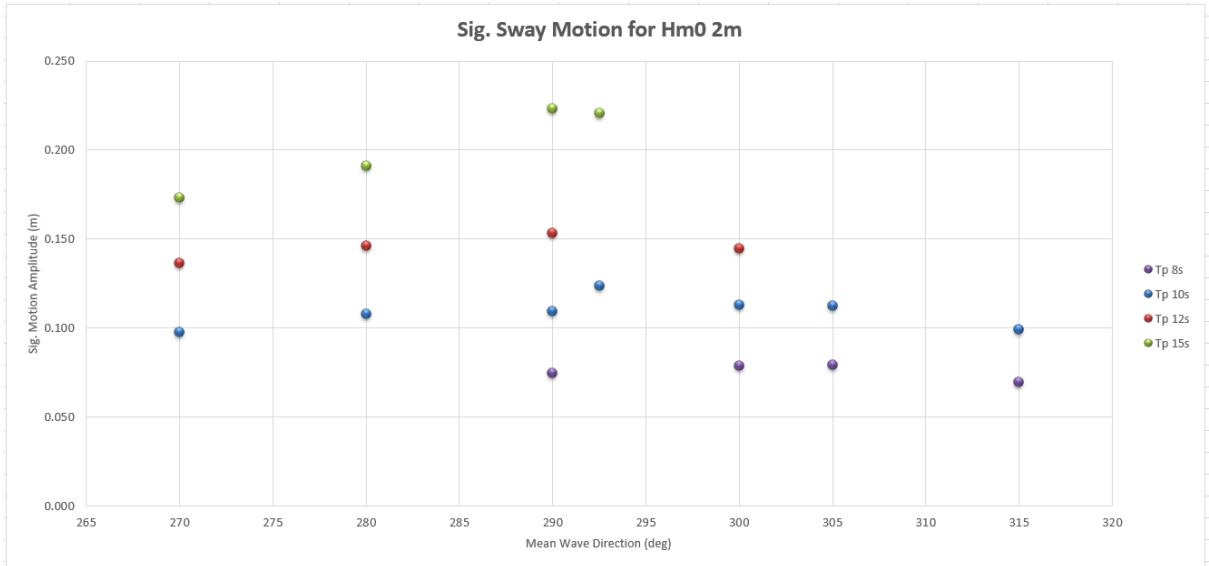


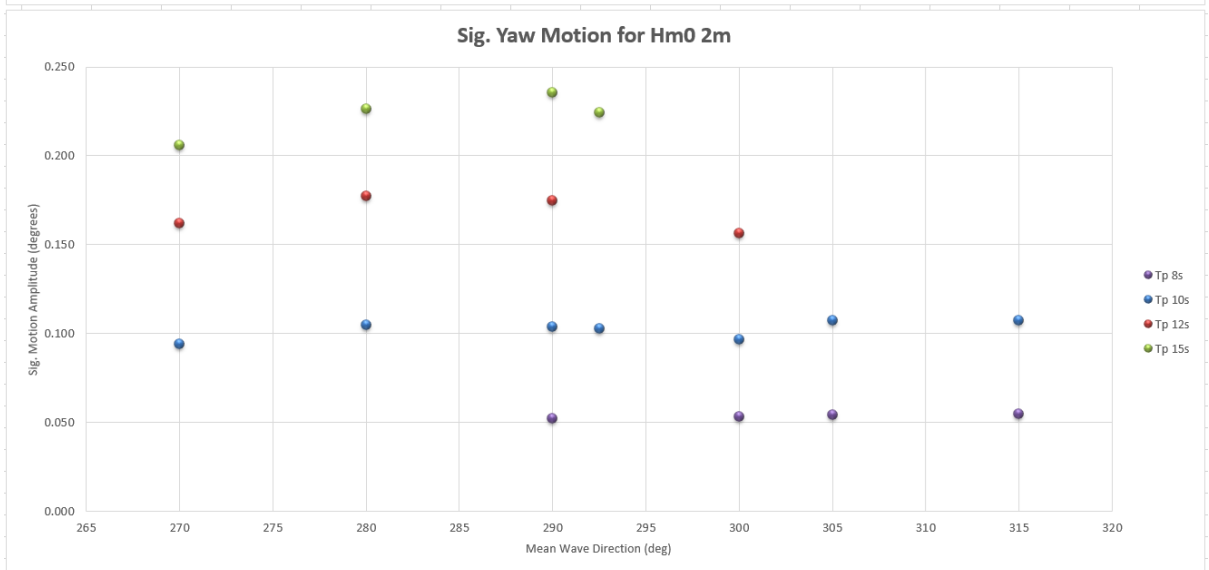
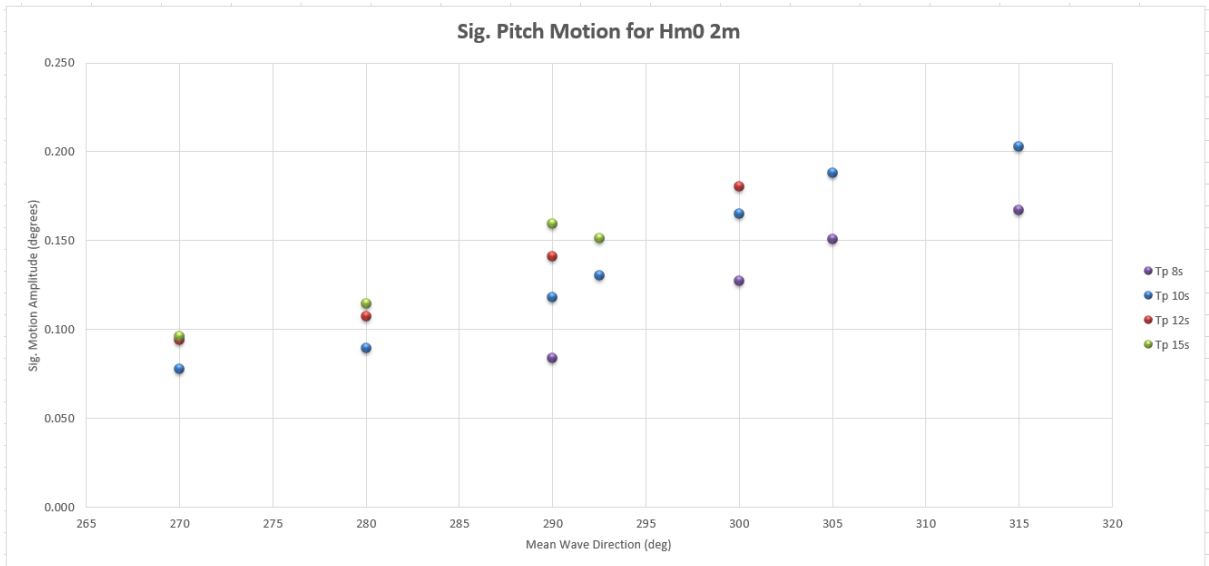




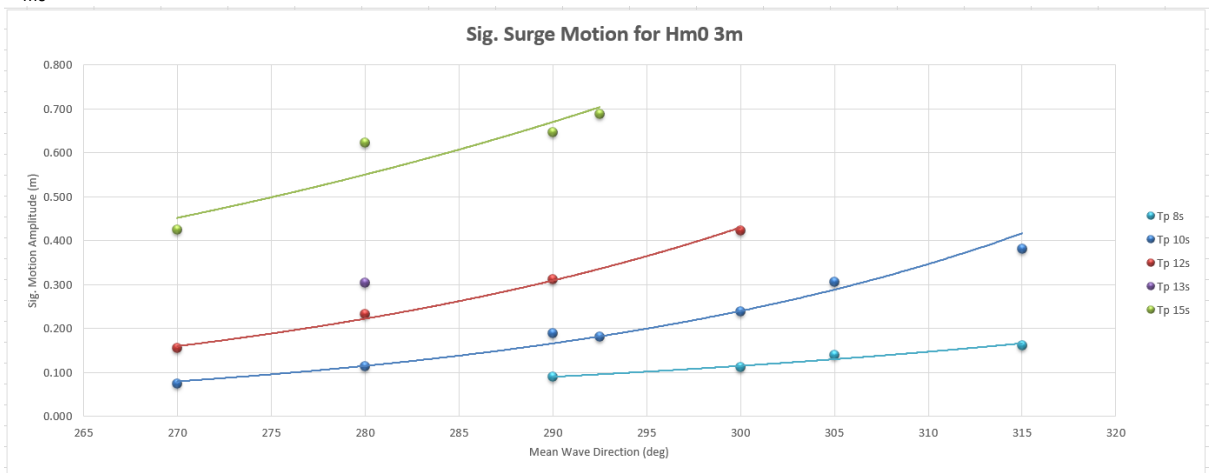
## H<sub>m0</sub> 2m

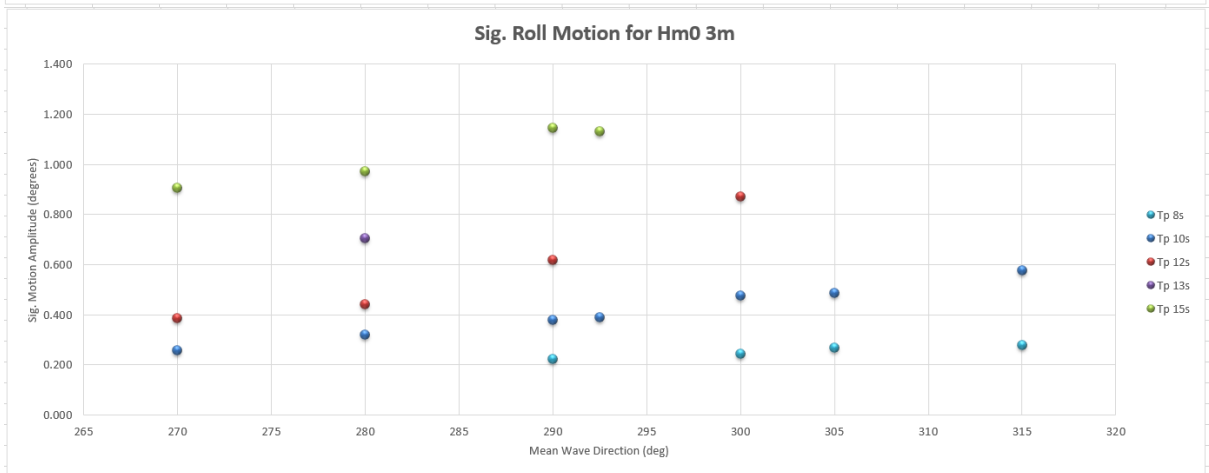
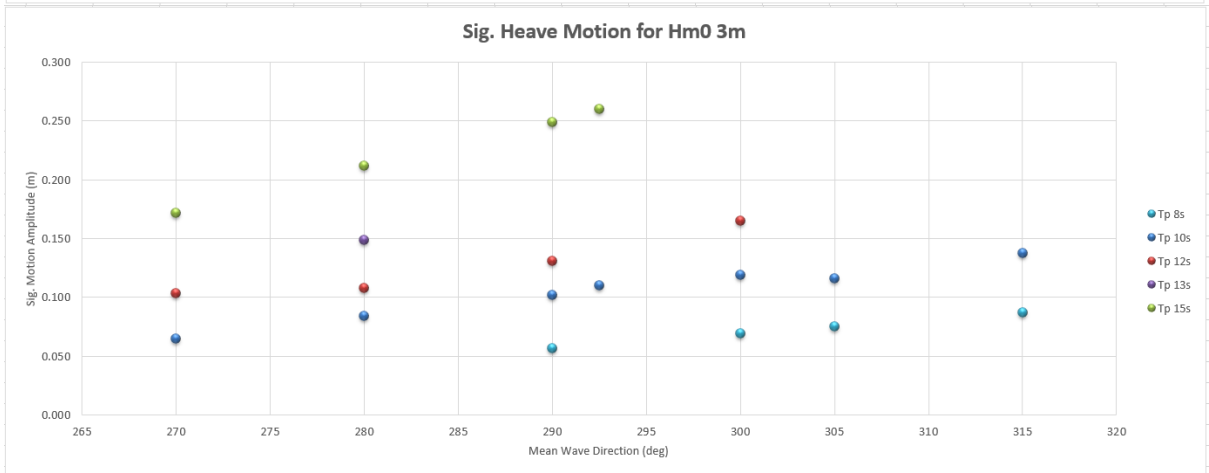
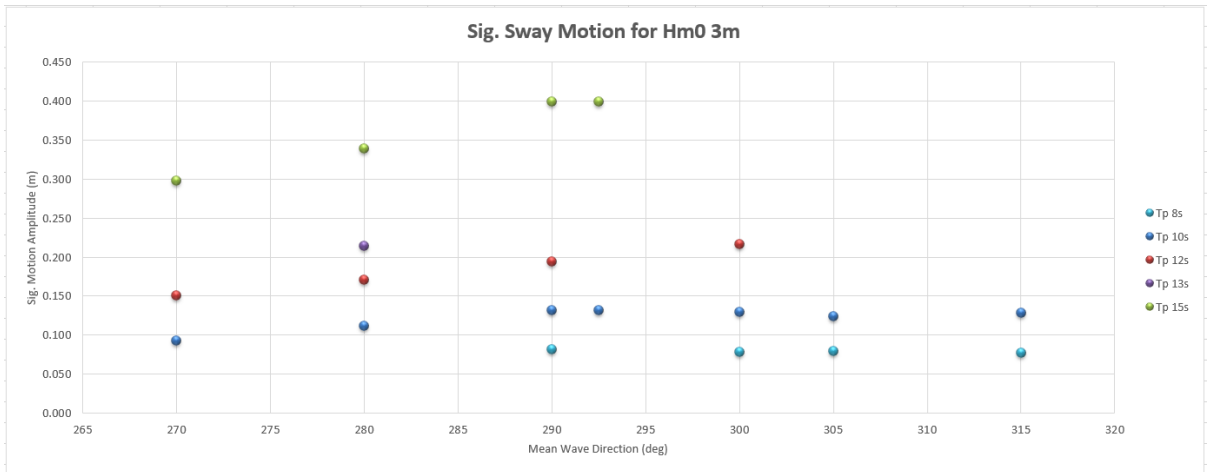


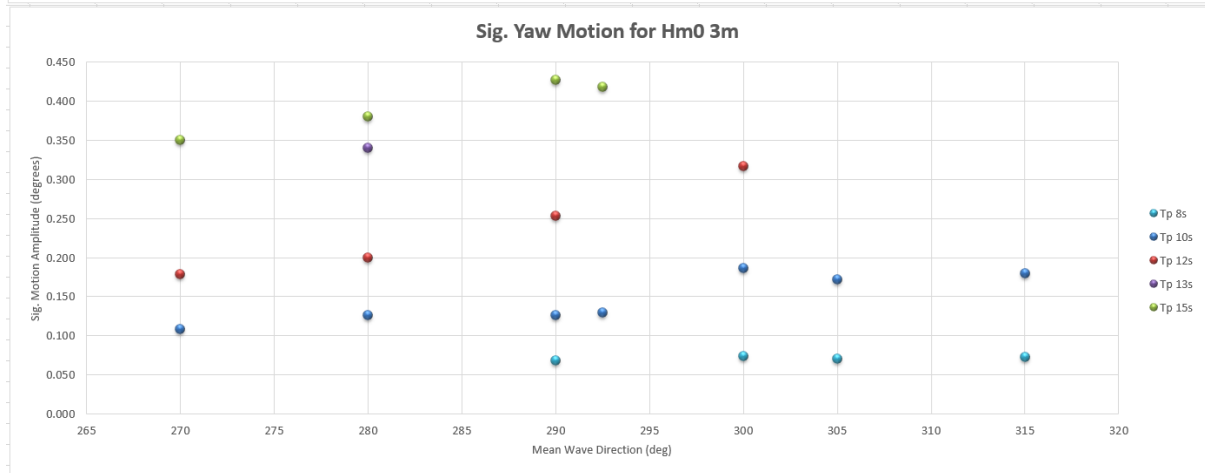
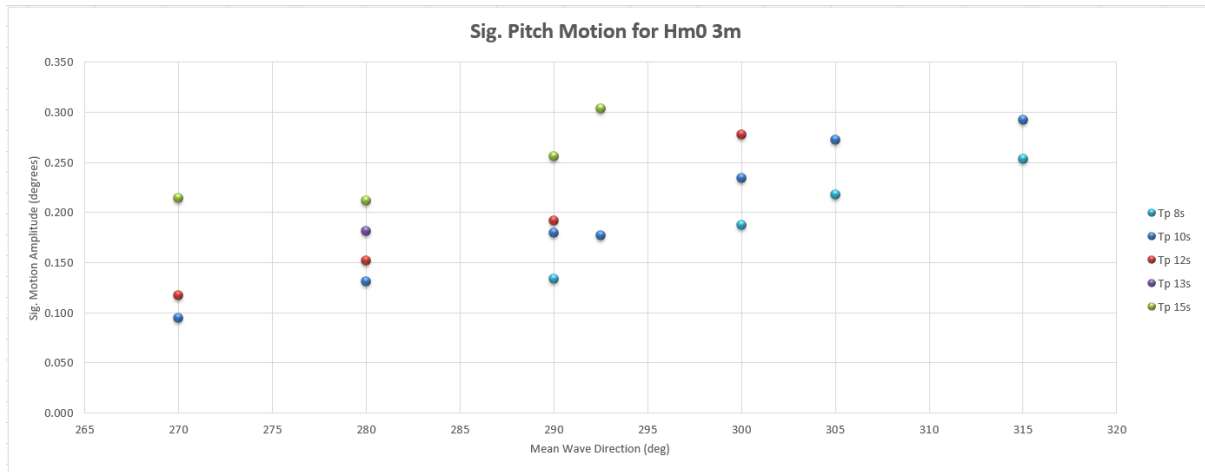




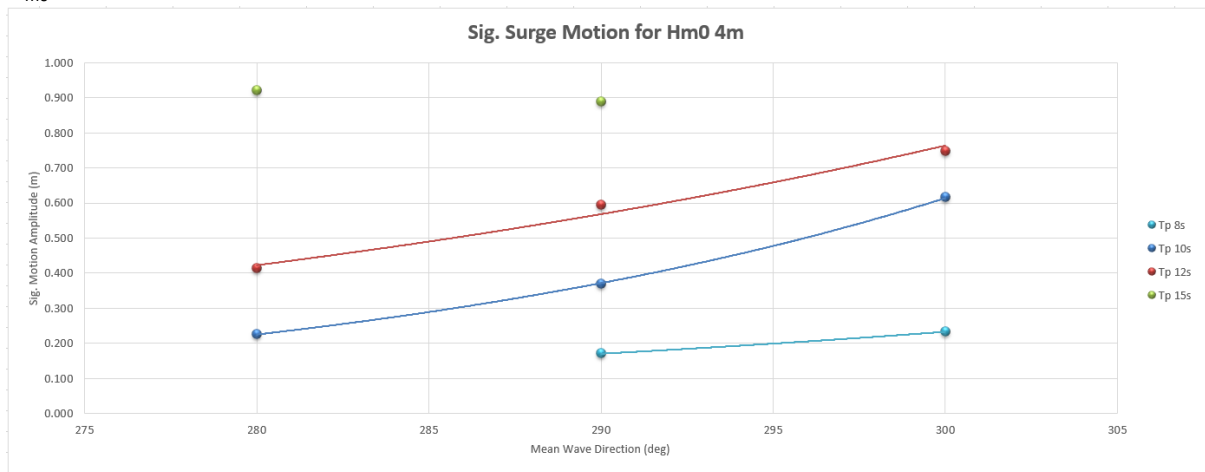
## H<sub>m0</sub> 3m



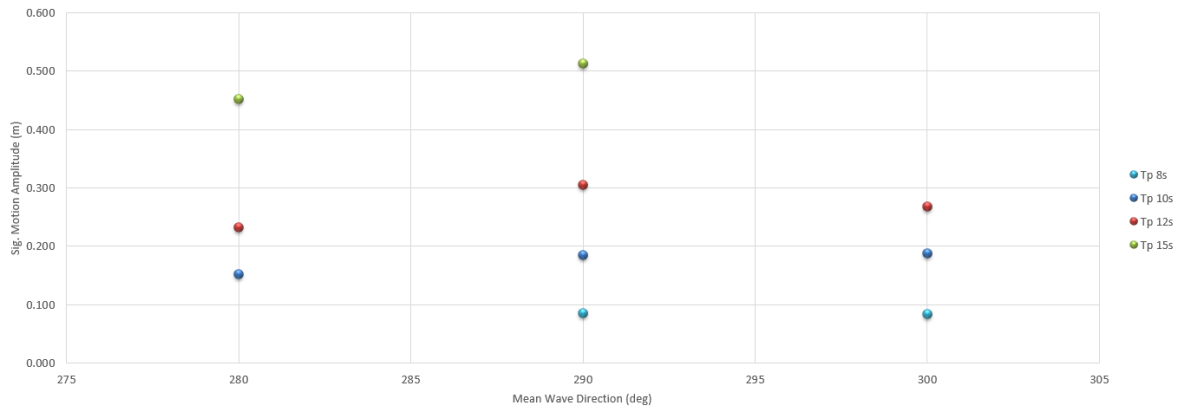




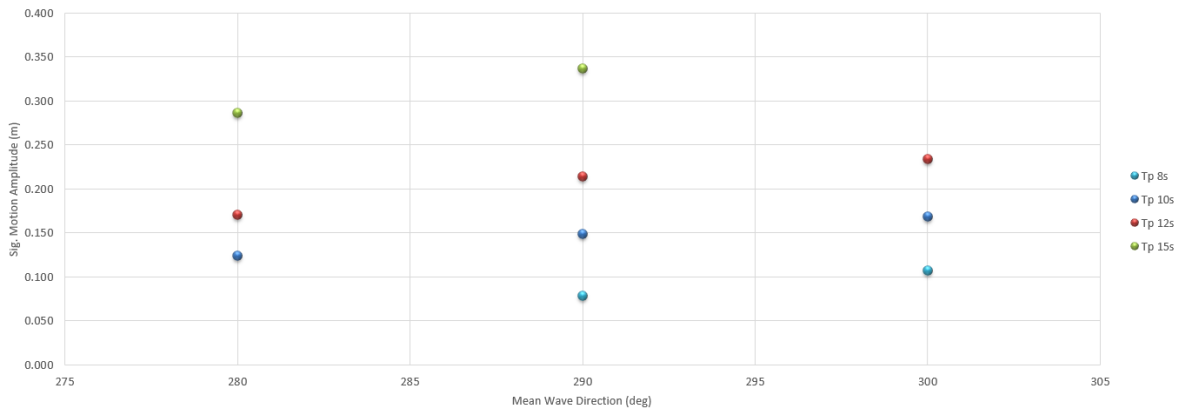
## H<sub>m0</sub> 4m



**Sig. Sway Motion for Hm0 4m**



**Sig. Heave Motion for Hm0 4m**



**Sig. Roll Motion for Hm0 4m**

